AN EVALUATION OF ESTIMATES OF STABILITY OF OSCILLATIONS IN NONLINEAR SYSTEMS

A THESIS
PRESENTED TO
THE FACULTY OF GRADUATE STUDIES
THE UNIVERSITY OF MANITOBA

IN PARTIAL FULFILLMENT
OF THE REQUIREMENTS FOR THE DEGREE
DOCTOR OF PHILOSOPHY

by

BARRIE WILLIAM LEACH

FEBRUARY, 1972

TABLE OF CONTENTS

ABSTRACT

Loeb's criterion and the IDF stability technique are compared for general nonlinear second and third order systems and selected nonlinear time delay systems. Situations in which the two stability techniques disagree are sought and studied in detail. The IDF stability technique is related directly to the variational approach for a general system, and Loeb's criterion is related to the variational approach for second order systems. The IDF stability technique is shown to involve the approximation of time averaging in addition to the inherent DF approximation. The simplified form of perturbations assumed in Loeb's criterion is shown to result in the approximation of ignoring certain modes of the variational system, leading to incorrect results in certain cases. Discrepancies between the two stability techniques in second and third order system examples are demonstrated to coincide with relatively poor DF approximations, and one technique cannot be considered better than the other in application - they should be used together for proper interpretation. However, for time delay systems the IDF stability technique is shown to be clearly superior to Loeb's criterion,since all discrepancies encountered in the time delay systems studied correspond to failures of Loeb's criterion, but correct stability prediction by the IDF stability technique.

LIST OF TABLES

LIST OF FIGURES

ACKNOWLEDGEMENTS

The inspiration and completion of this thesis have been possible because of many people. The National Research Council and the University of Manitoba provided the necessary financial support. My thesis supervisor, Professor R.A. Johnson, gave the time, ideas, and criticisms necessary for the thesis to evolve. My family, and especially my late mother, provided me with encouragement and support.

CHAPTER 1

INTRODUCTION

The analysis of nonlinear systems with respect to the existence, form, and stability of oscillations (periodic solutions) can be quite complicated. There are no general theories or methods - only a variety of techniques applicable to restricted classes of nonlinear systems. Some of these techniques are exact while others are only approximate. The problem of analysis is compounded when nonlinear systems with time delay (nonlinear differential - difference systems) are considered. Indeed, the theory for linear systems with time delay is far from being complete.

1.1 Approximate Techniques

In the study of oscillations in autonomous (time invariant and unforced) nonlinear systems, the approximate method known as the describing function (DF) method [1,2,3,4] has been a popular analytical tool. Other approximation techniques,such as harmonic linearization and the DIDF method,are related to the DF method, and are also quite familiar [1,5,6]. As an approximate method for determining the stability of oscillations, Loeb's criterion in conjunction with the DF method works well in a wide class of nonlinear systems [7,8,1,2]. However, it is known to fail, even when the describing function approximation seems reasonable - in systems involving time delay, for example. Gelb and VanderVelde [6], Brookes [9], Katzberg [10], and Menzies [11] cite examples of nonlinear systems with time delay for which Loeb's criterion fails. Gelb and VanderVelde suggest that another approximate stability method related to the DF, the incremental - input describing function

(IDF) stability technique, is more accurate than Loeb's criterion when applied to both delay and nondelay systems [6 p.246, pp.324-326]. However, both stability techniques are approximate and have in common the basic DF approximation. It cannot be concluded that the IDF stability technique is more accurate than Loeb's criterion in all situations without a thorough comparison of the two.

1.2 Purpose of the Thesis

Many questions concerning the use of the DF method, in conjunction with Loeb's criterion and the IDF stability technique, have not been answered satisfactorily. It is the intention in this thesis to try to resolve some of the problems in this area. The comparison of Loeb's criterion and the IDF stability technique for various systems is an important area of research in the light of the known failures of Loeb's criterion. Any discrepancies between the two techniques should be investigated as to which technique is predicting more correctly the actual stability. Reasons for failure of each stability technique in a given situation must be found in order to understand the approximations involved. From the practical point of view, a control engineer wants to know when these stability techniques can be used with confidence to ascertain the stability of predicted oscillations.

As well as a thorough comparison of the two approximate stability techniques, a comparison must be made between the approximate stability techniques and any exact stability information that is available. In this way the actual approximations involved in these two stability techniques can be determined. To this end an attempt must be made to relate them to the exact variational equation approach.

1.3 Outline of Chapters

In Chapter 2 the theory of stability of oscillations in nonlinear systems is developed using the variational equation approach. The types of stability to be considered are defined and the Floquet theory of variational equations is introduced. This chapter serves as the theoretical basis to which the approximate techniques outlined in succeeding chapters must be related.

Chapter 3 contains a description of the approximate DF method and related DIDF methods of oscillation prediction. The two important stability techniques, Loeb's criterion and the IDF stability technique, are also outlined. Convenient interpretations of these stability techniques are developed in terms of root locus plots, and the IDF stability technique is related by the author to the variational equation approach. Some general comparisons between the two stability techniques are made as well.

In Chapter 4 two types of nonlinearities to be considered, hard and soft spring, are studied. The shape of the nonlinearity is related to the DF equivalent gain, $K_{eq}(A)$. Also, the incremental gain, $N_B(A,0)$, of the IDF stability technique is related to $K_{eq}(A)$ for hard and soft spring nonlinearities. The nonlinearities to be used in simulations are introduced with the corresponding calculations of $K_{eq}(A)$ and $N_B(A,0)$.

After these preliminary chapters, a thorough study of the IDF stability technique and Loeb's criterion is made for second order systems in Chapter 5. Both stability techniques are compared to the variational equation, and it is shown that Loeb's criterion is the more accurate technique here. Simulation is used to verify the analysis - with some interesting results that bear further interpretation.

The comparison of Loeb's criterion and the IDF stability technique is continued in Chapter 6 for third order systems. A number of situations in which the two techniques disagree are found, and, with the aid of simulation, studied thoroughly. The unexpected results of the simulations shed new light on the use of the IDF stability technique in third order systems.

Systems involving time delay are dealt with in Chapter 7. Two system configurations for which exact periodic solutions are known are studied in some detail with respect to the DF method, DIDF technique, Loeb's criterion, and the IDF stability technique applied to them. Some exact stability information is derived from the exact variational equations for these systems. The problem of failure of Loeb's criterion in these and other time delay systems is investigated using root locus techniques.

Chapter 8 is a summary with suggestions for future work.

CHAPTER 2

THEORY OF STABILITY OF OSCILLATIONS

In order to determine the exact stability of an oscillation in an autonomous nonlinear system, it is sufficient in many cases to deal with the equation of the first (linear) variation from the periodic solution. This equation is termed the variational equation.

2.1 Calculation of the Variational Equation

A general autonomous nonlinear system having the block diagram configuration of Fig. 2.1 is considered. The nonlinearity f(x) is assumed to be static and single-valued while the transfer function of the linear plant, L(s), is either rational or in the form $G(s)e^{-\tau s}$ with G(s) rational (s is the Laplace Transform variable). If a periodic solution x*(t), of period T, exists in the system then the variational equation is found by considering a perturbed solution, x*(t) + e(t), with e(t) a small arbitrary perturbation term. An operational approach to the variational equation, due to Cosgriff [12], is conveniently applied to the system of Fig.2.1 to yield

$$L(D)\left\{f(x)\right\} + x = o \ , \ D \equiv d/dt. \tag{2.1}$$

Substitution of the perturbed solution, x* + e, into 2.1 results in

$$L(D)\left\{f(x^* + e)\right\} + x^* + e = o. \tag{2.2}$$

If f(x) has a Taylor series expansion about x* then 2.2 becomes

$$L(D)\left\{f(x^*) + e\,\frac{df}{dx}(x^*) + \frac{e^2}{2!}\,\frac{d^2f}{dx^2}(x^*) + \cdots\right\} + x^* + e = o, \tag{2.3}$$

which reduces to

$$L(D)\left\{\frac{df}{dx}(x^*)\ e\right\} + e = o \qquad (2.4)$$

when 2.1 is subtracted and the higher order terms in e are dropped. Equation 2.4 is then the (linear) variational equation for the periodic solution x* and the system of Fig.2.2 is the corresponding variational system. The coefficient $\frac{df}{dx}(x^*) \equiv \frac{df}{dx}\Big|_{x=x^*}$ will be a periodic time varying coefficient with period T - the same period as x*. Equation 2.4 is a linear differential equation with periodic time varying coefficients and the variational system of Fig. 2.2 is a linear periodic time varying system. If L(s) is of the form $G(s)e^{-\tau s}$, that is, the original nonlinear system involves time delay, then the variational equation (system) becomes a differential - difference equation (system) with periodic time varying coefficients.

An interesting lemma [9, p.11; 13, p.322], proved quite simply for this system, is that $\frac{dx^*}{dt}(t)$ $(\equiv \dot{x}^*)$ is always a solution to the variational equation. If 2.1 is differentiated with respect to time, the result is the variational equation 2.4 with e replaced by $\dot{x}^*$. This shows that the variational equation always has at least one periodic solution, since $\dot{x}^*$ is obviously periodic when x* is.

2.2 Stability Definitions [14]

Two types of stability are considered for periodic solutions to nonlinear systems - stability in the sense of Lyapunov (i.s.L) and orbital stability. The notion of orbital stability will be more important since it is devised especially for periodic motions in nonlinear systems. Stability i.s.L is more suited to the stability of equilibrium points and oscillations in linear systems.

Stable i.s.L - A periodic solution is stable i.s.L. if and only if any perturbation of this motion can be constrained to lie within a specified arbitrarily small distance of the periodic motion for each point in time by a suitable choice of the initial perturbation magnitude. Thus, if $x^*(t)$ is the periodic solution and $e(t)$ is an arbitrary perturbation, so that the perturbed solution is $x_p(t) \triangleq x^*(t) + e(t)$, then the mathematical statement of the definition would be: $\forall \epsilon > 0 \; \exists \delta > 0 \ni$

$$\left\| x^*(t_o) - x_p(t_o) \right\| = \left\| e(t_o) \right\| < \delta$$

$$\Rightarrow \left\| x^*(t) - x_p(t) \right\| = \left\| e(t) \right\| < \epsilon \quad , \forall t \geqslant t_o \; ,$$

where $\| \cdot \|$ denotes an arbitrary norm. Also, a periodic solution is asymptotically stable (a.s.) i.s.L. if and only if it is stable i.s.L. and

$$\lim_{t \to \infty} \left\| x^*(t) - x_p(t) \right\| = \lim_{t \to \infty} \left\| e(t) \right\| = o.$$

If a periodic solution is stable i.s.L., but not asymptotically stable i.s.L., it is said to be weakly stable i.s.L.

Orbitally Stable - A periodic solution is orbitally stable (o.s.) if and only if any perturbation of the motion can be constrained to lie within a specified arbitrarily small neighbourhood of the periodic solution trajectory C by a suitable choice of the initial perturbation magnitude. Mathematically the statement would be: $\forall \epsilon > 0 \; \exists \delta > 0 \ni$

$$\left\| x^*(t_o) - x_p(t_o) \right\| = \left\| e(t_o) \right\| < \delta \Rightarrow \left\| c - x_p(t) \right\| < \epsilon \quad ,$$

$\forall t \geqslant t_o$ and some $c \in C$. Note that c will vary with t. A periodic solution is asymptotically orbitally stable (a.o.s.) if and only if it is orbitally stable and $x_p(t)$ approaches the periodic motion trajectory C in norm as $t \to \infty$.

Note that the foregoing stability definitions are based on a state space formulation for the system and are only valid for systems without time delay. For systems with time delay, the corresponding stability definitions are complicated by the fact that time delay systems have an infinite dimensional state space. Stability definitions for time delay systems can be found in Mufti [15] and Bellman and Cooke [16].

A simple example from Minorsky [14] illustrates the difference between stability i.s.L. and orbital stability. Consider a system with state space representation in terms of x-y co-ordinates (phase plane) given by

$$\dot{x} = -y\sqrt{x^2+y^2} \quad ; \quad \dot{y} = x\sqrt{x^2+y^2} \quad . \tag{2.5}$$

Conversion to polar co-ordinates yields the simplified equations

$$\dot{r} = o \quad ; \quad \dot{\theta} = r \ . \tag{2.6}$$

The solutions of 2.6,

$$r(t) = r_o \ ; \quad \theta(t) = r_o t + \theta_o \ , \tag{2.7}$$

are periodic (the trajectories are concentric circles centred at the origin) with period $2\pi/r_o$ and amplitude r_o. Consider an arbitrary solution and a small perturbation, ϵ , in amplitude. The perturbed solution becomes

$$r_p(t) = r_o + \epsilon \ ; \ \theta_p(t) = (r_o + \epsilon)\ t + \theta_o . \tag{2.8}$$

The trajectories corresponding to solutions 2.7 and 2.8 can be constrained to be arbitrarily close by the choice of ϵ - this is all that is required for orbital stability. However, the two solutions cannot be kept arbitrarily close for each point in time, owing to the difference in their periods. The phase plane portrait of Fig. 2.3 shows how the perturbed solution (for $\epsilon > o$) gets farther and farther ahead of the original

solution as time increases. In fact, the phase difference, $\theta_p(t) - \theta(t)$, is ϵt, and increases without bound as $t \to \infty$. There will be an infinite number of times at which the solutions are 180^o out of phase and, hence, a distance $2r_o + \epsilon$ apart. Clearly, stability i.s.L. does not exist here, although orbital stability does.

2.3 The Variational Equation and Stability of Oscillations

The importance of the variational equation in the study of stability of oscillations stems from the close relationship between the stability of the zero solution of the variational equation and the stability of the oscillation itself.

2.3.1 Floquet Theory

Stability of the zero solution of the variational equation can be determined from its characteristic exponents as developed in Floquet theory which, for linear, n^{th} order, nondelay differential equations with periodic time varying coefficients, is described in Coddington and Levinson [13] and Kaplan [17]. Basically, it involves a characterization of n linearly independent solutions (the characteristic solutions) in the form $p_i(t)e^{\lambda_i t}$, $i = 1,\ldots,n$, where the p_i's are periodic time varying coefficients of period T (i.e., the same period as the time varying coefficients in the variational equation). The characteristic multipliers, $e^{\lambda_i t}$, are unique, and the characteristic exponents, λ_i, are unique modulo $2\pi j/T$ - thus the real parts of the λ_i's are unique.

Floquet theory for linear differential-difference equations with periodic time varying coefficients, as outlined by Stokes [18,19], is more complicated than for nondelay equations, although based on the same ideas. Characteristic solutions in the form $p_i(t)e^{\lambda_i t}$ are defined as before, but now there may be an uncountable infinity of these solutions!

It is shown that if the variational equation has all its characteristic exponents with negative real part then the zero solution of the variational equation is asymptotically stable i.s.L. Also, if at least one characteristic exponent has a positive real part then the zero solution is unstable i.s.L. In either of these two situations the variational equation is said to have significant stability behaviour. However, if it has one or more characteristic exponents with zero real part, and the rest with negative real parts, it is said to have critical stability behaviour.

2.3.2 Lyapunov's First Approximation Theorem [14,15]

This theorem, applicable to both delay and nondelay systems, states that if the variational equation has significant stability behaviour then the stability i.s.L. of the periodic motion is the same as the stability i.s.L. of the zero solution of the variational equation. If the variational equation exhibits critical stability behaviour then stability i.s.L. of the periodic motion is determined by higher order terms.

2.3.3 Orbital Stability Theorems

It has already been demonstrated that, for autonomous nonlinear systems with a periodic solution $x^*(t)$, the periodic function $\dot{x}^*(t)$ is a solution of the corresponding variational equation. This implies that at least one characteristic exponent of the variational equation has a zero real part, so that asymptotic stability i.s.L. of periodic solutions to autonomous nonlinear systems never occurs. However, Coddington and Levinson prove that if only one characteristic exponent has a zero real part, and the rest have negative real parts, then the corresponding periodic motion is asymptotically orbitally stable. Stokes [18] proves

the same result for systems with delay. These theorems then yield stability information in what would be critical stability situations according to Lyapunov.

2.4 Oscillations in Linear and Nonlinear Systems

Linear and nonlinear systems differ fundamentally in terms of the nature of stability of oscillations in each of them. It is very simple to show that autonomous linear systems have variational equations identical to their system equations. Now the condition for oscillation in an autonomous linear system is a complex conjugate pair of characteristic exponents of the system equation on the imaginary axis. This implies that the corresponding variational equation also exhibits a pair of characteristic exponents on the imaginary axis. If the other characteristic exponents have negative real parts, the zero solution of the variational equation is weakly stable i.s.L. and, hence, so is the oscillation itself. If at least one other characteristic exponent has a positive real part then the oscillation is unstable i.s.L. Stable oscillations in linear systems are always conservative oscillations in which a perturbation in the energy of the oscillation results in an oscillation at a new amplitude.

In autonomous nonlinear systems there are essentially two types of oscillations that can occur. One type is a conservative oscillation which is unstable i.s.L. but orbitally stable - see, for example, the system of equation 2.5. The corresponding variational equation exhibits critical stability with a conjugate pair of characteristic exponents on the imaginary axis. The other type of oscillation in autonomous nonlinear systems is the limit cycle, which is exclusive to nonlinear systems.

By definition a stable limit cycle is an asymptotically orbitally

stable oscillation which may be stable or unstable i.s.L. The corresponding variational equation has critical stability behaviour with one characteristic exponent having a zero real part. An unstable limit cycle is an orbitally unstable oscillation which is automatically unstable i.s.L. The corresponding variational equation has significant stability behaviour with one or more characteristic exponents having a positive real part.

2.5 Difficulties Involved in the Variational Approach

The use of the variational equation in determining the stability of an oscillation in an autonomous nonlinear system poses certain practical problems. For one thing, use of the variational equation implies knowledge of the exact expression for the periodic solution in the system. However, this exact expression is seldom known and some form of approximation must be used. Furthermore, the variational equation is always time varying, and the application of stability theory for time varying linear systems is not complete - especially for systems involving time delay.

In a practical sense, then, the variational equation approach is almost impossible to use. However, it is useful to compare any approximate stability techniques to the exact variational equation approach. Only in this way can the approximations involved in the use of these techniques be determined.

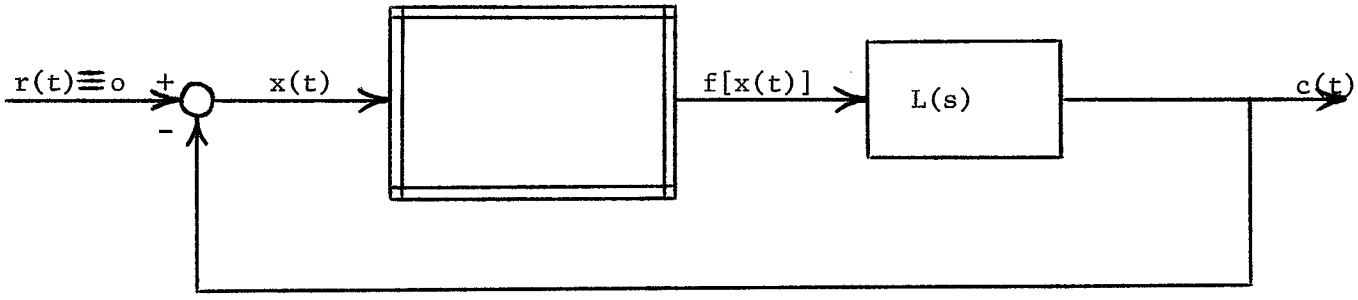

Fig. 2.1 GENERAL AUTONOMOUS NONLINEAR SYSTEM

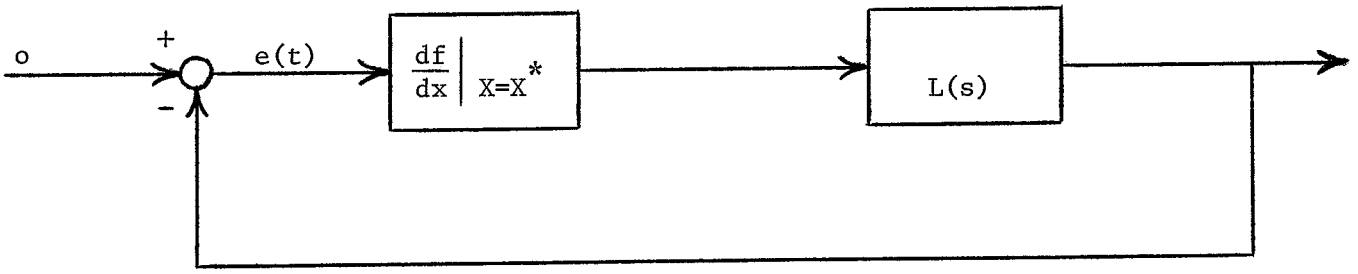

Fig. 2.2 VARIATIONAL SYSTEM

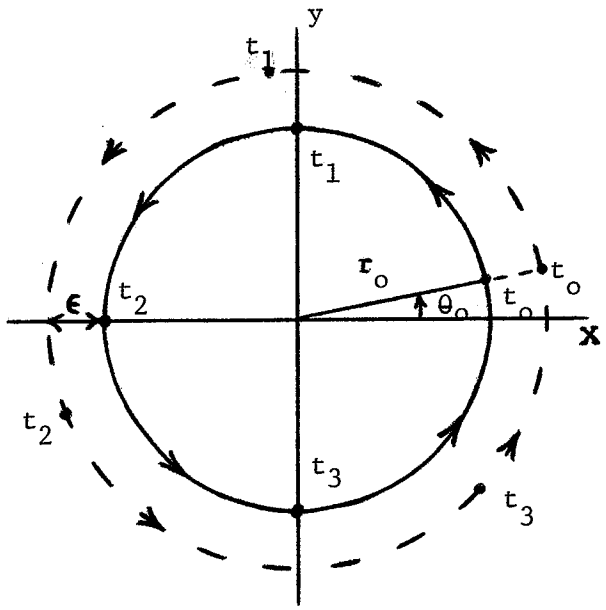

Fig. 2.3 PHASE PLANE PORTRAIT

CHAPTER 3

APPROXIMATE TECHNIQUES IN THE ANALYSIS OF OSCILLATIONS

The existence, form, and stability of oscillations in autonomous nonlinear systems are of prime importance here. The techniques to be described are approximate techniques used to study these aspects of nonlinear analysis.

3.1 Approximate Predictions of Oscillations

Inherent in most approximate methods for the prediction of oscillations is an approximation of the shape of the oscillation waveform. In fact, these methods normally assume a form for the oscillation, and then find conditions under which this form of oscillation will exist, approximately, in the system.

3.1.1. The Describing Function Method

The describing function (DF) method developed with the harmonic linearization method of Krylov and Bogoliubov [20], and can be attributed to a number of authors [21,22,23,24,25]. It has many uses in nonlinear systems analysis, but one of its most important uses is in the prediction of oscillations in autonomous nonlinear systems.

Consider the single-nonlinearity, closed-loop system of Fig.3.1. In general the nonlinear element may be i) static, single-valued; ii) multivalued; or iii) dynamic (static, single-valued nonlinearities will be studied almost exclusively in this thesis). The linear element L(s) may be rational or include a factor $e^{-\tau s}$ for the time delay. The basic assumption of the DF method, as applied to any oscillation in the system of Fig. 3.1, is that the input, x(t), to the nonlinearity may be approximated by a sinusoid, $x_{app}(t) = A \sin wt$. Conditions are then

found under which the system will support, approximately, a sinusoidal oscillation, and the values of A and w are determined. Two conditions are generally considered to be necessary in order that the DF method have meaning when applied here:

1. The nonlinear element is time-invariant.
2. The linear element acts as a low pass filter such that the higher harmonics of y(t) are sufficiently attenuated.

Condition 2 is known as the filter hypothesis.

The DF method involves finding the describing function (DF) for the nonlinear element. The ordinary DF for a general dynamic nonlinearity, $y = f(x,\dot{x})$, is the complex quantity,

$$Keq(A,w) = g\ (A,w) + j\ b\ (A,w), \tag{3.1}$$

where

$$g(A,w) \equiv \frac{1}{\pi A} \int_0^{2\pi} f[A \sin\theta\ ,\ Aw \cos\theta\ ] \sin\theta\, d\theta \tag{3.2}$$

and

$$b(A,w) \equiv \frac{1}{\pi A} \int_0^{2\pi} f[A \sin\theta\ ,\ Aw \cos\theta\ ] \cos\theta\, d\theta. \tag{3.3}$$

In general, then, the DF is both amplitude (A) and frequency (w) dependent, and has real and imaginary parts. However, if the nonlinearity is a static, single-valued nonlinearity, $y = f(x)$, then the DF is frequency independent and real:

$$Keq(A,w) = Keq(A) = g(A) = \frac{1}{\pi A} \int_0^{2\pi} f[A \sin\theta\ ] \sin\theta d\theta \tag{3.4}$$

with

$$b(A) = \frac{1}{\pi A} \int_0^{2\pi} f[A \sin\theta\ ] \cos\theta d\theta \equiv o. \tag{3.5}$$

If the nonlinearity is multivalued (hysteretic) then it cannot be expressed as a single-valued f(x), but the DF for it can still be computed. In this case $Keq(A) = g(A) + j\ b\ (A)$ is, in general, complex but frequency independent with

$$g(A) = \frac{1}{\pi A} \int_0^{2\pi} f[A \sin\theta] \sin\theta d\theta \tag{3.6}$$

and

$$b(A) = \frac{1}{\pi A} \int_0^{2\pi} f[A \sin\theta] \cos\theta d\theta . \tag{3.7}$$

Note that f[A sinθ] is not single-valued, so that, in the calculation of the integrals, the value of f[A sinθ] is determined from the past history of the function A sinθ .

DF predicted oscillations can be found by considering the DF linearized system of Fig. 3.2. This DF system is much simpler to work with since it is a constant coefficient linear system for each A and w. From linear system theory, a pair of conjugate characteristic exponents on the imaginary axis with the rest in the LHP (i.e. neutral stability) corresponds to existence of an oscillation in the DF system. However, most textbooks express the oscillation condition for this system as

$$K_{eq}(A,w)\, L(jw) = -1, \tag{3.8}$$

which simply constrains the loop gain to a sinusoidal signal to be 1 - the condition for sustaining a sinusoidal signal around the loop. Neutral stability and 3.8 are not synonomous in general, as will be seen in some of the systems discussed later in this thesis. Condition 3.8 is required if a pair of characteristic exponents are to be on the imaginary axis. It ignores completely the location of any other characteristic exponents of the DF system. If L(s) is higher than second order, or involves time delay, then other characteristic exponents exist. One or more of these could have a positive real part which would indicate an unstable DF system. If this is the situation then, clearly, neutral stability does not obtain. In terms of mode theory, this situation is one of having an oscillatory mode existing, due to the pair of imaginary characteristic exponents, but also unstable modes due to characteristic

exponents with positive real parts.

Gelb and Vander Velde suggest that the DF method should be applied only to the case of neutral stability of the DF system, and so seem to imply that an unstable DF system with 3.8 holding will never correspond to a possible oscillation in the original nonlinear system. Other authors [1,8,26] are vague, and use oscillation condition 3.8 but avoid any situations in which the DF system has additional unstable modes. Graham and McRuer [3, p.194] even assume that 3.8 and neutral stability are synonomous. It is the contention in this thesis that oscillation conditions with additional unstable modes should still be considered when the DF method is used. This contention is supported by experimental evidence in Chapter 6 in which a DF system with both an unstable and oscillatory mode corresponds to existence of a stable limit cycle of, approximately, the DF predicted amplitude and frequency.

The oscillation condition of 3.8 is often written in the form

$$L(jw) = -1/Keq(A,w), \tag{3.9}$$

and a graphical method (the "DF method") is employed to solve 3.9. L(jw) is plotted in polar form and calibrated in w, as in the standard Nyquist diagram; critical loci, -1/Keq(A,w), for fixed w values and variable A, are plotted on the same graph and calibrated in A. An intersection of L(jw) and -1/Keq(A,w) for which the w values match then yields an oscillation condition. If Keq is frequency independent then the critical locus plot, -1/Keq(A), intersecting with L(jw) yields an oscillation condition.

If the nonlinearity is static and single-valued,so that the DF is real and frequency independent, then Keq(A) can be considered as simply a real gain K in the DF system. For low order, nondelay systems the

analytic Routh-Hurwitz stability criterion for linear systems can be used to find conditions for oscillation. The root locus method may also be used to find the location of all roots of the DF system at the oscillation condition.

Approximate oscillations, $x_{app}(t) = A_o \sin w_o t$, which are symmetric, are assumed to exist in the nonlinear system when the ordinary DF method is used. Nonlinearities are, therefore, constrained to be odd symmetric ($f(x) = -f(-x)$), although this does not guarantee the absence of asymmetric oscillations. Nevertheless, odd symmetric nonlinearities are such that a sinusoidal input results in only odd harmonic components at the output and no dc offset (bias). A tacit assumption in the use of this form of the DF method is then that the actual oscillation in the system is symmetric - only then can the DF approximation, $A_o \sin w_o t$, be expected to be a reasonable approximation. Another form of the DF method may be used to consider offset oscillations.

3.1.2 Dual-Input Describing Function Techniques

Dual-input describing function (DIDF) techniques are used to improve the DF method. They involve an assumption of two terms in the approximation $x_{app}(t)$ rather than the single sinusoid of the DF method.

3.1.2.1 Bias-Plus-Sinusoid DIDF Technique

In this case the approximate input to the nonlinearity is assumed to be

$$x_{app}(t) = B + A \sin wt. \tag{3.10}$$

The equivalent gain of the nonlinearity to the bias input component B in the presence of the sinusoid A sin wt is given by

$$N_B(A,B,w) \equiv \frac{1}{2\pi B} \int_0^{2\pi} f[B+A\sin\theta\ ,\ Aw\cos\theta]\, d\theta \tag{3.11}$$

for general dynamic nonlinearities $f(x,\dot{x})$, and by

$$N_B(A,B) \equiv \frac{1}{2\pi B} \int_0^{2\pi} f[B+A \sin\theta]\, d\theta \tag{3.12}$$

for static nonlinearities. The describing function for the gain to the sinusoidal input component is given by

$$Keq(A,B,w) = g(A,B,w) + j\, b\,(A,B,w), \tag{3.13}$$

where

$$g(A,B,w) \equiv \frac{1}{\pi A} \int_0^{2\pi} f[B+A \sin\theta,\ Aw \cos\theta] \sin\theta d\theta \tag{3.14}$$

and

$$b(A,B,w) \equiv \frac{1}{\pi A} \int_0^{2\pi} f[B+A \sin\theta,\ Aw \cos\theta] \cos\theta d\theta \tag{3.15}$$

for a general dynamic nonlinearity, and for a static nonlinearity

$$Keq(A,B) = g(A,B) + j\, b\,(A,B) \tag{3.16}$$

with

$$g(A,B) \equiv \frac{1}{\pi A} \int_0^{2\pi} f[B+A \sin\theta] \sin\theta d\theta \tag{3.17}$$

and

$$b(A,B) \equiv \frac{1}{\pi A} \int_0^{2\pi} f[B+A \sin\theta] \cos\theta d\theta\ . \tag{3.18}$$

If the nonlinearity is single-valued as well as static then $b(A,B) \equiv o$, and $Keq(A,B)$ is real.

A biased oscillation, $B+A \sin wt$, is then predicted in the system of Fig.3.1 through two conditions, one for each input component, viz.,

$$Keq(A,B,w)\ L\ (jw) = -\ 1 \tag{3.19}$$

and

$$N_B(A,B,w)\ L\ (jo) = -\ 1. \tag{3.20}$$

These two conditions can be met for both odd symmetric and asymmetric nonlinearities as long as $|L(jo)|$ is finite. Gelb and Vander Velde are then in error when they state that "in a symmetric nonlinearity system no biases appear" [6, p.340]. Examples of symmetric nonlinearity systems in which biased oscillations occur will be given in Chapter 6.

3.1.2.2 Two-Sinusoid - Input Describing Function (TSIDF)

In the TSIDF technique the approximate input to the nonlinearity is assumed to be

$$x_{app}(t) = A \sin wt + B \sin (\gamma wt + \theta). \tag{3.21}$$

If γ is not rational then θ need not be included. One method of determining the equivalent gains (describing functions) of the nonlinearity to each of the sinusoidal components is to expand the output of the nonlinearity into its various frequency components for the input of 3.21. The describing function for component A sin wt is then defined as

$$K_A(A,B,w,\gamma,\theta) \equiv \frac{\text{phasor representation of output at frequency } w}{\text{phasor representation of input at frequency } w},$$

and for component B sin (γwt +θ) as

$$K_B(A,B,w,\gamma,\theta) \equiv \frac{\text{phasor representation of output at frequency } \gamma w}{\text{phasor representation of input at frequency } \gamma w}.$$

In general, K_A and K_B are complex functions of A,B,w,γ, and θ. However, for static nonlinearities the w dependence disappears. The special case of $\gamma = 3$, for odd symmetric nonlinearities, results in an improvement in the normal DF method through consideration of the third harmonic component as well as the fundamental component of the nonlinearity input. The loop conditions that must be satisfied are now

$$K_A(A,B,3,\theta)\ L\ (jw) = -1 \tag{3.22}$$

and

$$K_B(A,B,3,\theta)\ L\ (j3w) = -1. \tag{3.23}$$

3.2 Approximate Stability Techniques

The stability techniques discussed here usually refer to oscillations predicted by the ordinary DF method, and are thus subject to the DF approximation errors. However, a generalization of the IDF stability concept to an arbitrary oscillation approximation, $x_{app}(t)$, is also

developed.

3.2.1 Loeb's Criterion [2,6]

The analytical version of Loeb's criterion is based on the assumption of a certain specific form of perturbation about the DF predicted oscillation. Let A_o and w_o be the DF predicted amplitude and frequency of an oscillation given by

$$1 + Keq(A_o,w_o)\ L\ (jw_o) = o. \tag{3.24}$$

Define

$$U\ (A_o,w_o) \equiv Re\ \left\{ 1+Keq\ (A_o,w_o)\ L\ (jw_o)\right\} \tag{3.25}$$

and

$$V\ (A_o,w_o) \equiv Im\ \left\{ 1+Keq\ (A_o,w_o)\ L\ (jw_o)\right\}. \tag{3.26}$$

Then 3.24 can be written as

$$U\ (A_o,w_o) + j\ V\ (A_o,w_o) = o. \tag{3.27}$$

If the oscillation is expressed as $A_o e^{jw_o t}$ and is perturbed in amplitude by ΔA and in frequency by $\Delta w + j\Delta\sigma$, where $\Delta\sigma$ represents damping, then $(A_o+\Delta A)e^{j(w_o+\Delta w+j\Delta\sigma)t}$ is assumed to satisfy

$$U(A_o+\Delta A,w_o+\Delta w+ j\Delta\sigma) + jV(A_o+\Delta A,w_o+\Delta w+j\Delta\sigma) = o. \tag{3.28}$$

Expansion of 3.28 in a Taylor series about (A_o,w_o) and retention of only the linear terms produces

$$U(A_o,w_o)+ \frac{\partial U}{\partial w}\ (\Delta w+j\Delta\sigma)+ \frac{\partial U}{\partial A}\ \Delta A + j\left\{V(A_o,w_o)+ \frac{\partial V}{\partial w}\ (\Delta w+j\Delta\sigma)+ \frac{\partial V}{\partial A}\Delta A\right\}= o, \tag{3.29}$$

with all partial derivatives evaluated at (A_o,w_o). This implies that

$$\frac{\partial U}{\partial A}\ \Delta A - \frac{\partial V}{\partial w}\ \Delta\sigma + \frac{\partial U}{\partial w}\ \Delta w\ = o \tag{3.30}$$

and

$$\frac{\partial V}{\partial A}\ \Delta A + \frac{\partial U}{\partial w}\Delta\sigma + \frac{\partial V}{\partial w}\ \Delta w\ = o. \tag{3.31}$$

Elimination of Δw from 3.30 and 3.31 yields

$$\left[\frac{\partial U}{\partial A}\ .\ \frac{\partial V}{\partial w}\ -\ \frac{\partial U}{\partial w}\ .\ \frac{\partial V}{\partial A}\right]\ \Delta A = \left[\left(\frac{\partial U}{\partial w}\right)^2 + \left(\frac{\partial V}{\partial w}\right)^2\right]\Delta\sigma. \tag{3.32}$$

For an oscillation corresponding to a stable limit cycle it is required that ΔA and $\Delta\sigma$ have the same sign. From 3.32 the requirement then becomes

$$\left[\frac{\partial U}{\partial A} \cdot \frac{\partial V}{\partial w} - \frac{\partial U}{\partial w} \cdot \frac{\partial V}{\partial A}\right]_{(A_o,w_o)} > o \qquad (3.33)$$

for a stable limit cycle. Similarly, the requirement for an unstable limit cycle is

$$\left[\frac{\partial U}{\partial A} \cdot \frac{\partial V}{\partial w} - \frac{\partial U}{\partial w} \cdot \frac{\partial V}{\partial A}\right]_{(A_o,w_o)} < o. \qquad (3.34)$$

Also, the condition

$$\left[\frac{\partial U}{\partial A} \cdot \frac{\partial V}{\partial w} - \frac{\partial U}{\partial w} \cdot \frac{\partial V}{\partial A}\right]_{(A_o,w_o)} = o \qquad (3.35)$$

implies critical (neutral) stability and a conservative oscillation.

If the nonlinearity is static, so that Keq is only amplitude dependent, then a geometrical interpretation due to Gille et al.[2] may be used. In this interpretation L(jw) and $-Keq^{-1}(A)$ are written as vectors:

$$\underline{L}\,(jw) = \hat{i}\,X(jw) + \hat{j}\,Y(jw) \qquad (3.36)$$

and

$$-\underline{Keq}^{-1}(A) = \hat{i}\,P(A) + \hat{j}\,Q(A). \qquad (3.37)$$

The polar plot in the Nyquist plane is used, and directions of increasing w and A are indicated on the L(jw) and $-Keq^{-1}(A)$ plots respectively. For a stable limit cycle at (A_o,w_o) the stability condition corresponding to 3.33 is that the vector

$$\frac{dL(jw)}{dw} \times \frac{d}{dA}\left[-\underline{Keq}^{-1}(A)\right]\Bigg|_{(A_o,w_o)} \qquad (3.38)$$

point out of the page. Similarly, for an unstable limit cycle,vector 3.38 must point into the page. Neutral stability and a conservative oscillation situation exists if 3.38 is identically zero (i.e. the curves

are tangent). Fig.3.3 illustrates the hypothetical situation in which the oscillation (A_1,w_1) is a stable limit cycle and (A_2,w_2) is an unstable limit cycle.

It can also be shown that, if $Keq(A)$ is real, the Loeb's criterion condition becomes

$$\frac{d}{dw}\,\mathrm{ImL}(jw)\cdot\frac{d}{dA}\,Keq(A)\,\Big|_{(A_o,w_o)} < o \qquad (3.39)$$

for a stable limit cycle,

$$\frac{d}{dw}\,\mathrm{ImL}(jw)\cdot\frac{d}{dA}\,Keq(A)\,\Big|_{(A_o,w_o)} > o \qquad (3.40)$$

for an unstable limit cycle, and

$$\frac{d}{dw}\,\mathrm{ImL}(jw)\cdot\frac{d}{dA}\,Keq(A)\,\Big|_{(A_o,w_o)} = o \qquad (3.41)$$

for a neutrally stable (conservative) oscillation.

3.2.2 Graphical Stability Techniques

Graphical stability techniques based on the DF method employ the well known linear system stability techniques of the Nyquist criterion and root locus method [26]. In terms of the DF (linearized)system of Fig.3.2 a stable limit cycle is one in which a positive perturbation in amplitude results in a stable system configuration so that the amplitude decays towards its unperturbed value; a negative perturbation in amplitude results in an unstable system configuration in which the amplitude grows to its unperturbed value. An unstable limit cycle is defined by the reversal of these correspondences.

The modified Nyquist criterion and root locus graphical stability techniques are suited for static, single-valued nonlinearities with describing functions that are real and independent of w. In the modified Nyquist criterion,a polar plot of L(jw) and the critical locus

$-K_{eq}^{-1}(A)$ is made. Positive and negative perturbations in A about the oscillation condition are considered, and the corresponding variations in $-K_{eq}^{-1}(A)$ are noted. The point $-K_{eq}^{-1}(A+\Delta A)$ is considered to be the same as the -1 point in the ordinary Nyquist criterion, and stability of the DF system for both positive and negative perturbations in A can be determined using the Nyquist criterion.

The root locus method applied to the DF system involves considering $K_{eq}(A)$ as a variable gain K. Oscillation conditions correspond to intersections of the loci of complex pairs of roots with the jw axis. Positive and negative perturbations in A result in small changes in $K_{eq}(A)$, and movement of the root pairs from their jw axis positions. Figs. 3.4 and 3.5 indicate application of the modified Nyquist criterion and root locus method to a hypothetical system in which $K_{eq}(A)$ decreases with increasing A. Oscillations (A_1,w_1) and (A_3,w_3) are interpreted as stable limit cycles according to this analysis, with (A_2,w_2) unstable.

In most cases these two techniques are simply graphical interpretations of the analytical Loeb's criterion. This is as expected, since the graphical and analytical techniques are based on the same assumption with respect to the form of perturbation allowed. However, there is one situation in which the graphical stability techniques and Loeb's criterion appear to disagree. This is the situation in which the DF system has one or more unstable characteristic exponents (roots) as well as the root pair on the jw axis. The modified Nyquist criterion and root locus method will clearly consider the unstable mode (or modes) and predict an unstable limit cycle. On the other hand, Loeb's criterion could predict a stable limit cycle - depending upon how $-K_{eq}^{-1}(A)$ varies with A for a given L(jw). A graphical Loeb's criterion is then simply using these graphical stability techniques but ignoring any unstable

modes of the DF system. It has been mentioned previously that the literature is rather vague on the use of the DF method in these situations of unstable DF systems. Use of the IDF stability technique, to be described next, appears to clarify this type of situation.

3.2.3. The IDF Stability Technique and Its Extensions

The incremental-input describing function (IDF) stability technique, proposed by West et al.[27] and developed by Gelb and Vander Velde, is based on the calculation of the equivalent gain of the nonlinearity to an infinitesimal signal in the presence of the DF predicted sinusoidal oscillation. Two forms of infinitesimal signal are considered by Gelb and Vander Velde: an asynchronous sinusoid B sin γwt (B$\rightarrow$o, γ irrational) and an infinitesimal bias B(B$\rightarrow$o). If B sinγwt is the assumed infinitesimal signal then the input to the nonlinearity becomes $x_{app}(t)$ = A sin wt + B sinγwt. TSIDF analysis yields the equivalent gain, $K_B(A,B)$, of the nonlinearity to B sinγwt, and the IDF is then defined as

$$N_i(A) \equiv \lim_{B\rightarrow o} K_B(A,B). \tag{3.42}$$

If a bias B is the assumed infinitesimal signal then the input to the nonlinearity is B+A sin wt. From the bias-plus-sinusoid DIDF analysis the equivalent gain of the nonlinearity to B is given by 3.12. The corresponding IDF is then defined as

$$N_B(A,o) \equiv \lim_{B\rightarrow o} N_B(A,B) = \lim_{B\rightarrow o} \left\{ \frac{1}{2\pi B} \int_o^{2\pi} f[B+A\sin\theta]d\theta \right\}. \tag{3.43}$$

Note that the IDF s of 3.42 and 3.43 are shown for static, single-valued, odd symmetric nonlinearities, although they exist for more general nonlinearities. Application of L'Hospital's Rule to 3.43 yields

$$N_B(A,o) = \frac{1}{2\pi} \int_o^{2\pi} f'(A\sin\theta)\, d\theta\,, \tag{3.44}$$

so that $N_B(A,o)$ may be computed directly as long as f(x) is differentiable.

If f(x) is not differentiable then the limiting process of 3.43 must be used. Gelb and Vander Velde prove [6, pp.303-304] that $N_i(A) \equiv N_B(A,o)$ and, more generally, that the effective gain (i.e. the equivalent gain) of any static, single-valued, odd symmetric nonlinearity to an infinitesimal signal in the presence of any other statistically independent input signals is the same in the limit as the infinitesimal signal goes to zero, whether it be a bias, a sinusoid, or a random process [6,pp.34-37].

Once the IDF is calculated, the stability of the IDF equivalent linear system of Fig. 3.6 is considered. This IDF system is a linear, constant coefficient system and any linear system stability technique (Nyquist, Routh-Hurwitz, root locus) may be used. If the IDF system is asymptotically stable i.s.L. then the DF predicted oscillation is interpreted as a stable limit cycle; if the IDF system is unstable i.s.L. then the DF predicted oscillation is an unstable limit cycle; and if the IDF system is neutrally stable then the DF predicted oscillation is conservative.

The IDF stability technique described above is used in conjunction with the ordinary DF method. However, extensions of the IDF concept can [40, 41] be developed by applying it to DIDF techniques or more general approximations. For example, the TSIDF technique, when used to include the third harmonic component of the input to the nonlinearity, is an improvement of the ordinary DF method. In order to determine the stability of the oscillation approximated by $x_{app}(t) = A \sin \omega t + B \sin(3\omega t+\theta)$, consider an infinitesimal bias signal ϵ at the input. The equivalent gain of the nonlinearity to ϵ in the presence of $x_{app}(t)$ is then given by

$$K_\epsilon(A,B,\epsilon) \equiv \frac{1}{2\pi\epsilon} \int_0^{2\pi} f[\epsilon+A \sin\alpha+ B \sin(\alpha+\theta)]\, d\alpha \qquad (3.45)$$

for static, single-valued, odd symmetric nonlinearities. The corresponding IDF becomes

$$K_\epsilon(A,B,o) \equiv \lim_{\epsilon \to o} \left\{ \frac{1}{2\pi\epsilon} \int_o^{2\pi} f[\epsilon + A \sin\alpha + B \sin(\alpha+\theta)]\, d\alpha \right\} \tag{3.46}$$

$$= \frac{1}{2\pi} \int_o^{2\pi} f'[A \sin\alpha + B \sin(\alpha+\theta)]\, d\alpha \tag{3.47}$$

wherein $f(x)$ is assumed differentiable. Extending Gelb and Vander Velde's hypothesis, this IDF might also be calculated by using the perturbation $\epsilon \sin\gamma wt$ (γ irrational) as the infinitesimal signal, finding the equivalent gain of the nonlinearity to this signal, and taking the limit as $\epsilon \to o$.

The most general IDF would consist of calculating the equivalent gain of the nonlinearity to an infinitesimal signal in the presence of a general symmetric waveform, $x_{app}(wt)$, assumed as the oscillatory input to the nonlinearity. The result is

$$K_\epsilon \equiv \lim_{\epsilon \to o} \left\{ \frac{1}{2\pi\epsilon} \int_o^{2\pi} f[\epsilon + x_{app}(\theta)]\, d\theta \right\} \tag{3.48}$$

$$= \frac{1}{2\pi} \int_o^{2\pi} f'[x_{app}(\theta)]\, d\theta \,. \tag{3.49}$$

~~Unfortunately, an IDF cannot be constructed in the case of a bias plus sinusoid, B+A sin wt, because f[B+A sinθ] is not symmetric and the limit diverges.~~

3.2.4. Relationship Between the Variational System and the IDF Stability Technique

The IDF (equivalent linear) system can be related to the variational system of Fig.2.2 for linear variations about the actual oscillation $x^*(t)$. A DF approximate variational system (Fig.3.7), in which $x^*(t)$ is replaced by $x_{app}(t) = A_o \sin w_o t$, could be thought of. For the DF predicted oscillation, a stability study of this variational system would be the most accurate stability technique possible, since accuracy

of the stability prediction would only depend on the accuracy of the DF approximation. A more general approximate variational system [Fig.3.8] in which x*(t) is replaced by a general approximation to the oscillation, $x_{app}(t)$, could also be considered - DF and DIDF oscillation predictions would be particular cases of this. For a given approximation, $x_{app}(t)$, a stability study of the corresponding approximate variational system would be the most accurate stability technique to use. Of course, the fact that the approximate variational system and corresponding variational equation have time varying coefficients makes stability analysis of this system quite difficult, if not impossible, in general.

Consider now the "general" IDF of 3.48 and 3.49. K_ϵ may be written in the following form:

$$K_\epsilon = \lim_{\epsilon \to o} \left\{ \frac{1}{2\pi\epsilon} \int_o^{2\pi} f[\epsilon + x_{app}(\theta)]\, d\theta \right\}$$

$$= \lim_{\epsilon \to o} \left\{ \frac{1}{2\pi\epsilon} \int_o^{wT} f[\epsilon + x_{app}(wt)]\, d(wt) \right\}$$

$$= \lim_{\epsilon \to o} \left\{ \frac{w}{2\pi\epsilon} \int_o^{T} f[\epsilon + x_{app}(t)]\, dt \right\}$$

$$= \lim_{\epsilon \to o} \left\{ \frac{1}{T\epsilon} \int_o^{T} f[\epsilon + x_{app}(t)]\, dt \right\} \qquad (3.50)$$

$$= \frac{1}{T} \int_o^{T} f'[x_{app}(t)]\, dt = \overline{f'[x_{app}(t)]}. \qquad (3.51)$$

The foregoing is not strictly correct mathematically, since $x_{app}(wt)$ and $x_{app}(t)$ should really be two different functions. K_ϵ is now identified as the time-averaged value of the periodic time varying quantity $\left.\frac{df}{dx}\right|_{x=x_{app}(t)}$. The general IDF (equivalent linear) system can be represented as in Fig. 3.9. The relationship between it and the general approximate variational system of Fig. 3.8 is simply that the IDF system is the approximate variational system with the time-varying gain,

$\left.\frac{df}{dx}\right|_{x = x_{app}(t)}$ replaced by its average value, $\overline{f'[x_{app}(t)]}$. [42]

This substitution converts a time-varying linear system into a time invariant linear system for which stability analysis is straightforward.

For example, the particular case of the DF approximation yields

$$N_B(A,o) = \overline{f'[A_o \sin w_o t]}, \tag{3.52}$$

with the IDF system of Fig. 3.6 as the time-averaged approximation to the DF approximate variational system of Fig.3.7.

It should be noted that the time averaging approximation described above for the variational system is not equivalent to time averaging each of the coefficients in the corresponding variational equation. The system of Fig. 3.8 is governed by

$$L(D)\left\{\frac{df}{dx}(x_{app}) \cdot e\right\} + e = o, \tag{3.53}$$

whereas the time-averaged IDF system of Fig.3.9 yields

$$\overline{f'[x_{app}(t)]} \cdot L(D)\{e\} + e = o. \tag{3.54}$$

In general, it can be shown that time averaging the coefficients of the differential equation resulting from 3.53 yields an equation with more terms than the differential equation resulting from 3.54.

3.2.5 Approximations of the Stability Techniques

Some general observations can be made about the approximations involved in the use of Loeb's criterion and the IDF stability technique in conjunction with the DF method. One approximation common to both is the DF approximation - only when the DF method gives a reasonably good approximation to the actual oscillation can these stability techniques be expected to work properly. DIDF techniques improve the basic DF approximation, but only the IDF stability technique can be used with the

improved approximation.

However, both stability techniques involve approximations in addition to the DF approximation. In the case of Loeb's criterion, the assumption of a certain form of perturbation is considered to be an approximation. Recall that perturbations are assumed to be at the frequency of the predicted oscillation with only small perturbations in that frequency allowed. However, actual perturbations about an oscillation are governed (for infinitesimally small perturbations) by the characteristic exponents (modes) of the corresponding variational equation. There is always one mode related directly to the frequency of the oscillation, but other complex modes can exist - these other modes are ignored when using Loeb's criterion.

The IDF stability technique allows an arbitrary perturbation and involves the equivalent gain of the nonlinearity to the perturbation. This results in a time-averaged variational system governing stability of the oscillation. The IDF stability technique concludes with a study of the stability of this IDF system instead of the approximate variational system. The basic approximation here can be isolated by assuming that the exact oscillatory solution, $x^*(t)$, of the original nonlinear system is known. Stability of the variational system of Fig. 2.2 then gives the exact stability of the oscillation. However, application of the IDF stability technique involves defining the IDF or equivalent gain of the nonlinearity to arbitrary perturbations in the present of $x^*(t)$:

$$K_\epsilon(x^*) \equiv \lim_{\epsilon \to 0} \left\{ \frac{1}{T\epsilon} \int_0^T f[\epsilon + x^*(t)]dt \right\} \tag{3.55}$$

$$= \frac{1}{T} \int_0^T f'[x^*(t)]dt = \overline{f'[x^*(t)]}. \tag{3.56}$$

The corresponding IDF system (Fig. 3.10) is then the variational system with $\left.\frac{df}{dx}\right|_{x=x^*(t)}$ replaced by its time-averaged value, $\overline{f'[x^*(t)]}$.

In general, the stability properties of the variational system are not the same as those of the system of Fig. 3.10. This is exemplified by the second order Mathieu equation,

$$\ddot{e} + (a \pm 2q \cos 2t)\, e = o, \tag{3.57}$$

which is shown in system form in Fig. 3.11. The stability properties of 3.57, as outlined in McLachlan [28], differ significantly from those of the time-averaged equation,

$$\ddot{e} + a\, e = o, \tag{3.58}$$

corresponding to the system of Fig. 3.12. A general investigation of the differences in stability properties between a periodic time varying linear system and its time-averaged counterpart lies outside the scope of this thesis. Particular types of systems could, perhaps, yield some useful information.

For example, it is easy to show that a first order periodic time varying linear system has the same stability properties as its time-averaged counterpart. However, first order nonlinear systems do not exhibit autonomous oscillations, so a first order variational system will never exist in this context. In second and third order systems, some relationships can be found between stability of the variational system and stability of its time-averaged counterpart. These relationships will be demonstrated in later chapters.

3.2.6. Comparison of Loeb's Criterion and the IDF Stability Technique

Loeb's criterion and the IDF stability technique may be conveniently compared through the use of the root locus method. A typical root locus

for the system of Fig. 3.13 is shown in Fig. 3.14. The value of K for characteristic roots on the jw axis corresponds to the value of the DF for the nonlinearity, $Keq(A_o)$, necessary for an oscillation condition. From this the amplitude of the oscillation, A_o, may be determined. The value $w=w_o$ at the jw axis crossing is, of course, the predicted frequency of the oscillation. Now application of the IDF stability technique involves locating the roots of the system of Fig. 3.13 for $K = N_B(A_o,o)$. Fig. 3.14 indicates that all roots of the IDF system have negative real parts and, therefore, a stable limit cycle in the original nonlinear system is predicted. Loeb's criterion can be applied graphically, using the same root locus plot, by considering the motion of the imaginary root pair for small changes in $K = Keq(A)$, corresponding to small changes in A about A_o.

Once relationships between the shape of the nonlinearity, Keq(A), and $N_B(A,o)$ have been established, a detailed comparison of Loeb's criterion and the IDF stability technique may be made. These relationships and a general comparison are the subject of the next chapter.

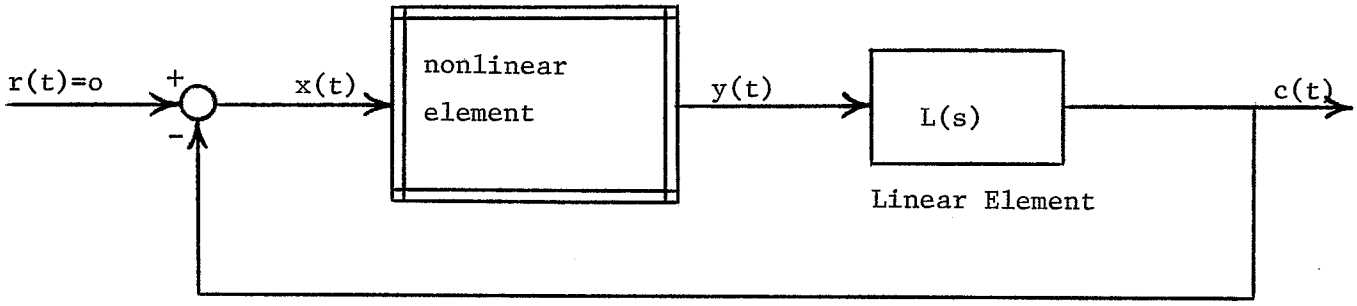

Fig. 3.1 SINGLE-NONLINEARITY CLOSED-LOOP SYSTEM

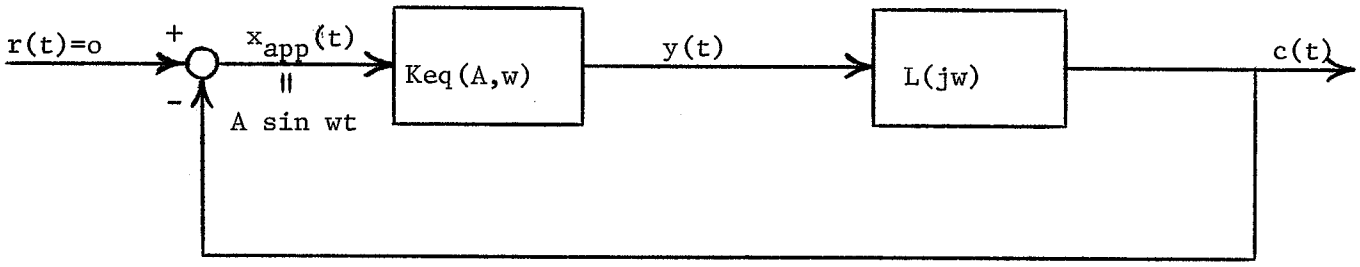

Fig. 3.2 DF LINEARIZED SYSTEM

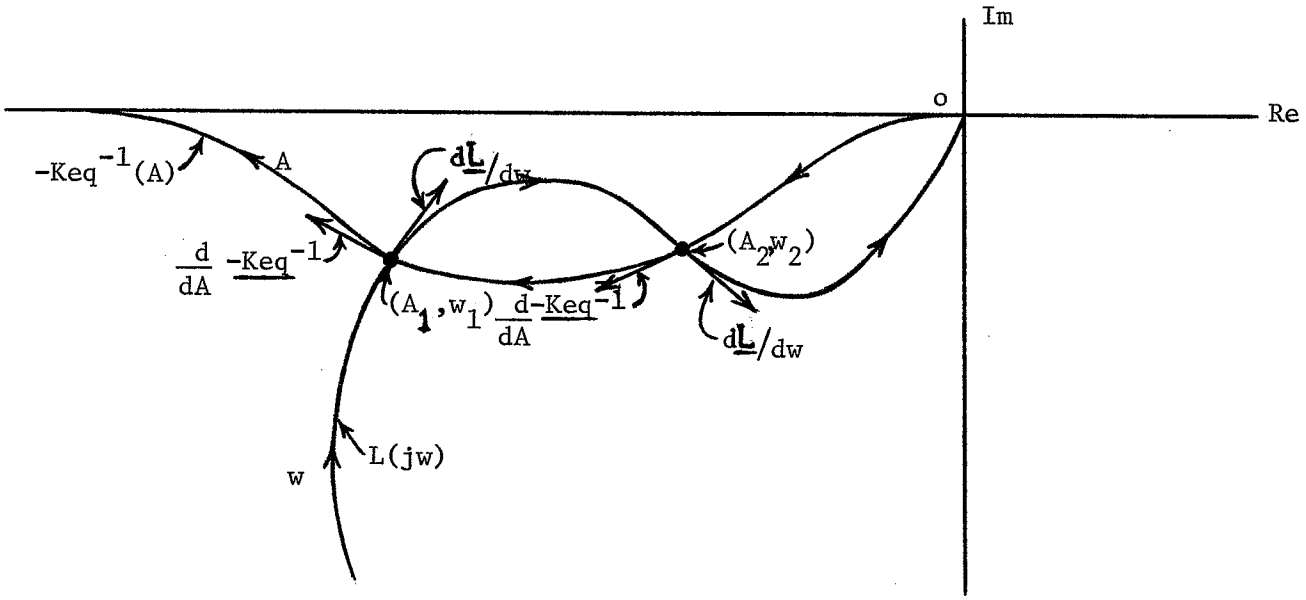

Fig. 3.3 GEOMETRICAL INTERPRETATION OF LOEB'S CRITERION

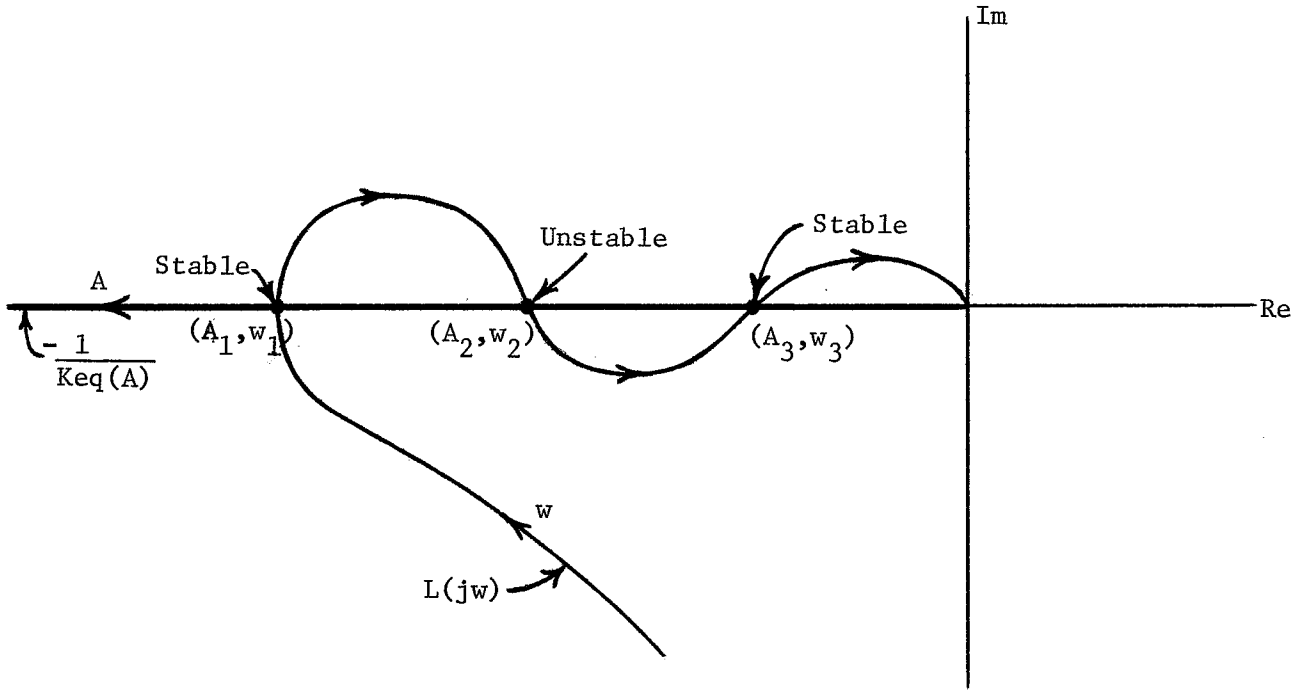

Fig. 3.4 MODIFIED NYQUIST CRITERION

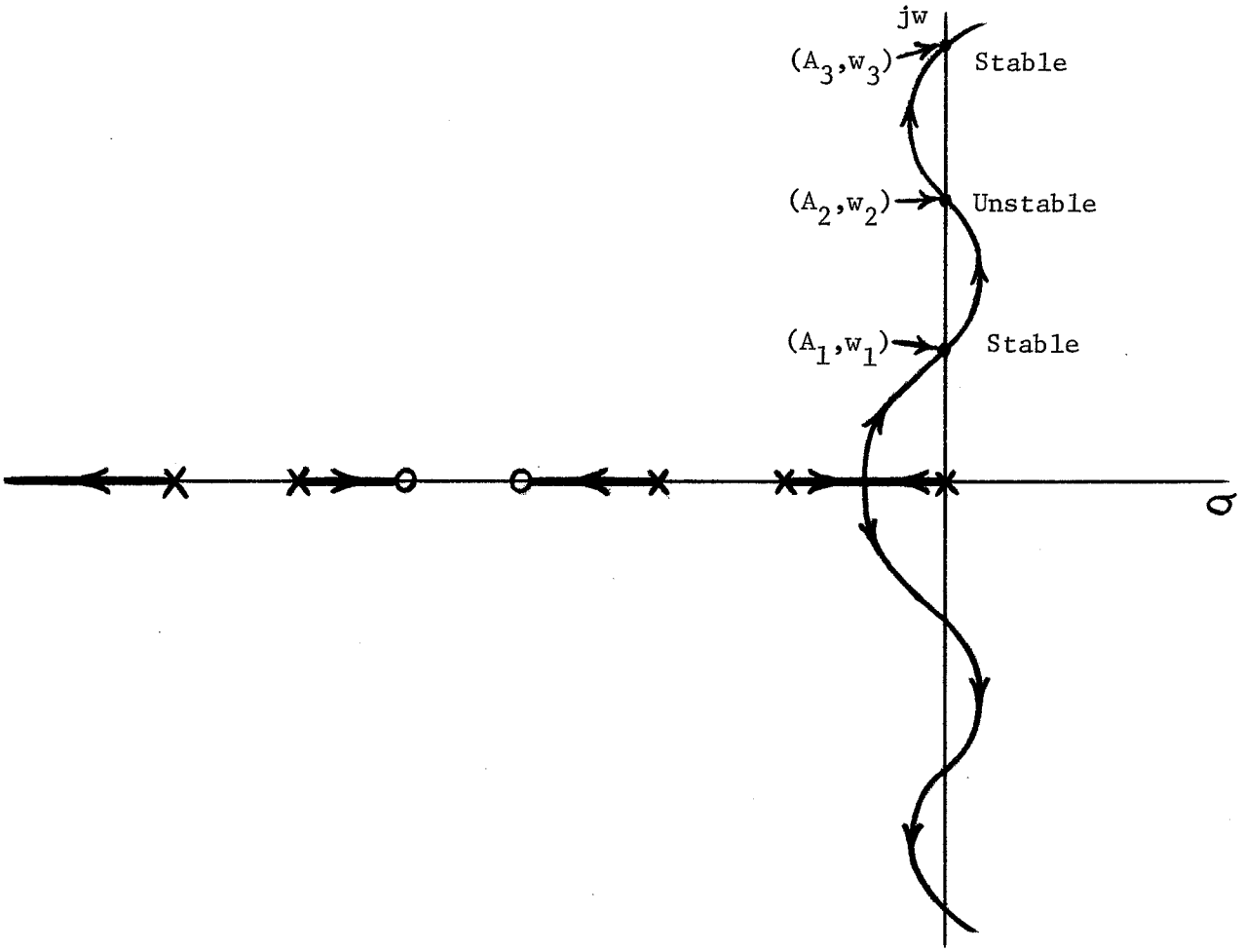

Fig. 3.5 ROOT LOCUS METHOD

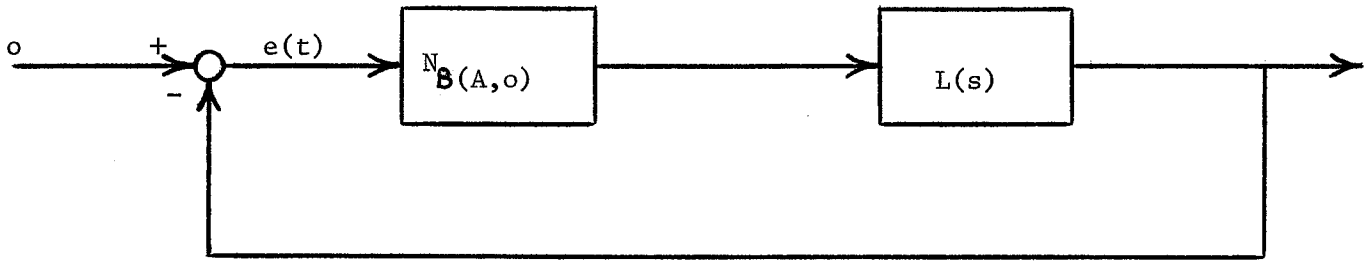

Fig. 3.6 IDF EQUIVALENT LINEAR SYSTEM

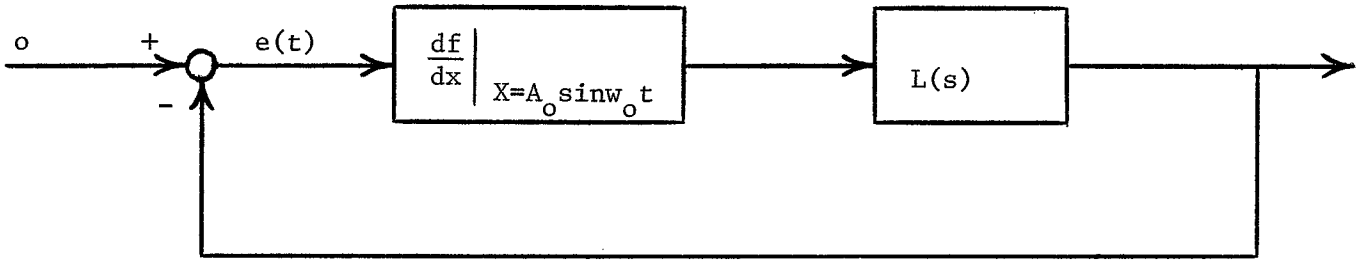

Fig. 3.7 DF APPROXIMATE VARIATIONAL SYSTEM

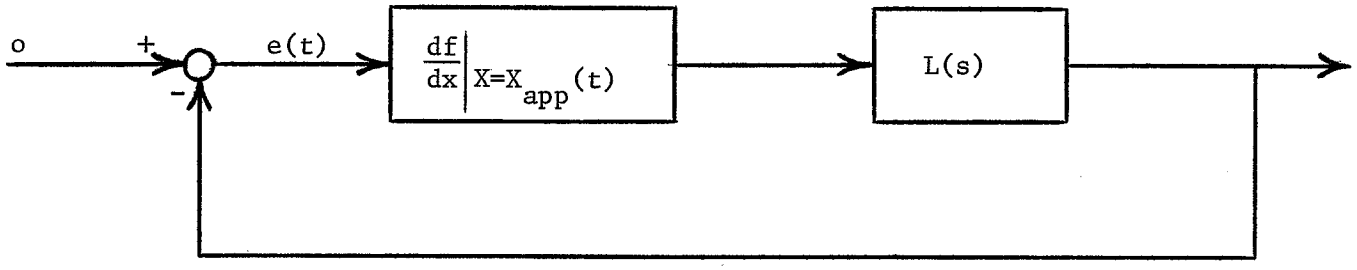

Fig. 3.8 GENERAL APPROXIMATE VARIATIONAL SYSTEM

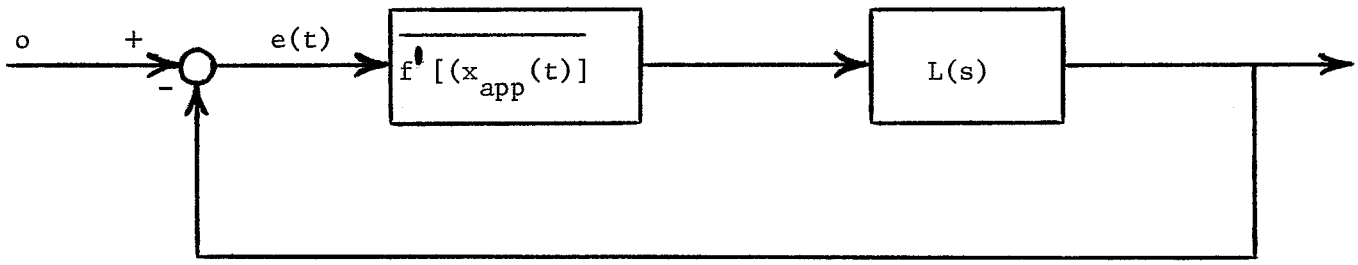

Fig. 3.9 GENERAL IDF EQUIVALENT LINEAR SYSTEM

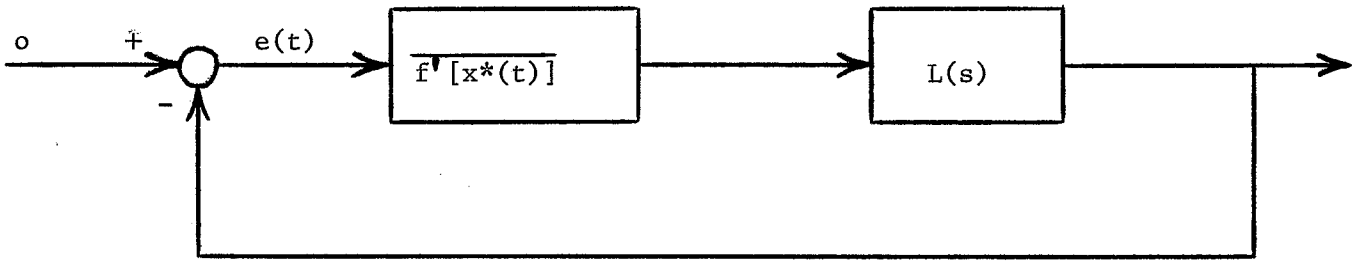

Fig. 3.10 IDF EQUIVALENT LINEAR SYSTEM FOR EXACT OSCILLATION

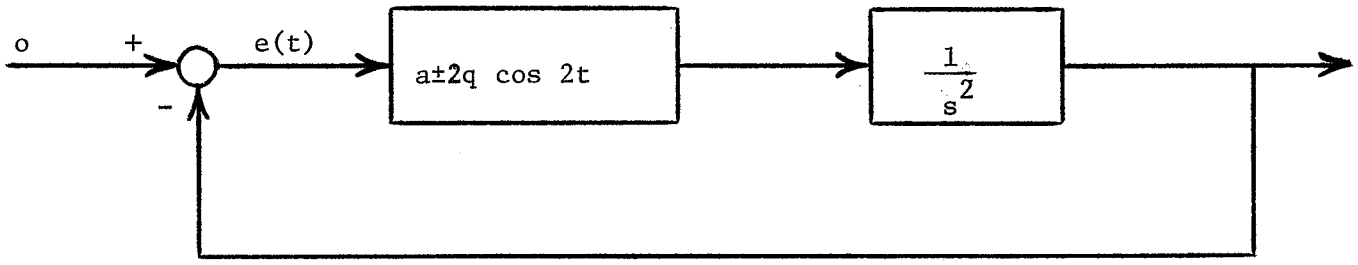

Fig. 3.11 SYSTEM FORM OF THE MATHIEU EQUATION

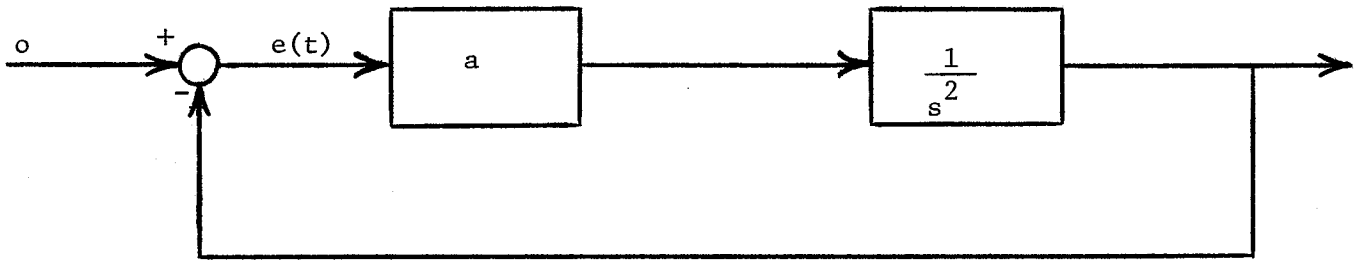

Fig. 3.12 TIME-AVERAGED MATHIEU SYSTEM

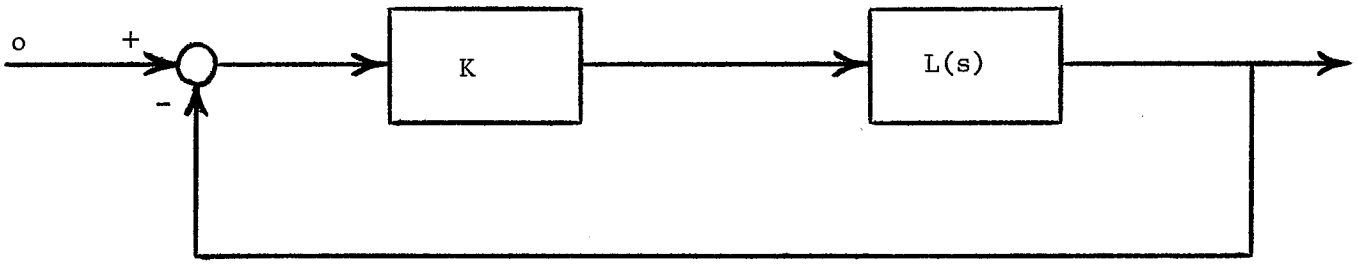

Fig. 3.13 LINEAR SYSTEM FOR ROOT LOCUS PLOT

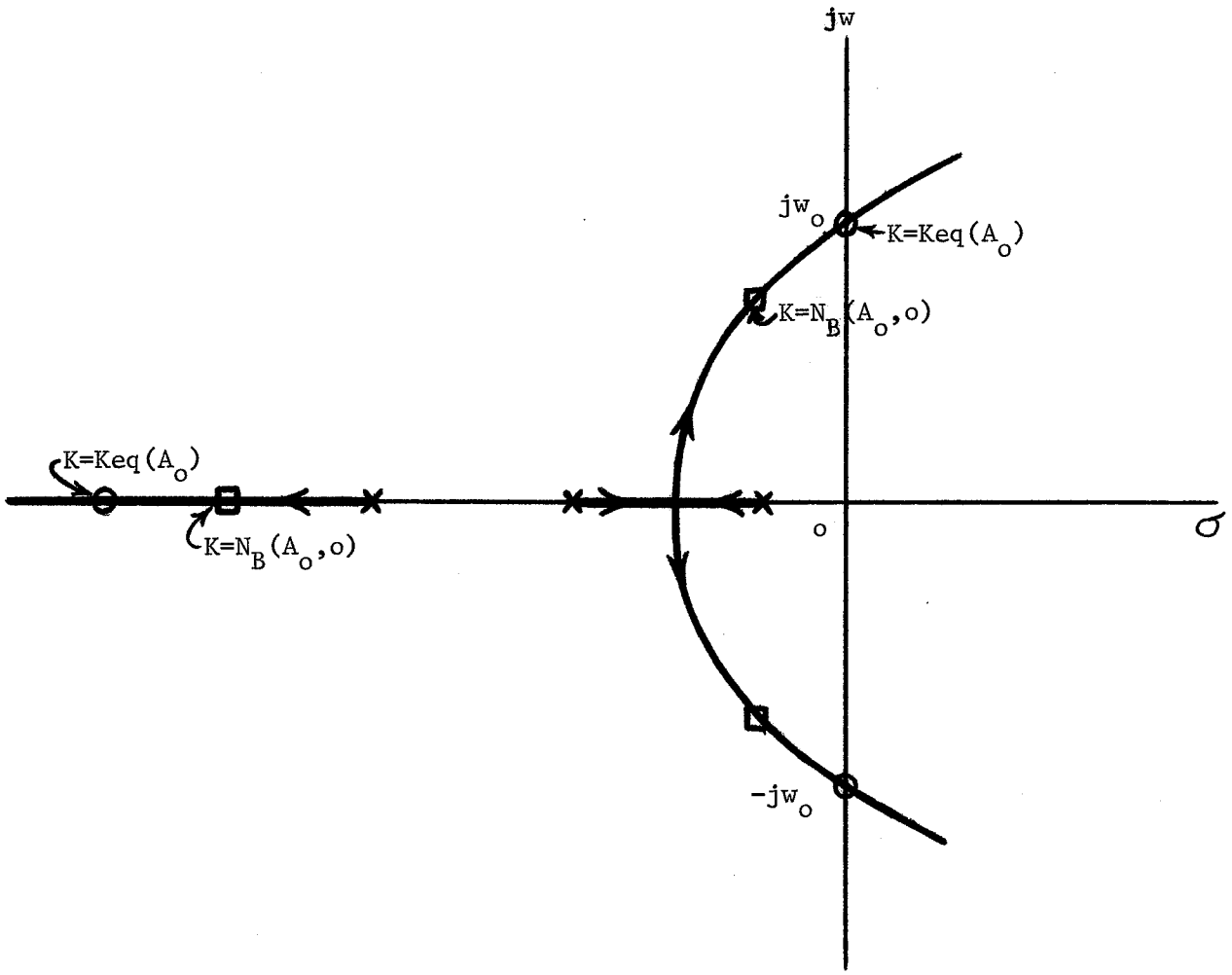

Fig. 3.14 ROOT LOCUS FOR STABILITY CALCULATIONS

CHAPTER 4

STABILITY TECHNIQUES FOR TWO GENERAL TYPES OF NONLINEARITY

Two general types of static, single-valued, odd symmetric nonlinearity are considered with respect to the corresponding forms for Keq(A) and $N_B(A,o)$. Once the forms of Keq(A) and $N_B(A,o)$ are established, Loeb's criterion and the IDF stability technique may be studied using the root locus method. A general comparison between the two stability techniques reveals possible situations in which they will disagree. These discrepancies are explored in detail in subsequent chapters.

4.1 Relationships Involving the Nonlinearity

The two types of static, single-valued, odd symmetric nonlinearity f(x) to be considered are the hard spring and soft spring (saturation) types. A hard spring nonlinearity is defined as one for which $f'(x)$ is non-negative and monotonic non decreasing, while a soft spring nonlinearity has $f'(x)$ non-negative but monotonic non increasing. Fig. 4.1 shows typical hard and soft spring nonlinearities. It should be noted that discontinuous nonlinearities are included as limiting cases, the ideal relay of Fig.4.2(a) being one such "soft spring".

The ordinary DF, Keq(A), for f(x), as defined in Chapter 3,is

$$Keq(A) = \frac{1}{\pi A} \int_0^{2\pi} f(A \sin\theta) \sin\theta \, d\theta \,, \tag{4.1}$$

which, upon integration by parts, yields

$$Keq(A) = \frac{1}{\pi} \int_0^{2\pi} f'(A \sin\theta) \cos^2\theta \, d\theta = \frac{4}{\pi} \int_0^{\pi/2} f'(A\sin\theta) \cos^2\theta \, d\theta. \tag{4.2}$$

Thus $f'(x) \geqslant o$ implies $Keq(A) \geqslant o$. Furthermore, if f(x) is hard spring, $f'(x)$ is monotonic non decreasing and, therefore, by 4.2 Keq(A) is also.

Similarly, if f(x) is soft spring so that $f'(x)$ is monotonic non increasing then Keq(A) is non-negative and monotonic non increasing.

The IDF, $N_B(A,o)$, for such a f(x) has been defined in Chapter 3 as

$$N_B(A,o) = \frac{1}{2\pi}\int_o^{2\pi} f'(A\sin\theta)d\theta = \frac{2}{\pi}\int_o^{\pi/2} f'(A\sin\theta)d\theta. \qquad (4.3)$$

Thus, if f(x) is hard spring then $N_B(A,o) \geqslant o$ and is monotonic non decreasing; if f(x) is soft spring then $N_B(A,o) \geqslant o$ and is monotonic non increasing.

Furthermore, differentiation of 4.1 yields

$$\frac{d}{dA}\{Keq(A)\} = -\frac{1}{\pi A^2}\int_o^{2\pi} f(A\sin\theta)\sin\theta d\theta + \frac{1}{\pi A}\int_o^{2\pi} f'(A\sin\theta)\sin^2\theta d\theta$$

$$= \frac{-Keq(A)}{A} + \frac{2N_B(A,o)}{A} - \frac{1}{\pi A}\int_o^{2\pi} f'(A\sin\theta)\cos^2\theta d\theta. \qquad (4.4)$$

Transformation of the third term by 4.2 then yields

$$\frac{d}{dA}\{Keq(A)\} = \frac{2}{A}\{N_B(A,o) - Keq(A)\}. \qquad (4.5)$$

Equation 4.5 relates Keq(A) to $N_B(A,o)$. In particular, if Keq(A) is monotonic increasing (f(x) hard spring), so that $\frac{d}{dA}\{Keq(A)\} > o$, then 4.5 yields $N_B(A,o) > Keq(A)$. Also, if Keq(A) is monotonic decreasing (f(x) soft spring), so that $\frac{d}{dA}\{Keq(A)\} < o$, then $N_B(A,o) < Keq(A)$. A further relationship between $N_B(A,o)$ and Keq(A) can be found for soft spring nonlinearities. From 4.2 Keq(A) can be expressed as

$$Keq(A) = \frac{1}{\pi}\int_o^{2\pi} f'(A\sin\theta)\cos^2\theta d\theta = \frac{1}{\pi}\int_o^{2\pi} f'(A\sin\theta)(1-\sin^2\theta)d\theta$$

$$= \frac{1}{\pi}\int_o^{2\pi} f'(A\sin\theta)d\theta - \frac{1}{\pi}\int_o^{2\pi} f'(A\sin\theta)\sin^2\theta d\theta$$

$$= 2N_B(A,o) - \frac{1}{\pi}\int_o^{2\pi} f'(A\sin\theta)\sin^2\theta d\theta. \qquad (4.6)$$

Equation 4.6 then yields $Keq(A) \leqslant 2N_B(A,o)$ and the following inequalities for soft spring nonlinearities:

$$\frac{1}{2} Keq(A) \leqslant N_B(A,o) < Keq(A). \tag{4.7}$$

This places a general lower bound on $N_B(A,o)$ relative to $Keq(A)$ for soft spring nonlinearities.

However, there is no general upper bound on $N_B(A,o)$ relative to $Keq(A)$ for hard spring nonlinearities; this can be demonstrated by the following counterexample. Gelb and Vander Velde[6, pp.313-315] develop the expressions $Keq(A)$ and $N_B(A,o)$ for the general power law nonlinearity, $f(x) = x^n$, n odd. These expressions are

$$Keq(A) = 2A^{n-1} \frac{1 \cdot 3 \cdot 5 \text{ ---}(n)}{2 \cdot 4 \cdot 6 \text{ ---}(n+1)} \tag{4.8}$$

and

$$N_B(A,o) = A^{n-1} \frac{1 \cdot 3 \cdot 5 \text{ ---}(n)}{2 \cdot 4 \cdot 6 \text{ ---}(n-1)} \quad , \tag{4.9}$$

with the ratio

$$\frac{N_B(A,o)}{Keq(A)} = \frac{n+1}{2} \tag{4.10}$$

yielding

$$N_B(A,o) = \frac{n+1}{2} \cdot Keq(A). \tag{4.11}$$

There is no general upper bound we can place on $N_B(A,o)$ with respect to $Keq(A)$ because $N_B(A,o)$ can be made arbitrarily large compared to $Keq(A)$ by increasing the value of n appropriately.

4.2 Calculations for Selected Nonlinearities

The calculations of $Keq(A)$ and $N_B(A,o)$ are usually straightforward for most static, single-valued, odd symmetric nonlinearities. In fact, Gelb and Vander Velde tabulate $Keq(A)$ and $N_B(A,o)$ for a number of the

common nonlinearities. The nonlinearities considered here are to be used in systems discussed in subsequent chapters.

i) Ideal Relay ($f(x) = M \operatorname{sgn} x$)

This nonlinearity, shown in Fig. 4.2(a), is a limiting case of a soft spring nonlinearity because of its discontinuity. Calculations [6, pp.306-309] yield

$$Keq(A) = 4M/(\pi A) \tag{4.12}$$

and

$$N_B(A,o) = 2M/(\pi A). \tag{4.13}$$

Both $Keq(A)$ and $N_B(A,o)$ are monotonic decreasing and $N_B(A,o) = \frac{1}{2} Keq(A)$ - the lower bound on $N_B(A,o)$ in 4.7 is attained.

ii) Odd Square Law ($f(x) = x|x|$)

This nonlinearity (Fig. 4.2(b)) is an example of a continuous hard spring nonlinearity. Calculations yield

$$Keq(A) = 8A/(3\pi) \tag{4.14}$$

and

$$N_B(A,o) = 4A/\pi \ , \tag{4.15}$$

with $Keq(A)$ and $N_B(A,o)$ monotonic increasing and $N_B(A,o) = \frac{3}{2} Keq(A)$.

iii) Cubic ($f(x)=x^3$)

This nonlinearity (Fig. 4.2(c)) is a particular case of the general power law nonlinearity already described. Equations 4.8 and 4.9 yield

$$Keq(A) = \frac{3}{4} A^2 \tag{4.16}$$

and

$$N_B(A,o) = \frac{3}{2} A^2 \ , \tag{4.17}$$

with $Keq(A)$ and $N_B(A,o)$ monotonic increasing and $N_B(A,o) = 2\ Keq(A)$.

4.3 Stability Techniques and the Type of Nonlinearity

With the relationships developed in Section 4.1 it is now possible to state something definite about the application of Loeb's criterion and the IDF stability technique to hard and soft spring nonlinearity systems. As mentioned in Chapter 3, the root locus method is a convenient way of applying these two techniques together.

4.3.1 Hard Spring Nonlinearity

If the nonlinear system has a hard spring nonlinearity f(x), then Keq(A) and $N_B(A,o)$ are usually monotonic increasing (rather than simply monotonic non decreasing) and $N_B(A,o) > Keq(A)$. A root locus plot of the linear system of Fig. 3.13 indicates possible oscillation conditions and the direction in which the characteristic roots will move for increasing or decreasing K. Application of the graphical Loeb's criterion involves a consideration of the movement of the imaginary pair of roots (corresponding to the oscillation condition) for small perturbations in A, with K = Keq(A). The direction of movement depends on the shape and calibration of the root locus. For the hard spring nonlinearity, if the root locus crosses the imaginary axis from left to right for increasing K (Fig. 4.3(a)), then the graphical Loeb's criterion predicts an unstable limit cycle. If the root locus crosses from right to left (Fig. 4.3(b)) then the Loeb's criterion prediction is a stable limit cycle.

Application of the IDF stability technique involves the location of the roots for the gain value $K = N_B(A_o,o)$. For hardspring nonlinearities $N_B(A_o,o) > Keq(A_o)$ so that this gain value is larger than that required for the oscillation condition. If the root locus crosses the imaginary axis from left to right (Fig. 4.3(a)) then $K = N_B(A_o,o)$

usually corresponds to the imaginary root pair moving into the RHP and an unstable limit cycle predicted. Similarly, a crossing from right to left (Fig. 4.3(b)) means that $K = N_B(A_o,o)$ usually corresponds to the root pair in the LHP and a stable limit cycle, provided the other roots of the system are in the LHP.

4.3.2 Soft Spring Nonlinearity

If the nonlinear system has a soft spring nonlinearity then Keq(A) and $N_B(A,o)$ are usually monotonic decreasing with $N_B(A,o) < Keq(A)$. When the root locus crosses the imaginary axis from left to right (Fig.4.4(a)) the graphical Loeb's criterion predicts a stable limit cycle. Alternatively, if the root locus crosses from right to left (Fig. 4.4(b)) then Loeb's criterion predicts an unstable limit cycle.

In terms of the IDF stability technique, the root locus crossing from left to right (Fig. 4.4(a)) places the root pair in the LHP at $K = N_B(A_o,o)$, and a stable limit cycle is predicted provided the other roots stay in the LHP. A crossing from right to left (Fig. 4.4(b)) places the root pair in the RHP for $K = N_B(A_o,o)$ and the prediction is an unstable limit cycle.

4.4 General Comparison of the IDF Stability Technique and Loeb's Criterion

The hypothetical DF oscillation situations of Figs. 4.3 and 4.4 show Loeb's criterion and the IDF stability technique in agreement. However, in general these two stability techniques are not always in agreement. Possibilities of discrepancies between them are directly dependent upon the shape of the root locus, and hence are dependent upon the form of the linear plant L(s). Specific forms of L(s) will bring to light particular root loci that yield discrepancy situations. In general, though, the reason for any discrepancy situation may be

demonstrated in the following way. Loeb's criterion is seen to consider only the imaginary root pair at the oscillation condition and how this pair of roots is perturbed for the specific form of perturbation assumed. The IDF stability technique, on the other hand, produces a time-averaged approximate variational equation, and in root locus form indicates the approximate characteristic modes by all the root locations and not just the pair yielding the oscillation condition. Furthermore, a more general form of perturbation is assumed. The movement of roots for K changing from the oscillation condition $K = Keq(A_o)$ to the IDF stability condition $K = N_B(A_o,o)$ can be quite drastic due to the possibly large difference between $Keq(A_o)$ and $N_B(A_o,o)$. Essentially anything could happen to the location of the roots, and the IDF stability would be affected accordingly. This is certainly more complicated than Loeb's criterion, which predicts stability through local perturbations about the imaginary root pair.

Fig. 4.5 illustrates the root locus for a third order L(s). For a soft spring nonlinearity there is a possibility of discrepancy depending upon the gain calibration of the root locus. Loeb's criterion predicts a stable limit cycle, but the IDF stability technique would predict an unstable limit cycle if the situation depicted in Fig. 4.5 occurred. Details of this and other discrepancies in third order systems will be dealt with in Chapter 6.

4.5 The Quasi Linear Region and Linear Systems

The DF approximation is inherent in both Loeb's criterion and the IDF stability technique. As a result, the most meaningful comparison of the two techniques would be one made under the condition that the DF predicted oscillation is a close approximation to the actual oscillation.

Apart from good filtering properties of L(s), a good DF approximation is ensured when the nonlinear system is close to being linear (i.e. quasi linear). Of course, the DF approximate oscillation approaches the actual oscillation in the limit as the nonlinear system approaches a linear one. For continuous hard and soft spring nonlinearities the linear situation is approached as A_o decreases to zero.

Let f(x) be such that the following Maclaurin series exists:

$$f(x) = f(o) + xf'(o) + \frac{x^2}{2!} f''(o) + \text{---} . \tag{4.18}$$

Odd symmetry of f(x) implies that 4.18 becomes

$$f(x) = xf'(o) + \frac{x^3}{3!} f'''(o) + \frac{x^5}{5!} f^{v}(o) + \text{---} . \tag{4.19}$$

Then the DF, Keq(A), can be expressed in series form as

$$Keq(A) = \frac{1}{\pi A} \int_o^{2\pi} \left\{ A \sin\theta f'(o) + \frac{(A \sin\theta)^3}{3!} f'''(o) + \frac{(A\sin\theta)^5}{5!} f^{v}(o) + \text{---} \right\} \sin\theta d\theta = f'(o) + \frac{A^2}{8} f'''(o) + \frac{A^4}{192} f^{v}(o) + \text{---}. \tag{4.20}$$

Expansion of $f'(x)$ in a Maclaurin series yields

$$f'(x) = f'(o) + xf''(o) + \frac{x^2}{2!} f'''(o) + \text{---} , \tag{4.21}$$

or

$$f'(x) = f'(o) + \frac{x^2}{2!} f'''(o) + \frac{x^4}{4!} f^{v}(o) + \text{---} , \tag{4.22}$$

since f(x) is odd symmetric. The IDF, $N_B(A,o)$, can then be similarly expressed as

$$N_B(A,o) = \frac{1}{2\pi} \int_o^{2\pi} \left\{ f'(o) + \frac{(A\sin\theta)^2}{2!} f'''(o) + \frac{(A\sin\theta)^4}{4!} f^{v}(o) + \text{---} \right\} d\theta$$
$$= f'(o) + \frac{A^2}{4} f'''(o) + \frac{A^4}{64} f^{v}(o) + \text{---} . \tag{4.23}$$

The difference then becomes

$$Keq(A) - N_B(A,o) = - \frac{A^2}{8} f'''(o) - \frac{A^4}{96} f^{v}(o) - \text{--} , \tag{4.24}$$

and $\lim_{A \to o} [Keq(A) - N_B(A,o)] = o$, so that $Keq(o) = N_B(o,o)$.

Now $|Keq(A) - N_B(A,o)|$ can be considered as a measure of the degree of nonlinearity of f(x). If and only if f(x) is odd symmetric and quasi linear will the difference be small. From 4.24 it is seen that $|Keq(A) - N_B(A,o)|$ increases with A. This means that, as A increases, the input to the nonlinearity, A sin wt, makes larger excursions into the nonlinear region of f(x). On the other hand, for $A \ll 1$, $|Keq(A) - N_B(A,o)| \sim A^2$, and the difference between Keq(A) and $N_B(A,o)$ is very small. This is the quasi linear region of f(x) in which the DF approximation continuously improves, and Keq(A) approaches $N_B(A,o)$, as A decreases to zero.

A comparison of Loeb's criterion and the IDF stability technique in the quasi linear region of f(x) is quite revealing. The error due to the DF approximation is virtually suppressed, and any differences between the two techniques become more evident. In terms of the root locus, the roots of the linear system of Fig. 3.13 move very little during the gain change from $K = Keq(A_o)$ to $K = N_B(A_o,o)$ since the gains are almost equal. Loeb's criterion and the IDF stability technique are then essentially equivalent in terms of the contribution that the imaginary root pair producing the oscillation condition makes to the stability of the system. However, the situation of an unstable DF system is clearly a case where the two techniques can differ. At the gain value $K = N_B(A_o,o)$ the unstable roots of the DF system will have moved very little and the IDF system will also be unstable. Loeb's criterion ignores these unstable roots entirely and just considers the imaginary root pair and how it moves for small perturbations. Fig. 4.6 illustrates the situation where the DF system is unstable; the IDF stability technique predicts an un-

stable limit cycle, but Loeb's criterion predicts a stable limit cycle for a soft spring nonlinearity. $Keq(A_o)$ and $N_B(A_o,o)$ are shown close together in order to represent the quasi linear situation.

Loeb's criterion becomes suspect in this type of situation because of linear system considerations. If a linear system is considered as a special case of the general nonlinear system then DF analysis applied to it becomes an exact procedure. A linear system implies that $f(x) = cx$ with $Keq = N_B = c$. It would be expected that Loeb's criterion and the IDF stability technique are exact for a linear system since they are based on equivalent linearization of the general nonlinear system. In fact, for a linear system the IDF system is exactly the variational system - a constant coefficient linear system as in Fig. 3.13 with $K = c$. The root locus for $K = c$ then indicates the imaginary root pair corresponding to the linear oscillation. If all other roots are in the LHP then a neutrally stable, conservative oscillation is predicted by the IDF stability technique, while if unstable roots exist, as well, at $K = c$ then an unstable oscillation is predicted - these are equivalent to the variational equation predictions. However, Loeb's criterion predicts a neutrally stable, conservative oscillation no matter where the other roots are located. It is clear, in this situation, that Loeb's criterion is incorrect when unstable modes are present and, since it is incorrect for a linear system when the DF system is unstable, it is doubted whether it should be applied in nonlinear systems under the same condition.

Recall that graphical stability criteria recognize the existence of unstable modes at the oscillation condition. In fact, application of these to a linear system is equivalent to use of the IDF stability technique. However, in nonlinear systems this equivalence no longer holds,

since the DF system uses K = Keq while the IDF system uses K = N_B. In light of the known relationship of the IDF system to the variational system, use of the DF system to determine stability has really no theoretical basis. This situation of an unstable DF system is treated in detail for third order systems in Chapter 6.

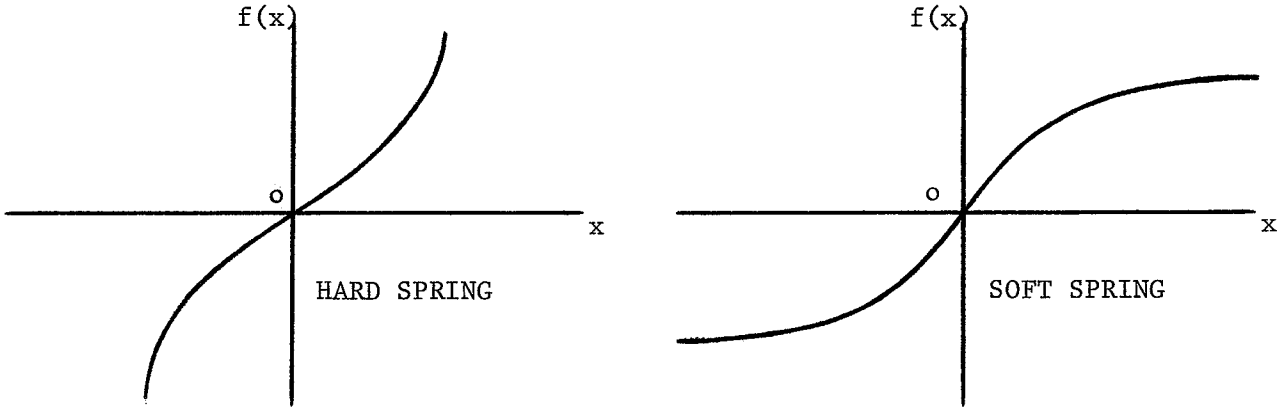

Fig. 4.1 HARD SPRING AND SOFT SPRING NONLINEARITIES

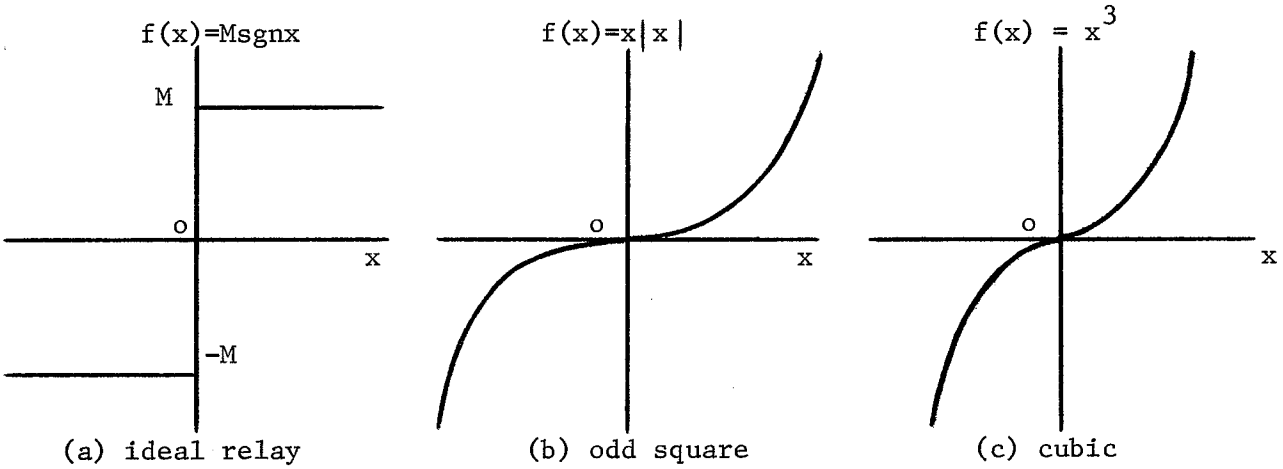

Fig. 4.2 EXAMPLES OF NONLINEARITIES

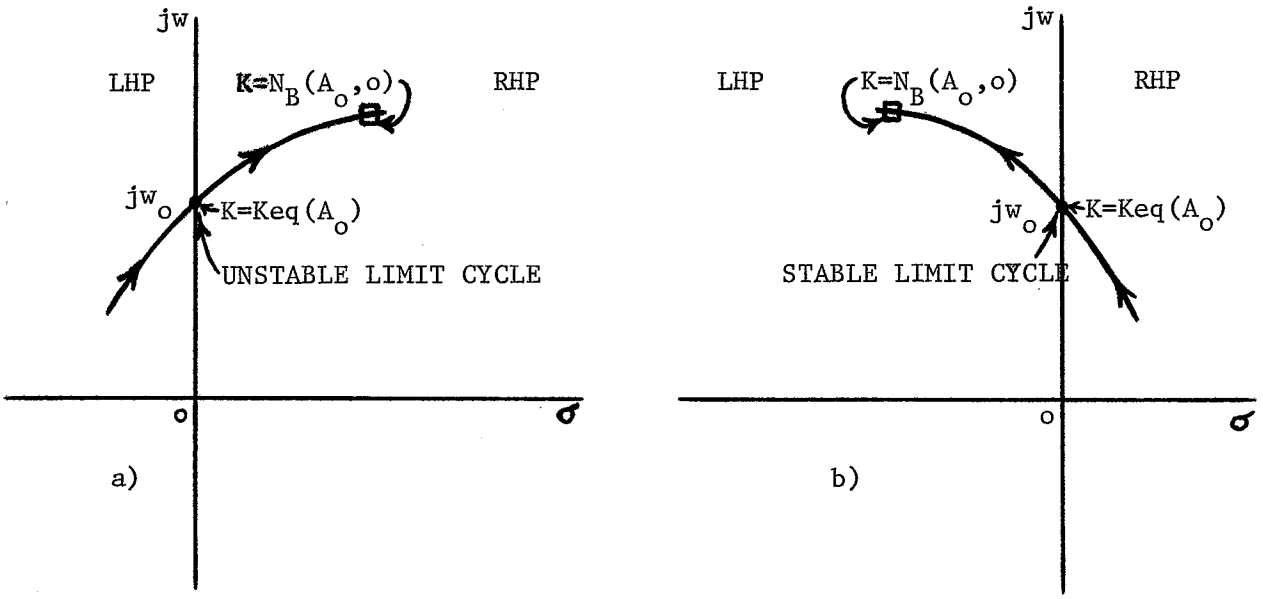

Fig. 4.3 STABILITY TECHNIQUES FOR HARD SPRING NONLINEARITY

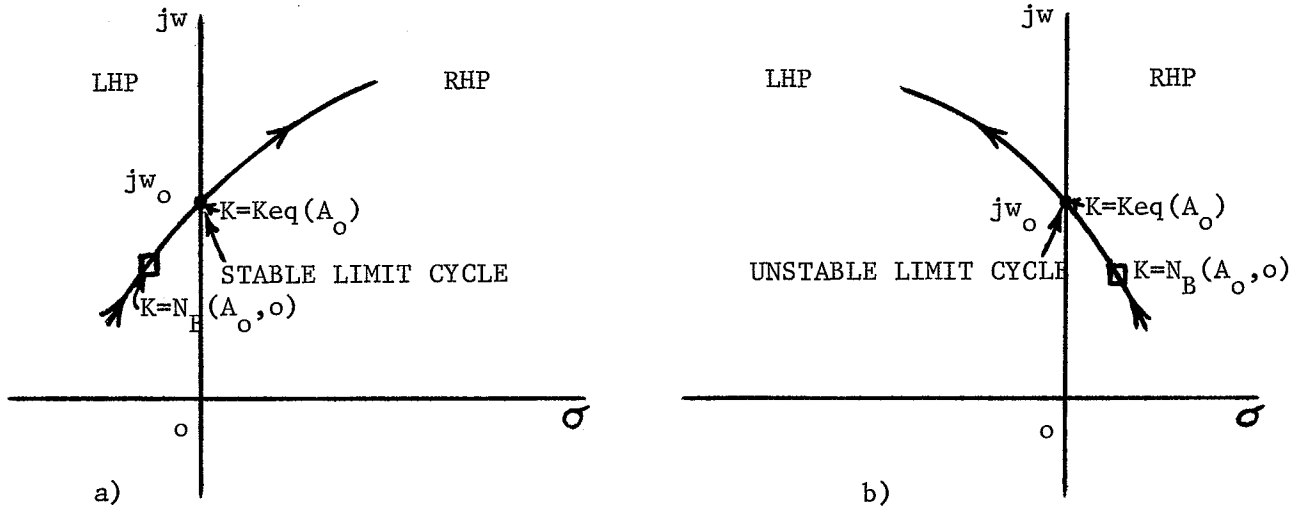

Fig. 4.4 STABILITY TECHNIQUES FOR SOFT SPRING NONLINEARITY

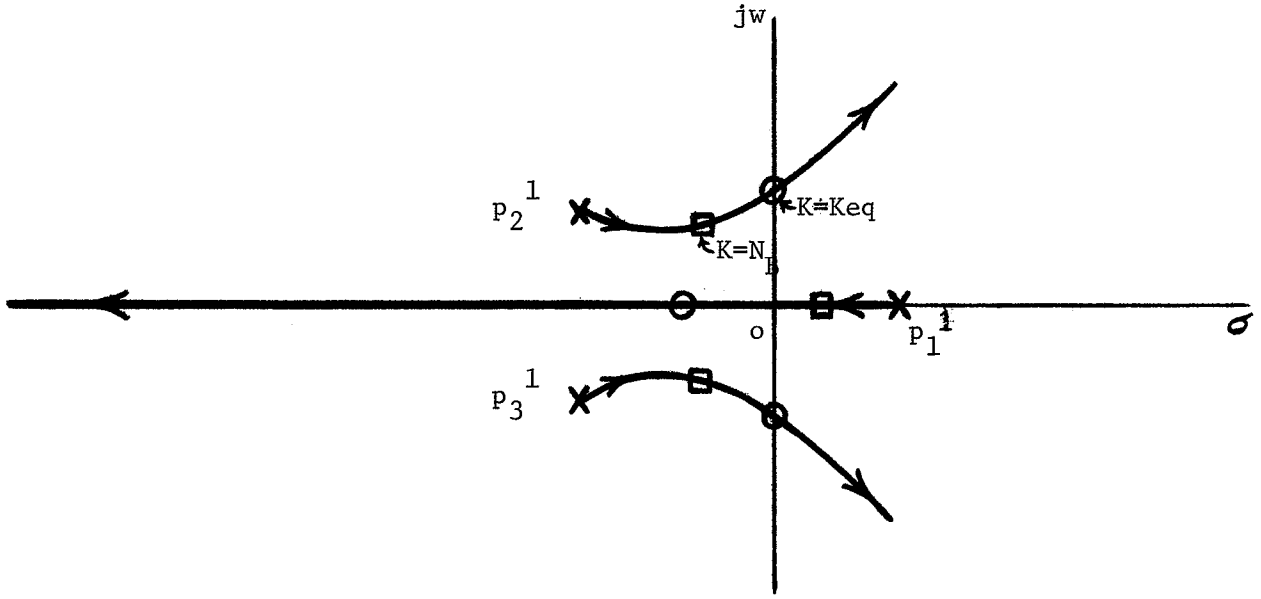

Fig. 4.5 EXAMPLE DISCREPANCY SITUATION

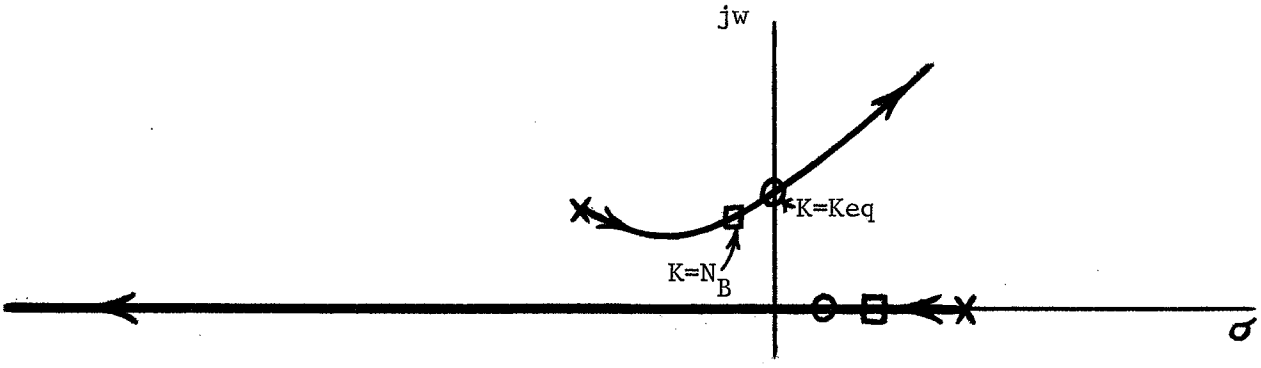

Fig. 4.6 UNSTABLE DF LINEARIZED SYSTEM SITUATION

CHAPTER 5

STABILITY OF OSCILLATIONS IN SECOND ORDER SYSTEMS

Second order nonlinear systems are the lowest order systems for which autonomous oscillations can occur. A number of theoretical results are available for them, and these results can be used to study the accuracy of the DF method and approximate stability techniques. Because of the low order, second order systems are easy to work with in terms of obtaining analytical expressions for the DF method and associated stability techniques. The IDF stability technique and Loeb's criterion may then be compared analytically, and any discrepancies may be studied in detail.

5.1 Floquet Theory and Time Averaging

Consider the general second order nonlinear system of Fig.5.1 with f(x) a static, single-valued, odd symmetric nonlinearity and

$$L(s) = \frac{q_1 s + q_o}{s^2 + p_1 s + p_o} \quad . \tag{5.1}$$

Let $x(t) = x^*(t)$ be a periodic solution of the system with period T; then the variational system for perturbations about $x^*(t)$ is given in Fig. 5.2. The corresponding variational equation becomes

$$\ddot{e}(t) + \left\{p_1 + q_1 g[x^*(t)]\right\} \dot{e}(t) + \left\{p_o + q_o g[x^*(t)] + q_1 \dot{g}[x^*(t)]\right\} e(t) = o, \tag{5.2}$$

where $g[x^*(t)] \equiv \left\{df(x)/dx\right\}\Big|_{x=x^*}$. Floquet theory applied to 5.2 will yield the two characteristic exponents of the variational equation. There exist complex constants λ_1, λ_2 such that 5.2 has the two linearly independent (characteristic) solutions,

$$e_i(t) = P_i(t) e^{\lambda_i t} \quad ; \quad i = 1,2 \tag{5.3}$$

with the P_i periodic of period T. Now $\dot{x}^*(t)$ is a periodic solution of the variational equation so that one solution, say $e_1(t)$, is $\dot{x}^*(t) = P_1(t)e^{\lambda_1 t}$ with $P_1(t) = \dot{x}^*(t)$ and $\lambda_1 = o$. The second solution, $e_2(t)$, may be found through the form $e_2(t) = a(t)e_1(t)$, where a (t) is a time-varying coefficient to be determined. Appendix I shows the detailed calculations that yield

$$\lambda_2 = -\left\{p_1+q_1 \cdot \frac{1}{T} \int_o^T g[x^*(t)]dt\right\} = -\left\{p_1+q_1\overline{g[x^*(t)]}\right\}. \quad (5.4)$$

A stable (unstable) limit cycle then exists if and only if

$$-\lambda_2 = p_1+ q_1\overline{g[x^*(t)]} > 0 \ (< o). \quad (5.5)$$

Also, a conservative oscillation exists if and only if

$$-\lambda_2 = p_1+ q_1\overline{g[x^*(t)]} \equiv o. \quad (5.6)$$

In Chapter 3 it is demonstrated that the IDF stability approach involves a time averaging of the variational system. For second order systems, stability of the variational system and its time-averaged counterpart can be readily compared. The time-averaged variational system is shown in Fig. 5.3 and the corresponding differential equation with constant coefficients becomes

$$\ddot{e}(t)+\left\{p_1+q_1\overline{g[x^*(t)]}\right\}\dot{e}(t)+\left\{p_o+q_o\overline{g[x^*(t)]}\right\}e(t) = o. \quad (5.7)$$

Analysis of the roots of the characteristic equation,

$$s^2 +\left\{p_1+q_1\overline{g[x^*]}\right\}s +\left\{p_o+q_o\overline{g[x^*]}\right\} = o, \quad (5.8)$$

yields the conditions

$$p_o+ q_o\overline{g[x^*]} \geqslant o \quad (5.9)$$

and

$$p_1+ q_1\overline{g[x^*]} > o \quad (5.10)$$

for stability. This situation would correspond to the time-averaged variational system predicting a stable limit cycle. Note that, since time averaging in general eliminates the oscillatory solution $\dot{x}^*(t)$ from 5.7, the condition that one root of 5.8 be zero is not required for a stable limit cycle. Now conditions 5.9 and

$$p_1+q_1 \overline{g[x^*]} = o \tag{5.11}$$

correspond to a conservative oscillation, while

$$p_o+q_o \overline{g[x^*]} < o \tag{5.12}$$

or

$$p_1+q_1 \overline{g[x^*]} < o \tag{5.13}$$

corresponds to an unstable limit cycle.

A comparison of the stability of the variational system and its time-averaged counterpart indicates that the two will disagree under the conditions

$$p_1+q_1 \overline{g[\dot{x}^*]} \gtrless o \; ; \quad p_o+q_o \overline{g[x^*]} < o. \tag{5.14}$$

The actual stability situation (that of the variational equation) is one of a stable limit cycle or conservative oscillation existing, depending upon whether 5.5 or 5.6 is satisfied. However, the time-averaged variational equation predicts an unstable limit cycle due to the extra condition, $p_o+q_o \overline{g[x^*]} < o$. Time averaging of a second order variational equation can, therefore, lead to incorrect stability results.

5.2. Approximate Stability Techniques

Application of the DF method to a general second order system yields the DF conditions

$$p_1 + q_1 \, Keq(A_o) = o \tag{5.15}$$

and

$$w_o^2 = p_o + q_o \, Keq(A_o) = p_o - \frac{q_o p_1}{q_1} > o \qquad (5.16)$$

for the existence of the solution $x_{app}(t) = A_o \sin w_o t$. Loeb's criterion, in the analytical form of 3.39, 3.40, and 3.41, involves calculation of the expression $\frac{d}{dw} ImL(jw) \cdot \frac{d}{dA} Keq(A)\Big|_{(A_o, w_o)}$. A derivation, due to Willems [29], relates this expression to one involving the IDF, $N_B(A,o)$. This derivation is given in Appendix II and shows that Loeb's criterion is equivalent to the condition

$$p_1 + q_1 \, N_B(A_o, o) > o \quad (< o) \qquad (5.17)$$

for a stable (unstable) limit cycle and

$$p_1 + q_1 \, N_B(A_o, o) = o \qquad (5.18)$$

for a conservative oscillation.

If the expression

$$N_B(A_o, o) = \frac{1}{T} \int_o^T f'(A_o \sin w_o t) dt = \overline{g(A_o \sin w_o t)} \qquad (5.19)$$

is used in the above conditions then they become identical to the actual stability conditions of 5.5 and 5.6 with the actual oscillation, $x^*(t)$, replaced by the DF approximation, $x_{app}(t) = A_o \sin w_o t$. A Floquet analysis of the variational equation

$$\ddot{e}(t) + \left\{ p_1 + q_1 g[A_o \sin w_o t] \right\} \dot{e}(t) + \left\{ p_o + q_o g[A_o \sin w_o t] + q_1 \dot{g}[A_o \sin w_o t] \right\} e(t) = o. \qquad (5.20)$$

corresponding to the DF approximate variational system of Fig. 5.4, yields stability conditions 5.17 and 5.18 under the assumption of one periodic solution of 5.20. Loeb's criterion, applied to second order systems, is therefore equivalent to a stability study of the DF approximate variational system, and is thus an exact stability criterion for second order systems, apart from the DF approximation.

Recall that the IDF stability technique has already been related, in general, to the variational equation. IDF stability for second order systems is equivalent to a stability study of the time-averaged DF approximate variational system of Fig. 5.5. It is demonstrated in Section 5.1 that time averaging can be an approximation, in general, with respect to stability of oscillations in second order systems. Thus it is seen that the IDF stability technique involves an approximation in addition to the DF approximation, namely that of time averaging, for second order systems at least. Loeb's criterion, in these systems, involves only the DF approximation and is therefore the better technique to apply in such cases.

Consideration of the characteristic equation,

$$s^2+[p_1+q_1N_B(A_o,o)]s + [p_o+q_oN_B(A_o,o)] = o, \tag{5.21}$$

of the time-averaged (IDF) system of Fig. 5.5 yields

$$p_o+q_oN_B(A_o,o) \geqslant o; \quad p_1+q_1N_B(A_o,o) > o \tag{5.22}$$

for a stable limit cycle,

$$p_o+q_oN_B(A_o,o) \geqslant o; \quad p_1+q_1N_B(A_o,o) = o \tag{5.23}$$

for a conservative oscillation, and

$$p_o+q_oN_B(A_o,o) < o \tag{5.24}$$

or

$$p_1+q_1N_B(A_o,o) < o \tag{5.25}$$

for an unstable limit cycle. Comparison of these stability conditions with those of 5.17 and 5.18 for Loeb's criterion reveals a discrepancy between the two stability techniques under the conditions

$$p_o+q_oN_B(A_o,o) < o ; \quad p_1+q_1N_B(A_o,o) \geqslant o. \tag{5.26}$$

When conditions 5.26 obtain, Loeb's criterion predicts a stable limit

cycle or a conservative oscillation depending upon whether 5.17 or 5.18 holds. The IDF stability technique, on the other hand, predicts an unstable limit cycle. This discrepancy is due to the time averaging approximation of the IDF stability technique; it only remains to identify more closely second order situations in which conditions 5.26 occur. Although Loeb's criterion should be correct in these situations, experimentation will reveal the extent of the DF approximation when a discrepancy exists.

5.3 Detailed Study

Conservative second order systems are considered separately because of the many analytical results available to determine the actual stability situation. For non conservative second order systems, simulation is used to determine actual stability since convenient analytical results are not available.

5.3.1 Conservative Systems

The general second order system of Fig. 5.1 has a differential equation given by

$$\ddot{x}(t)+\left\{p_1+q_1 f'[x(t)]\right\}\dot{x}(t)+\left\{p_o x(t)+q_o f[x(t)]\right\} = o. \qquad (5.27)$$

Second order nonlinear conservative systems have differential equations of the form

$$\ddot{x}(t)+ F[x(t)] = o\ , \qquad (5.28)$$

so that the system of Fig. 5.1 is conservative if $p_1 = q_1 = o$, and then $F(x) \equiv p_o x + q_o f(x)$. Since $f(x)$ is assumed odd symmetric, $F(x)$ will also be odd symmetric. Conditions for existence of conservative oscillations can be found by defining a potential energy, $V(x)$, where

$$V(x) \equiv \int_o^x F(x^1)dx^1 = \int_o^x [p_o x^1 + q_o f(x^1)]\, dx^1$$
$$= \frac{p_o x^2}{2} + q_o \int_o^x f(x^1)dx^1. \qquad (5.29)$$

A graph of V(x) will indicate maxima and minima, and conservative oscillation trajectories can be constructed in the phase plane. This procedure is described in Minorsky [14].

Stability of conservative oscillations here is orbital stability, and stability i.s.L. need not hold. This is reflected in the variational equation through 5.6, which is now $p_1+q_1\overline{g[x^*(t)]} = o$, and implies that the variational equation has both characteristic exponents with real part zero - a doubly critical situation.

The DF condition for the conservative case becomes simply

$$w_o^2 = p_o + q_o\, Keq(A_o) > o, \qquad (5.30)$$

and a continuum of oscillations, $A_o \sin w_o t$, is predicted as long as 5.30 is satisfied. The Loeb's criterion condition is that of 5.18, $p_1+q_1N_B(A_o,o) = o$, indicating a conservative oscillation. Loeb's criterion is then in agreement with the actual situation, assuming the DF method approximates an oscillation that actually exists.

The discrepancy situation, 5.26, requires $p_o+q_oN_B(A_o,o) < o$ in order that the IDF stability technique predict an unstable limit cycle when the actual situation is a conservative oscillation. Conditions are now found so that $p_o+ q_oN_B(A_o,o) < o$ but a conservative oscillation exists and is predicted by the DF method. In such cases Loeb's criterion is correct while the IDF stability technique is incorrect. Various possibilities, in terms of the properties of L(s), are as follows:

i) $p_o \geqslant o$, $q_o > o$

L(s) is a stable, minimum phase transfer function. The linear

system for application of the root locus method when using the stability techniques is shown in Fig. 5.6, and the corresponding root locus is given in Fig. 5.7. The DF condition, $w_o^2 = p_o + q_o Keq(A_o) > o$, is satisfied for $Keq(A_o) > o$, and Loeb's criterion and the IDF stability technique are seen to be equivalent in predicting a conservative oscillation, since $p_o + q_o N_B(A_o,o) > o$. The theory of conservative oscillations in second order systems verifies that such oscillations do exist at all amplitudes.

ii) $p_o < o$, $q_o > o$

L(s) is now an unstable, minimum phase transfer function and the root locus for the corresponding linear system is given in Fig. 5.8. The DF method predicts an oscillation as long as

$$Keq(A_o) > - p_o/q_o. \tag{5.31}$$

Loeb's criterion and the IDF stability technique will then be in disagreement if and only if

$$N_B(A_o,o) < - p_o/q_o < Keq(A_o). \tag{5.32}$$

In order that 5.32 obtains, f(x) must be a soft spring nonlinearity so that $N_B(A_o,o) < Keq(A_o)$.

The DF condition for existence of an oscillation is $p_o+q_oKeq(A_o) > o$, but the exact existence condition can be found by employing conservative system theory. Recall that $F(x) = p_o x + q_o f(x)$ and $V(x) \equiv \int_o^x F(x^1)dx^1$ - typical plots of F(x) and the corresponding V(x) are shown in Fig. 5.11. Phase plane analysis of Fig. 5.11 indicates that conservative oscillations will exist provided $p_o + q_o f'(o) > o$. Oscillations of amplitudes in the range $o < A < A_{o_{CR}}$ then exist, where

$$p_o A_{o_{CR}} + q_o f(A_{o_{CR}}) = o, \tag{5.33}$$

or

$$\frac{f(A_{o_{CR}})}{A_{o_{CR}}} = -\frac{p_o}{q_o} \quad . \tag{5.34}$$

The exact condition for existence of a conservative oscillation of amplitude A_o is then

$$p_o A_o + q_o f(A_o) > o \ , \tag{5.35}$$

or

$$\frac{f(A_o)}{A_o} > \frac{-p_o}{q_o} \ , \tag{5.36}$$

while the DF existence condition is

$$Keq(A_o) > -\frac{p_o}{q_o} \ . \tag{5.37}$$

The exact frequency of the oscillation of amplitude A_o is shown in Gelb and Vander Velde [6, p.164] to be

$$w_{o_{exact}} = \frac{\pi}{\sqrt{2}} \left\{ \int_o^{A_o} \left[\int_x^{A_o} F(x^1)dx^1 \right]^{-\frac{1}{2}} dx \right\}^{-1} . \tag{5.38}$$

In Appendix III it is proved that $N_B(A,o) \lessapprox \frac{f(A)}{A} \lessapprox Keq(A)$ for soft spring nonlinearities. Then the condition for actual existence of a conservative oscillation of amplitude A_o, predicted by the DF method, with 5.32 holding is

$$N_B(A_o,o) < -\frac{p_o}{q_o} < \frac{f(A_o)}{A_o} < Keq(A_o). \tag{5.39}$$

If the ideal relay nonlinearity, $f(x) = M\ sgn(x)$, is used, for example, then 5.39 becomes

$$\frac{2M}{\pi A_o} < -\frac{p_o}{q_o} < \frac{M}{A_o} < \frac{4M}{\pi A_o} \ . \tag{5.40}$$

For definiteness let $A_o = 1$, $M = 3\pi/2$, $q_o = 1$, then 5.40 becomes

$$3 < -p_o < 3\pi/2 = 4.71 < 6. \tag{5.41}$$

The DF frequency prediction is now

$$w_{o_{DF}} = \sqrt{p_o + q_o \, Keq(A_o)} = \sqrt{6 + p_o} \quad , \tag{5.42}$$

while the exact frequency expression is calculated as

$$w_{o_{exact}} = \frac{\sqrt{-p_o}\ \pi}{\text{arc cosh}\left\{ \dfrac{M^2 - 2A_o M\, p_o/q_o - A_o{}^2 (p_o/q_o)^2}{(M + A_o p_o/q_o)^2} \right\}}$$

$$= \frac{\sqrt{-p_o}\ \pi}{\text{arc cosh}\left\{ \dfrac{22.21 - 9.42\, p_o - p_o{}^2}{(4.71 + p_o)^2} \right\}} \tag{5.43}$$

from analysis of on-off systems (Appendix IV) rather than from 5.38.

Table 5.1 Amplitude and Frequency Calculations for Case ii) Example System

	$A_o = 1$			$w_o = w_{o_{exact}}$		
p_o	$w_{o_{DF}}$	$w_{o_{exact}}$	% Error	$A_{o_{DF}}$	$A_{o_{exact}}$	% Error
-3.0	1.732	1.625	6.6%	1.065	1.0	6.5%
-3.5	1.581	1.441	9.7%	1.076	1.0	7.6%
-4.0	1.414	1.215	16.4%	1.095	1.0	9.5%
-4.5	1.225	0.950	29.0%	1.110	1.0	11.1%
-4.6	1.183	0.756	56.5%	1.160	1.0	16.0%
-4.71	1.136	0.000	∞	1.272	1.0	27.2%

Table 5.1 shows calculations of $w_{o_{DF}}$, $w_{o_{exact}}$, $A_{o_{DF}}$, $A_{o_{exact}}$, and the corresponding percentage errors for p_o in the range $-3 \geqslant p_o \geqslant -4.71$.

It is seen from Table 5.1 that both amplitude and frequency errors increase as p_o decreases. The value $p_o = -4.71$ implies that the actual oscillation corresponds to the separatrix in Fig. 5.11 which divides the

phase plane into a region in which oscillations exist and one in which they do not. The separatrix motion has an infinite period and hence $w_{o_{exact}} = o$. However, the DF method still predicts an oscillation of non-zero frequency for this value of p_o, and the frequency error increases as this separatrix condition is approached. Thus, for this example, the region in which the IDF stability technique is incorrect is a region in which the DF approximation is decreasing in accuracy.

iii) $p_o \gg o$, $q_o < o$

L(s) is a stable nonminimum phase transfer function, and the root locus for the corresponding linear system is shown in Fig. 5.9. The DF method predicts an oscillation as long as

$$Keq(A_o) < - p_o/q_o \ . \tag{5.44}$$

Loeb's criterion and the IDF stability technique will then be in disagreement if and only if

$$Keq(A_o) < - p_o/q_o < N_B(A_o,o) \ . \tag{5.45}$$

In order that 5.45 obtains, f(x) must be a hard spring nonlinearity so that $Keq(A_o) < N_B(A_o,o)$.

The exact existence condition can be found by employing conservative system theory, as done previously. The plots of F(x), V(x), and the phase plane trajectories shown in Fig. 5.11 still apply, and phase plane analysis yields $p_o A_o + q_o f(A_o) > o$ as the exact condition for existence of an oscillation of amplitude A_o. This condition can be rewritten as

$$\frac{f(A_o)}{A_o} < - p_o/q_o \ . \tag{5.46}$$

The exact frequency of the oscillation of amplitude A_o is given in 5.38.

In Appendix III it is proved that $Keq(A) \lessapprox \frac{f(A)}{A} \lessapprox N_B(A,o)$ for hard

spring nonlinearities. The condition for existence of a conservative oscillation of amplitude A_o, predicted by the DF method, with 5.45 holding is

$$Keq(A_o) < \frac{f(A_o)}{A_o} < -\frac{p_o}{q_o} < N_B(A_o,o). \tag{5.47}$$

If the cubic nonlinearity, $f(x) = c\,x^3$, is used, for example, then 5.47 becomes

$$\frac{3}{4}\,c\,A_o^2 < c\,A_o^2 < -\frac{p_o}{q_o} < \frac{3}{2}\,c\,A_o^2 . \tag{5.48}$$

With $A_o = 1$, $c = 16/3$, $q_o = -1$, 5.48 becomes

$$4 < 5.33 < p_o < 8 . \tag{5.49}$$

The DF frequency prediction is then

$$w_{o_{DF}} = \sqrt{p_o + q_o\,Keq(A_o)} = \sqrt{p_o - 4}\ , \tag{5.50}$$

while the exact frequency expression is calculated from 5.38 as

$$w_{o_{exact}} = \frac{\pi}{\sqrt{2}}\sqrt{\frac{p_o}{2} - \frac{4}{3}} \Big/ \int_0^1 \frac{dx}{\sqrt{(1-x^2)\left[1 - \frac{4x^2}{(3p_o/2-4)}\right]}} = \frac{\frac{\pi}{\sqrt{2}}\sqrt{\frac{p_o}{2} - \frac{4}{3}}}{K\left(\frac{1}{\sqrt{3p_o/8 - 1}}\right)}, \tag{5.51}$$

where $K(\cdot)$ is the complete elliptic normal integral.

Table 5.2 shows calculations of $w_{o_{DF}}$, $w_{o_{exact}}$, $A_{o_{DF}}$, $A_{o_{exact}}$, and the corresponding percentage errors for p_o in the range $8 \geqslant p_o \geqslant 5.33$. Both amplitude and frequency errors increase as p_o decreases. The value $p_o = 5.33$ corresponds to the separatrix motion and hence $w_{o_{exact}} = o$. This is the identical trend to that of the case ii) example, namely, a worsening of the DF approximation as the separatrix motion is approached.

Table 5.2 Amplitude and Frequency Calculations for Case iii) Example System

p_o	$A_o = 1$			$w_o = {}^{w_o}{}_{exact}$		
	$w_{o_{DF}}$	$w_{o_{exact}}$	% Error	$A_{o_{DF}}$	$A_{o_{exact}}$	% Error
8.0	2.000	1.957	2.20%	1.022	1.0	2.2%
7.0	1.732	1.666	3.96%	1.027	1.0	2.7%
6.5	1.581	1.485	6.46%	1.036	1.0	3.6%
6.0	1.414	1.270	11.35%	1.055	1.0	5.5%
5.5	1.225	0.933	31.30%	1.075	1.0	7.5%
5.4	1.183	0.800	47.88%	1.090	1.0	9.0%
5.33	1.153	0.000	∞	1.155	1.0	11.6%

iv) $p_o < o$, $q_o < o$

L(s) is an unstable, nonminimum phase transfer function, and the root locus for the linear system is given in Fig. 5.10. The DF method predicts that no oscillations are possible, and this is verified by analytical theory of conservative systems.

5.3.2 Non Conservative Systems

For $p_1 \neq o$, $q_1 \neq o$, existing oscillations will be in the form of stable or unstable limit cycles. The Routh-Hurwitz criterion and root locus method can be used to discover possible discrepancy situations in which conditions 5.26 are satisfied (Loeb's criterion predicts a stable limit cycle while the IDF stability technique predicts an unstable limit cycle). Investigations have produced two system configurations in which conditions 5.26 hold with a DF oscillation predicted (i.e. 5.15 and 5.16 are also satisfied). These two system configurations can be classified according to the shape of the root locus of the corresponding linear system.

System Configuration I

Fig. 5.12 shows the root locus for this first system configuration in which a discrepancy between Loeb's criterion and the IDF stability technique can exist. In terms of poles and zeros, L(s) is expressed as

$$L(s) = \frac{-(s-z_1)}{(s-p_1^{\,1})(s-p_2^{\,1})} = \frac{-s+z_1}{s^2-(p_1^{\,1}+p_2^{\,1})s+p_1^{\,1}p_2^{\,1}}, \tag{5.52}$$

which, by identification, gives

$$q_1 = -1(<o);\ q_o = z_1(>o);\ p_1 = -(p_1^{\,1}+p_2^{\,1})(>o);\ p_o = p_1^{\,1}p_2^{\,1}(<o). \tag{5.53}$$

L(s) is an unstable, nonminimum phase transfer function, and the system has, essentially, positive feedback instead of the usual negative feedback. The DF conditions 5.15 and 5.16 become

$$Keq(A_o) = -(p_1^{\,1} + p_2^{\,1}) \tag{5.54}$$

and

$$w_o^{\,2} = p_1^{\,1}p_2^{\,1} + z_1 Keq(A_o) = p_1^{\,1}p_2^{\,1} - z_1(p_1^{\,1}+p_2^{\,1}) > o; \tag{5.55}$$

the discrepancy conditions of 5.26 become

$$p_1^{\,1}p_2^{\,1} + z_1 N_B(A_o, o) < o \text{ and } -(p_1^{\,1}+p_2^{\,1}) - N_B(A_o, o) > o, \tag{5.56}$$

or

$$N_B(A_o,o) < -p_1^{\,1}p_2^{\,1}/z_1 \text{ and } N_B(A_o,o) < -(p_1^{\,1}+p_2^{\,1}). \tag{5.57}$$

Since $N_B(A_o,o) < Keq(A_o)$ is necessary in order to satisfy 5.57, f(x) must be a soft spring nonlinearity. If $f(x) = M\,sgn(x)$, $M = \pi/2$, $p_1^{\,1} = -4$, $p_2^{\,1} = 2$, then DF conditions 5.54 and 5.55 become

$$Keq(A_o) = 2/A_o = 2 \tag{5.58}$$

yielding $A_o = 1$, and

$$w_o^{\,2} = -8 + 2\,z_1. \tag{5.59}$$

Also, discrepancy conditions 5.57 become

$$\frac{1}{A_o} = 1 < \frac{8}{z_1} \quad \text{and} \quad \frac{1}{A_o} = 1 < 2 \ . \tag{5.60}$$

The DF method predicts an oscillation of amplitude $A_o = 1$ and a discrepancy exists between Loeb's criterion and the IDF stability technique if and only if $4 < z_1 < 8$.

Similarly, for the case $M = \pi$, $p_1^1 = -6$, $p_2^1 = 2$, the DF conditions become

$$Keq(A_o) = 4/A_o = 4 \tag{5.61}$$

yielding $A_o = 1$, and

$$w_o^2 = -12 + 4 z_1. \tag{5.62}$$

Discrepancy conditions 5.57 become

$$\frac{2}{A_o} = 2 < \frac{12}{z_1} \text{ and } \frac{2}{A_o} = 2 < 4 \ , \tag{5.63}$$

so that the DF method predicts an oscillation of amplitude $A_o = 1$ and a discrepancy exists between Loeb's criterion and the IDF stability technique if and only if $3 < z_1 < 6$.

Table 5.3 exhibits values of $w_{o_{DF}}$, $w_{o_{exact}}$, $A_{o_{DF}}$, $A_{o_{exact}}$, and the corresponding percentage errors for various values of z_1 in each of the two examples defined above. The exact amplitude and frequency were measured in experimental simulations of the systems on an EAI 580 analog computer.

An interesting observation from the results of experimental simulations is that, in both systems, limit cycles become nonexistent before the discrepancy regions of z_1 are reached. For the first system ($M = \pi/2, p_1^1 = -4$),

Table 5.3 Amplitude and Frequency Calculations for System Configuration I Examples

z_1	$M = \pi/2$, $p_1^1 = -4$, $p_2^1 = 2$, $4 < z_1 < 8$ for discrepancy					
	$w_{o_{DF}}$	$w_{o_{exact}}$	% Error	$A_{o_{DF}}$	$A_{o_{exact}}$	% Error
10.0	3.46	2.42	43.0%	1.0	1.348	25.8%
9.5	3.32	2.24	48.2%	1.0	1.366	26.8%
9.0	3.16	1.96	61.3%	1.0	1.396	28.4%
8.5	3.00	1.65	81.8%	1.0	1.443	30.7%
8.02	2.84	.90	215.6%	1.0	1.570	36.3%
z_1	$M = \pi$, $p_1^1 = -6$, $p_2^1 = 2$, $3 < z_1 < 6$ for discrepancy					
	$w_{o_{DF}}$	$w_{o_{exact}}$	% Error	$A_{o_{DF}}$	$A_{o_{exact}}$	% Error
8.0	4.47	3.14	42.4%	1.0	1.347	25.8%
7.5	4.24	2.80	51.5%	1.0	1.370	27.0%
7.0	4.00	2.42	65.4%	1.0	1.400	28.6%
6.5	3.74	1.96	90.8%	1.0	1.450	31.0%
6.02	3.47	.90	285.6%	1.0	1.570	36.3%

no limit cycles exist for $z_1 < 8.02$, the discrepancy region being $4 < z_1 < 8$. For the second system, oscillations are non existent for $z_1 < 6.02$ with the discrepancy region $3 < z_1 < 6$. Percentage errors in amplitude and frequency are large in both cases, and increase as the limits ($z_1 = 8.02$ and $z_1 = 6.02$ respectively) are approached from above. The limits of existence correspond to the oscillations approaching a separatrix motion in the phase plane. This is evidenced in Table 5.3 by $w_{o_{exact}}$ approaching zero as z_1 approaches the existence limit. Observations of the oscillations as the limits were approached indicated that the waveform was approaching a square wave. Large DF approximation errors are quite likely for such a waveform. Fig. 5.14a) shows a phase plane plot of the separatrix and Fig. 5.14b) the waveform for $z_1 = 8.02$ in the

first example of System Configuration I.

System Configuration II

In Fig. 5.13 root loci are shown for the second system configuration in which the two stability techniques can disagree. Fig. 5.13a) shows p_1^1 and p_2^1 as real roots in the RHP while Fig. 5.13b) shows p_1^1 and p_2^1 as complex conjugate roots in the RHP. In terms of poles and zeros, L(s) is expressed as

$$L(s) = \frac{s - z_1}{(s-p_1^1)(s-p_2^1)} = \frac{s - z_1}{s^2-(p_1^1+p_2^1)s+p_1^1p_2^1}, \quad (5.64)$$

with the identification

$$q_1=1(>o);\ q_o=-z_1(<o);\ p_1=-(p_1^1+p_2^1)(<o);\ p_o=p_1^1p_2^1(>o). \quad (5.65)$$

L(s) is then an unstable, nonminimum phase transfer function. The DF conditions 5.15 and 5.16 become

$$Keq(A_o) = p_1^1 + p_2^1 \quad (5.66)$$

and

$$w_o^2 = p_1^1p_2^1 - z_1\,Keq(A_o) = p_1^1p_2^1 - z_1(p_1^1+p_2^1) > o, \quad (5.67)$$

and the discrepancy conditions of 5.26 are now

$$p_1^1p_2^1 - z_1N_B(A_o,o) < o \text{ and } -(p_1^1+p_2^1) + N_B(A_o,o) > o \quad (5.68)$$

or

$$N_B(A_o,o) > p_1^1p_2^1/z_1 \text{ and } N_B(A_o,o) > p_1^1+p_2^1. \quad (5.69)$$

Since $N_B(A_o,o) > Keq(A_o)$ is necessary in order that 5.69 hold, f(x) must be a hard spring nonlinearity. Let $f(x) = M\,x^3$, M= 4.614, $p_1^1 = 4$, $p_2^1 = 6$, then DF conditions 5.66 and 5.67 become

$$Keq(A_o) = \frac{3}{4}\ (4.614)\ A_o^2 = 10 \quad (5.70)$$

yielding $A_o = 1.7$, and

$$w_o^2 = 24 - 10\, z_1 > o \ . \tag{5.71}$$

Also, discrepancy conditions 5.69 become

$$20 > \frac{24}{z_1} \quad \text{and} \quad 20 > 10 \ . \tag{5.72}$$

The DF Method predicts an oscillation of amplitude $A_o = 1.7$ and a discrepancy exists between Loeb's criterion and the IDF stability technique if and only if $1.2 < z_1 < 2.4$.

Similarly, if $M = 8/3$, $p_1^1 = 4+j2$, $p_2^1 = 4 - j2$, then the DF conditions are

$$Keq(A_o) = \frac{3}{4}\ (2.667)\ \ A_o^2 = 8 \tag{5.73}$$

yielding $A_o = 2$, and

$$w_o^2 = 20 - 8\, z_1 > o \ . \tag{5.74}$$

Discrepancy conditions 5.69 become

$$16 > \frac{20}{z_1} \quad \text{and} \quad 16 > 8 \ , \tag{5.75}$$

so that the DF method predicts an oscillation of amplitude $A_o = 2$, and a discrepancy exists between the two stability techniques if and only if $1.25 < z_1 < 2.5$.

Table 5.4 shows values of $w_{o_{DF}}$, $w_{o_{exact}}$, $A_{o_{DF}}$, $A_{o_{exact}}$, and the corresponding percentage errors for various values of z_1 in each of the two examples defined above.

For each system oscillations are observed in the discrepancy region of z_1. In the first system ($M = 4.614$, $p_1^1 = 4$, $p_2^1 = 6$) the limit of existence of oscillations is found to be $z_1 = 1.625$ while in the second system it is found to be $z_1 = 1.677$. In both systems, percentage errors in amplitude and frequency increase as the limits are approached from

Table 5.4 Amplitude and Frequency Calculations for System Configuration II Examples

z_1	$M = 4.614$, $p_1^1 = 4$, $p_2^1 = 6$, $1.2 < z_1 < 2.4$ for discrepancy					
	$w_{o_{DF}}$	$w_{o_{exact}}$	% Error	$A_{o_{DF}}$	$A_{o_{exact}}$	% Error
1.00	3.74	2.74	36.5%	1.70	1.750	2.86%
1.20	3.46	2.37	46.0%	1.70	1.760	3.41%
1.30	3.32	2.17	53.0%	1.70	1.764	3.63%
1.40	3.16	1.91	66.0%	1.70	1.770	3.96%
1.50	3.00	1.57	91.0%	1.70	1.777	4.33%
1.60	2.83	1.08	162.0%	1.70	1.790	5.03%
1.625	2.78	0.67	315.0%	1.70	1.790	5.03%
z_1	$M = 2.667$, $p_1^1 = 4+ j2$, $p_2^1 = 4-j2$, $1.25 < z_1 < 2.5$ for discrepancy					
	$w_{o_{DF}}$	$w_{o_{exact}}$	% Error	$A_{o_{DF}}$	$A_{o_{exact}}$	% Error
1.00	3.46	2.74	26.3%	2.00	2.060	2.92%
1.25	3.16	2.24	41.0%	2.00	2.073	3.52%
1.30	3.10	2.17	42.9%	2.00	2.077	3.71%
1.40	2.97	1.96	51.5%	2.00	2.084	4.03%
1.50	2.83	1.70	66.5%	2.00	2.094	4.49%
1.60	2.68	1.34	100.0%	2.00	2.103	4.90%
1.677	2.57	0.66	289.5%	2.00	2.115	5.40%

below. The ever increasing frequency errors, with $w_{o_{exact}}$ approaching zero, indicate that the limit cycles are approaching a separatrix motion as the limits are approached. Observation of the oscillations as these limits are attained shows that the waveforms again resemble square waves, thus explaining the large DF frequency errors.

5.4 Conclusions

Loeb's criterion, for second order systems, is shown to be equivalent to a stability study of the DF approximate variational system of Fig. 5.4 while the IDF stability technique is shown to be equivalent to a stability

study of the time-averaged DF approximate variational system of Fig. 5.5. Loeb's criterion then involves only the DF approximation, while the IDF stability technique involves the additional approximation of time averaging. Theoretically, then, Loeb's criterion should be the more accurate stability technique to apply to second order systems.

Application of the two stability techniques to specific forms of second order system has produced situations in which Loeb's criterion predicts stability while the IDF stability technique predicts instability. However, in both conservative and non conservative systems exhibiting this discrepancy situation, it is found that the discrepancy region is a region in which the DF approximation is becoming progressively worse, especially in its frequency prediction, $^{w}o_{DF}$, as $^{w}o_{DF}$ approaches zero. In all examples considered, $^{w}o_{DF}$ approaching zero in the DF predicted oscillation corresponds to the actual oscillation approaching a separatrix motion for which $^{w}o_{exact}$ is zero. However, every system studied is such that, in the oscillation region close to the separatrix motion, $^{w}o_{exact} < {}^{w}o_{DF}$ - the separatrix motion is reached before $^{w}o_{DF}$ reaches zero. There is then always an interval of $^{w}o_{DF}$ values, $o \lessapprox w_o \lessapprox w^*$, in which DF predicted oscillations do not correspond to any existing oscillations. In the System Configuration I this situation is reached even before the discrepancy region of z_1 is entered.

From the evidence of the examples studied, it may be concluded that DF oscillations, with $^{w}o_{DF}$ approaching zero, correspond, in an approximate way, to actual oscillations approaching a separatrix motion. Also, as $^{w}o_{DF}$ goes to zero it seems to be generally true that DF errors, especially those in frequency, increase drastically. From the root loci of Figs. 5.8, 5.9, 5.12 and 5.13 it is evident that $^{w}o_{DF}$ must be

relatively close to zero in order to have a discrepancy situation existing. Thus discrepancy regions seem to correspond to regions of larger DF error, and perhaps the IDF stability technique indicates this with its instability prediction. In fact, the DF approximation can be so poor in these discrepancy situations that an actual oscillation does not even exist. Although the IDF stability technique is seemingly in error in discrepancy situations, it could actually be interpreted as yielding information about the accuracy of the DF predicted oscillations.

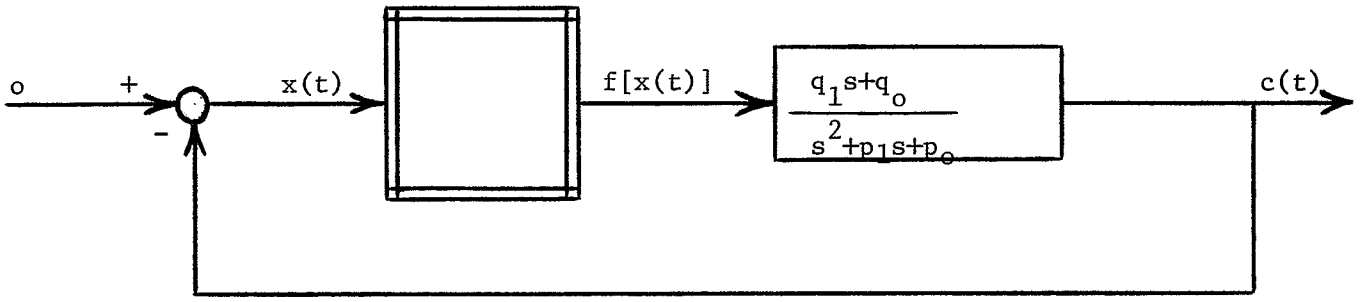

Fig. 5.1 GENERAL SECOND ORDER NONLINEAR SYSTEM

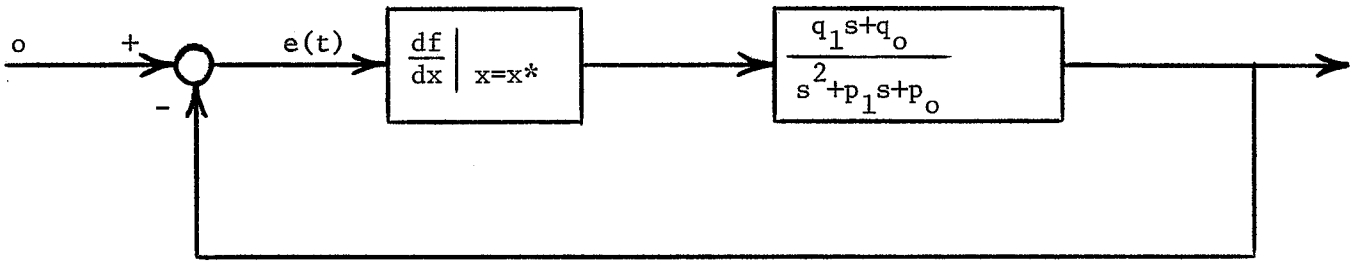

Fig. 5.2 SECOND ORDER VARIATIONAL SYSTEM

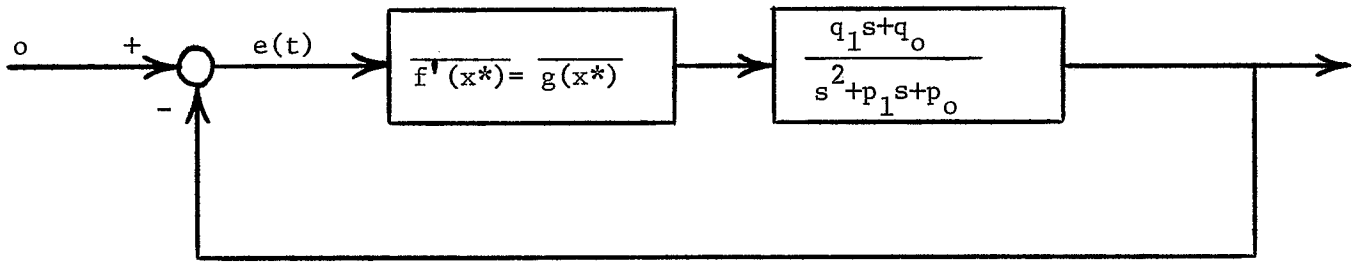

Fig. 5.3 TIME-AVERAGED SECOND ORDER VARIATIONAL SYSTEM

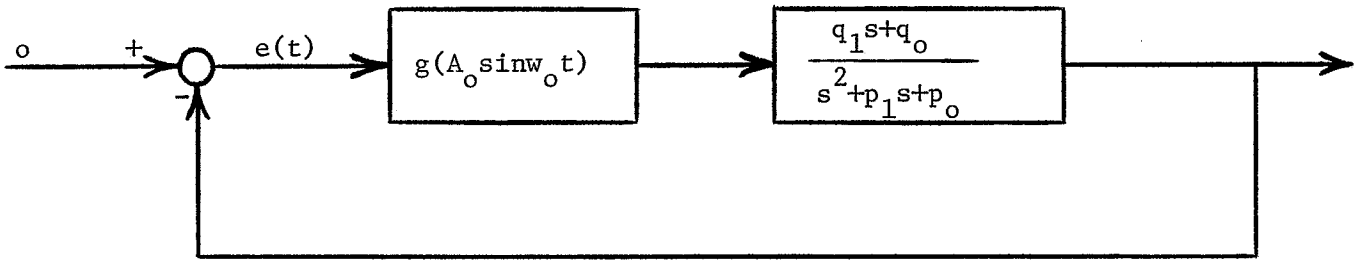

Fig. 5.4 DF APPROXIMATE VARIATIONAL SYSTEM

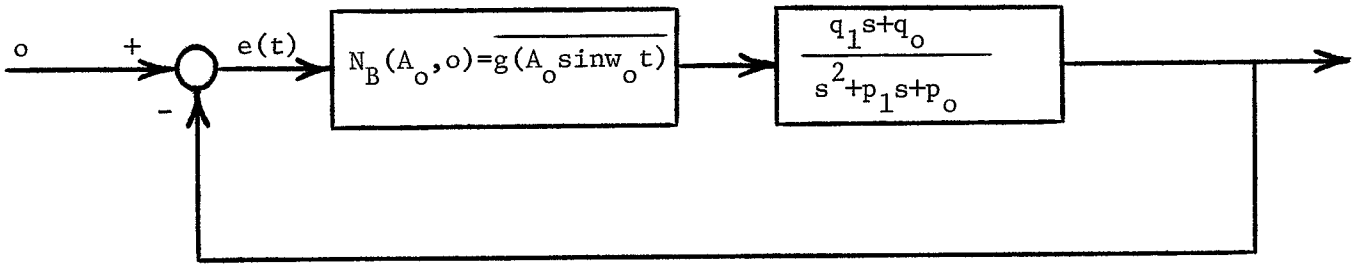

Fig. 5.5 TIME-AVERAGED DF APPROXIMATE VARIATIONAL SYSTEM

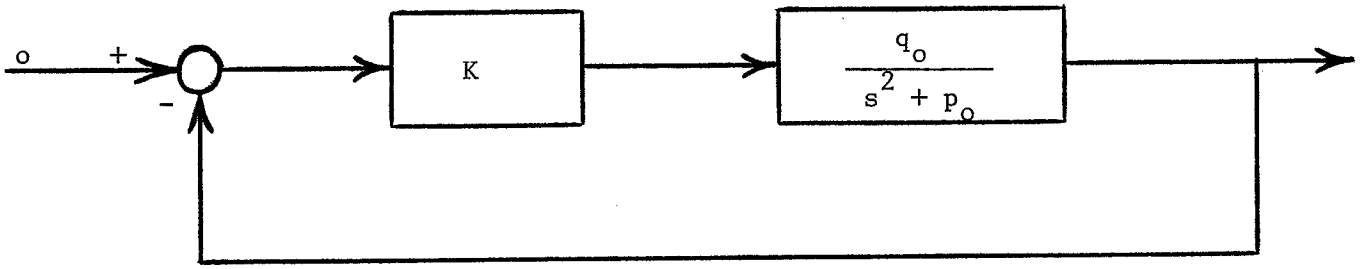

Fig. 5.6 LINEAR SYSTEM FOR ROOT LOCUS - CONSERVATIVE CASE

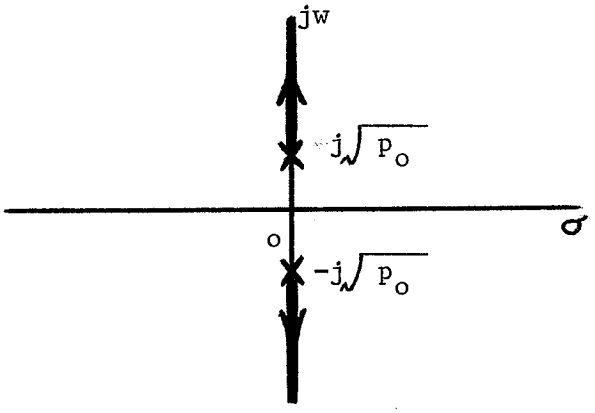

Fig. 5.7 ROOT LOCUS: $p_o \geq o, q_o > o$

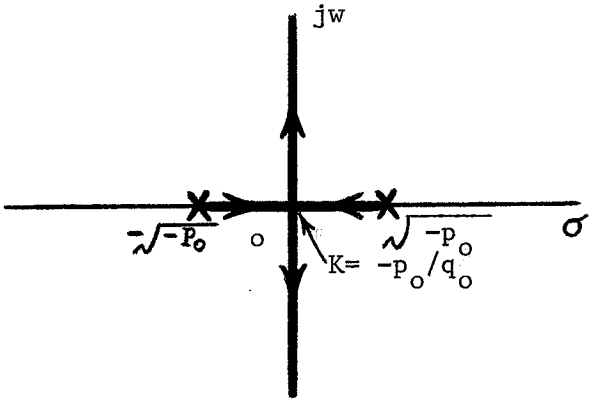

Fig. 5.8 ROOT LOCUS : $p_o < o, q_o > o$

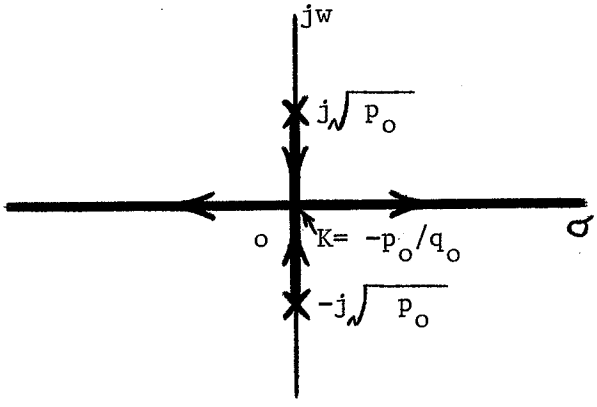

Fig. 5.9 ROOT LOCUS : $p_o \geq o, q_o < o$

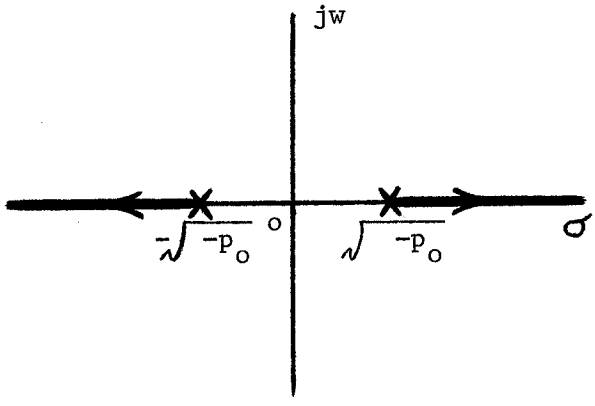

Fig. 5.10 ROOT LOCUS : $p_o < o, q_o < o$

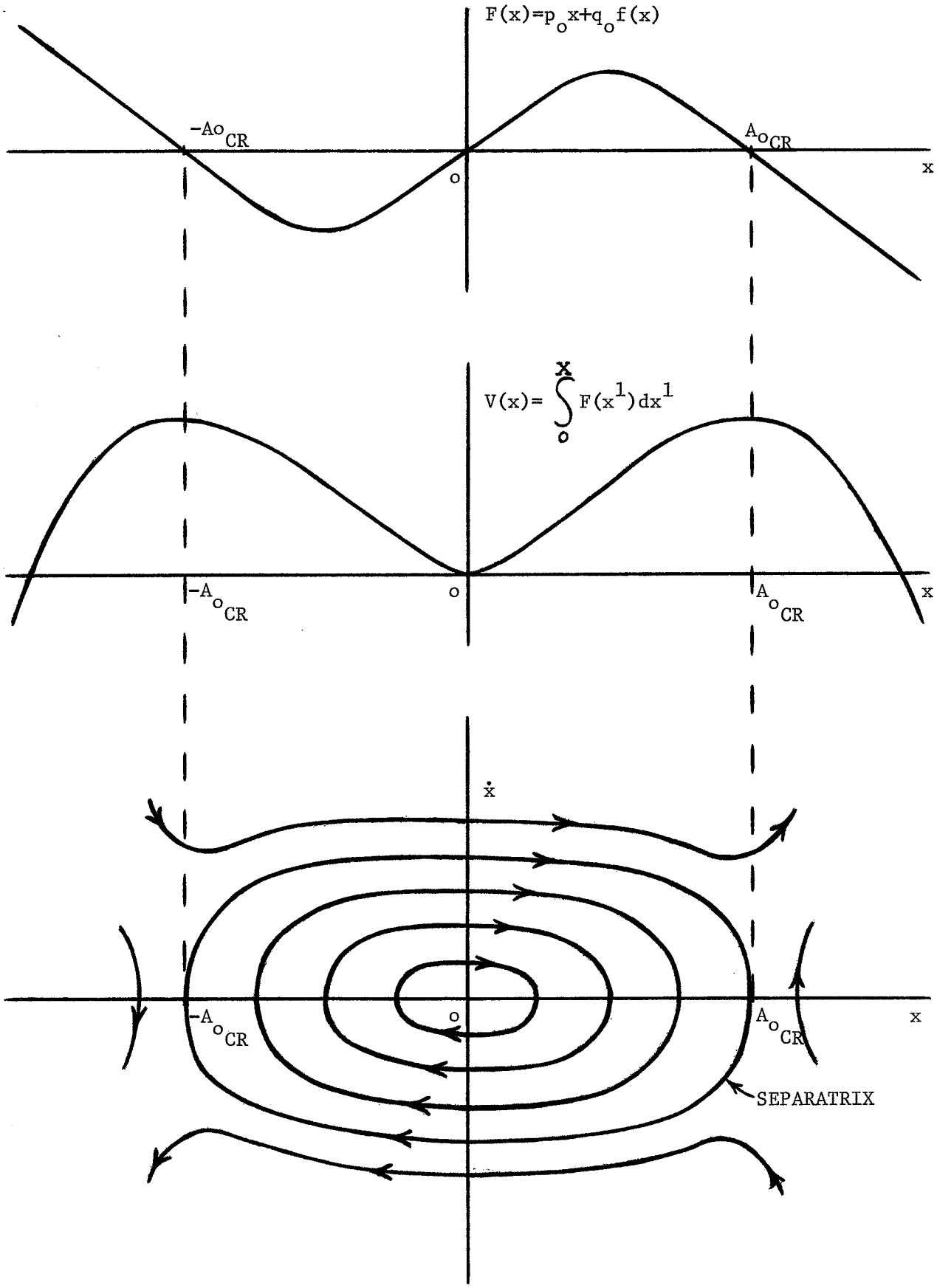

Fig. 5.11 CONSERVATIVE SYSTEM ANALYSIS

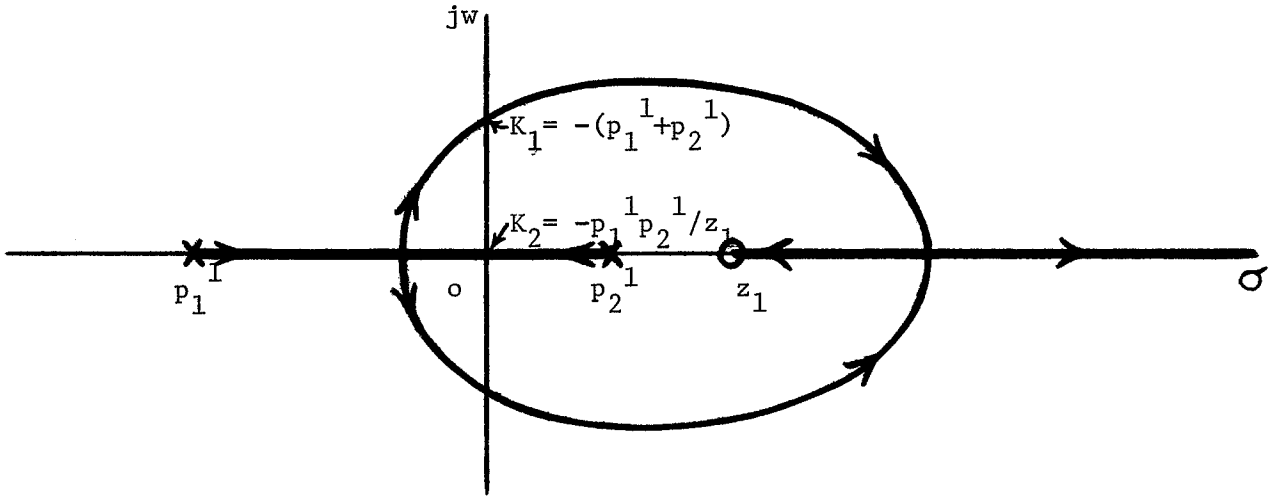

Fig. 5.12 ROOT LOCUS FOR SYSTEM CONFIGURATION I

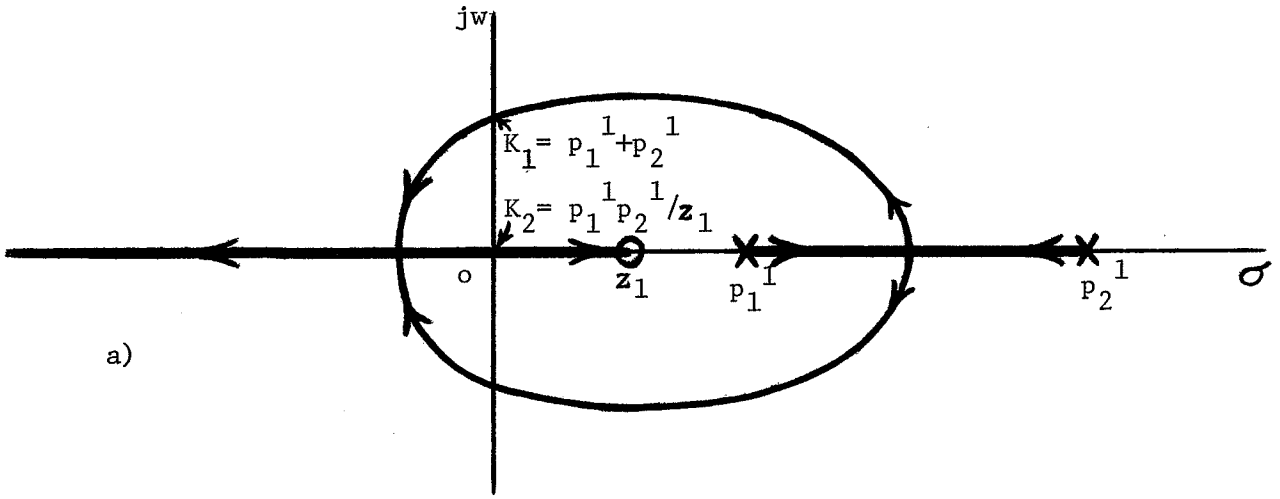

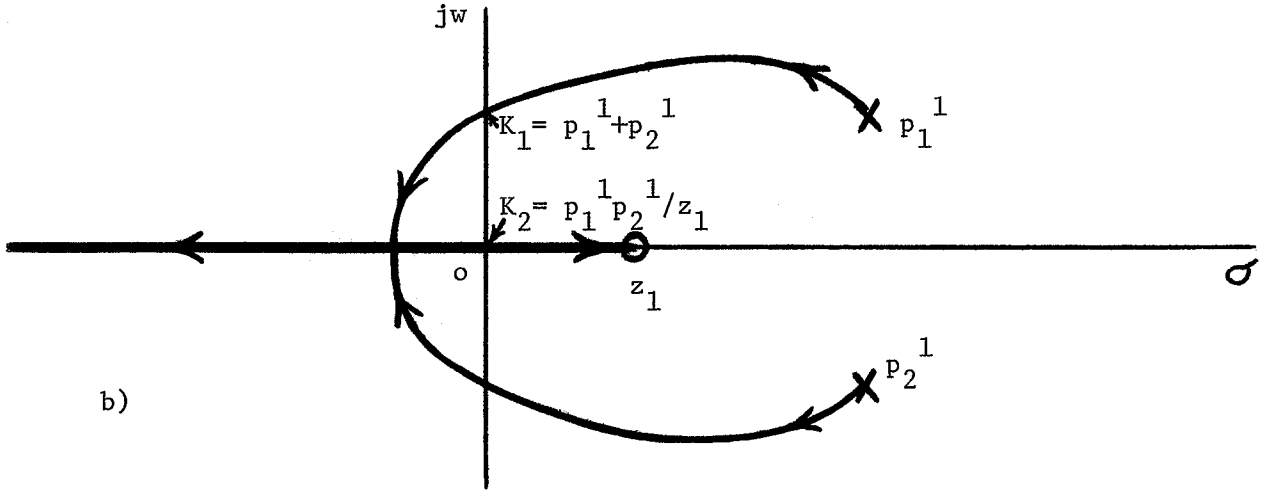

Fig. 5.13 ROOT LOCI FOR SYSTEM CONFIGURATION II

CHAPTER 6

STABILITY OF OSCILLATIONS IN THIRD ORDER SYSTEMS

Third order nonlinear systems are of sufficiently low order to be dealt with in detail, yielding analytical expressions for the DF method and the approximate stability techniques. However, few theoretical results concerning stability of oscillations can be obtained, and simulation must always be used to determine the actual stability properties.

6.1 Floquet Theory and Time Averaging

Consider the general third order nonlinear system of Fig. 6.1 with f(x) a static, single-valued, odd symmetric nonlinearity and

$$L(s) = \frac{q_2 s^2 + q_1 s + q_o}{s^3 + p_2 s^2 + p_1 s + p_o} \quad . \tag{6.1}$$

Let $x(t) = x^*(t)$ be a periodic solution of the system with period T. Then the variational system of Fig. 6.2 corresponds to the variational equation

$$\dddot{e}(t) + \left\{p_2 + q_2 g\,[x^*(t)]\right\} \ddot{e}(t) + \left\{p_1 + q_1 g\,[x^*(t)] + 2q_2 \dot{g}\,[x^*(t)]\right\} \dot{e}(t)$$
$$+ \left\{p_o + q_o g\,[x^*(t)] + q_1 \dot{g}\,[x^*(t)] + q_2 \ddot{g}[x^*(t)]\right\} e(t) = o, \tag{6.2}$$

with $g[x^*(t)] \equiv f'(x^*) = [df(x)/dx]\,\big|_{x=x^*}$. Kaplan [17, pp.474-476] shows that the three characteristic exponents $\lambda_1, \lambda_2, \lambda_3$, corresponding to the three linearly independent solutions of 6.2, are related by the following equation:

$$\lambda_1 + \lambda_2 + \lambda_3 = -\frac{1}{T}\int_o^T \left\{p_2 + q_2 g\,[x^*(t)]\right\} dt = -\left\{p_2 + q_2 \overline{g[x^*(t)]}\right\}. \tag{6.3}$$

Since $\dot{x}^*(t)$ is a periodic solution of the variational equation, one characteristic exponent, say λ_1, is zero. A necessary (sufficient)

condition for $x^*(t)$ to be a stable (unstable) limit cycle is $\lambda_2+\lambda_3 < 0 (> o)$, or

$$p_2 + q_2\overline{g\,[x^*(t)]} > o \;(< o), \tag{6.4}$$

from 6.3.

The time-averaged third order variational system of Fig. 6.3 has a differential equation given by

$$\dddot{e}(t) + \left\{p_2+q_2\overline{g[x^*(t)]}\right\}\ddot{e}(t) + \left\{p_1+q_1\overline{g[x^*(t)]}\right\}\dot{e}(t)$$
$$+\left\{p_o+ q_o\overline{g[x^*(t)]}\right\}e(t) = o. \tag{6.5}$$

Analysis of the roots of the corresponding characteristic equation,

$$s^3+[p_2+q_2\overline{g(x^*)}]\, s^2 + [p_1+q_1\overline{g(x^*)}]\, s + [p_o+q_o\overline{g(x^*)}] = o, \tag{6.6}$$

by the Routh-Hurwitz criterion yields

$$p_2 + q_2\,\overline{g(x^*)} > o \tag{6.7}$$

as a necessary condition in order to have all three characteristic roots of 6.6 in the LHP. Alternatively,

$$p_2 + q_2\,\overline{g(x^*)} < o \tag{6.8}$$

is one of the sufficient conditions in order to have at least one of the characteristic roots of 6.6 in the RHP. The necessary condition of 6.7 for stability of the time-averaged variational system is then the same as the necessary condition of 6.4 for stability of the variational system. Similarly, the sufficient condition of 6.8 for instability of the time-averaged variational system is identical to the sufficient condition of 6.4 for an unstable variational system. It is rather unlikely, however, that the remaining Routh-Hurwitz necessary and sufficient conditions for stability or instability of the time-averaged variational system will coincide with those of the original variational system. Unfortunately, the problem of determining necessary and sufficient conditions for stable

or unstable limit cycles in third order systems, using the variational system, is too intractable to be of any use.

If the DF approximate variational system of Fig. 6.4 is considered, then a necessary condition for asymptotic orbital stability is

$$p_2 + q_2 \overline{g\ [A_o \sin w_o t]} > o\ , \tag{6.9}$$

and a sufficient condition for instability is

$$p_2 + q_2 \overline{g\ [A_o \sin w_o t]} < o\ . \tag{6.10}$$

Analysis of the time-averaged DF approximate variational system of Fig. 6.5 yields the same condition 6.9 as a necessary condition for all roots to lie in the LHP, and 6.10 as a sufficient condition for at least one root in the RHP. A complete analysis using the Routh-Hurwitz criterion will be presented in the next section, and yields necessary and sufficient conditions for stability or instability.

6.2 Approximate Stability Techniques

The DF method and approximate stability techniques are applied to three classes of third order systems: L(s) having i) no zeros, ii) one zero, and iii) two zeros. For each class, both positive and negative feedback situations are considered. The linear system of Fig. 6.6 is used to apply the DF method and stability techniques by way of the Routh-Hurwitz criterion and root locus method.

With L(s) in its most general form, the characteristic equation for the linear system of Fig. 6.6 is

$$s^3+(p_2+q_2K)\ s^2 + (p_1+q_1K)\ s + p_o+q_oK = o, \tag{6.11}$$

for which the Routh array,

$$\begin{array}{c|ccc} s^3 & 1 & p_1+q_1K & o \\ s^2 & p_2+q_2K & p_o+q_oK & o \\ s^1 & \dfrac{(p_1+q_1K)(p_2+q_2K)-(p_o+q_oK)}{p_2+q_2K} & o & o \\ s^o & p_o+q_oK & o & o \end{array} \qquad (6.12)$$

gives the DF condition,

$$(p_1+q_1Keq)\ (p_2+q_2Keq) - (p_o+q_oKeq) = o, \qquad (6.13)$$

and, from the auxiliary equation, $(p_2+q_2Keq)\ s^2+p_o+q_oKeq = o$,

$$w_o^{\,2} = \frac{p_o+q_oKeq}{p_2+q_2Keq} = p_1+q_1Keq > o\ . \qquad (6.14)$$

6.2.1 L(s) with No Zeros

If L(s) has no zeros then $q_1 = q_2 = o$ and, without loss of generality, it can be assumed that $|q_o| = 1$ since the gain can be associated with K.

6.2.1.1 Negative Feedback

If $q_o = 1$ then the negative feedback situation occurs. A pole - zero representation of L(s) would be

$$L(s) = \frac{1}{s^3+p_2\,s^2+p_1s+p_o} = \frac{1}{(s-p_1^{\,1})(s-p_2^{\,1})(s-p_3^{\,1})}\ , \qquad (6.15)$$

with the identifications

$$p_o = -\,p_1^{\,1}p_2^{\,1}p_3^{\,1}\ ;\ p_1 = p_1^{\,1}p_2^{\,1} + p_1^{\,1}p_3^{\,1} + p_2^{\,1}p_3^{\,1}\ ;$$

$$p_2 = -\,(p_1^{\,1} + p_2^{\,1} + p_3^{\,1})\ . \qquad (6.16)$$

From 6.13 and 6.14 the DF conditions are

$$Keq(A_o) = p_1p_2 - p_o > o \qquad (6.17)$$

and

$$w_o^{\,2} = p_1 > o\ . \qquad (6.18)$$

The third root at the DF conditions is $s_3 = - p_2$, and $p_o + Keq(A_o) = p_2 w_o^2$. The Routh array (6.12), with the DF conditions substituted and $q_1 = q_2 = o$, $q_o = 1$, shows that the DF system is neutrally stable if and only if the third root $s_3 = - p_2 < o$, i.e. $p_2 > o$. Thus a neutrally stable DF system exists if and only if

$$p_1^{-1} + p_2^{-1} + p_3^{-1} < o \ , \tag{6.19}$$

and an unstable DF system exists if and only if

$$p_1^{-1} + p_2^{-1} + p_3^{-1} > o \ , \tag{6.20}$$

In fact, 6.20 is a sufficient condition for an unstable system independant of the value of K.

Since $q_2 = o$, the necessary condition for a stable limit cycle (6.4) is simply 6.19, and the sufficient condition for an unstable limit cycle (6.4) is 6.20. Also, in the root locus method, the centre of the asymptotes, $\sigma_A = \dfrac{p_1^{-1} + p_2^{-1} + p_3^{-1}}{3} = - \dfrac{p_2}{3}$, substituted into 6.19 and 6.20, yields $\sigma_A < o$ for a neutrally stable DF system and $\sigma_A > o$ for an unstable DF system. The root loci of Fig. 6.7 show, in terms of the location of the poles of L(s), the various possible situations in which the DF conditions obtain.

Application of Loeb's criterion results in a prediction of a stable limit cycle if f(x) is soft spring ($N_B(A_o,o) < Keq\ (A_o)$), and an unstable limit cycle if f(x) is hard spring ($N_B(A_o,o) > Keq(A_o)$). This can be expressed as

$$p_1 p_2 - p_o - N_B(A_o,o) > o \ , \tag{6.21}$$

for a stable limit cycle, and

$$p_1 p_2 - p_o - N_B(A_o,o) < o \tag{6.22}$$

for an unstable limit cycle (for details see Appendix V).

On the other hand, the IDF stability technique requires the following conditions to be satisfied in order to have a stable (unstable) limit cycle:

$$p_2 > o \ (< o) \ , \tag{6.23}$$

$$p_1 p_2 - p_o - N_B(A_o,o) > o \ (< o) \ , \tag{6.24}$$

and

$$p_o + N_B(A_o,o) > o \ (< o) \ . \tag{6.25}$$

For a stable limit cycle all three stability conditions must be satisfied, whereas for an unstable limit cycle only one of the three instability conditions need be satisfied. Also, 6.24 is identical to the Loeb conditions of 6.21 and 6.22.

Now $p_2 < o$ implies that the DF system is unstable, and this is also an exact sufficient condition for an unstable limit cycle. Thus, in this case, if any oscillation exists with $p_2 < o$ it must be an unstable limit cycle. The IDF stability technique is in complete agreement with the theoretical result in this situation, whereas Loeb's criterion will still predict a stable limit cycle (as long as f(x) is a soft spring). This is then one possibility for a discrepancy between Loeb's criterion and the IDF stability technique, and it is depicted in the root locus of Fig. 6.7 c), where $p_1^{\,1} + p_2^{\,1} + p_3^{\,1} > o$ and $N_B(A_o,o) < Keq(A_o)$.

Another possible discrepancy occurs for $p_2 > o$, so that the DF system is still neutrally stable. If $p_2 > o$ and $p_1 p_2 - p_o - N_B(A_o,o) > o$, but $p_o + N_B(A_o,o) < o$, then the IDF stability technique predicts an unstable limit cycle while Loeb's criterion predicts a stable limit cycle. This situation is depicted in the root locus of Fig. 6.7 d) if $N_B(A_o,o) < - p_o$, and in the root locus of Fig. 6.7 c) if $p_2 > o$ and $N_B(A_o,o) < - p_o$.

Figs. 6.7 a) and 6.7 b) show root locus situations in which the

two stability techniques agree that the limit cycle is stable for f(x) a soft spring and unstable for f(x) a hard spring.

6.2.1.2. Positive Feedback

If $q_o = -1$ then a positive feedback situation occurs. L(s) can be expressed as

$$L(s) = \frac{-1}{s^3+p_2s^2+p_1s+p_o} = \frac{-1}{(s-p_1^1)(s-p_2^1)(s-p_3^1)} \tag{6.26}$$

with the same identifications as in 6.16. The DF conditions are

$$Keq(A_o) = p_o - p_1p_2 \tag{6.27}$$

and 6.18. The third root at the DF conditions is still $s_3 = -p_2$, and $p_o - Keq(A_o) = p_2w_o^2$. Also, 6.19 and 6.20 still apply, so that a neutrally stable DF system exists if and only if $p_2 > o$, and $p_2 < o$ always ensures at least one root in the RHP. The root loci of Fig. 6.8 indicate, in terms of pole locations, the various possible situations in which the DF conditions obtain.

Loeb's criterion will predict a stable limit cycle if f(x) is a hard spring ($N_B(A_o,o) > Keq(A_o)$), and an unstable limit cycle if f(x) is a soft spring ($N_B(A_o,o) < Keq(A_o)$). This can be expressed as

$$p_1p_2 - p_o + N_B(A_o,o) > o, \tag{6.28}$$

for a stable limit cycle, and

$$p_1p_2 - p_o + N_B(A_o,o) < o \tag{6.29}$$

for an unstable limit cycle (details in Appendix V).

For a stable (unstable) limit cycle the IDF stability technique requires

$$p_2 > o \ (< o) , \tag{6.30}$$

$$p_1p_2 - p_o + N_B(A_o,o) > o \ (< o) , \tag{6.31}$$

and

$$p_o - N_B(A_o,o) > o \ (< o) \ . \qquad (6.32)$$

Again, all three stability conditions are required for a stable limit cycle, but only one of the three instability conditions is required for an unstable limit cycle.

The condition $p_2 < o$ is an exact sufficient condition for an unstable limit cycle, as well as being a sufficient condition for IDF stability. If any oscillation exists with $p_2 < o$, then the IDF stability technique is in agreement with the theoretical result that the oscillation is an unstable limit cycle. Loeb's criterion will still predict a stable limit cycle as long as f(x) is a hard spring, and this is one possibility for a discrepancy between the two stability techniques. This discrepancy is depicted in all four root loci of Fig. 6.8.

If $p_2 > o$, so that the DF system is neutrally stable, then a discrepancy is still possible. Let $p_1p_2 - p_o + N_B(A_o,o) > o$, but $p_o - N_B(A_o,o) < o$; then the IDF stability technique predicts an unstable limit cycle while Loeb's criterion predicts a stable limit cycle. This situation is depicted in the root locus of Fig. 6.8 c) if $\sigma_A < o$ and $N_B(A_o,o) > p_o$.

The only possibility of Loeb's criterion and the IDF stability technique being in agreement for f(x) a hard spring nonlinearity occurs in the root locus of Fig. 6.8 c), when $\sigma_A < o$ and $N_B(A_o,o) < p_o$. Then the two stability techniques agree that a stable limit cycle exists.

6.2.1.3 Comments

Two basically different discrepancies are found for the case of L(s) with no zeros. The first kind of discrepancy is the situation where the DF system is neutrally stable ($p_2 > o$), Loeb's criterion predicts a stable limit cycle, but $N_B(A_o,o)$ is such that a root of the linear

system lies in the RHP. The IDF stability technique thus predicts an unstable limit cycle. This situation is very similar to the discrepancies found in second order nonconservative systems.

The second kind of discrepancy occurs when the DF system is unstable ($p_2 < o$) and, in fact, a root of the linear system always exists in the RHP. A discrepancy exists when Loeb's criterion predicts a stable limit cycle while the IDF stability technique is, of course, predicting an unstable limit cycle. The theoretical sufficient condition for instability, $p_2 < o$, then indicates that the IDF stability technique is correct in this situation. This second discrepancy possibility occurs because a third root, not present in second order systems, exists, and is accounted for, in the IDF stability technique.

A relationship is found between stability of oscillations and the root locus method applied to the linear system of Fig. 6.6 for the no zero case. The centre of asymptotes, $\sigma_A = \frac{p_1^{-1} + p_2^{-1} + p_3^{-1}}{3} = -\frac{p_2}{3}$, can be used as a stability criterion - $\sigma_A < o$ is a necessary condition for a stable limit cycle while $\sigma_A > o$ is a sufficient condition for an unstable limit cycle.

6.2.2 L(s) with One Zero

If L(s) has one zero then $q_2 = o$. Without loss of generality it can be assumed that $|q_1| = 1$.

6.2.2.1 Negative Feedback

With $q_1 = 1$ the negative feedback situation occurs. A pole-zero representation of L(s) would be

$$L(s) = \frac{s + q_o}{s^3+p_2s^2+p_1s+p_o} = \frac{s - z_1}{(s-p_1^{-1})(s-p_2^{-1})(s-p_3^{-1})} \qquad (6.33)$$

with $q_o = - z_1$ and the p_i given by 6.16. The DF conditions are now

$$Keq(A_o) = \frac{p_o - p_1 p_2}{p_2 - q_o} > o \ , \tag{6.34}$$

and

$$w_o^2 = \frac{p_o - p_1 q_o}{p_2 - q_o} > o \ . \tag{6.35}$$

The third root at the DF conditions is still $s_3 = - p_2$, and $p_o + q_o Keq(A_o) = p_2 w_o^2$. As in the no zero case, the DF system is neutrally stable if and only if $p_2 > o$ and unstable if and only if $p_2 < o$. Also, the necessary condition of 6.4 for a stable limit cycle is again $p_2 > o$, and the sufficient condition of 6.4 for an unstable limit cycle is $p_2 < o$. The root loci of Fig. 6.9 show some of the interesting cases in which DF oscillations are predicted.

Loeb's criterion, in analytical form, becomes

$$(p_2 - q_o)\ N_B(A_o,o) + p_1 p_2 - p_o > o \ (< o) \tag{6.36}$$

for a stable (unstable) limit cycle (see Appendix V). The IDF stability technique predicts a stable (unstable) limit cycle under the following conditions:

$$p_2 > o \ (< o), \tag{6.37}$$

$$(p_2 - q_o)\ N_B(A_o,o) + p_1 p_2 - p_o > o (< o), \tag{6.38}$$

and

$$p_o + q_o\ N_B(A_o,o) > o \ (< o). \tag{6.39}$$

Again, all three stability conditions are required for stability, but only one instability condition is required for instability.

If $p_2 < o$ the IDF stability technique predicts an unstable limit cycle, which is in agreement with the theoretical result. Loeb's criterion still predicts a stable limit cycle as long as the stability condition of 6.36 holds. This discrepancy is depicted in the root loci of Figs. 6.9 a), b), and c) if $p_o + q_o Keq(A_o) < o$, and in Fig. 6.9 d).

If $p_2 > o$, a discrepancy still exists when stability condition 6.36 and instability condition 6.39 are satisfied. Loeb's criterion predicts a stable limit cycle while the IDF stability technique predicts an unstable limit cycle. This discrepancy exists in the root loci of Figs. 6.9 a), b), and c) when $p_o + q_o\, Keq(A_o) > o$ and $p_o + q_o\, N_B(A_o,o) < o$.

6.2.2.2 Positive Feedback

If $q_1 = -1$ the positive feedback situation occurs. L(s) is expressed as

$$L(s) = \frac{-s + q_o}{s^3+p_2s^2+p_1s+p_o} = \frac{-(s - z_1)}{(s-p_1^1)(s-p_2^1)(s-p_3^1)}, \qquad (6.40)$$

with $q_o = z_1$ and the p_i given by 6.16. The DF conditions are

$$Keq(A_o) = \frac{p_1p_2 - p_o}{p_2 + q_o} > o \qquad (6.41)$$

and

$$w_o^2 = \frac{p_o + p_1\, q_o}{p_2 + q_o} > o. \qquad (6.42)$$

The third root at the DF conditions is $s_3 = -p_2$, and $p_o + q_oKeq(A_o) = p_2w_o^2$. Also, $p_2 > o$ remains a necessary condition for a stable limit cycle with $p_2 < o$ a sufficient condition for an unstable limit cycle. The root loci of Fig. 6.10 indicate some of the possibilities in which DF oscillations are predicted.

Loeb's criterion, in the analytical form (Appendix V), is now

$$-(p_2 + q_o)\, N_B(A_o,o) + p_1p_2 - p_o > o \ (< o) \qquad (6.43)$$

for a stable (unstable) limit cycle. For a stable (unstable) limit cycle the IDF stability technique requires

$$p_2 > o \ (< o), \qquad (6.44)$$

$$-(p_2 + q_o)\, N_B(A_o,o) + p_1p_2 - p_o > o \ (< o), \qquad (6.45)$$

and

$$p_o + q_o N_B(A_o,o) > o \ (< o), \tag{6.46}$$

with any one of the instability conditions sufficient for an unstable limit cycle, but all three stability conditions needed for a stable limit cycle.

Again, $p_2 < o$ implies an unstable limit cycle according to the IDF stability technique, and this is in agreement with the theoretical result. Loeb's criterion will predict a stable limit cycle as long as stability condition 6.43 is satisfied. This discrepancy is shown in the root loci of Figs. 6.10 a), b), and c). If $p_2 > o$, a discrepancy will still exist when stability condition 6.43 and instability condition 6.46 are satisfied - Loeb's criterion then predicts a stable limit cycle while the IDF stability technique predicts an unstable limit cycle. This discrepancy will exist in the root locus of Fig. 6.10 d) if $N_B(A_o,o) < - p_o/q_o$.

6.2.2.3 Comments

The two different kinds of discrepancy found in the no zero case are also found in the one zero case. In fact, most results for this case are very similar to those for the no zero case, including the root loci for DF oscillation situations. As in the no zero case, the DF system is neutrally stable if and only if $p_2 > o$ and unstable if and only if $p_2 < o$. Also, $p_2 < o$ remains a theoretical sufficient condition for instability, and this result is in agreement with the IDF stability technique prediction of an unstable limit cycle when $p_2 < o$.

6.2.3. L(s) With Two Zeros

If L(s) has two zeros then $q_2 \neq o$ and, without loss of generality, it can be assumed that $|q_2| = 1$.

6.2.3.1 Negative Feedback

With $q_2 = 1$ the negative feedback situation occurs and L(s) can be written as

$$L(s) = \frac{s^2 + q_1 s + q_o}{s^3 + p_2 s^2 + p_1 s + p_o} = \frac{(s-z_1)(s-z_2)}{(s-p_1)(s-p_2)(s-p_3)}, \quad (6.47)$$

with $q_1 = -(z_1 + z_2)$, $q_o = z_1 z_2$, and the p_i given in 6.16. The DF conditions of 6.13 and 6.14 become

$$Keq_{1,2} = -\frac{(p_1 - q_o + q_1 p_2)}{2 q_1} \pm \sqrt{\frac{(p_1 - q_o + q_1 p_2)^2}{4 q_1^2} - \frac{(p_1 p_2 - p_o)}{q_1}}, \quad (6.48)$$

with

$$\sqrt{\frac{(p_1 - q_o + q_1 p_2)^2}{4 q_1^2} - \frac{(p_1 p_2 - p_o)}{q_1}} > \left| \frac{p_1 - q_o + q_1 p_2}{2 q_1} \right| \quad (6.49)$$

implying a unique $Keq(A_o) > o$, and

$$w_o^2 = \frac{p_o + q_o Keq}{p_2 + Keq} = p_1 + q_1 Keq(A_o) > o. \quad (6.50)$$

The third root at the DF conditions is now $s_3 = -(p_2 + Keq)$, and $p_o + q_o Keq = (p_2 + Keq)(p_1 + q_1 Keq)$.

The exact necessary (sufficient) condition of 6.4 for a stable (unstable) limit cycle is now $p_2 + \overline{g[x^*(t)]} > o$ ($< o$). In terms of the DF approximate variational system, an approximate necessary condition for a stable limit cycle (6.9) becomes $p_2 + N_B(A_o, o) > o$, and an approximate sufficient condition for an unstable limit cycle (6.10) is $p_2 + N_B(A_o, o) < o$. From the Routh array (6.12), the DF system is neutrally stable if and only if $p_2 + Keq(A_o) > o$ ($s_3 < o$) and unstable if and only if $p_2 + Keq(A_o) < o$ ($s_3 > o$). The root loci of Fig. 6.11 show some of the important situations in which DF oscillations can exist.

The analytical form of Loeb's criterion (Appendix V) yields

$$q_1 N_B^2(A_o,o) + (p_1 + q_1p_2-q_o) N_B(A_o,o) + p_1p_2-p_o > o (< o) \quad (6.51)$$

for a stable (unstable) limit cycle. The IDF stability technique requires

$$p_2 + N_B(A_o,o) > o, \quad (6.52)$$

$$q_1 N_B^2(A_o,o) + (p_1 + q_1p_2-q_o) N_B(A_o,o) + p_1p_2-p_o > o, \quad (6.53)$$

and

$$p_o + q_o N_B(A_o,o) > o \quad (6.54)$$

for a stable limit cycle, and

$$p_2 + N_B(A_o,o) < o, \quad (6.55)$$

or

$$q_1 N_B^2(A_o,o) + (p_1+q_1p_2-q_o) N_B(A_o,o) + p_1p_2-p_o < o, \quad (6.56)$$

or

$$p_o + q_o N_B(A_o,o) < o \quad (6.57)$$

for an unstable limit cycle.

If the DF system is neutrally stable (p_2 + Keq > o), and the DF conditions are satisfied, then a discrepancy occurs when 6.52, 6.53, and 6.57 obtain or 6.53, 6.55, and 6.57 are satisfied. In either case, Loeb's criterion predicts a stable limit cycle while the IDF stability technique predicts an unstable limit cycle. This discrepancy is shown in the root locus of Fig. 6.11 a) with $N_B(A_o,o) < - p_o/q_o < Keq(A_o)$ and the root locus of Fig. 6.11 d) with $N_B(A_o,o) > - p_o/q_o > Keq(A_o)$.

If the DF system is unstable (p_2 + Keq < o) then a discrepancy occurs when 6.53, 6.55 and 6.57 obtain or 6.52, 6.53, and 6.57 are satisfied, with Loeb's criterion predicting a stable limit cycle while the IDF stability technique predicts an unstable limit cycle. This discrepancy is shown in Fig. 6.11 a) for $N_B(A_o,o) < Keq(A_o) < - p_o/q_o$, in Figs. 6.11b) and c) for $Keq(A_o) < N_B(A_o,o) < -p_o/q_o$, and in Fig. 6.11d) for $N_B(A_o,o) > Keq(A_o) > -p_o/q_o$. However, a situation is still possible for which the DF system is unstable but the IDF stability technique and

Loeb's criterion agree that a stable limit cycle exists. This occurs when 6.52, 6.53, and 6.54 are satisfied. Note that this situation does not occur in the no zero and one zero cases - there, an unstable DF system automatically implies an unstable limit cycle predicted by the IDF stability technique. This situation is shown in the root loci of Figs. 6.11 b) and c) for $Keq(A_o) < -p_o/q_o < N_B(A_o,o)$.

6.2.3.2 Positive Feedback

A positive feedback situation occurs for $q_2 = -1$. L(s) can be written as

$$L(s) = \frac{-s^2 + q_1 s + q_o}{s^3 + p_2 s^2 + p_1 s + p_o} = \frac{-(s-z_1)(s-z_2)}{(s-p_1^1)(s-p_2^1)(s-p_3^1)} \qquad (6.58)$$

with $q_1 = z_1 + z_2$, $q_o = -z_1 z_2$, and the p_i given in 6.16. The DF conditions are

$$Keq_{1,2} = -\frac{(p_1+q_o-q_1p_2)}{2q_1} \pm \sqrt{\frac{(p_1+q_o-q_1p_2)^2}{4q_1^2} - \frac{(p_o-p_1p_2)}{q_1}}, \qquad (6.59)$$

with

$$\sqrt{\frac{(p_1+q_o-q_1p_2)^2}{4q_1^2} - \frac{(p_o-p_1p_2)}{q_1}} > \left| \frac{p_1+q_o-q_1p_2}{2q_1} \right| \qquad (6.60)$$

implying a unique $Keq(A_o) > o$, and

$$w_o^2 = \frac{p_o + q_o Keq}{p_2 - Keq} = p_1 + q_1 Keq > o \; . \qquad (6.61)$$

The third root at the DF conditions is $s_3 = -(p_2 - Keq)$, and $p_o + q_o Keq = (p_2 - Keq)(p_1 + q_1 Keq)$.

The exact necessary (sufficient) condition of 6.4 for a stable (unstable) limit cycle is $p_2 - \overline{g[x^*(t)]} > o$ ($< o$). From the DF approximate variational system an approximate necessary condition for a stable

limit cycle is $p_2 - N_B(A_o,o) > o$, and an approximate sufficient condition for an unstable limit cycle is $p_2 - N_B(A_o,o) < o$. The DF system is unstable (neutrally stable) if and only if $p_2 - Keq(A_o) < o \quad (> o)$. The root loci of Fig. 6.12 show some of the important situations in which DF oscillations exist for this case.

The analytical Loeb's criterion (Appendix V) is now

$$-q_1 N_B^2(A_o,o) + (-p_1+q_1p_2-q_o)\, N_B(A_o,o) + p_1p_2-p_o > o(<o) \qquad (6.62)$$

for a stable (unstable) limit cycle, while the IDF stability technique requires

$$p_2 - N_B(A_o,o) > o\ , \qquad (6.63)$$

$$q_1\, N_B^2(A_o,o) + (-p_1 + q_1p_2-q_0)\, N_B(A_o,o) + p_1p_2-p_o > o\ , \qquad (6.64)$$

and

$$p_o + q_o\, N_B(A_o,o) > o \qquad (6.65)$$

for a stable limit cycle, and

$$p_2 - N_B(A_o,o) < o\ , \qquad (6.66)$$

or

$$q_1 N_B^2(A_o,o) + (-p_1+q_1p_2-q_o)\, N_B(A_o,o) + p_1p_2-p_o < o\ , \qquad (6.67)$$

or

$$p_o + q_o\, N_B(A_o,o) < o \qquad (6.68)$$

for an unstable limit cycle.

When the DF system is neutrally stable (p_2-Keq $> o$) a discrepancy occurs if 6.63, 6.64, and 6.68 obtain or 6.64, 6.66 and 6.68 are satisfied. Loeb's criterion predicts a stable limit cycle while the IDF stability technique predicts an unstable limit cycle. The root locus of Fig.6.12 c) with $N_B(A_o,o) < -p_o/q_o < Keq(A_o)$ illustrates this situation.

Conditions 6.63, 6.64, and 6.68 or 6.64, 6.66 and 6.68 also imply a discrepancy when the DF system is unstable (p_2 - Keq $< o$) - again Loeb's

criterion predicts a stable limit cycle while the IDF stability technique predicts an unstable limit cycle. This discrepancy is shown in Figs. 6.12 a) and b) for $Keq(A_o) > N_B(A_o,o) > -p_o/q_o$, in Fig. 6.12 c) for $N_B(A_o,o) < Keq(A_o) < -p_o/q_o$, and in Fig. 6.12 d) for $N_B(A_o,o) > Keq(A_o) > -p_o/q_o$. There is also the possibility of the DF system being unstable with 6.63, 6.64, and 6.65 holding, so that Loeb's criterion and the IDF stability technique agree that a stable limit cycle exists. This situation is shown in the root loci of Figs. 6.12 a) and b) for $Keq(A_o) > -p_o/q_o > N_B(A_o,o)$.

6.2.4 Comments

A detailed comparison of Loeb's criterion and the IDF stability technique for third order systems leads to a classification of DF situations as follows:

i) The DF system is neutrally stable, and Loeb's criterion and the IDF stability technique are in agreement as to the stability or instability of the limit cycle.

ii) The DF system is neutrally stable, and Loeb's criterion predicts a stable limit cycle while the IDF stability technique predicts an unstable limit cycle.

iii) The DF system is unstable, and Loeb's criterion predicts a stable limit cycle while the IDF stability technique predicts an unstable limit cycle.

iv) The DF system is unstable, and Loeb's criterion and the IDF stability technique agree that a stable limit cycle exists.

v) The DF system is unstable, and Loeb's criterion and the IDF stability technique agree that an unstable limit cycle exists.

The class ii), iii), and iv) situations are of particular interest,

and specific examples will be studied in detail in the next section. The discrepancies of classes ii) and iii) exist for L(s) with two, one, or no zeros, whereas the situation of class iv) only occurs for L(s) with two zeros. A particular example of this last situation will demonstrate that a stable limit cycle can exist even if the DF system is unstable.

6.3 A Detailed Study of Examples

Since the results for L(s) with one zero are very similar to those for L(s) with no zeros, only this latter, less complicated linear plant is used for examples demonstrating class ii) and iii) discrepancies.

6.3.1 Example I

The system configuration is shown in Fig. 6.13 with p_1^1 and K as variables and $p_2^1, p_3^1 = -1 \pm j3$. The root locus for fixed p_1^1 and K variable would appear as in Fig. 6.7 c). Application of the results of subsection 6.2.1 yields a class iii) situation when $5 > p_1^1 > 2$, a class ii) situation when $2 > p_1^1 > .901$, and a class i) situation (with a stable limit cycle predicted) when $p_1^1 < .901$.

Simulation of the system with p_1^1 variable yields a stable limit cycle, corresponding to the DF prediction, for $p_1^1 < .901$. However, with $p_1^1 > .901$ a biased sinusoid form of stable limit cycle is observed. The bias-plus-sinusoid DIDF technique can be used to predict the existence of this form of limit cycle in the system. Conditions 3.19 and 3.20 then become

$$\frac{4K\sqrt{1-(B/A)^2}}{\pi A} \cdot \frac{1}{2p_1^{1\,2} - 4p_1^1 + 20} = -1 \; ; \; w_o^2 = 10 - 2p_1^1 \tag{6.69}$$

and

$$\frac{2K \sin^{-1}(B/A)}{\pi B} \cdot \frac{1}{10p_1^1} = -1 \; ; \quad \left|\frac{B}{A}\right| < 1 \tag{6.70}$$

respectively. These two equations can be combined to yield

$$B/A \cdot \frac{\sqrt{1 - (B/A)^2}}{\sin^{-1}(B/A)} = \frac{{p_1}^1{}^2 - 2{p_1}^1 + 10}{10{p_1}^1} \quad . \tag{6.71}$$

Now

$$\lim_{B/A \to o} \left\{ \frac{B/A \cdot \sqrt{1-(B/A)^2}}{\sin^{-1}(B/A)} \right\} = 1, \tag{6.72}$$

and solution of the RHS of 6.71 yields ${p_1}^1 = .901, 11.099$ when $B/A = o$. The region of a predicted biased sinusoid limit cycle then begins at ${p_1}^1 = .901$ and corresponds to the transition point between a class i) situation and a class ii) situation. This is not unexpected since, in terms of the root locus of Fig. 6.7 c), the transition point corresponds to the third root located at the origin in the IDF system. The IDF system can then support a bias of zero value in the presence of the DF sinusoid.

In Table 6.1 predictions using the bias-plus-sinusoid DIDF technique are compared with simulation measurements, and percentage errors are calculated.

Table 6.1 DIDF Calculations and Measurements for Example I

${p_1}^1$	$A_{o_{DIDF}}$	$A_{o_{exact}}$	% Error	$B_{o_{DIDF}}$	$B_{o_{exact}}$	% Error	$w_{o_{DIDF}}$	$w_{o_{exact}}$	% Error
.901	1.00	1.007	.70%	.00	.007	100.0%	2.864	2.92	1.92%
.95	1.00	1.034	3.29%	.28	.168	66.7%	2.846	2.86	.49%
1.00	1.00	1.046	4.40%	.39	.341	14.37%	2.828	2.82	.11%
1.05	1.00	1.033	3.19%	.46	.425	8.24%	2.811	2.80	.57%
1.10	1.00	1.037	3.57%	.51	.497	2.62%	2.793	2.76	1.20%
1.15	1.00	1.042	4.03%	.55	.547	.55%	2.775	2.70	2.78%
1.20	1.00	1.055	5.21%	.59	.589	.17%	2.757	2.68	2.87%

The percentage errors are reasonable, and it can be safely concluded that the bias-plus-sinusoid DIDF technique is predicting the existing limit cycle in the range $.901 < p_1^1 < 1.2$. However, an interesting phenomenon occurs for $p_1^1 > 1.2$ - a new form of stable limit cycle exists for p_1^1 slightly above 1.2, but when $p_1^1 = 1.37$ is attained, no limit cycle, stable or unstable, exists. Fig. 6.17 shows recordings of the biased sinusoid limit cycle for $p_1^1 = 1.2$ and the new waveform, which is clearly no longer a simple biased sinusoid, for $p_1^1 = 1.25$. The bias-plus-sinusoid DIDF technique predicts the existence of biased sinusoid limit cycles right up to $p_1^1 = 5.0$, but the simulation indicates that the prediction is valid only up to $p_1^1 = 1.20$.

Comparison of the stability techniques for this system indicates that in the class i) situation, with $p_1^1 < .901$, Loeb's criterion and the IDF stability technique are correct in predicting a stable limit cycle. In the class ii) region ($2 > p_1^1 > .901$), a DF predicted oscillation no longer exists, but a stable biased sinusoid limit cycle does exist in the portion, $.901 < p_1^1 < 1.20$, of this region. The IDF stability technique was not applied to a biased limit cycle in order to predict its stability. For $.901 < p_1^1 < 2$ Loeb's criterion predicts a stable limit cycle while the IDF stability technique predicts an unstable limit cycle. However, both approximate stability techniques refer to the unbiased DF predicted oscillation, which no longer exists in this region. As p_1^1 increases above .901 the DF oscillation becomes a progressively poorer approximation to the biased limit cycle (since bias value increases with p_1^1). The IDF stability technique apparently reflects this poor approximation by predicting that the unbiased DF oscillation is unstable (given the discrepancy situation).

For the class iii) situation ($5 > p_1^1 > 2$), Loeb's criterion still predicts a stable limit cycle while the IDF stability technique predicts an unstable limit cycle, but no actual limit cycle exists. A theoretical sufficient condition for an unstable limit cycle exists in this region, but this condition is not valid when no limit cycle exists. Sometimes the existence of an unstable limit cycle cannot be recognized easily in a system without reversing time, and, in a practical sense, is not much different than absence of a limit cycle. In this sense, the IDF stability technique may have some validity in predicting an unstable limit cycle. Loeb's criterion is definitely incorrect in predicting a stable limit cycle in this region.

6.3.2. Example II

This system configuration is shown in Fig. 6.14 with p_1^1 and K variable and $p_2^1 = -2, p_3^1 = 1$. The root locus for fixed p_1^1 and variable K is as shown in Fig. 6.7 d). In terms of p_1^1, the results of subsection 6.2.1 (with negative feedback) yield a class ii) situation when $-2.0 > p_1^1 > -3.5615$, and a class i) situation (with a stable limit cycle predicted) when $p_1^1 < -3.5615$.

Simulation of the system with p_1^1 variable indicates a stable, unbiased limit cycle existing for $p_1^1 < -3.04$ and no limit cycle existing in the region $-2.0 > p_1^1 > -3.04$. Table 6.2 shows DF calculations, experimental measurements, and percentage errors for values of p_1^1 in the interval $-4.0 \leqslant p_1^1 \leqslant -3.04$.

Percentage errors in both amplitude and frequency are seen to be quite high and increasing as p_1^1 approaches -3.04. It should be noted that $w_{o_{DF}}^2 = -p_1^1 - 2$, so that $w_{o_{DF}}$ decreases to zero as p_1^1 approaches -2. The situation described here is identical to the situation found in

Table 6.2 DF Calculations and Measurements for Example II

p_1^1	$A_{o_{DF}}$	$A_{o_{exact}}$	% Error	$w_{o_{DF}}$	$w_{o_{exact}}$	% Error
-4.0	1.00	1.150	13.05%	1.414	1.256	12.6%
-3.75	1.00	1.158	13.65%	1.323	1.120	18.1%
-3.50	1.00	1.177	15.05%	1.225	.982	24.8%
-3.25	1.00	1.202	16.80%	1.120	.785	42.7%
-3.04	1.00	1.285	22.20%	1.020	.560	82.1%

second order systems corresponding to System Configuration I, where a class ii) region exists when $w_{o_{DF}}^2$ is made sufficiently small. The root loci of Figs. 5.12 and 6.7d) are alike near the origin, and the same general trend in percentage errors holds. The motion appears to be approaching a separatrix with $w_{o_{exact}}$ going to zero as p_1^1 approaches - 3.04. Also, the waveform is observed to become more like a square wave as p_1^1 approaches - 3.04 in value. The same interpretation of the IDF stability technique result appears to apply - in the class ii) region the DF approximation is becoming progressively worse as p_1^1 approaches the limit at -2, and this is reflected by the IDF stability technique predicting an unstable limit cycle in this region.

6.3.3 Example III

This system configuration is shown in Fig. 6.15 with p_1^1 and K again variable and p_2^1, $p_3^1 = 1 \pm j5$. The root locus for fixed p_1^1 and variable K is given in Fig. 6.8 c). The results of subsection 6.2.1 for positive feedback yield a class iii) situation when $p_1^1 > -2$, class ii) situations when $-2 > p_1^1 > -3.77$ or $-6.897 > p_1^1 > -13$, and a class i) situation (with a stable limit cycle predicted) when $-3.77 > p_1^1 > -6.897$. Simulation indicates a stable, unbiased limit cycle for $-3.77 > p_1^1 > -9.3$,

a stable, biased sinusoid limit cycle for $-3.77 < p_1^1 < -2.23$, and an unstable, biased sinusoid limit cycle for $-1.895 < p_1^1 < -.9615$.

Application of the bias-plus-sinusoid DIDF technique yields

$$\frac{8AK}{3\pi}\left\{\left[1+\frac{1}{2}(B/A)^2\right]\sqrt{1-(B/A)^2}+\frac{3}{2}\frac{B}{A}\sin^{-1}(B/A)\right\}\cdot\frac{1}{2p_1^{1\,2}+4p_1^1+52}=1, \tag{6.73}$$

with $w_o^2 = 2p_1^1 + 26$, and

$$\frac{A^2K}{\pi B}\left\{\left[1+2(B/A)^2\right]\sin^{-1}(B/A)+3\frac{B}{A}\sqrt{1-(B/A)^2}\right\}\cdot\frac{1}{-26p_1^1}=1 \tag{6.74}$$

for $|B/A| \leqslant 1$; or

$$\frac{2BK}{2p_1^{1\,2}+4p_1^1+52}=1\ ,\ w_o^2=2p_1^1+26\ , \tag{6.75}$$

and

$$\frac{(B^2+A^2/2)\,K}{B}\cdot\frac{1}{-26p_1^1}=1 \tag{6.76}$$

for $|B/A| \geqslant 1$. Combination of 6.73 and 6.74 yields

$$\frac{8B/(3A)\left\{\left[1+\frac{1}{2}(B/A)^2\right]\sqrt{1-(B/A)^2}+\frac{3B}{2A}\sin^{-1}(B/A)\right\}}{\left[1+2(B/A)^2\right]\sin^{-1}(B/A)+\frac{3B}{A}\sqrt{1-(B/A)^2}}=\frac{2p_1^{1\,2}+4p_1^1+52}{-26p_1^1} \tag{6.77}$$

with $|B/A| \leqslant 1$, and 6.75 and 6.76 together yield

$$\frac{4}{2+A^2/B^2}=\frac{2p_1^{1\,2}+4p_1^1+52}{-26p_1^1} \tag{6.78}$$

with $|B/A| \geqslant 1$. Two regions of existence of a biased sinusoid limit cycle are predicted - the interval $-3.77 < p_1^1 < -.9615$, and the interval $-13 < p_1^1 < -6.897$. The beginning ($B/A = o$) of the regions,

- 3.77 and - 6.897 respectively, in each case corresponds to the transition point between a class i) situation and a class ii) situation. The reason for this has already been explained.

One interesting result of the simulation is the fact that a biased sinusoid limit cycle does not exist in the interval $-13 < p_1^1 < -6.897$, although the bias-plus-sinusoid DIDF technique predicts a biased sinusoid solution in this interval. On the other hand, the prediction of a biased sinusoid limit cycle in the interval $-3.77 < p_1^1 < -.9615$ is correct. However, a difference in the bias-plus-sinusoid DIDF technique when applied in each of the two intervals can be found to exist. If no bias is assumed (B = o) then 6.77 can be written as

$$\frac{2}{3} = \frac{2{p_1^1}^2 + 4\, p_1^1 + 52}{-26\, p_1^1} . \qquad (6.79)$$

Fig. 6.16 shows a graph of the error, RHS - 2/3, between the two sides of 6.79 for values of p_1^1 in each of the two intervals. It is seen that the RHS of 6.79 is less sensitive to variations in p_1^1 in the interval $-13 < p_1^1 < -6.897$ than in the interval $-3.77 < p_1^1 < -.9615$. Also, $w_{o_{DF}}$ is decreasing to zero as p_1^1 approaches - 13. These two differences between the two intervals must account for the existence of biased sinusoid limit cycles in the one interval but not in the other. Of course, the bias-plus-sinusoid DIDF technique is only approximate, and there is no guarantee that limit cycles predicted by it actually exist.

Table 6.3 shows a comparison of DF calculations and experimental results in the interval $-3.77 > p_1^1 > -13$.

In the class ii) region $-6.897 > p_1^1 > -13$, both frequency and amplitude errors increase as p_1^1 approaches - 13. As in other situations of this sort, with $w_{o_{DF}}$ going to zero, the limit cycle is approaching a

Table 6.3 DF Calculations and Measurements for Example III

p_1^1	$A_{o_{DF}}$	$A_{o_{exact}}$	% Error	$w_{o_{DF}}$	$w_{o_{exact}}$	% Error
-3.77	2.000	2.001	.05%	4.295	4.360	1.49%
-4.00	2.000	2.001	.05%	4.243	4.200	1.02%
-5.00	2.000	2.006	.30%	4.000	4.050	1.23%
-6.00	2.000	2.011	.55%	3.742	3.700	1.13%
-6.90	2.002	2.025	1.14%	3.493	3.480	.37%
-7.15	2.005	2.032	1.33%	3.421	3.400	.62%
-7.42	2.065	2.101	1.71%	3.340	3.305	1.06%
-7.78	2.130	2.170	1.84%	3.231	3.142	2.84%
-8.21	2.185	2.249	2.84%	3.094	2.950	4.89%
-8.69	2.270	2.366	4.05%	2.936	2.735	7.35%
-9.21	2.360	2.545	7.12%	2.752	2.165	27.10%
-9.30	2.400	2.616	8.26%	2.720	1.910	42.50%

separatrix indicated by $w_{o_{exact}}$ approaching zero (the waveform is approaching a square wave). In this case, the separatrix condition is close to $p_1^1 = -9.30$, according to simulation (the separatrix cannot be approached any closer due to noise inherent in the system simulation). For $-9.3 > p_1^1 > -13$ no limit cycle exists. The IDF stability technique again seems to indicate this situation of poorer DF approximation in the class ii) region by predicting an unstable limit cycle. This example is then quite similar to the second order example of System Configuration II in this class ii) region.

Table 6.4 gives a comparison of bias-plus-sinusoid DIDF calculations and experimental results in the interval $-3.77 < p_1^1 < -1.08$. Clearly, the errors are quite reasonable, so there is no doubt that the bias-plus-sinusoid DIDF technique is predicting the existing limit cycle. In the region $-3.77 < p_1^1 < -2.228$ a stable, biased limit cycle exists, but

for p_1^1 slightly larger than - 2.228 the waveform changes. Fig. 6.18 shows recordings of the biased sinusoid waveform for p_1^1 = - 2.228, and the new waveform for p_1^1 = - 2.1.

Table 6.4 DIDF Calculations and Measurements for Example III

p_1^1	$A_{o_{DIDF}}$	$A_{o_{exact}}$	% Error	$B_{o_{DIDF}}$	$B_{o_{exact}}$	% Error	$w_{o_{DIDF}}$	$w_{o_{exact}}$	% Error
-3.770	2.000	2.001	.05%	.00	.024	100.00%	4.295	4.36	1.49%
-3.637	2.000	1.988	.60%	.20	.158	26.60%	4.330	4.36	.69%
-3.342	2.000	2.020	.99%	.40	.380	5.26%	4.395	4.42	.56%
-2.992	2.000	2.010	.50%	.60	.593	1.18%	4.472	4.49	.40%
-2.658	2.000	2.003	.15%	.80	.797	.38%	4.550	4.55	.00%
-2.363	2.000	2.002	.10%	1.00	.997	.30%	4.615	4.62	.11%
-2.228	2.000	2.010	.50%	1.10	1.105	.45%	4.640	4.65	.21%
-1.895	1.000	1.006	.60%	.70	.701	.07%	4.710	4.83	2.48%
-1.723	1.000	1.006	.60%	.80	.800	.00%	4.748	4.83	1.70%
-1.565	1.000	1.007	.70%	.90	.903	.33%	4.785	4.83	.93%
-1.454	1.000	1.009	.84%	1.00	.999	.05%	4.805	4.83	.52%
-1.303	1.000	1.018	1.82%	1.20	1.186	1.22%	4.838	4.83	.17%
-1.204	1.000	1.026	2.48%	1.40	1.386	1.05%	4.857	4.83	.56%
-1.142	1.000	1.023	2.24%	1.60	1.586	.88%	4.870	4.83	.83%
-1.106	1.000	1.016	1.53%	1.80	1.792	.42%	4.877	4.83	.97%
-1.080	1.000	1.020	1.91%	2.00	1.988	.63%	4.885	4.93	.91%

In the interval - 2.06 $< p_1^1 <$ - 1.895 no limit cycle exists, and in the region - 1.895 $< p_1^1 <$ - .9615 an unstable, biased sinusoid limit cycle exists. Note that a sufficient condition for an unstable limit cycle is $p_1^1 > -2$, and, in this case, the condition is almost a necessary one as well.

Again the IDF stability technique seems to indicate a change in the DF oscillation when a class i) to class ii) transition ($p_1^1 <$ - 3.77 to $p_1^1 >$ - 3.77) occurs. In this case the change is from an unbiased limit cycle to a biased limit cycle. The DF approximation then becomes very

poor in approximating a biased waveform, and the IDF stability technique predicts an unstable limit cycle in order to indicate this.

Example III is rather interesting in that, with two class ii) regions, it exhibits the two types of behaviour in the class ii) region illustrated by Examples I and II, but with positive feedback and a different type of nonlinearity.

6.3.4 Examples IV, V, VI and VII

These examples are used to illustrate the existence of a stable limit cycle, predicted by the DF method, when the DF system is unstable. System configurations IV and V are shown in Figs. 6.19 and 6.20 with z_1 and K as variables. The root loci for these systems are those of Figs. 6.11 b) and c) respectively. Application of the results of subsection 6.2.3 to Example IV yields a class iii) situation when $z_1 > -.58$, a class iv) situation when $-.58 > z_1 > -1.1$, and a class i) situation (with a stable limit cycle predicted) when $z_1 < -1.1$. Application to Example V yields a class iii) situation when $z_1 > -.65$, a class iv) situation when $-.65 > z_1 > -1.3$, and a class i) situation (with a stable limit cycle predicted) when $z_1 < -1.3$.

Simulation of Example IV indicates that no limit cycle exists for $z_1 > -.75$, but rather a stable bias level or equilibrium point exists. For $z_1 < -.75$, stable, unbiased limit cycles exist as predicted by the DF method. Table 6.5 compares DF calculations and experimental results for $z_1 < -.75$. The errors are reasonable for the DF method, although the frequency errors are rather high. Fig. 6.23 a) shows the waveform for $z_1 = -1$, and the fact that it is not symmetrical is probably related to the high DF frequency error. All three limit cycles measured in Table 6.5 correspond to class iv) situations in which the DF system

Table 6.5 DF Calculations and Measurements for Example IV

z_1	$A_{o_{DF}}$	$A_{o_{exact}}$	% Error	$w_{o_{DF}}$	$w_{o_{exact}}$	% Error
-.8	1.000	.989	1.16%	8.225	7.66	7.37%
-.9	1.000	.988	1.21%	8.290	7.85	5.60%
-1.0	1.000	.991	.96%	8.349	7.85	6.36%

is unstable.

Simulation of Example V shows that a stable equilibrium point, but no limit cycle, exists for $z_1 > -.88$, and a stable, unbiased, DF predicted limit cycle exists for $z_1 < -.88$. Table 6.6 shows DF calculations and experimental results for $z_1 < -.88$. The errors are again reasonable, with the frequency errors slightly higher than in the case of Example IV. The two limit cycles measured in Table 6.6 correspond to class iv) situations with the DF system unstable.

Table 6.6 DF Calculations and Measurements for Example V

z_1	$A_{o_{DF}}$	$A_{o_{exact}}$	% Error	$w_{o_{DF}}$	$w_{o_{exact}}$	% Error
-.9	1.000	1.008	.80%	10.25	9.25	10.8%
-1.0	1.000	1.010	1.04%	10.32	9.25	11.5%

System configurations VI and VII are shown in Figs. 6.21 and 6.22 with the root loci given by Figs. 6.12 a) and b) respectively. These two systems are the complements of Examples IV and V for the positive feedback case. The results of subsection 6.2.3 for Example VI yield a class iii) situation when $z_1 > 1.63$, a class iv) situation when $1.63 > z_1 > .9$, and a class i) situation (with a stable limit cycle predicted) when $z_1 < .9$. For Example VII a class iii) situation exists when $z_1 > 2.9$,

a class iv) situation exists when $2.9 > z_1 > 1.5$, and a class i) situation (with a stable limit cycle predicted) exists when $z_1 < 1.5$.

Simulation of Example VI indicates that a stable equilibrium point, but no limit cycle, exists for $z_1 > 1.43$, and DF predicted stable limit cycles exist for $z_1 < 1.43$. Fig. 6.23 b) shows the limit cycle waveform for $z_1 = 1$. Simulation of Example VII shows that a stable equilibrium point, but no limit cycle, exists for $z_1 > 2.1$, and DF predicted stable limit cycles exist for $z_1 < 2.1$. Table 6.7 compares DF calculations and experimental results for Examples VI and VII. Both amplitude and frequency errors are rather high, with the amplitude errors substantially higher here than for Examples IV and V.

Table 6.7 DF Calculations and Measurements for Examples VI and VII

z_1	$A_{o_{DF}}$	$A_{o_{exact}}$	% Error	$w_{o_{DF}}$	$w_{o_{exact}}$	% Error
VI:						
1.0	1.000	1.140	12.3%	6.10	5.71	6.83%
1.2	.990	1.129	12.3%	6.22	5.71	8.93%
1.4	.975	1.115	12.6%	6.32	5.71	10.70%
VII:						
2.0	1.000	1.167	14.3%	6.58	5.71	15.20%

The large DF errors and distorted waveforms of limit cycles in Examples IV, V, VI and VII are due to the poor filtering characteristics of a third order linear plant with two zeros. The IDF stability technique correctly predicts stable limit cycles even for an unstable DF system. However, the limit of the stable limit cycle region is not predicted exactly, probably due to the rather large DF errors.

6.4 Existence of Unstable Limit Cycles

Experimental evidence seems to indicate that there is no real guideline when it comes to determining whether or not an unstable limit cycle exists. The IDF stability technique, in conjunction with the root locus method, does not seem to correlate existence of unstable limit cycles with the modes or root locations in the IDF system. For example, it would be expected that if the complex conjugate root pair moved into the RHP in the IDF system then this would correspond to an unstable limit cycle situation. It certainly corresponds to a class i) situation with an unstable limit cycle predicted by both Loeb's criterion and the IDF stability technique. However, an unstable limit cycle does not always exist under these circumstances. Examples I and II with $f(x) = x^3$ (see the root loci of Figs. 6.7 c) and d)) are situations in which unstable limit cycles are predicted by the DF method, as above, but do not exist.

A sufficient condition for an unstable limit cycle does not guarantee existence of an (unstable) limit cycle. Consider a system configuration with the root locus of Fig. 6.8 b), $p_2^1 = 1$, $p_3^1 = 2$, and $p_1^1 > 2$. The sufficient condition of 6.4 holds so that, if a limit cycle exists, it must be unstable. If the nonlinearity is the hard spring $f(x) = x^3$ then no limit cycle exists whereas, if the nonlinearity is the soft spring $f(x) = \text{sgn}(x)$, then an unstable limit cycle exists. Table 6.8 compares DF calculations and experimental results for the unstable limit cycle. It is seen that the errors are quite reasonable, so that the DF predicted unstable limit cycle actually exists.

The complex conjugate root pair moving into the RHP in the IDF system is not a sufficient condition for existence of an unstable limit cycle, and it may not be a necessary condition either. The system

Table 6.8 DF Calculations and Measurements for an Unstable Limit Cycle

p_1^1	$A_{o_{DF}}$	$A_{o_{exact}}$	% Error	$w_{o_{DF}}$	$w_{o_{exact}}$	% Error
2.0	1.274	1.314	3.04%	2.828	2.86	1.12%
3.0	1.274	1.320	3.48%	3.317	3.30	.51%
4.0	1.274	1.322	3.63%	3.742	3.70	1.13%

situation just described seems to suggest that it is a necessary condition since, for $f(x) = \text{sgn}(x)$, the root pair moves into the RHP while for $f(x) = x^3$ the root pair moves into the LHP. Further experimental evidence to support this is found by simulating Example III for $p_1^1 > -.9615$. No limit cycle exists for $f(x) = x\,|x|$, which corresponds to a root pair moving into the LHP. However, an unstable limit cycle, predicted by the DF method, does exist for $f(x) = \text{sgn}(x)$, and this corresponds to the root pair moving into the RHP. Table 6.9 shows a comparison of DF calculations and experimental results for the unstable limit cycle of Example III with $f(x) = \text{sgn}(x)$. The errors are fairly small and verify that the limit cycle corresponds to the DF predicted one.

Table 6.9 DF Calculations and Measurements for the Unstable Limit Cycle of Example III

p_1^1	$A_{o_{DF}}$	$A_{o_{exact}}$	% Error	$w_{o_{DF}}$	$w_{o_{exact}}$	% Error
-.9615	1.000	1.009	.89%	4.910	4.83	1.66%
0.00	1.000	1.013	1.28%	5.099	5.03	1.37%
1.00	1.000	1.015	1.48%	5.292	5.24	.99%

For $p_1^1 < -.9615$ there is a region in which an unstable, biased sinusoid limit cycle exists for both $f(x) = x\,|x|$ and $f(x) = \text{sgn}(x)$. The situation for $f(x) = x\,|x|$ is then a case where the root pair is

not in the RHP and yet an unstable limit cycle exists. However, the fact that the limit cycle is biased means that it does not correspond to the DF predicted limit cycle. Thus it may be that a necessary condition for an unstable DF predicted limit cycle is that the root pair moves into the RHP.

6.5 Conclusions

There are a number of possible situations in third order systems in which Loeb's criterion and the IDF stability technique can disagree. Disagreement always occurs with Loeb's criterion predicting stability while the IDF stability technique predicts instability. Simulation of typical systems indicates two distinct possibilities that occur when a discrepancy arises.

The first possibility is identical to what happens in second order systems in the same situation. In the parameter region where the IDF stability technique predicts an unstable limit cycle (a class ii) situation) the actual stable limit cycle is approaching a separatrix. The frequency error in the DF method grows without bound as the separatrix is approached.

In the second possibility, when a class ii) situation occurs, the actual stable limit cycle is biased and predicted by the bias-plus-sinusoid DIDF technique. In both possibilities the interpretation is that the DF predicted limit cycle is becoming an increasingly poorer approximation to the actual limit cycle, and this is indicated by the IDF stability technique predicting instability for the DF predicted limit cycle. Thus the IDF stability technique is considered not entirely incorrect in these situations because the existing stable limit cycle does not really correspond closely to the DF predicted limit cycle.

A theoretical sufficient condition for an unstable limit cycle can hold with Loeb's criterion predicting a stable limit cycle. However, no example could be found illustrating an unstable DF predicted limit cycle with Loeb's criterion predicting stability. It may be that DF predicted unstable limit cycles only occur when Loeb's criterion and the IDF stability technique predict instability due to the root pair moving into the RHP in the IDF system.

It has been demonstrated that stable, DF predicted limit cycles can exist when the DF system is unstable. The IDF stability technique does a reasonably good job of predicting the existence of this situation.

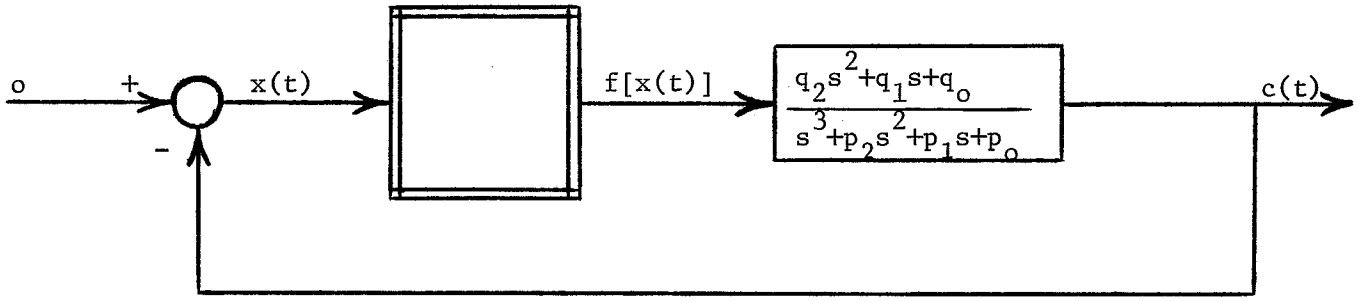

Fig. 6.1 GENERAL THIRD ORDER NONLINEAR SYSTEM

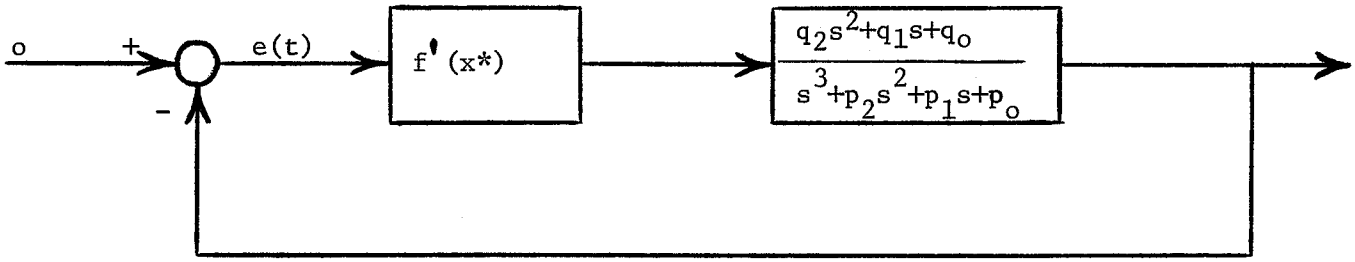

Fig. 6.2 THIRD ORDER VARIATIONAL SYSTEM

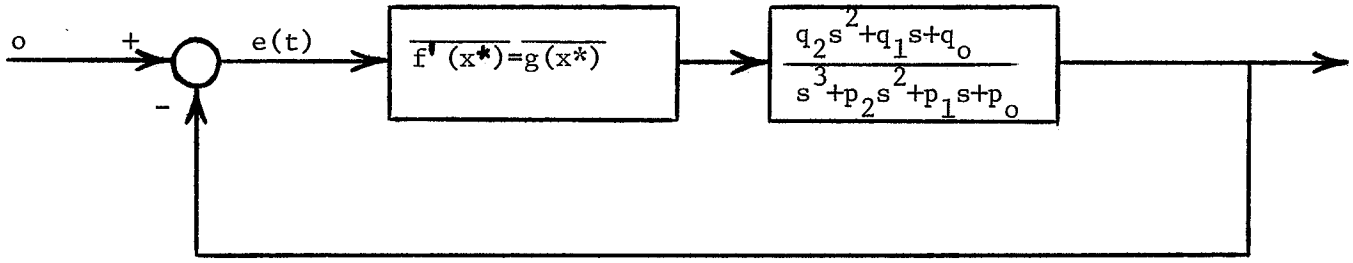

Fig. 6.3 TIME-AVERAGED THIRD ORDER VARIATIONAL SYSTEM

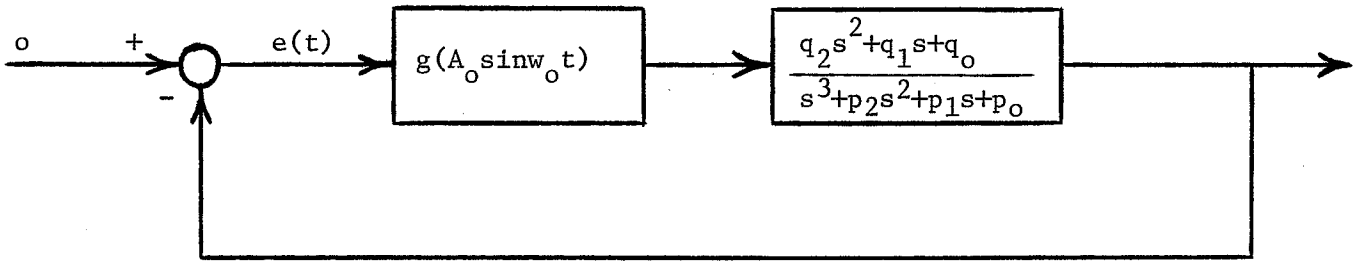

Fig. 6.4 DF APPROXIMATE VARIATIONAL SYSTEM

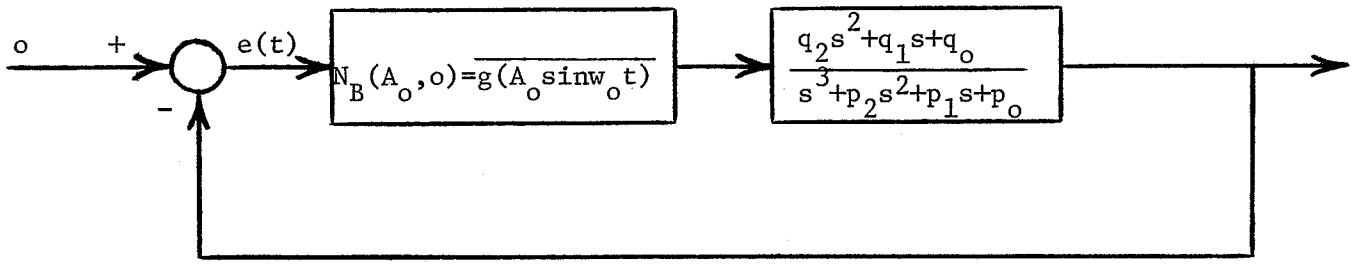

Fig. 6.5 TIME-AVERAGED DF APPROXIMATE VARIATIONAL SYSTEM

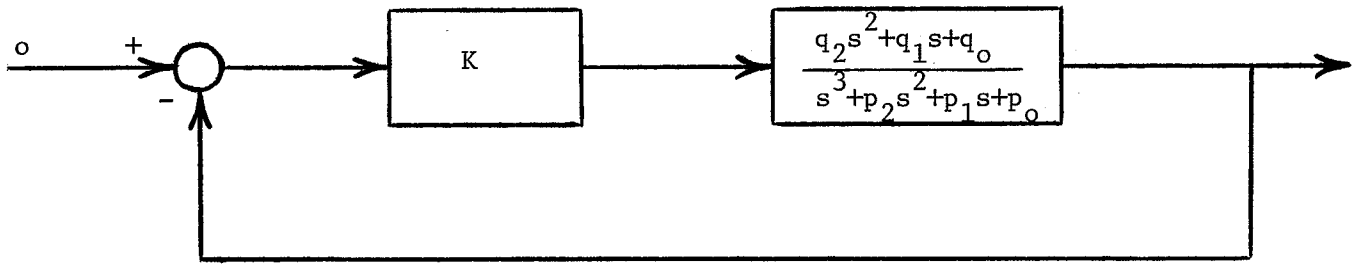

Fig. 6.6 LINEAR SYSTEM FOR DF AND STABILITY ANALYSIS

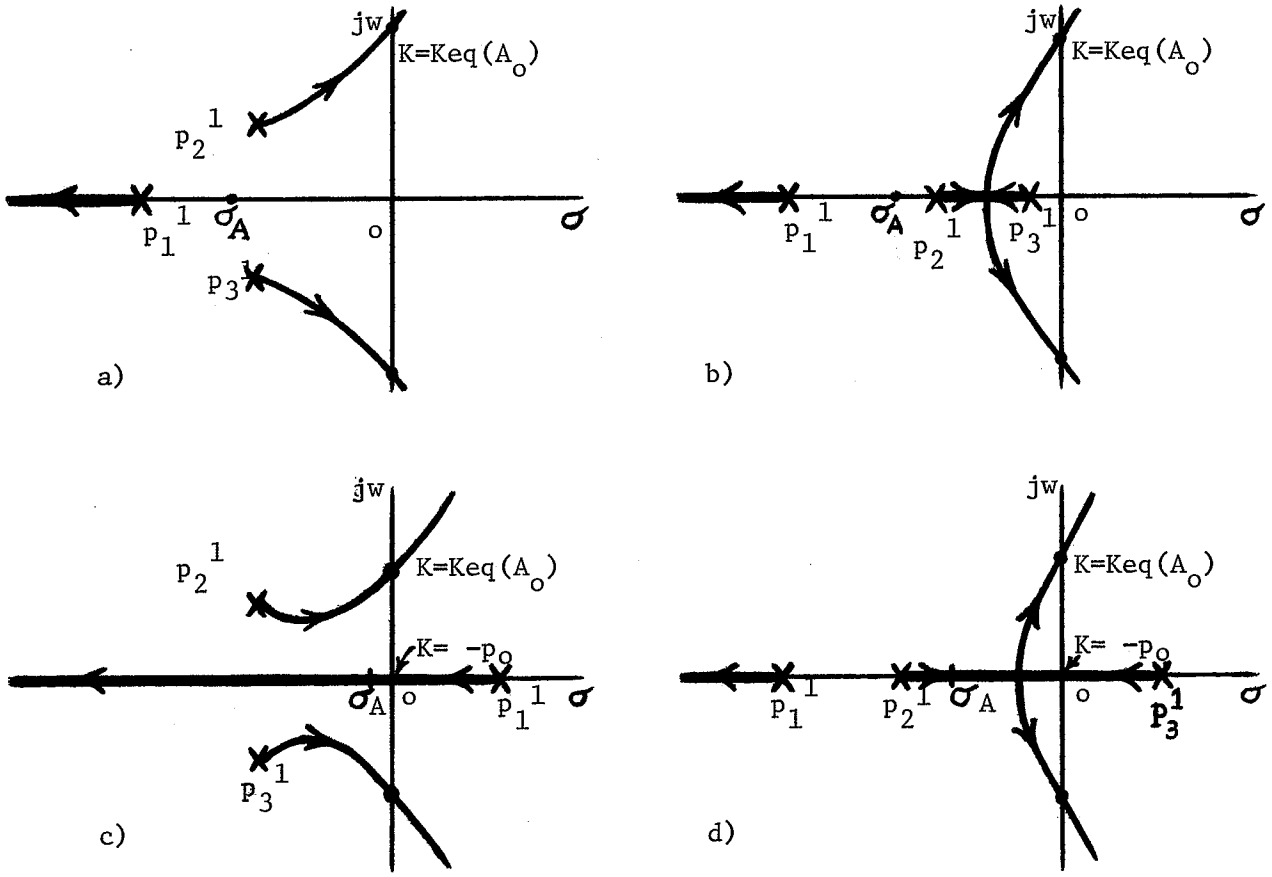

Fig. 6.7 ROOT LOCI FOR L(s) WITH NO ZEROS AND NEGATIVE FEEDBACK

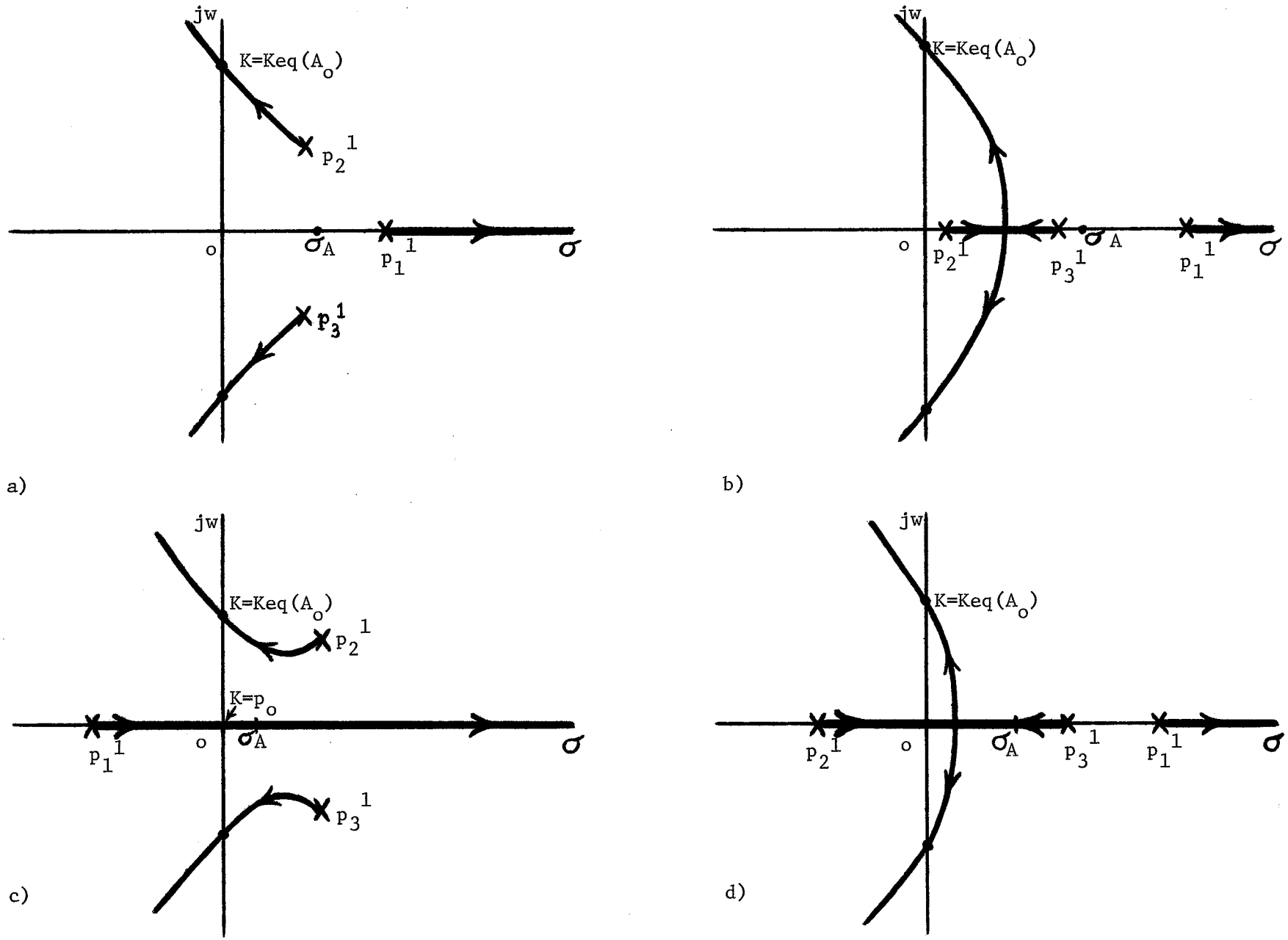

Fig. 6.8 ROOT LOCI FOR L(s) WITH NO ZEROS AND POSITIVE FEEDBACK

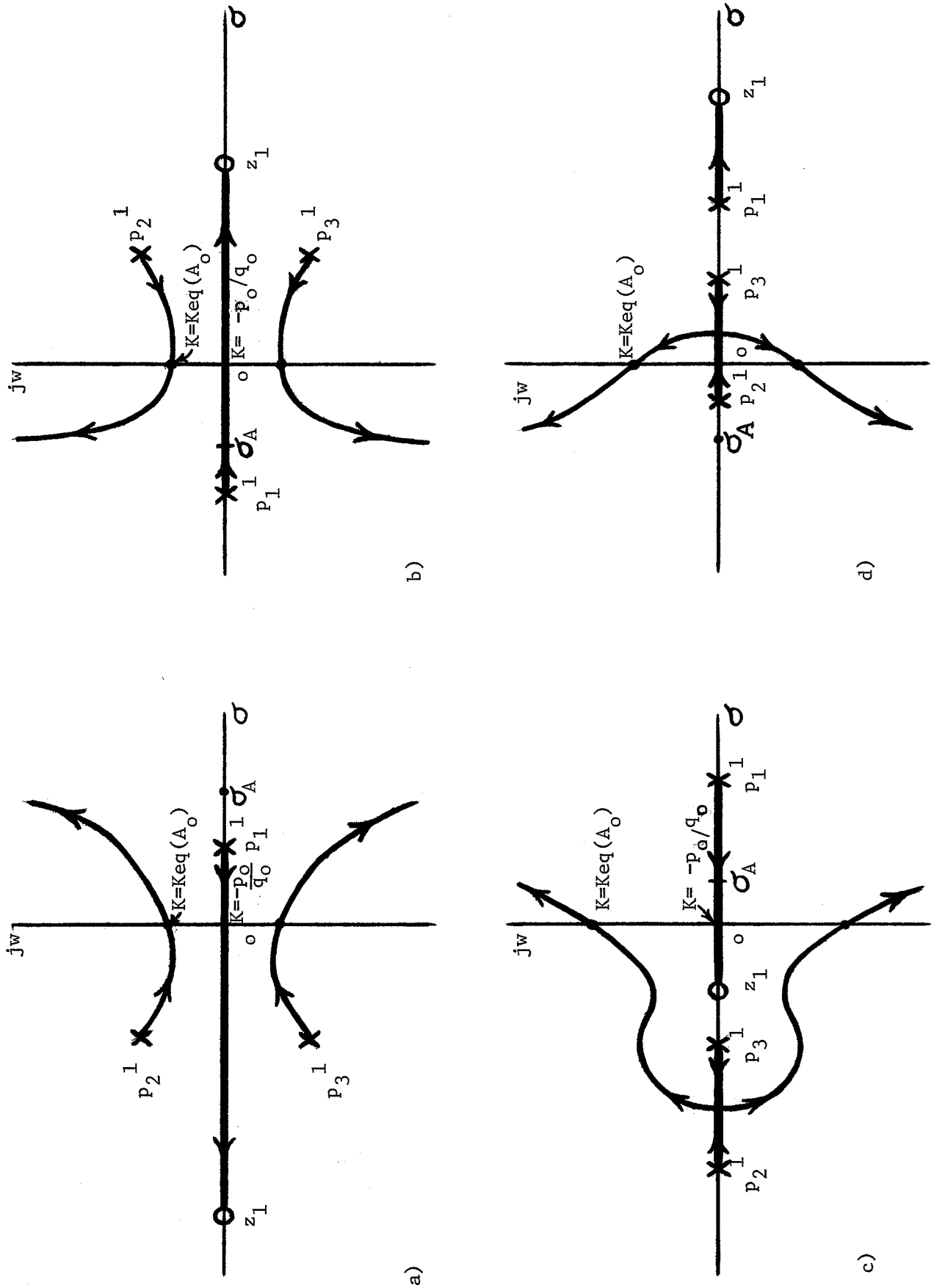

Fig. 6.9 ROOT LOCI FOR L(s) WITH ONE ZERO AND NEGATIVE FEEDBACK

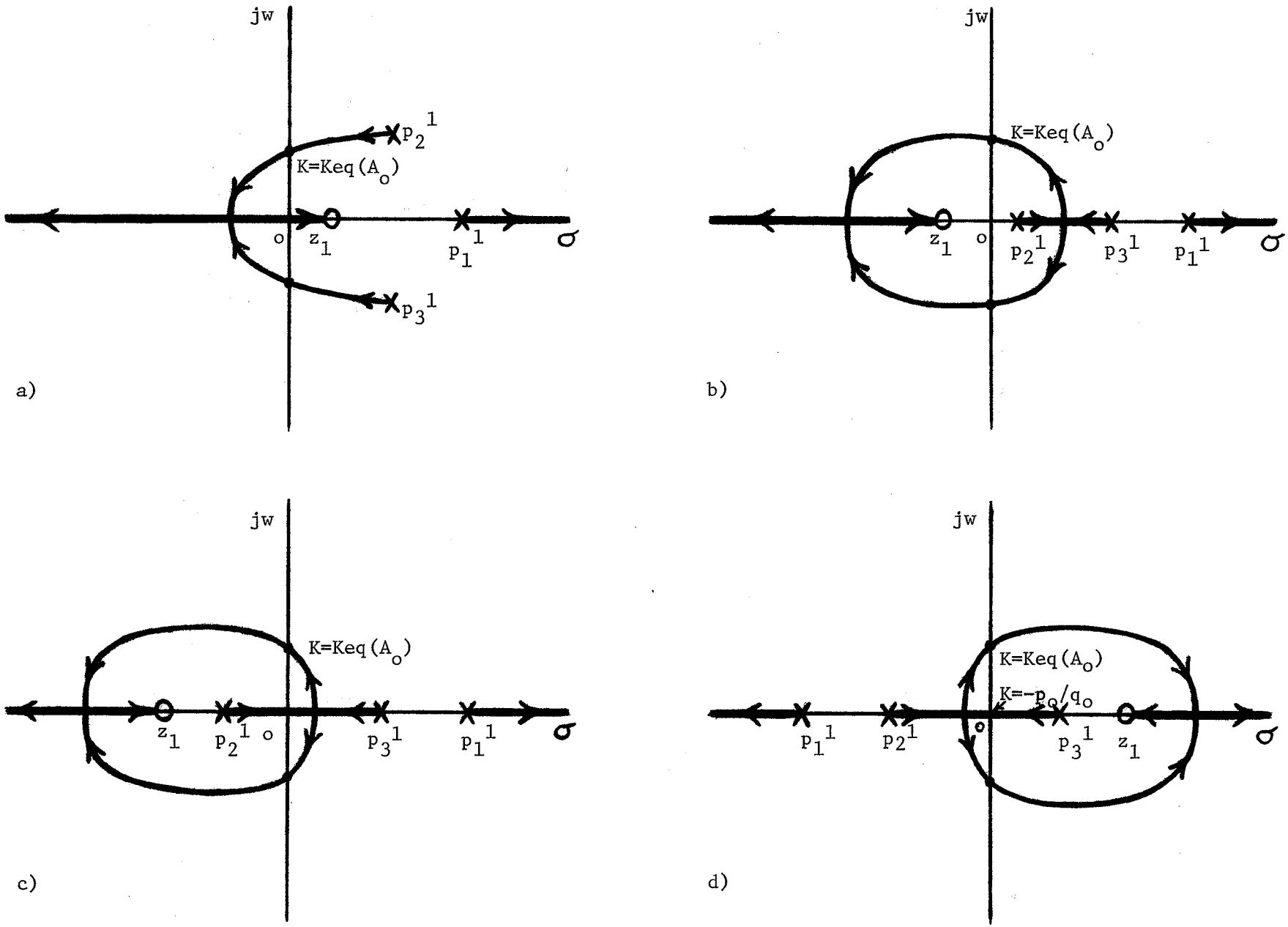

Fig. 6.10 ROOT LOCI FOR L(s) WITH ONE ZERO AND POSITIVE FEEDBACK

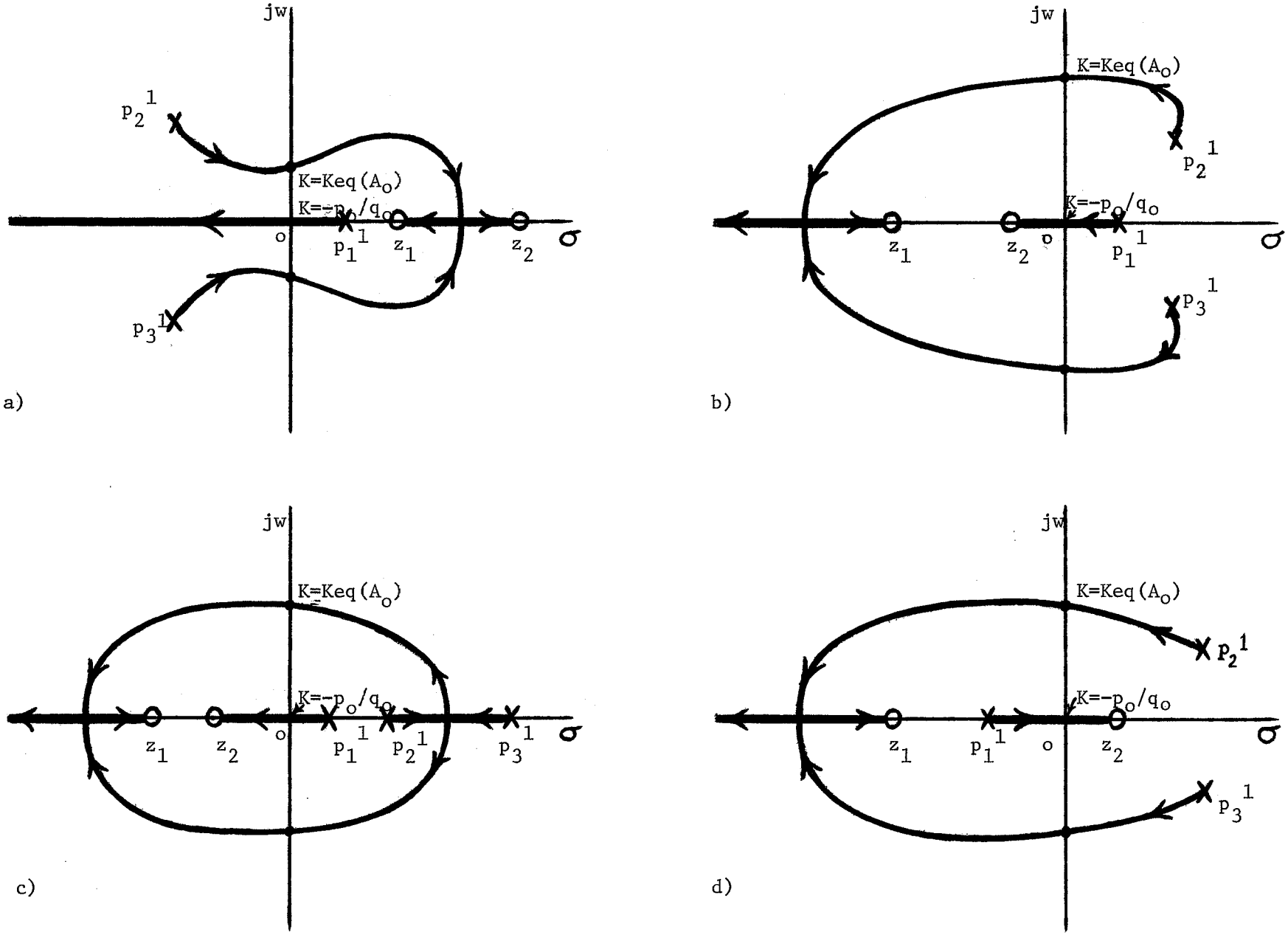

Fig. 6.11 ROOT LOCI FOR L(s) WITH TWO ZEROS AND NEGATIVE FEEDBACK

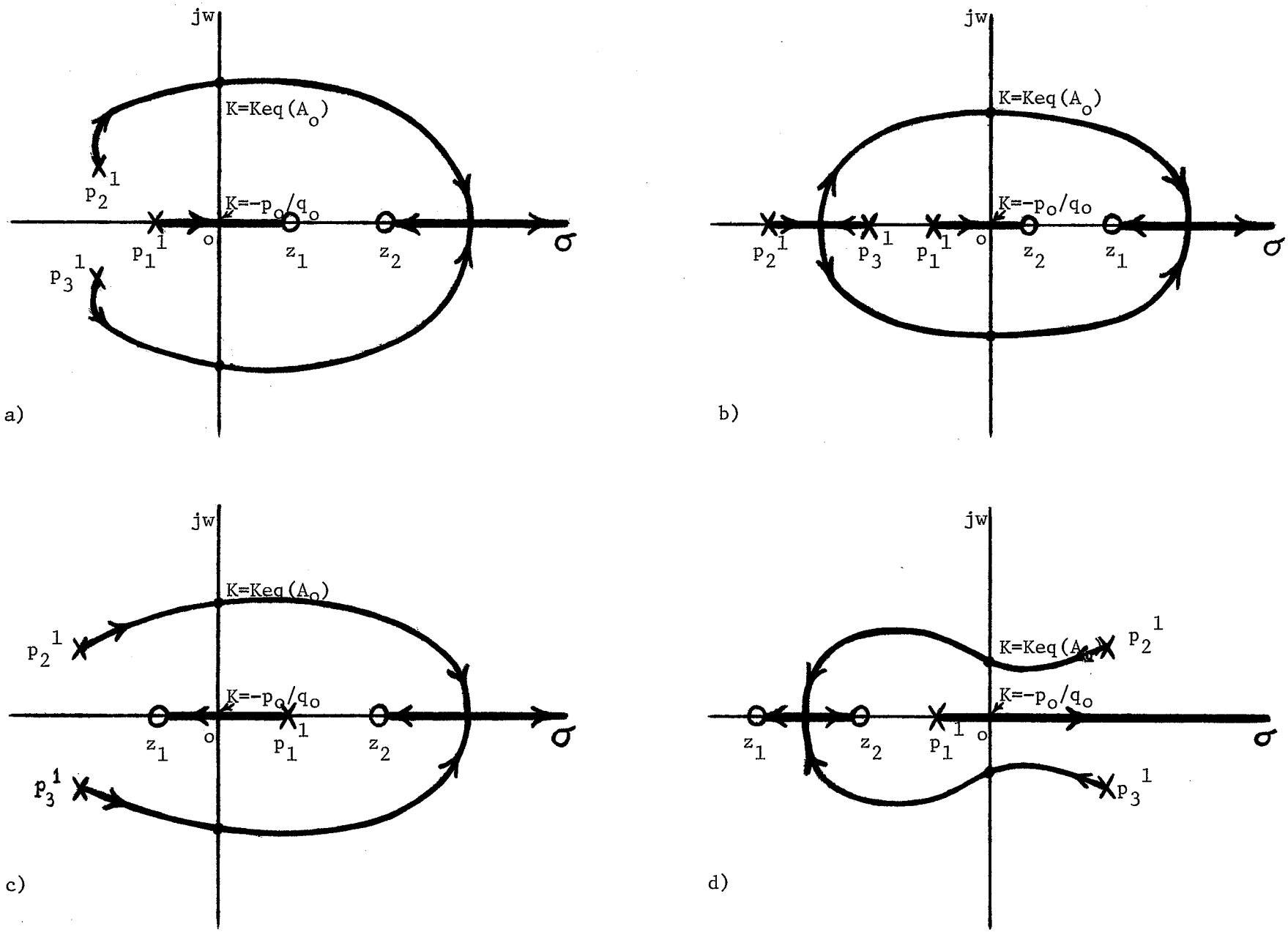

Fig. 6.12 ROOT LOCI FOR L(s) WITH TWO ZEROS AND POSITIVE FEEDBACK

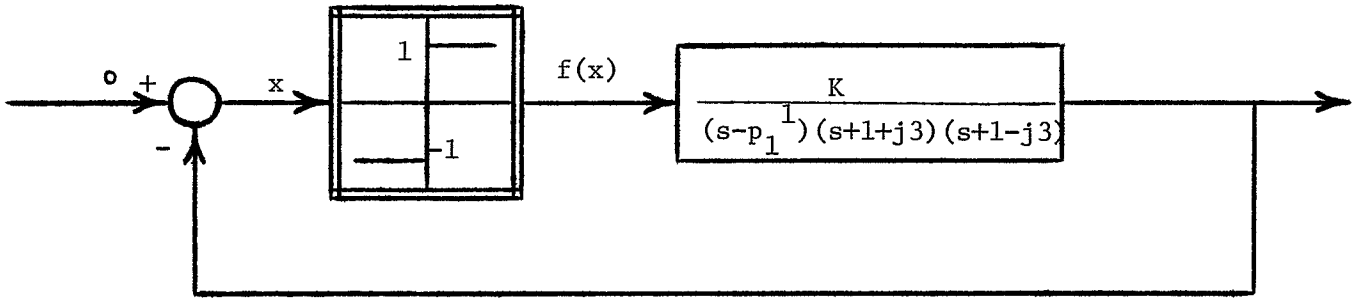

Fig. 6.13 EXAMPLE I

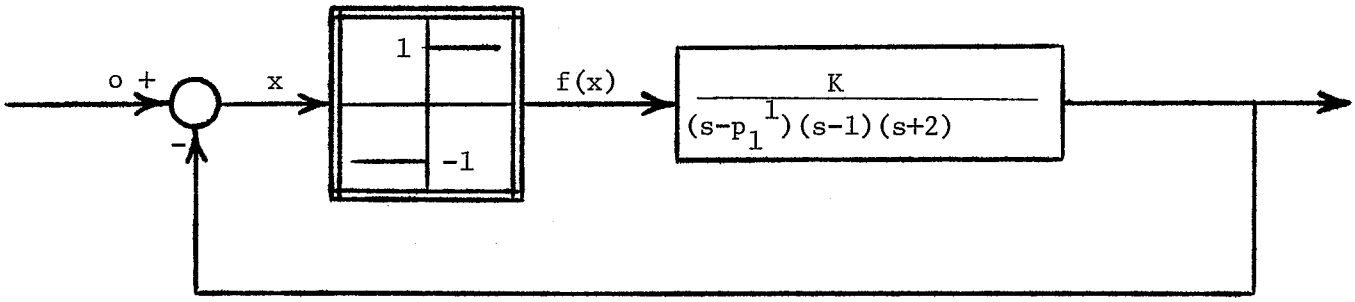

Fig. 6.14 EXAMPLE II

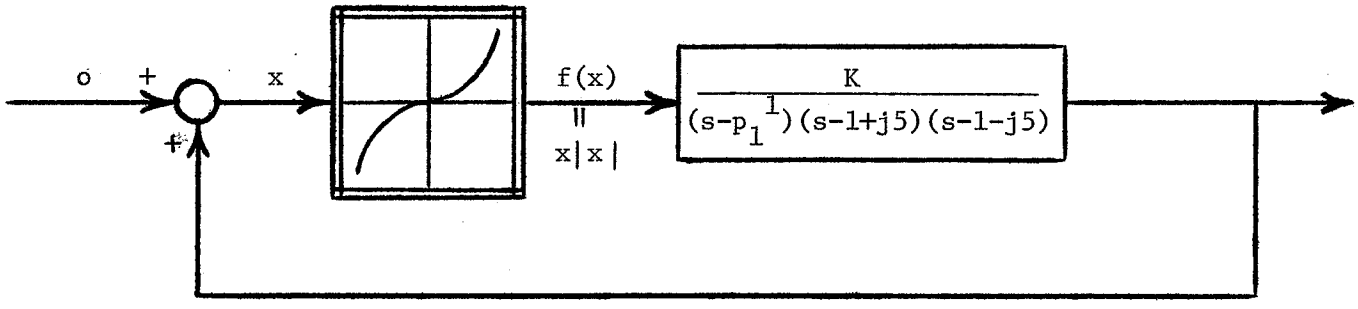

Fig. 6.15 EXAMPLE III

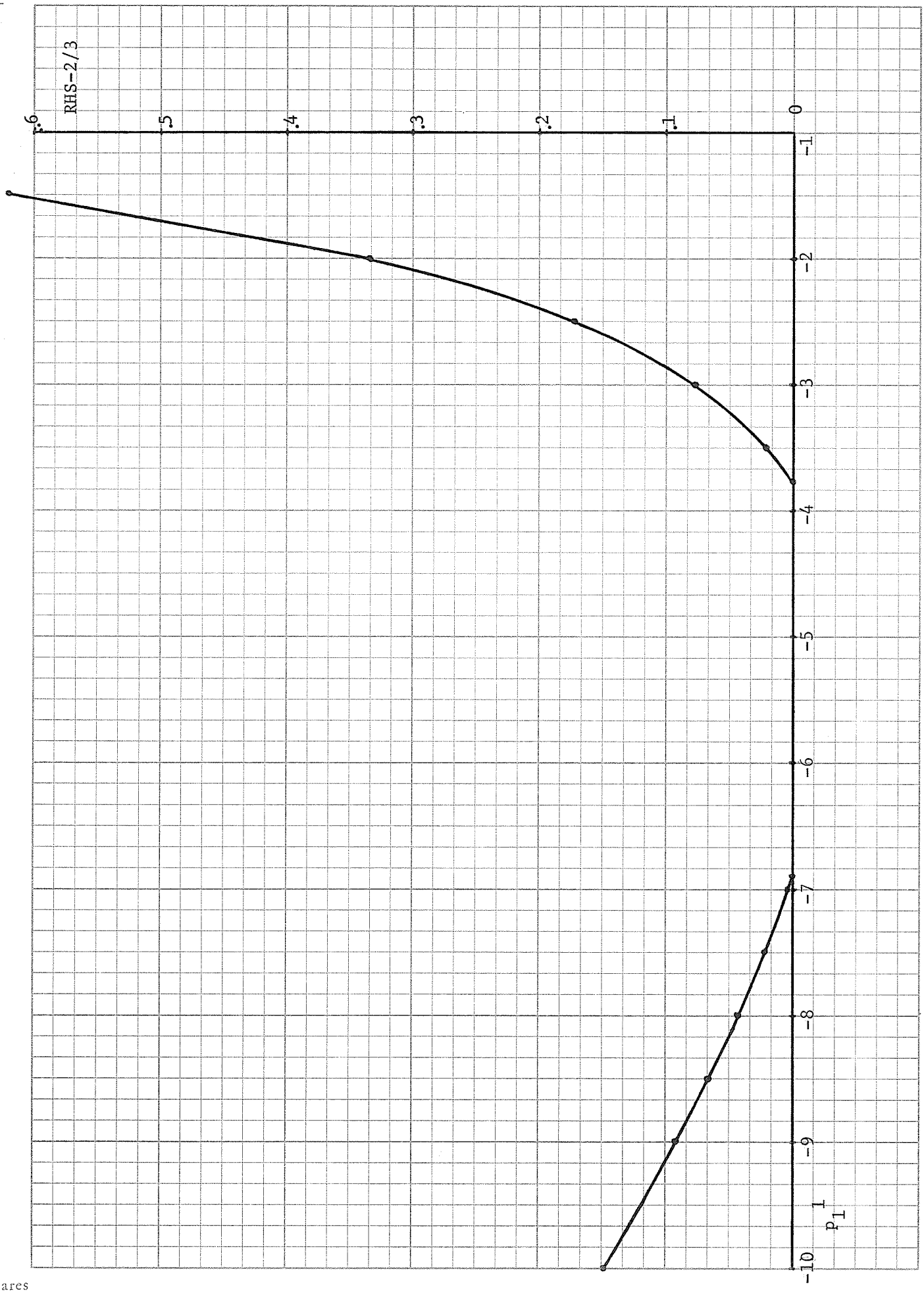

Fig. 6.16 GRAPH OF RHS-2/3 IN 6.79

Squares
he Inch

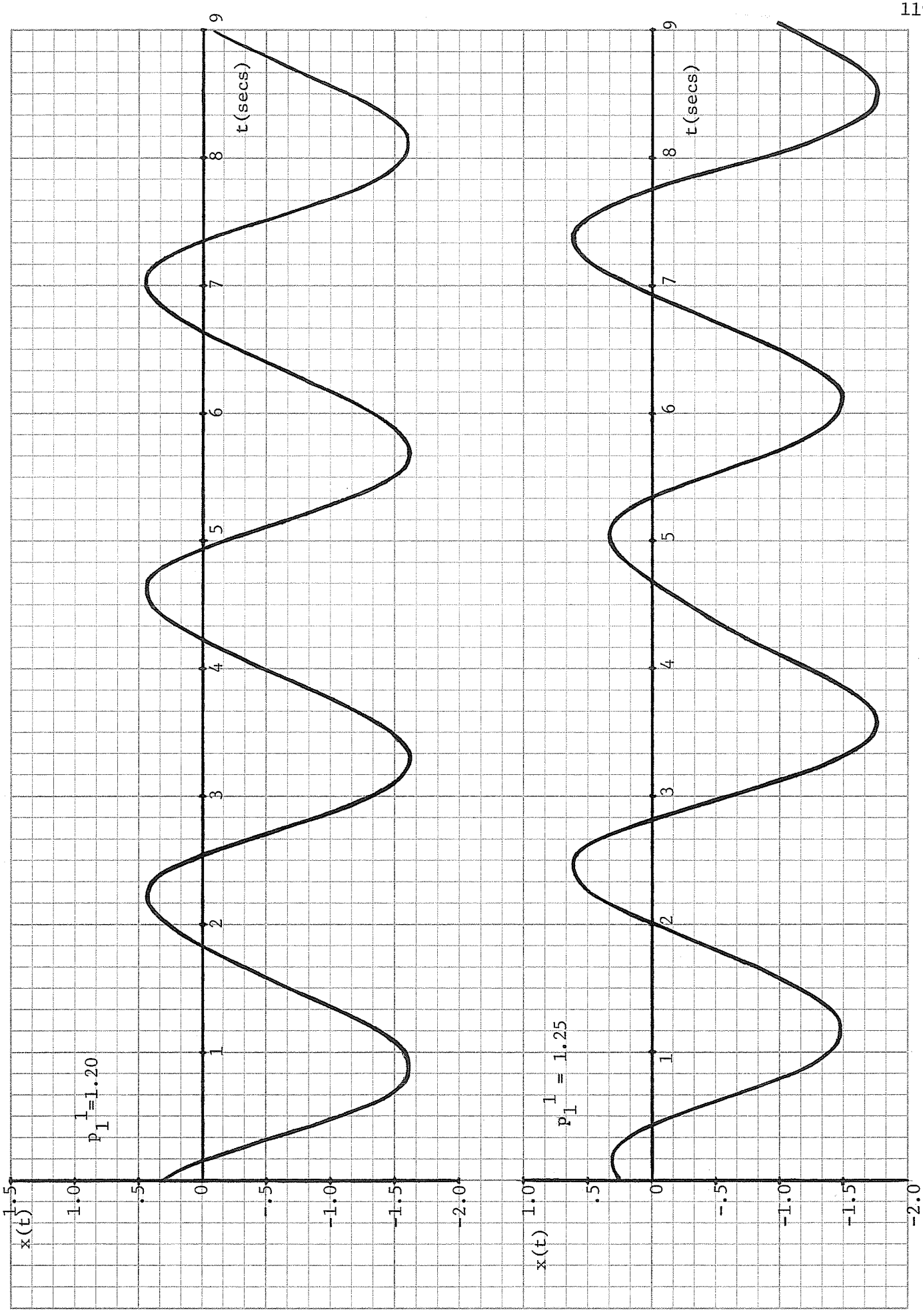

Fig. 6.17 WAVEFORM RECORDINGS FOR EXAMPLE I

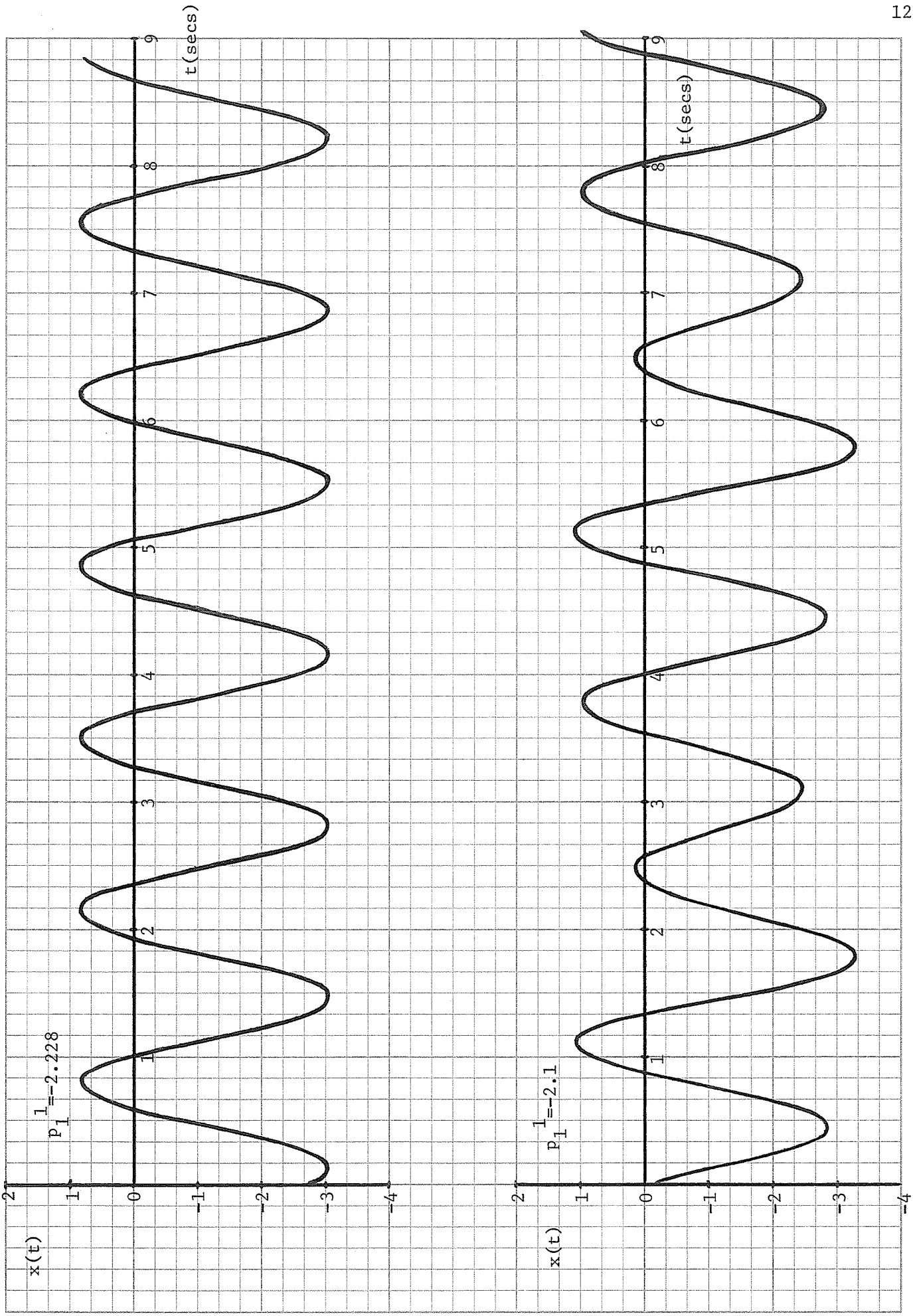

Fig. 6.18 WAVEFORM RECORDINGS FOR EXAMPLE III

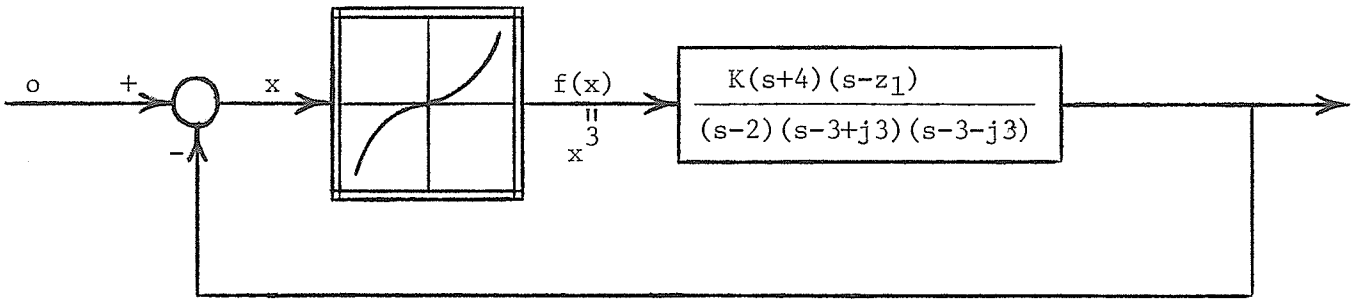

Fig. 6.19 EXAMPLE IV

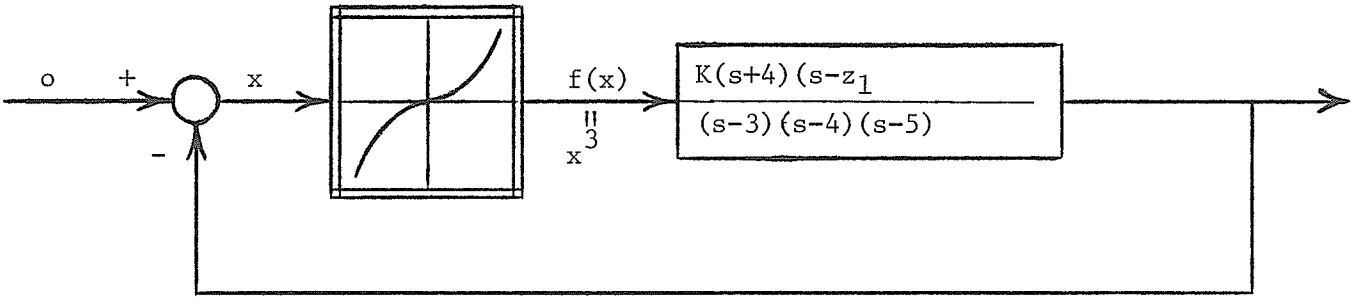

Fig. 6.20 EXAMPLE V

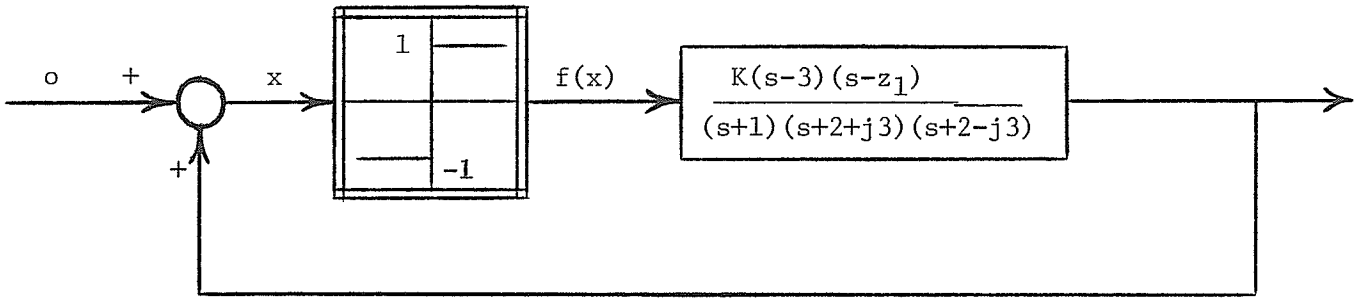

Fig. 6.21 EXAMPLE VI

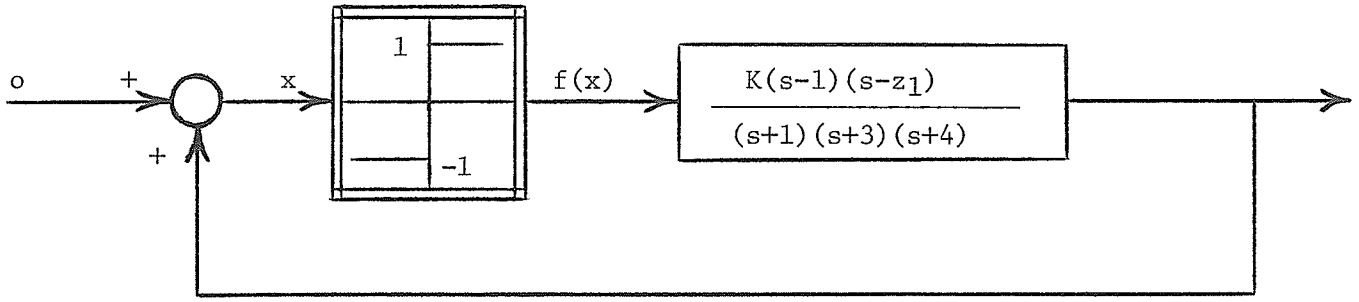

Fig. 6.22 EXAMPLE VII

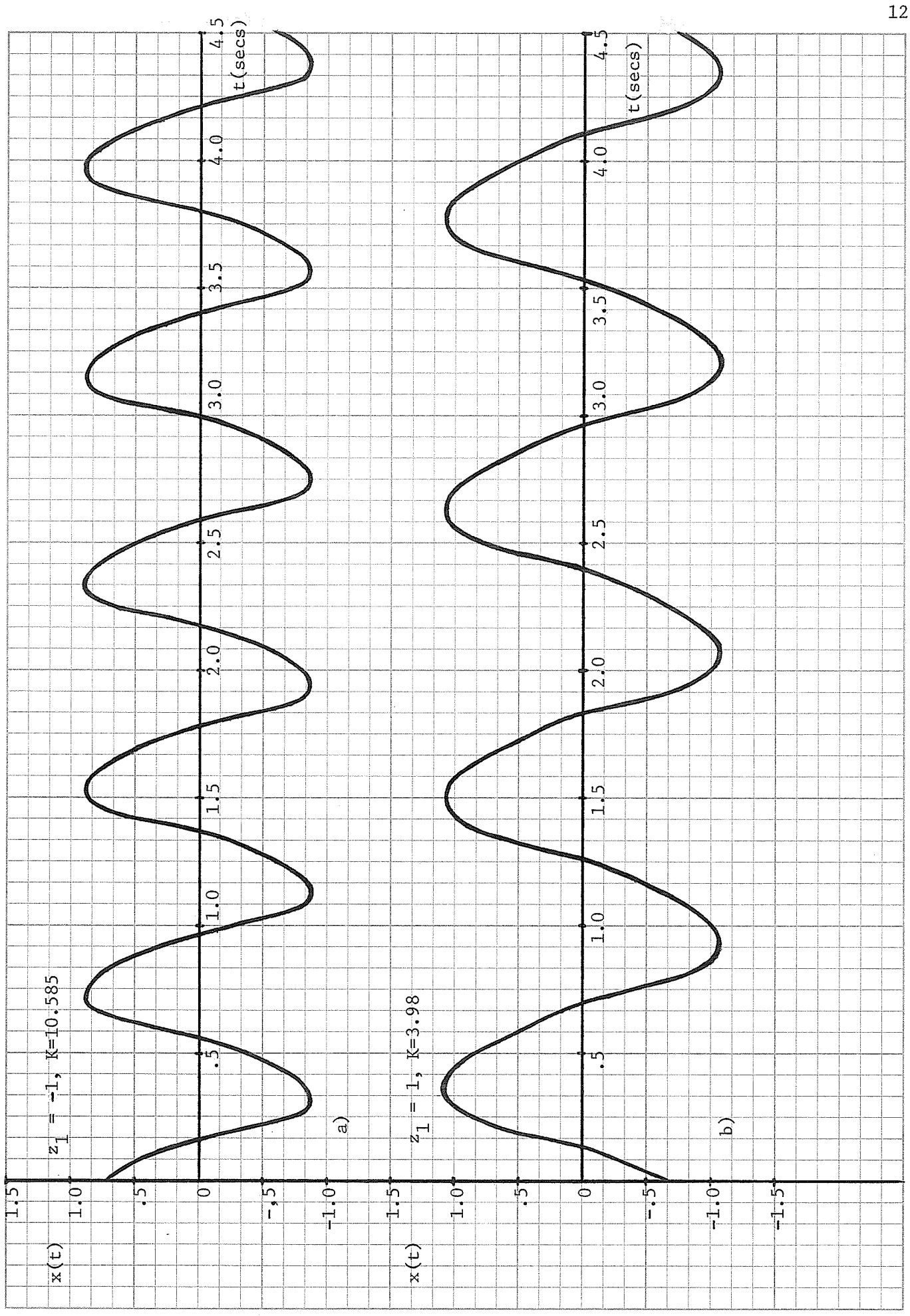

Fig. 6.23 WAVEFORM RECORDINGS FOR EXAMPLES IV AND VI

CHAPTER 7

OSCILLATIONS IN SYSTEMS WITH TIME DELAY

Certain forms of autonomous nonlinear systems involving time delay can be analyzed, approximately, by the DF method. Also, Loeb's criterion and the IDF stability technique can be applied to determine stability of oscillations. In this chapter, specific time delay systems are studied in detail to determine how well these approximate techniques work, and why the two stability techniques disagree in certain cases.

7.1 Two Systems With Known Exact Solutions

The exact analytical limit cycle solutions are known for two nonlinear systems with time delay, so these systems are studied in great detail.

7.1.1 A System Studied by Jones

Jones [30, 31] has studied the nonlinear differential-difference equation

$$\dot{x}(t) = -\alpha\, x(t-1)\,[1-x^2(t)]\ ,\ \alpha \text{ constant} \qquad (7.1)$$

in some detail, and gives conditions for the existence of periodic solutions. A system block diagram representation of 7.1 is given in Fig. 7.1, and a simpler representation is indicated in Fig. 7.2, with the nonlinearity given by $f\,[x(t),x(t-1)] = \alpha\, x(t-1)\,[1-x^2(t)]$. The nonlinearity involves time delay and is similar to a dynamic nonlinearity.

7.1.1.1 Exact Solutions

Jones [31, pp. 32-33] indicates a proof, due to Macintyre, that a periodic solution of 7.1 of period 4 exists in the form $x^*(t) = k\ sn[\alpha t,k]$, with sn the Jacobian elliptic sine function. More generally, an entire family of periodic solutions of 7.1 are found in terms of elliptic

functions by using relationships in Jahnke, Emde, and Lösch [32].

First of all,

$$\frac{d}{du}\ sn(u) = cn(u)\ dn(u) = \frac{cn(u)}{dn(u)}\ dn^2(u)$$

$$= \frac{cn(u)}{dn(u)}\ [\ 1 - k^2 sn^2(u)]. \tag{7.2}$$

Now

$$\frac{cn(u)}{dn(u)} = -\ sn(u-K) = -\ sn(u-K-4nK);\quad n= o,\pm\ 1,\ \ldots, \tag{7.3}$$

since sn has a real period 4K. Thus,

$$\frac{d}{du}\ sn(u) = -\ sn(u-K-4nK)\ [1-k^2 sn^2(u)]. \tag{7.4}$$

With the substitutions u =ct and x(t) = k sn (ct), 7.4 becomes

$$\frac{1}{c}\ \frac{d}{dt}\ [\ \frac{x(t)}{k}\ ] = \frac{-x(t-K/c-4nK/c)[1-x^2(t)]}{k}, \tag{7.5}$$

or

$$\dot{x}(t) = -\ c\ x(t-K/c\ -\ 4nK/c)\ [1\ -\ x^2(t)]. \tag{7.6}$$

With the identifications $\frac{K}{c} + 4nK/c$ =1 and c = α , 7.6 becomes 7.1.

Thus the periodic solutions $x_n(t)$ = k sn [(4n+1)Kt,k] , α = (4n+1)K, of period $T_n = \frac{4}{|4n+1|}$, all satisfy the Jones equation 7.1. Since α(k) = (4n+1)K(k), α varies from (4n+1) π /2 to (4n+1)·∞ as k varies from o to 1 for the n^{th} solution. There are two countably infinite sets of periodic solutions, n = o, 1, 2, ... and n = - 1, -2, -3, ...

7.1.1.2 A Convenient Transformation

If the transformation x(t) = tanh[y(t)] is considered then

$$\dot{x}(t) = [1-x^2(t)]\ \dot{y}(t), \tag{7.7}$$

and substitution into 7.1 yields

$$\dot{y}(t) = -\ \alpha \tanh\ [y(t-1)]\ . \tag{7.8}$$

The transformation is a bijective (one-one and onto) map, and is defined

in the interval $-1 < x < 1$, $-\infty < y < \infty$. By the nature of the transformation, stability properties of the solutions must remain the same. A system block diagram corresponding to 7.8 is shown in Fig. 7.3. The nonlinearity $f(y) = \tanh(y)$ is single-valued and odd symmetric, and of the soft spring class. The exact periodic solutions, $x_n(t) = k\ sn\ [(4n+1)Kt,k]$, of 7.1 now correspond to periodic solutions, $y_n(t) = \tanh^{-1}\{k\ sn\ [(4n+1)Kt,k]\}$ of 7.8.

7.1.1.3 The Exact Variational Equation

Since the exact periodic solutions are known for the transformed equation 7.8, the variational equation governing behaviour about any one of the periodic motions may be found exactly. For $y_n(t)$ it is

$$\frac{\alpha e^{-D}}{D}\left\{\frac{d}{dy}\tanh(y)\Big|_{y=y_n(t)} \cdot \varepsilon\right\} + \varepsilon = 0. \tag{7.9}$$

With $\frac{d}{dy}\tanh(y) = 1 - \tanh^2(y)$, the variational equation becomes

$$\dot{\varepsilon}(t) = -\alpha\left\{1 - \tanh^2[y_n(t-1)]\right\}\varepsilon(t-1), \tag{7.10}$$

or

$$\dot{\varepsilon}(t) = -\alpha\,[1 - x_n^2(t-1)]\;\varepsilon(t-1) \tag{7.11}$$

in terms of the original solution $x_n(t)$. Thus 7.11 is a linear differential-difference equation with a periodic time varying coefficient (the corresponding system is shown in Fig. 7.4). The periodic time varying coefficient of 7.11, $-\alpha\,[1-x_n^2(t-1)]$, may be expressed in terms of elliptic functions, again using relationships found in [32], as follows:

$$\begin{aligned} x_n(t-1) &= k\ sn[(4n+1)K\,(t-1),k] = k\ sn\ [(4n+1)Kt-K,k] \\ &= -\frac{k\ cn\ [(4n+1)Kt,k]}{dn[(4n+1)Kt,k]}\ . \end{aligned} \tag{7.12}$$

Therefore,

$$1 - x_n^2\,(t-1) = \frac{dn^2\ [(4n+1)Kt,k]\ - k^2cn^2[(4n+1)Kt,k]}{dn^2[(4n+1)Kt,k]}$$

$$= \frac{1 - k^2}{dn^2[(4n+1)Kt,k]} \quad , \tag{7.13}$$

and

$$-\alpha[1-x_n^2(t-1)] = \frac{-\alpha k'^2}{dn^2[(4n+1)Kt,k]} = \frac{-(4n+1)Kk'^2}{dn^2[(4n+1)Kt,k]} . \tag{7.14}$$

The time varying coefficient is therefore periodic with period $T_n/2 = 2/|4n+1|$. For a given value of k, corresponding to a given value of $\alpha(k)$, the limits of variation of the time varying coefficient are found as $-(4n+1)K(1-k^2)$ and $-(4n+1)K$. These limits vary from $-(4n+1)\pi/2$ and $-(4n+1)\pi/2$ to o and $-(4n+1)\infty$ respectively as k varies from o to 1.

Although the exact variational equation is known for each of the periodic motions of 7.8, it is very difficult to solve. However, one important result is available for the variational equation corresponding to negative n, for which the time varying coefficient is always positive. Birkhoff and Kotin [33, p.15] prove a theorem which, when applied to 7.11, yields that if 7.14 is greater than zero for all $t > o$, and

$$\int_0^\infty \left\{ \frac{-(4n+1)Kk'^2}{dn^2[(4n+1)Kt,k]} \right\} dt = \infty \quad , \tag{7.15}$$

then every positive solution (i.e. initial function positive) of 7.11 tends to infinity as t goes to infinity. It will be proved subsequently that the time average value of 7.14 is positive for negative n, and this implies that 7.15 is satisfied. Thus unstable solutions of the variational equation always exist when n is negative, and periodic solutions of 7.8 with negative n must correspond to unstable limit cycles.

Unfortunately, definite stability results when n is non negative cannot be found in the literature. However, useful information may be obtained for this case at least through simulation. Menzies [11] has

conducted extensive simulation studies of 7.1 for α positive (corresponding to n non negative). Only the limit cycle for n = o, with period $T_o = 4$ and frequency $w_o = \pi/2$, could be excited. The author has also simulated this Jones system, and the n = o limit cycle (for α = 1.7, 2, and 4) is shown in Fig. 7.27. No higher frequency limit cycles (i.e. $n > o$) are observed when α is in the region of their existence. In fact, even the n = o periodic solution is found to go unstable for $\alpha > 5$, but this is due to finite disturbances making $|x(t)| > 1$, which leads to unstable solutions. Jones [30, p.110] has exhibited numerical solutions of the n = o limit cycle up to $\alpha = 8$, so it is believed that this limit cycle is stable for all $k < 1$. Nonobservance of the higher value of n modes for a variety of initial functions seems to suggest that they correspond to unstable limit cycles. Fig. 7.28 shows the nature of the instability for the n=±1 limit cycles - the solutions quickly move away from the mathematically predicted periodic motions which have been stored as initial functions. Verification of the existence and instability of these limit cycles by reversing time in the simulation cannot be done because the time delay becomes a time advance in reverse time, but at least their existence has been established mathematically.

There is one nonrigorous argument that can be applied in order to determine the stability properties of the non negative n periodic motions in the small amplitude region (i.e. k close to o). Consider the variational equation of 7.11 in the form $\dot{\varepsilon}(t) = \phi(t)\,\varepsilon(t-1)$ with $\phi(t) = -(4n+1)Kk'^2/dn^2[(4n+1)Kt,k]$. With the change of variables, $\varepsilon(t) = b(t)\,\delta(t)$, the variational equation becomes

$$\dot{\delta}(t) = -\frac{\dot{b}(t)}{b(t)}\,\delta(t) + \phi(t)\,\frac{b(t-1)}{b(t)}\,\delta(t-1) \quad . \tag{7.16}$$

With the choice, $b(t) = 1/dn[(4n+1)Kt,k]$, and relationships found in [32],

7.16 becomes

$$\dot{\sigma}(t) = h(t)\,\sigma(t) + c\,\sigma(t-1), \tag{7.17}$$

where

$$h(t) = -(4n+1)Kk^2\ \mathrm{sn}[(4n+1)Kt,k]\ \mathrm{sn}\ [(4n+1)Kt-K,k] \tag{7.18}$$

is periodic with period $T_n = 4/|4n+1|$, and

$$c = -\ (4n+1)Kk' \tag{7.19}$$

is a constant. If k = o then 7.17 becomes

$$\dot{\sigma}(t) = -\ (4n+1)\,\frac{\pi}{2}\,\sigma(t-1). \tag{7.20}$$

For the constant coefficient equation, $\dot{\sigma}(t) = c\,\sigma(t-1)$, the location of characteristic exponents can be determined by the D-decomposition method [34, pp. 54-60] or the root locus technique for time delay systems (to be outlined subsequently). The result is that a stable situation occurs when $o \geqslant c \geqslant -\pi/2$, and an unstable situation occurs otherwise. With respect to 7.20, only n = o corresponds to a stable situation - at the borderline of stability.

If the assumption is made that the characteristic exponents of 7.17 vary in a continuous manner as k is varied continuously, then something can be said concerning stability of periodic motions for small k. For $n > o$ and k = o there exists at least one characteristic exponent of 7.17 in the open RHP. In fact, as n increases the number of characteristic exponents with positive real parts increases. By the continuity of motion of these characteristic exponents, there exists at least a small interval, $[o, k_\epsilon]$, of k values for which one or more characteristic exponents of 7.17 remain in the RHP. Then, at least for small amplitudes corresponding to $k \in [o,k_\epsilon]$, the periodic motion for any $n > o$ must be an unstable limit cycle. For n = o nothing can be said because at k = o 7.17 has a characteristic exponent with zero value.

7.1.1.4 DF and TSIDF Analysis

The DF method can be applied to both the original Jones system of Figs. 7.1 and 7.2 and the transformed system of Fig. 7.3. Application of the DF method to the original Jones system yields the describing function (for nonlinearity $f[x(t),x(t-1)] = \alpha x(t-1)\ [1-x^2(t)]$), $Keq(A,w) = g(A,w) + j\ b(A,w)$ with

$$g(A,w) = (1 - \frac{3}{4} A^2)\ \alpha \cos w \qquad (7.21)$$

and

$$b(A,w) = (\frac{1}{4} A^2 - 1)\ \alpha \sin w\ . \qquad (7.22)$$

The DF is complex and both amplitude and frequency dependent. The equations governing limit cycle prediction are derived from $Keq(A,w) \cdot L(jw) = -1$, with $L(jw) = 1/jw$, and are given by

$$(1 - \frac{3}{4} A^2)\ \alpha \cos w = o \qquad (7.23)$$

and

$$w = (1 - \frac{1}{4} A^2)\ \alpha \sin w\ . \qquad (7.24)$$

Equations 7.23 and 7.24 predict two possible limit cycles. The first one requires a constant amplitude $A_o = 2/\sqrt{3}$ and frequencies given by $3\ w_o/(2\alpha) = \sin w_o$. The second possibility is related to the known limit cycles, k sn [(4n+1)Kt,k] , existing in the system. It yields frequencies $w_n = |\ 4n+1\ |\ \pi/2$; n = o, ± 1, ± 2, ... and corresponding amplitudes $A_n = 2\sqrt{1 - (4n+1)\pi/(2\alpha)}$. The frequency predictions correspond to the actual frequencies, and the starting point (A_n = o) for a DF predicted limit cycle at $\alpha = (4n+1)\ \pi/2$ also corresponds to the starting point (k = o) for an actual limit cycle. The obvious discrepancy is that $\lim_{|\alpha|\to\infty} A_n = 2$ whereas $\lim_{|\alpha|\to\infty} A_{exact} = 1$ for all n.

Table 7.1 shows DF amplitude calculations compared to the actual n = o limit cycle amplitude (k) and fundamental component amplitude for

various values of α. In the small amplitude region the errors are reasonably small, as expected, but increase rather drastically with increasing amplitude. Also, the DF amplitude, $A_{o_{DF}}$, corresponds closer to the amplitude of the limit cycle's fundamental component, $A_{1_{exact}}$, than to the limit cycle amplitude, $A_{exact} = k$. The same trends of Table 7.1 occur for the other possible limit cycles ($n \neq o$) in the system.

Table 7.1 Comparison of DF Amplitude Calculations and Amplitudes of the Actual n = o Limit Cycle

α	$A_{o_{DF}}$	$A_{o_{exact}}$ (=k)	% Error	$A_{1_{exact}}$	% Error
1.5708(π/2)	0	0	-	0	-
1.6098	.3113	.3066	1.5373%	.3085	.9185%
1.6502	.4386	.4254	3.1006%	.4307	1.8459%
1.6901	.5314	.5079	4.6180%	.5172	2.7391%
1.8499	.7768	.7036	10.4106%	.7322	6.0915%
2.0496	.9667	.8258	17.0578%	.8801	9.8350%
2.2504	1.0991	.8927	23.1142%	.9713	13.1617%
2.6493	1.2761	.9560	33.4746%	1.0750	18.6994%
3.0539	1.3938	.9813	42.0284%	1.1316	23.1644%
3.6056	1.5024	.9940	51.1548%	1.1749	27.8742%
4.8411	1.6438	.9995	64.4637%	1.2194	34.8042%

The TSIDF technique, applied here to improve the DF approximation, involves assuming an approximate input to the nonlinearity in the form $x_{app}(t) = A \sin wt + B \sin (3 wt + \theta)$. This results in the four equations in the four unknowns A, B, w, and θ given by

$$\left(\frac{-AB \sin\theta}{2}\right) \sin w + \left(\frac{AB \sin\theta}{4}\right) \sin 3w + \left(1 - 3A^2/4 - B^2/2 + \frac{AB\cos\theta}{2}\right)\cos w$$

$$+ \left(-B^2 + \frac{AB \cos\theta}{4}\right) \cos 3w = o, \qquad (7.25)$$

$$(-\alpha + A^2\alpha/4 + B^2\alpha/2 + \frac{\alpha AB\cos\theta}{2})\sin w + (\frac{-\alpha AB\cos\theta}{4})\sin 3w$$

$$+ (\frac{\alpha AB\sin\theta}{2})\cos w + (\frac{\alpha AB\sin\theta}{4})\cos 3w + w = o, \qquad (7.26)$$

$$- 3Bw\sin\theta + (\alpha B - \alpha A^2B/2 - \alpha B^3/4)\sin\theta\sin 3w + (\alpha A^3/4 - A^2B\alpha\cos\theta)\cos w$$

$$+ (\alpha B - \alpha A^2B/2 - 3\alpha B^3/4)\cos\theta\cos 3w = o, \qquad (7.27)$$

and

$$(-\alpha A^3/4)\sin w + (-\alpha B + \alpha A^2B/2 + \alpha B^3/4)\cos\theta\sin 3w$$

$$+ (-\alpha A^2B\sin\theta)\cos w + (\alpha B - \alpha A^2B/2 - 3\alpha B^3/4)\sin\theta\cos 3w$$

$$+ 3Bw\cos\theta = o. \qquad (7.28)$$

With the DF frequency prediction, $w_n = |4n+1|\pi/2$, 7.25 - 7.28 become

$$-\frac{3AB\sin\theta}{4} = o, \qquad (7.29)$$

$$-\alpha(1 - A^2/4 - B^2/2 - \frac{AB\cos\theta}{2}) + \frac{\alpha AB\cos\theta}{4} + w_n = o, \qquad (7.30)$$

$$- 3Bw_n\sin\theta - \alpha(B - A^2B/2 - B^3/4)\sin\theta\sin w_n = o, \qquad (7.31)$$

and

$$-\frac{\alpha A^3\sin w_n}{4} - \alpha(-B + A^2B/2 + B^3/4)\cos\theta\sin w_n + 3Bw_n\cos\theta = o \qquad (7.32)$$

respectively. Since, from 7.29, $\theta = o$ (except in the trivial case), these equations reduce to

$$w_n = \alpha(1 - A^2/4 - B^2/2 - 3AB/4), \qquad (7.33)$$

and

$$-\alpha(-B + B^3/4 + A^2B/2 + A^3/4)\sin w_n + 3Bw_n = o. \qquad (7.34)$$

Equations 7.33 and 7.34 may be solved simultaneously for A and B when n and α are specified. For example, with n = o 7.33 can be solved for A in terms of B to yield

$$A = -3B/2 + \sqrt{B^2/4 + 4 - 2\pi/\alpha}. \qquad (7.35)$$

This solution, substituted into 7.34, produces the equation

$$B^6 - 24B^4 + (80 + 32\pi/\alpha - 4\pi^2/\alpha^2)B^2 + (-32 + 48\pi/\alpha - 24\pi^2/\alpha^2 + 4\pi^3/\alpha^3) = o. \qquad (7.36)$$

This equation may be solved to yield B, and A is then determined from 7.35.

Table 7.2 shows A and B values from this TSIDF analysis compared with the amplitudes of the fundamental and third harmonic components of the exact limit cycle. A comparison of the errors here with those of Table 7.1 for the ordinary DF approximation clearly indicates the substantial improvement in the approximation when the third harmonic component is included. These results are expected to hold for all other limit cycles ($n \neq o$) as well. It should be noted that this vast improvement in the approximation requires a significant amount of additional work compared to the work required in the ordinary DF method.

Table 7.2 Comparison of TSIDF Amplitude Calculations and Fundamental and Third Harmonic Amplitudes of Actual Limit Cycle

α	A_{TSIDF}	A_{exact}	% Error	B_{TSIDF}	B_{exact}	% Error
1.5708($\pi/2$)	0	0	-	0	0	-
1.6098	.3085	.3085	.0011%	.0019	.0019	.0008%
1.6502	.4307	.4307	.0008%	.0053	.0053	.0140%
1.6901	.5172	.5172	.0019%	.0095	.0095	.0322%
1.8499	.7321	.7322	.0168%	.0299	.0299	.1639%
2.0496	.8795	.8801	.0711%	.0584	.0582	.4313%
2.2504	.9696	.9713	.1721%	.0869	.0862	.7846%
2.6493	1.0696	1.0750	.5084%	.1389	.1366	1.6602%
3.0539	1.1203	1.1316	1.0003%	.1843	.1795	2.7111%
3.6056	1.1535	1.1749	1.8260%	.2357	.2260	4.3178%
4.8411	1.1723	1.2194	3.8638%	.3195	.2951	8.2884%

Analysis so far has been restricted to the original Jones system of Figs. 7.1 and 7.2. However, the DF method can also be applied to the transformed system of Fig. 7.3. Unfortunately, the describing function

for the nonlinearity tanh(y), expressed as

$$Keq(A) = g(A) = \frac{1}{\pi A} \int_0^{2\pi} \tanh [A \sin\theta_1] \sin\theta_1 d\theta_1, \qquad (7.37)$$

cannot be integrated. However, since tanh(y) is a soft spring type of nonlinearity, it is known that Keq(A) will be monotonic decreasing with A, and will vary from 1 to 0 as A varies from 0 to ∞. The DF condition, Keq(A) L (jw) = - 1, with L (jw) = $\alpha e^{-jw}/jw$, yields the limit cycle conditions,

$$w = \alpha\, Keq(A) \sin w \qquad (7.38)$$

and

$$\frac{\alpha \cos w}{w} = o. \qquad (7.39)$$

Then limit cycles with frequencies $w_n = |4n+1|\pi/2$ are predicted, and DF amplitudes are given by $Keq(A_n) = (4n+1)\pi/(2\alpha)$. Thus the limit cycle frequencies are predicted exactly, and the starting point (A_n = o) for a limit cycle of frequency w_n is predicted correctly at $\alpha = (4n+1)\pi/2$, just as for the DF method applied to the original Jones system.

7.1.1.5 Approximate Stability Techniques

Application of Loeb's criterion to the original Jones system involves expressing Keq(A,w) L (jw) + 1 in the form X (A,w) + j Y(A,w). The result is

$$X(A,w) = 1 + \frac{\alpha \sin w(A^2/4-1)}{w}, \qquad (7.40)$$

and

$$Y(A,w) = -\frac{(1-3A^2/4)\,\alpha \cos w}{w}. \qquad (7.41)$$

Then

$$\left.\frac{\partial X}{\partial A}\frac{\partial Y}{\partial w} - \frac{\partial Y}{\partial A}\frac{\partial X}{\partial w}\right|_{(A_n w_n)} = A_n \alpha^2 \sin^2 w_n (1-3A_n^2/4)/2w_n^2, \qquad (7.42)$$

which is positive for $o \leq A_n < 2/\sqrt{3}$ and negative for $A_n > 2/\sqrt{3}$,

thereby predicting a stable limit cycle for An $< 2/\sqrt{3}$ and an unstable limit cycle for $A_n > 2/\sqrt{3}$, for all n. For small amplitudes, with the DF approximation reasonably accurate, Loeb's criterion is seen to fail for the $n \neq o$ limit cycles (since they are known to be unstable). The DF error is so large for $A_n > 2/\sqrt{3}$ that any stability information by way of Loeb's criterion is probably invalid anyway.

Loeb's criterion applied to the transformed system of Fig. 7.3 involves evaluation of the expression $\frac{d}{dw}\,\mathrm{ImL}(jw)\frac{d}{dA}\,\mathrm{Keq}(A)$. The result is

$$\frac{d}{dw}\,\mathrm{ImL}(jw)\,\frac{d}{dA}\,\mathrm{Keq}(A)\Big|_{(A_n,w_n)} = \frac{\alpha \sin w_n}{w_n}\,\mathrm{Keq}'(A_n). \qquad (7.43)$$

Since $\alpha \sin w_n/w_n > o$ $\forall$ n, and $\mathrm{Keq}'(A_n) < o$ because tanh(y) is a soft spring nonlinearity, 7.43 is always negative, and Loeb's criterion then predicts a stable limit cycle $\forall$ n. Again Loeb's criterion fails for the $n \neq o$ limit cycles, this time predicting stability at all amplitude levels.

The IDF stability technique can be applied to the original Jones system, but care must be taken with time delay in the nonlinearity. If an incremental bias B is assumed to exist in conjunction with the DF prediction, A sin w t, then the incremental gain, $N_B(A,w) \equiv \lim_{B\to o} N_B(A,B,w)$, becomes

$$N_B(A,w) = \alpha(1-A^2/2 - A^2 \cos w). \qquad (7.44)$$

Stability analysis of the IDF system of Fig. 7.5 yields $N_B(A_n,w_n) > 0$ for a stable limit cycle and $N_B(A_n,w_n) < o$ for an unstable one. Since

$$N_B(A_n,w_n,) = \alpha[-1+(4n+1)\pi/\alpha], \quad n = o,\pm1,\pm2.. \qquad (7.45)$$

the stability conditions are

$$(4n+1)\pi/2 < \alpha < (4n+1)\pi, \; n \geq o$$
$$\alpha < (4n+1)\pi, \; n < o \qquad (7.46)$$

for a stable limit cycle, and

$$\alpha > (4n+1)\pi \ , \ n \geqslant o$$
$$(4n+1)\pi/2 > \alpha > (4n+1)\pi \ , \ n < o \qquad (7.47)$$

for an unstable limit cycle. It should be noted that, because an incremental dc bias is assumed, the effect of the time delay in the nonlinearity is not reflected in the IDF system. This is then felt to be an incorrect application of the IDF stability technique to a time delay system.

The correct procedure, in this case, is to include the effect of the time delay in the nonlinearity by assuming a perturbation signal in the form $\epsilon e^{at} \sin\Omega t$ so that the input to the nonlinearity is $x(t) = \epsilon e^{at} \sin \Omega t + A_n \sin w_n t$. Expansion of the output of the nonlinearity $f[x(t),x(t-1)]$ yields, from Appendix VI, the incremental gain

$$N_i(A_n,a,\Omega,w_n) = \alpha(1-A_n^2/2)\ e^{-(a+j\Omega)}. \qquad (7.48)$$

The IDF system for this form of perturbation is shown in Fig. 7.6. If the arbitrary complex frequency, $a + j\Omega$, is generalized to s, then the equivalent linear system can be considered as in Fig. 7.7. Stability analysis of this form of time delay system (seen in detail later in the chapter) yields $o \leqslant \alpha(1-A_n^2/2) \leqslant \pi/2$ for a stable limit cycle and $\alpha(1-A_n^2/2) > \pi/2$, $\alpha(1-A_n^2/2) < o$ for an unstable limit cycle. The stability conditions are then

$$(4n+1)\pi - \pi/2 \leqslant \alpha \leqslant (4n+1)\pi \ , \ n \geqslant o$$
$$(4n+1)\pi \geqslant \alpha \geqslant (4n+1)\pi - \pi/2, \ n < o \qquad (7.49)$$

for a stable limit cycle, and

$$\alpha < (4n+1)\pi - \pi/2, \ \alpha > (4n+1)\pi \ , \ n \geqslant o$$
$$\alpha > (4n+1)\pi \ , \ \alpha < (4n+1)\pi - \pi/2, \ n < o \qquad (7.50)$$

for an unstable limit cycle. The stability conditions predicted here

differ from those predicted for a bias perturbation. However, here the correct stability results are predicted for the small amplitude region of A_n corresponding to α close to $(4n+1)\,\pi/2$. This is not true for the analysis with a bias perturbation. For large amplitude A_n, the DF prediction is shown to be very inaccurate, and possibly this inaccuracy is reflected in the incorrect stability results here for large A_n.

To verify the basic correctness of the IDF stability technique, the DF approximation can be eliminated by considering the actual limit cycle solutions. The same perturbation signal, $\epsilon e^{at} \sin \Omega t$, is considered, and the input to the nonlinearity is $\epsilon e^{at} \sin \Omega t + k\,\mathrm{sn}[(4n+1)Kt,k]$. The incremental gain of the perturbation signal in the presence of the actual limit cycle signal is, from Appendix VI,

$$N_i(k,a,\Omega,n) = \frac{\alpha}{T} \cdot \int_0^T dn^2[(4n+1)Kt,k]dt = (4n+1)E(k)e^{-(a+j\Omega)} \quad (7.51)$$

and the equivalent linear system, with $a + j\Omega$ generalized to s, is shown in Fig. 7.8. The Jacobian elliptic integral E(k) varies monotonically from $\pi/2$ to 1 as k varies from o to 1. Stability analysis of the system of Fig. 7.8 results in

$$o \leqslant (4n+1)\,E(k) \leqslant \pi/2 \quad (7.52)$$

for a stable limit cycle, and

$$(4n+1)E(k) < o,\ (4n+1)E(k) > \pi/2 \quad (7.53)$$

for an unstable limit cycle. Only the n = o limit cycle is predicted as stable $\forall k$ - all other limit cycles are predicted as unstable $\forall k$. This analysis then corresponds exactly to the actual stability situation for all limit cycles. The IDF stability technique is seen to be basically correct applied here, and the previous inaccuracies are attributed to the DF approximation itself.

The transformed system of Fig. 7.3 can be analyzed using the DF method and the IDF stability technique, very much as is done for second and third order systems in Chapters 5 and 6. The DF system and the IDF system are related to the root locus of the linear time delay system of Fig. 7.9. Bower and Schultheiss [26] give a good description of the root locus method applied to systems with time delay. For the system of Fig. 7.9 the root locus is shown in Fig. 7.10. If the system of Fig. 7.9 is positive feedback instead of negative feedback then the root locus is that of Fig. 7.11. These root loci are seen to be quite different from the root loci for nondelay systems in that here there are an infinite number of branches. They cross the imaginary axis at the values $jw_n = \pm j(4n+1)\,\pi/2$; $n=o,1,2,..$ for negative feedback and $jw_n = \pm j|4n+1|\pi/2$, $n=-1,-2,..$ for positive feedback. DF conditions at the imaginary axis crossings are $K = \alpha\, Keq(A_n) = (4n+1)\,\pi/2$; $n = o,\pm1,\pm2,--$ or $Keq(A_n) = (4n+1)\,\pi/2\alpha$. The $n \geq o$ DF limit cycles correspond to $\alpha > o$ (negative feedback) and the $n < o$ limit cycles correspond to $\alpha < o$ (positive feedback).

Since the nonlinearity in the system of Fig. 7.3 is the soft spring, tanh(y), straightforward application of Loeb's criterion in the graphical root locus form indicates stable limit cycles $\forall$ n - the same result as application of 7.43. However, the root locus approach clearly indicates that the DF system is unstable for all but the n = o limit cycle. This casts doubt on the validity of Loeb's criterion as applied here, and this doubt is further amplified by the application of the IDF stability technique. The incremental gain for a bias perturbation can be used because no delay exists in the nonlinearity, and the result is

$$N_B(A,o) = \frac{1}{2\pi}\int_o^{2\pi} f'(A\sin\theta)\,d\theta = 1 - \frac{1}{2\pi}\int_o^{2\pi}\tanh^2(A\sin\theta)\,d\theta \quad (7.54)$$

Although 7.54 cannot be evaluated in closed form, the general result, $Keq(A)/2 < N_B(A,o) < Keq(A)$, for soft spring nonlinearities is sufficient to ensure that all limit cycles other than n = o are unstable.

The interesting result is that the IDF stability technique, applied to the transformed system, yields the correct stability result for all amplitude levels. On the other hand, when it is applied to the original Jones system, correct stability results are predicted only for the small amplitude region. This seems to suggest that the DF approximation is more accurate for the transformed system, especially for large amplitudes, than for the original system. The nature of the transformation is such that, with $y(t) \approx A \sin wt$, $x(t) = \tanh [y(t)] \approx \tanh [A \sin wt]$ is probably a better approximation to sn $[(4n+1)Kt,k]$ than simply a sinusoid. This then agrees with the conclusion of the IDF stability analysis.

Any DF inaccuracy in the IDF stability technique applied to the transformed system may be eliminated by considering perturbations about the actual limit cycle. The input to the nonlinearity is $B + y_n(t) = B + \tanh^{-1}\{k \text{ sn } [(4n+1)Kt,k]\}$, with B an incremental bias, and the incremental gain is calculated as $N_B^*(k,n) = (4n+1)E(k)$ in Appendix VI. The equivalent linear system for stability studies is then that of Fig. 7.8, the same as for the original Jones system with perturbations about the exact solutions. As would be expected, the correct stability results are predicted for all limit cycles.

In Chapter 3 it is shown that the IDF stability technique is equivalent to the time averaging of the DF approximate variational system, and elimination of the DF approximation results in an equivalent linear system which is the time average of the exact variational system. Verification of this general result for the transformed system involves

calculation of the time average value of $[1-x_n^2(t-1)] = (4n+1)Kk'^2/dn^2[(4n+1)Kt,k]$, the time varying coefficient of the variational system of Fig. 7.4. With relationships found in [32], the time average value is expressed as

$$\frac{1}{Tn}\int_0^{Tn} \alpha[1-x_n^2(t-1)]\,dt = \frac{|4n+1|}{4}\int_0^{4/|4n+1|} \frac{(4n+1)Kk'^2\,dt}{dn^2[(4n+1)Kt,k]}$$

$$= (4n+1)\int_0^K dn^2[u,k]\,du$$

$$= (4n+1)\,E(k), \qquad (7.55)$$

which is, of course, the same expression as the incremental gain in the IDF technique when the actual limit cycle solutions are used. In this particular system, the process of time averaging the variational equation does not affect the stability results.

7.1.2 A Complementary System

The author has found that the nonlinear differential-difference equation

$$\dot{x}(t) = -\alpha\, x(t-1)\,[1+x^2(t)]\ ,\ \alpha \text{ constant} \qquad (7.56)$$

is in many ways complementary to the Jones equation 7.1. The system block diagram for the complementary system can be considered as in Fig. 7.2 with the nonlinearity now $f[x(t),x(t-1)] = \alpha\, x(t-1)\,[1+x^2(t)]$.

7.1.2.1. Exact Solutions

A family of periodic solutions of 7.56 can be found in terms of elliptic functions using relationships in [32] . It can be shown that

$$\frac{d}{du}\,cn(u) = -\,cn(u-K-4nK)k'\left[1+\frac{k^2}{k'^2}\,cn^2(u)\right]\ , \qquad (7.57)$$

and, with $u = ct$ and $x(t) = \frac{k}{k'}\,cn(ct)$, 7.57 becomes

$$\dot{x}(t) = - c\, k' x(t-K/c - 4nK/c)\, [1+x^2(t)] \,. \qquad (7.58)$$

With the identifications $K/c + 4nK/c = 1$ and $ck' = \alpha$, 7.58 becomes 7.56. The periodic solutions $x_n(t) = \frac{k}{k'}\, cn\, [(4n+1)Kt,k]$, $\alpha = k'(4n+1)K$, of period $T_n = 4/|4n+1|$; $n = o, \pm1, \pm2, --$ then satisfy 7.56. Since $\alpha(k) = (4n+1)k'K(k)$, α varies from $(4n+1)\,\pi/2$ to o as k varies from o to 1 for the n^{th} solution. As in the Jones system, there are two countably infinite sets of periodic solutions, $n = o,1,2,---$ and $n = -1,-2,-3,---$.

7.1.2.2 Transformation of 7.56

If the transformation $x(t) = \tan[y(t)]$ is considered then

$$\dot{x}(t) = [1+x^2(t)]\, \dot{y}(t), \qquad (7.59)$$

and substitution into 7.56 yields

$$\dot{y}(t) = - \alpha \tan [y(t-1)] \,. \qquad (7.60)$$

The transformation is bijective and defined in the interval $-\infty < x < \infty$, $-\pi/2 < y < \pi/2$. The system block diagram for 7.60 is shown in Fig. 7.12 with the nonlinearity $f(y) = \tan(y)$ single-valued and odd symmetric, and of the hard spring class. The periodic solutions $x_n(t) = \frac{k}{k'}\, cn\, [(4n+1)Kt,k]$, of 7.56 correspond to periodic solutions $y_n(t) = \tan^{-1}\left\{ \frac{k}{k'}\, cn\, [(4n+1)Kt,k] \right\}$ of 7.60.

7.1.2.3 The Exact Variational Equation

The variational equation for $y_n(t)$ is

$$\dot{\varepsilon}(t) = - \alpha \left\{1+\tan^2[y_n(t-1)]\right\} \cdot \varepsilon(t-1)$$
$$= - \alpha \left\{1+x_n^2(t-1)\right\} \varepsilon(t-1), \qquad (7.61)$$

and the corresponding variational system is shown in Fig. 7.13. The periodic time varying coefficient, $- \alpha [1+x_n^2(t-1)]$, may be expressed in terms of elliptic functions, the result being $- \alpha [1+x_n^2(t-1)] = - \alpha/dn^2\, [(4n+1)Kt,k] = - k'(4n+1)K/dn^2\, [(4n+1)Kt,k]$. (7.62)

This time varying coefficient is periodic with period $T_n/2 = 2/|4n+1|$.

For given k, the limits of variation of the coefficient are $-(4n+1)K/k'$ and $-(4n+1)Kk'$, and these limits vary from $-(4n+1)\pi/2$ and $-(4n+1)\pi/2$ to $-(4n+1)\infty$ and o respectively as k varies from o to 1. Note that k varying from o to 1 corresponds to α varying from $(4n+1)\pi/2$ to o.

The theorem of Birkhoff and Kotin [33, p.15] can again be applied. With n negative, 7.62 is always positive, and so is its time average value. Hence

$$\int_0^\infty \left\{ \frac{-k'(4n+1)K}{dn^2[(4n+1)Kt,k]} \right\} dt = \infty \,, \tag{7.63}$$

and the conditions of the theorem are satisfied. Thus, unstable solutions of the variational equation always exist for negative n, and the limit cycles for $n < o$ must be unstable.

Simulation of 7.56 for various initial functions and values of α produced no stable limit cycles. Fig. 7.29 shows an attempt to generate the n = o limit cycle, but the solution decays to zero. Fig. 7.30 shows that the $n = \pm 1$ limit cycles are also unstable. All limit cycles for $n \geq o$ are then expected to be unstable. Verification of this result, analytically, is possible for the small amplitude region (k close to zero) of the limit cycles. The variational equation 7.61 is transformed by $\xi(t) = b(t)\cdot\sigma(t)$, resulting in

$$\dot{\sigma}(t) = h(t)\cdot\sigma(t) + c\,\sigma(t-1) \tag{7.64}$$

with

$$h(t) = -(4n+1)Kk^2 sn[(4n+1)Kt,k]\, sn[(4n+1)Kt-K,k] \tag{7.65}$$

periodic with period $T_n = 4/|4n+1|$, $c = -(4n+1)K$, and $b(t) = 1/dn[(4n+1)Kt,k]$. If k = o then 7.64 becomes

$$\dot{\sigma}(t) = -(4n+1)\,\frac{\pi}{2}\cdot\sigma(t-1), \tag{7.66}$$

identical to 7.20 for the transformed Jones system. The argument used in

that case then applies here and shows that, at least for $k \in [o,k_\epsilon]$, limit cycles for $n > o$ must be unstable. Again nothing can be said about the $n = o$ limit cycle.

The stability situation here is very similar to that of the Jones system, except that the $n = o$ limit cycle is also unstable now.

7.1.2.4 DF and TSIDF Analysis

Application of the DF method to the untransformed complementary system yields the describing function for $f[x(t),x(t-1)] = \alpha \cdot x(t-1)[1+x^2(t)]$, $Keq(A,w) = g(A,w) + j\, b(A,w)$, with

$$g(A,w) = (-1-3A^2/4)\,\alpha \cos w \tag{7.67}$$

and

$$b(A,w) = (A^2/4 + 1)\,\alpha \sin w. \tag{7.68}$$

The equations governing limit cycle prediction are

$$(-1-3A^2/4)\,\alpha \cos w = o \tag{7.69}$$

and

$$w = (1+A^2/4)\,\alpha \sin w. \tag{7.70}$$

From 7.69 and 7.70, limit cycles of frequencies $w_n = |4n+1|\,\pi/2$, $n = o, \pm1, \pm2, \cdots$ and amplitudes $A_n = 2\sqrt{-1+(4n+1)\pi/(2\alpha)}$ are predicted. The frequency predictions are exact, as are the starting points (amplitude = o) of the limit cycles at $\alpha = (4n+1)\,\pi/2$.

Table 7.3 shows DF amplitude calculations compared to the actual $n = o$ limit cycle amplitude (k/k') and fundamental component amplitude for various values of α.

As with the Jones system, amplitude errors are small at low amplitude but increase rapidly with increasing amplitude. Again the DF amplitude approximates the fundamental component amplitude, $A_{1_{exact}}$, better than it does the limit cycle amplitude, $A_{o_{exact}}$. The behaviour

Table 7.3 Comparison of DF Amplitude Calculations and Amplitudes of Actual n = o Limit Cycle

α	$A_{o_{DF}}$	$A_{o_{exact}}$ $(=k/k')$	% Error	$A_{1_{exact}}$	% Error
1.5708$(\pi/2)$	o	o	—	o	—
1.5507	.226	.229	1.27%	.229	1.18%
1.5297	.328	.334	1.77%	.332	1.21%
1.5076	.405	.420	3.57%	.414	2.18%
1.4844	.482	.500	3.66%	.493	2.30%
1.4339	.616	.654	5.82%	.640	3.76%
1.3769	.748	.817	8.41%	.790	5.28%
1.3110	.890	1.000	11.00%	.957	7.00%
1.2330	1.044	1.224	14.70%	1.150	9.22%
1.1367	1.237	1.530	19.15%	1.407	12.10%
1.0094	1.493	2.000	25.35%	1.785	16.37%
.8153	1.926	3.000	35.80%	2.530	23.85%

of the calculations for other than the n = o limit cycle is expected to be similar to that of Table 7.3.

TSIDF analysis is similar to that detailed for the Jones system, and results in an approximate limit cycle, $x_{app}(t) = A \sin wt + B \sin 3wt, B < o$, with frequencies $w_n = |4n+1|\,\pi/2$. For the n = o limit cycle, A and B are given by the solution of

$$A = -3B/2 + \sqrt{B^2/4 - 4 + 2\pi/\alpha} \tag{7.71}$$

and

$$B^6+24B^4+(80+32\pi/\alpha - 4\pi^2/\alpha^2)B^2+(32-48\pi/\alpha+24\pi^2/\alpha^2-4\pi^3/\alpha^3)= o. \tag{7.72}$$

Table 7.4 shows a few TSIDF calculations along with the exact amplitudes of the fundamental and third harmonic components of the limit cycle in the larger amplitude region. The errors remain reasonable for large amplitude, and indicate the significant improvement in accuracy when the third harmonic is included in the approximation. This same improvement

in amplitude prediction should occur for the other limit cycles as well.

Table 7.4 Comparison of TSIDF Amplitude Calculations and Fundamental and Third Harmonic Amplitudes of Actual Limit Cycle

α	A_{TSIDF}	A_{exact}	% Error	B_{TSIDF}	B_{exact}	% Error
1.1367	1.409	1.407	.142%	-.1138	-.1129	.797%
1.0783	1.579	1.573	.381%	-.1485	-.1464	1.433%
1.0094	1.793	1.785	.448%	-.1977	-.1948	1.490%
.9253	2.088	2.076	.578%	-.2746	-.2695	1.893%
.8153	2.560	2.530	1.186%	-.4152	-.4043	2.700%
.6503	3.556	3.470	2.480%	-.7641	-.7290	4.810%

Application of the DF method to the transformed system of Fig. 7.12 yields the describing function,

$$Keq(A) = g(A) = \frac{1}{\pi A} \int_0^{2\pi} \tan [A \sin \theta_1] \sin \theta_1 d\theta_1. \qquad (7.73)$$

Since tan(y) is a hard spring, Keq(A) is monotonic increasing with A, and varies from 1 to ∞ as A varies from o to $\pi/2$. Limit cycle conditions here are identical to those of 7.38 and 7.39, so that frequencies $w_n = |4n+1| \pi/2$ are predicted, and DF amplitudes may be calculated from $Keq(A_n) = (4n+1)\pi/(2\alpha)$.

7.1.2.5 Approximate Stability Techniques

Application of Loeb's criterion to the untransformed system results in

$$\frac{\partial X}{\partial A}\frac{\partial Y}{\partial w} - \frac{\partial Y}{\partial A}\frac{\partial X}{\partial w}\Bigg|_{(A_n, w_n)} = -A_n \alpha^2 \sin^2 w_n (1+3A_n^2/4)/(2w_n^2), \qquad (7.74)$$

which is always negative. Hence Loeb's criterion predicts an unstable limit cycle $\forall$ n. Also, Loeb's criterion applied to the transformed system of Fig. 7.12 involves 7.43. With $Keq'(A_n) > o$ (since tan(y) is a hard spring), 7.43 is always positive, and Loeb's criterion again predicts

an unstable limit cycle $\forall$ n.

The IDF stability technique applied to the untransformed system involves assuming a perturbation $\epsilon e^{at} \sin \Omega t$, so that the incremental gain becomes

$$N_i(A_n, a, \Omega, w_n) = \alpha (1+A_n^2/2)\ e^{-(a+j\Omega)}. \qquad (7.75)$$

With $a+j\Omega$ generalized to s, the equivalent linear system for perturbations is shown in Fig. 7.14. Stability analysis of this form of linear time delay system has already been shown to yield

$$o \leqslant \alpha(1+A_n^2/2) \leqslant \pi/2 \qquad (7.76)$$

for a stable limit cycle, and

$$\alpha (1+A_n^2/2) > \pi/2\ ;\quad \alpha(1+A_n^2/2) < o \qquad (7.77)$$

for an unstable limit cycle. Since $\alpha(1+A_n^2/2) = (4n+1)\pi - \alpha$, the stability conditions become

$$(4n+1)\pi - \pi/2 \leqslant \alpha \leqslant (4n+1)\pi/2,\ n \geqslant o \qquad (7.78)$$

for a stable limit cycle, and

$$\alpha < (4n+1)\pi/2 < (4n+1)\pi - \pi/2,\ n \geqslant o$$
$$\alpha < o,\quad n < o \qquad (7.79)$$

for an unstable limit cycle. Condition 7.78 is only satisfied trivially ($\alpha = \frac{\pi}{2}$), so all limit cycles are predicted as unstable.

The DF method, Loeb's criterion, and the IDF stability technique applied to the transformed system of Fig. 7.12 can be related easily to the root locus of the linear time delay system of Fig. 7.9 (Figs.7.10 and 7.11). DF oscillation conditions correspond to jw axis crossings of the root locus and yield the exact frequencies $w_n = |\ 4n+1\ |\ \pi/2$. DF amplitudes are calculated from the DF condition $K = \alpha Keq(A_n) = (4n+1)\pi/2$ or $Keq(A_n) = (4n+1)\pi/(2\alpha)$. Since the nonlinearity tan(y) is a hard spring, application of Loeb's criterion in the graphical root locus form

indicates unstable limit cycles $\forall n$. The IDF stability technique involves evaluation of the incremental gain

$$N_B(A,o) = \frac{1}{2\pi}\int_o^{2\pi} f'(A\sin\theta)\,d\theta = 1 + \frac{1}{2\pi}\int_o^{2\pi}\tan^2(A\sin\theta)d\theta\,, \tag{7.80}$$

with the general result : $N_B(A,o) > Keq(A)$ because of the hard spring character. This is sufficient to ensure that all limit cycles are unstable.

DF inaccuracies may be eliminated from the IDF stability technique by considering perturbations about the actual limit cycles. For both the untransformed and transformed systems the resulting equivalent linear system for stability studies is that of Fig. 7.15, with the incremental gain $N_B^*(k,n) = (4n+1)\,E(k)/k'$. $N_B^*(k,n)$ varies monotonically from $(4n+1)\pi/2$ to $(4n+1)\infty$ as k varies from o to 1. Hence the system of Fig. 7.15 is unstable $\forall k, \forall n$. It can be shown that the time average value of the periodic time varying coefficient, $\propto [1+x_n^2(t-1)]$, of the variational system of Fig. 7.13 is also given by $(4n+1)E(k)/k'$, thus verifying the time averaging nature of the IDF technique for this system.

7.1.3 Comments

Loeb's criterion fails for the Jones system but predicts stability correctly for the complementary system. For the transformed Jones system, application of Loeb's criterion in the graphical root locus form (Figs. 7.10 and 7.11) does not take into account the characteristic roots other than the pair indicating the particular limit cycle mode. Location of all characteristic exponents (roots) of the variational system is found, approximately, through the IDF approach, and indicates unstable modes for $n \neq o$ leading to unstable limit cycles.

For the transformed complementary system, Loeb's criterion still

neglects the infinity of other characteristic roots, but the hard spring nature of the nonlinearity results in a correct prediction of instability just by considering the motion of the root pair for the particular limit cycle mode. The other modes of the variational system, or the IDF approximation to it, are neglected in Loeb's criterion because of the assumed form that perturbations must have in the Loeb analysis.

7.2. Two Other Systems

Two additional systems studied by other authors are further studied here since they relate closely to the transformed systems already discussed.

7.2.1. The System of Gelb and Vander Velde [6,pp.243-246]

The nonlinear time delay system of Gelb and Vander Velde is shown in Fig. 7.16. The nonlinearity is $f(x) = \sigma x - \epsilon x^3$; $\sigma, \epsilon > o$, and the linear plant e^{-s}/s. This system is identical in form to the transformed systems of Section 7.1 except for the nonlinearity. The describing function for this nonlinearity is $Keq(A) = \sigma - 3\epsilon A^2/4$, and application of the DF method yields limit cycle frequencies $w_n = |4n+1|\pi/2$, $n=o,\pm1,\pm2,---$ with amplitudes

$$A_n^2 = \frac{4}{3\epsilon}\ [\sigma - (4n+1)\pi/2]. \tag{7.81}$$

The condition for existence of a limit cycle (A_n, w_n) is $A_n^2 \geq o$ or $\sigma \geq (4n+1)\pi/2$. Loeb's criterion applied here results in the evaluation of

$$\frac{d}{dw}\,ImL(jw)\frac{d}{dA}\,Keq(A)\Big|_{(A_n,w_n)} = \frac{-3\epsilon A_n}{(4n+1)\pi}\ . \tag{7.82}$$

Since 7.82 is negative for $n \geq o$ and positive for $n < o$, Loeb's criterion predicts stable limit cycles for $n \geq o$ and unstable ones for $n < o$.

Simulation studies reported by Gelb and Vander Velde indicate that only the n = o limit cycle is stable. Furthermore, the n = o limit cycle is only stable for σ in the range $\pi/2 < \sigma < \sim 4$ or 5. Loeb's criterion is

thus incorrect in predicting stability for the $n > o$ limit cycles.

The IDF incremental gain, $N_B = \sigma - 3\epsilon A^2/2$ for this nonlinearity, leads to the IDF system of Fig. 7.17 for limit cycle (A_n, w_n). The stable region of this system is $o \leqslant \sigma - 3\epsilon A_n^2/2 \leqslant \pi/2$, and since

$$N_B(A_n, o) = \sigma - 3\epsilon A_n^2/2 = -\sigma + (4n+1)\pi, \tag{7.83}$$

the condition becomes

$$(4n+1)\pi - \pi/2 \leqslant \sigma \leqslant (4n+1)\pi \tag{7.84}$$

for a stable limit cycle. For $n < o$ it is obvious that 7.84 is not satisfied since $\sigma > o$, and all $n < o$ limit cycles are predicted as unstable. However, for $n \geqslant o$ the existence condition is $\sigma \geqslant (4n+1)\pi/2$ for limit cycle (A_n, w_n), and 7.84 can be satisfied. In particular, for $n = o$ the IDF region for a stable limit cycle is $\pi/2 \leqslant \sigma \leqslant \pi$.

Certain discrepancies are noted between the IDF results and simulation studies. The upper limit of stability of the $n = o$ limit cycle is not predicted correctly, and regions of stable limit cycles for $n > o$ are predicted which have not been observed. These discrepancies are attributed to the DF approximation, since previous studies have indicated the basic accuracy of the time averaging approximation in the IDF technique for this form of system. Stability condition 7.84 may be written in terms of A_n as

$$\frac{8n\pi}{3\epsilon} \leqslant A_n^2 \leqslant \frac{2(4n+1)\pi}{3\epsilon} . \tag{7.85}$$

For $n = o$ this becomes $o \leqslant A_o^2 \leqslant \frac{2\pi}{3\epsilon}$, for $n = 1$: $\frac{8\pi}{3\epsilon} < A_1^2 < \frac{10\pi}{3\epsilon}$, etc. The $n = o$ limit cycle mode is the only one for which the stability interval starts out at $A = o$. Of course the best DF approximation occurs in the small amplitude region, and DF error then increases with amplitude. In the small amplitude regions $-(4n+1)\pi/2 \leqslant \sigma \leqslant (4n+1)\pi - \pi/2$, or

$o \leq A_n^2 \leq 8n\pi/3\epsilon$ - correct stability is predicted by the IDF stability technique.

A closer look at the nonlinearity $f(x) = \sigma x - \epsilon x^3$ (Fig. 7.18) indicates the typical region of operation (in terms of a saturation characteristic) as $-\sqrt{\sigma/(3\epsilon)} < x < \sqrt{\sigma/(3\epsilon)}$. In this region f(x) is a soft spring and the DF approximation should be reasonable. For the n = o limit cycle, $A_o^2 > \frac{2\sigma}{3\epsilon}$ is equivalent to $\sigma > \pi$, so it is seen that amplitudes yielding the IDF stability discrepancy for n = o correspond to amplitudes outside the typical region of f(x). Similarly, $\frac{\sigma}{2\epsilon} < A_n^2 < \frac{2\sigma}{3\epsilon}$ is equivalent to $\frac{4}{5}(4n+1)\pi < \sigma < (4n+1)\pi$, and for $n > o$ A_n must lie in this interval if 7.84 is to hold. Again, amplitudes yielding an IDF stability discrepancy for $n > o$ correspond to x out of the typical region of f(x).

A further indication of DF accuracy may be derived by calculating the ratio $\frac{\text{third harmonic amplitude}}{\text{fundamental amplitude}}$ for the output of the nonlinearity with a sinusoidal input. Since

$$f(A \sin wt) = \left(\sigma - \frac{3}{4}\epsilon A^2\right) A \sin wt + \frac{\epsilon}{4} A^3 \sin 3wt, \qquad (7.86)$$

this ratio is

$$\frac{\text{third harmonic}}{\text{fundamental}} = \frac{A^2}{\frac{4\sigma}{\epsilon} - 3A^2} . \qquad (7.87)$$

Fig. 7.19 shows a plot of 7.87 versus A^2. In the region $\frac{\sigma}{2\epsilon} < A^2 < \frac{2\sigma}{3\epsilon}$ the ratio varies from .2 to .33, and indicates substantial third harmonic content. This implies that the DF approximation will be relatively poor for amplitudes in the region of the IDF stability discrepancy.

The DF method, Loeb's criterion, and IDF stability technique may be related to graphical root locus interpretations using Figs. 7.10 and 7.11. Of course the results are the same as those already derived. Again the

failure of Loeb's criterion for the $n > o$ limit cycles is attributed to the ignoring of the unstable modes indicated, approximately, by the IDF system. The $n < o$ limit cycles are predicted correctly as unstable by Loeb's criterion because they correspond to $A_n^2 > \frac{4\sigma}{3\epsilon}$ and, hence, negative $Keq(A_n)$ and $N_B(A_n,o)$. If the DF system and IDF system are considered to have positive feedback then $Keq(A_n) = \frac{3}{4}\epsilon A_n^2 - \sigma > o$ and $N_B(A_n,o) = \frac{3}{2}\epsilon A_n^2 - \sigma > o$, with the nonlinearity essentially behaving like a hard spring. Application of Loeb's criterion and the IDF stability technique, using the root locus of Fig. 7.11, indicates that the motion of the root pair corresponding to the particular limit cycle mode always determines instability, even though the infinity of other roots are neglected in Loeb's criterion. This is exactly the same situation as that for the transformed complementary system.

7.2.2 The System of Brookes and Katzberg [9,10]

Brookes and Katzberg studied the nonlinear time delay relay system of Fig. 7.20 in some detail. For the ideal unit relay, $Keq(A) = \frac{4}{\pi A}$ and the DF limit cycle conditions become

$$\tan w = 1/w \tag{7.88}$$

and

$$A = \frac{4 \sin w}{\pi w} \quad . \tag{7.89}$$

Limit cycles (A_n,w_n) are predicted, with w_n identified in the graphical solution (Fig. 7.21) of 7.88, where $2n\pi < w_n < (4n+1)\pi/2$ so that $A_n > o$. Note that as n approaches ∞, w_n approaches $2n\pi$. For $n = o$ the result is $A_o = 1.123, w_o = .86$ and for $n = 1$ it is $A_1 = .03$, $w_1 = 6.437$. The corresponding values of Keq are $Keq(A_o) = 1.132$ and $Keq(A_1) = 42$. Brookes shows, using the Hamel Locus, that the exact frequencies are $w_o = .84$ and $w_1 = 6.41$ yielding DF frequency percentage errors of 2.38% and .42% respectively - certainly quite reasonable. He also demonstrates

that the infinity of limit cycles (A_n, w_n) exist by using the exact Hamel Locus, thus verifying the approximate DF limit cycle predictions.

Loeb's criterion in the analytical form involves establishing the sign of

$$\frac{d}{dw}\,\mathrm{ImL}(jw)\,\frac{d}{dA}\,\mathrm{Keq}(A)\Big|_{(A_n,w_n)} = \frac{-4[1+w_n+2w_n^2+w_n^3+w_n^4]\cos w_n}{w_n^2(1+w_n^2)^2\,\pi A_n^2} \quad (7.90)$$

Since $\cos w_n > o\ \forall n$, 7.90 is always negative, and Loeb's criterion predicts all limit cycles as stable.

Katzberg establishes in an exact fashion the infinity of limit cycles, and proves that only the n = o limit cycle is stable, with the higher frequency limit cycles unstable. Thus Loeb's criterion again fails for the higher frequency limit cycles in a time delay system.

The IDF stability technique yields $N_B(A,o) = \frac{2}{\pi A}$ for the ideal unit relay, and the IDF system is shown in Fig. 7.22. Stability of this system may be found by plotting the root locus of the system with $N_B(A_n,o)$ replaced by the general K. The root locus for this form of linear time delay system is shown in Fig. 7.23 (see Bower and Schultheiss [26] for details). Only the upper half plane is shown since the bottom half must be symmetrical. From Fig. 7.23 it is seen that additional pairs of roots move into the RHP as the gain K passes through the critical values $K_n = w_n/\sin w_n$ in sequence. The values w_n are calculated from 7.88 and shown graphically in Fig. 7.21, and the K_n of course correspond to the values of $\mathrm{Keq}(A_n)$ required by the DF conditions. The system of Fig. 7.22 is stable if and only if $o \lessgtr \frac{2}{\pi A_n} \lessgtr K_o = 1.132$. Since $\frac{2}{\pi A_n} = \frac{w_n}{2\sin w_n}$, the stability condition becomes

$$o \lessgtr \frac{w_n}{2\sin w_n} \lessgtr 1.132\ . \quad (7.91)$$

Now 7.91 can be shown to be satisfied only for n = o where $\frac{w_o}{2\sin w_o} = .566$. For $n > o$, $\frac{w_n}{2\sin w_n} > 1.132$, so that a prediction of instability results for the $n > o$ limit cycles. Thus the IDF stability technique gives the true stability situation for all limit cycles in this system.

Again the reason for the failure of Loeb's criterion may be observed graphically in terms of the IDF system and the root locus of Fig. 7.23. For the DF limit cycles corresponding to higher frequency intersections the root locus indicates roots in the RHP for $K = N_B(A_n,o)$, $n > o$. Loeb's criterion neglects these roots and considers only the root pair corresponding to the intersection $j w_n$. With the soft spring nonlinearity, Loeb's criterion then predicts stability from this simplified "local" perturbation analysis.

Brookes shows that for the variational system of the second intersection ($w = w_1$) limit cycle, one solution mode is $e^{(1.22+j\ 1.55)t}$. In other words, one characteristic value of this variational equation is 1.22 + j 1.55. It is this unstable mode which causes the limit cycle instability. Now in terms of the IDF system and its root locus of Fig. 7.23, the location of the principal root at gain $K = N_B(A_1,o) = 21$ may be found from the characteristic equation

$$s^2 + s + 21e^{-s} = o. \qquad (7.92)$$

Setting $s = \sigma + jw$ and substituting into 7.92 yields the solution $s = 1.28 + j\ 1.62$ as the value of the principal root. This obviously corresponds to the unstable mode found by Brookes, and the value is reasonably close to the characteristic value. In fact, the percentage error in σ is 4.92% and in w is 4.52% - both quite small considering that the IDF system is the DF approximate time-averaged counterpart of the exact variational system. This result is then very encouraging in

support of the use of the IDF stability technique in time delay systems both to determine limit cycle stability and to predict the actual modes of instability. Note that Loeb's criterion could not predict the presence of this unstable mode at a frequency different than the limit cycle frequency because of the assumption of perturbations of the same frequency as the limit cycle.

Using ideas due to Grensted [35,36] , Katzberg develops a nonrigorous argument for the failure of Loeb's criterion in this and other time delay systems. He considers general solutions of the system of Fig. 7.20 in the form $x(t) = A\, e^{\sigma_i t} \sin wt$ with the corresponding describing function

$$Keq(A) = \frac{4}{\pi A e^{\sigma_i t}} \quad , \tag{7.93}$$

due to Grensted. From Nyquist analysis, using the critical locus $-Keq^{-1}(A) = -\pi A\, e^{\sigma_i t}/4$ (see Fig. 7.24), oscillation conditions are found as intersections of the critical locus and Nyquist plot $L(jw) = e^{-jw}/[jw(jw+1)]$ with $\sigma_i = o$, but other modes at the oscillation conditions with $\sigma_i > o$ are established as intersections of $L(\sigma_i+jw) = e^{-\sigma_i - jw}/[(\sigma_i+jw)(1+\sigma_i+jw)]$ with the oscillation condition. Additional modes of the form $A\, e^{\sigma_i t} \sin wt$, $\sigma_i > o$ are clearly unstable, and imply that the corresponding oscillation (limit cycle) is also unstable. In this manner the higher frequency limit cycles are predicted as unstable. Although correct stability results are predicted, the analysis is not correct. This analysis is equivalent to finding the unstable roots of the DF system corresponding to a particular limit cycle (A_n, w_n). However, it has been shown that it is the IDF system which approximates to the variational system, and unstable roots of the IDF system determine unstable limit cycles. Hence talk of two or more modes existing simultaneously in the

nonlinear system of Fig. 7.20 is meaningless, and only the IDF system should be used for determining possible unstable modes. For example, Katzberg calculates the unstable mode, supposedly existing simultaneously with the limit cycle (A_1, w_1), as 1.66 + j 1.74. This mode, compared to the exact unstable mode of the variational system, 1.22 + j 1.55, shows 36.9% error in σ and 12.25% error in jw. The IDF unstable mode is then much more accurate, as it should be.

7.3 Time Averaging in a Special System

El'sgol'ts [34] studies the periodic time varying linear system of Fig. 7.25, where a (t) is periodic with period T and n is an arbitrary positive integer. This system is then quite similar to the variational systems for the transformed Jones and complementary systems. However, the difference lies in the fact that here there is an integer relationship between the period of the time varying coefficient and the time delay. The differential-difference equation corresponding to the system is

$$\dot{\epsilon}(t) = - a(t-nT)\ \epsilon(t-nT)$$
$$= - a(t)\ \epsilon(t-nT)\ . \qquad (7.94)$$

Now an infinite set of solutions of 7.94 exists in the form $\epsilon(t)=e^{\int_0^t g(u)du}$, with g(u) periodic of period T. If this form of solution is substituted into 7.94 then

$$g(t) = - a(t)\ e^{-nTk}, \qquad (7.95)$$

with $k \equiv \frac{1}{T} \cdot \int_0^T g(u)du = \overline{g(t)}$. Now from 7.95

$$k = \frac{1}{T} \int_0^T g(u)du = - e^{-nTk} \cdot \frac{1}{T} \int_0^T a(u)du = - \overline{a(t)}\ e^{-nTk}, \qquad (7.96)$$

so that solutions for k from 7.96 are equivalent to finding the roots of the constant coefficient time delay system of Fig. 7.26 with s replaced

by k. However, this system is simply the time-averaged system of the original system of Fig. 7.25. Also, stable or unstable solutions $\varepsilon(t) = e^{\int_0^t g(u)du}$ are determined by Re k < o or Re k > o respectively. Determination of the characteristic values $s_i = k_i$, i = 1,2,-- of the time-averaged system of Fig. 7.26 then yields solutions $\varepsilon_i(t) = e^{\int_0^t g(u,k_i)du}$ with $g(t,k_i) = -a(t)e^{-nTk_i}$ and $k_i = \overline{g(t,k_i)}$. The solutions $\varepsilon_i(t)$ are stable if Re k_i < o, unstable if Re k_i > o, and periodic if Re k_i = o.

If the infinite set of solutions is fundamental (linearly independent and spanning the solution space) then stability of the system of Fig. 7.25 is equivalent to the stability of the time-averaged system of Fig. 7.26. Even if the solutions do not form a fundamental set, certainly a sufficient condition for the instability of the time varying system is the instability of the time-averaged system caused by at least one characteristic root with positive real part. Zverkin [37,38] has done work on this and more general time varying delay systems which indicates that stability may be determined by studying the stability properties of their time-averaged counterparts.

The purpose of illustrating this special time varying delay system is to indicate at least one form of delay system for which time averaging is not an approximation in terms of stability analysis. This gives further support to the idea that time averaging in the IDF system for time delay systems is reasonably accurate with regard to stability results.

7.4 Conclusions

For the time delay systems examined in this chapter a result common to all of them is the accuracy of the time averaging involved in the IDF system. The only serious source of error in the use of the IDF stability technique here is the DF approximation itself. Although time averaging

probably works reasonably well away from stability boundaries, a surprising feature of the IDF stability technique applied to the system of Brookes and Katzberg is its ability to predict the unstable mode of the variational system rather accurately (considering that the DF approximation is involved as well). With the consistently good IDF results of the examples, the possibility of the IDF stability technique working well in other time delay systems exists, and should be investigated.

Loeb's criterion is clearly seen to fail for time delay systems due to the simplified assumption of perturbations only about the limit cycle amplitude and frequency. The IDF stability technique indicates approximate unstable modes, at lower frequencies, for the higher frequency limit cycle possibilities. Brookes' exact variational system analysis for the one system is evidence that the IDF system is indeed approximating the variational system well in terms of predicting the unstable characteristic values.

The IDF stability technique is preferred to the argument of Katzberg and Grensted regarding failure of Loeb's criterion in time delay systems. This technique is related directly to the theoretical variational analysis and, although approximate, appears to predict the unstable modes rather well. Katzberg's argument in terms of different modes in the nonlinear system is unsound theoretically since it does not relate to the variational system.

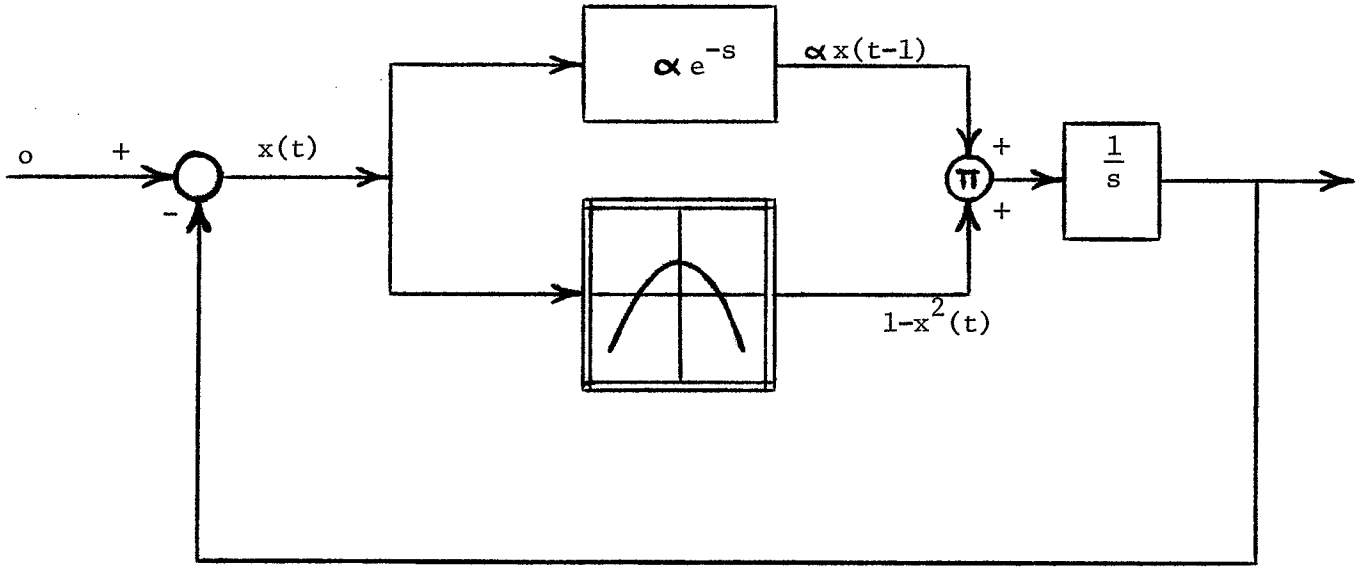

Fig. 7.1 BLOCK DIAGRAM OF JONES SYSTEM

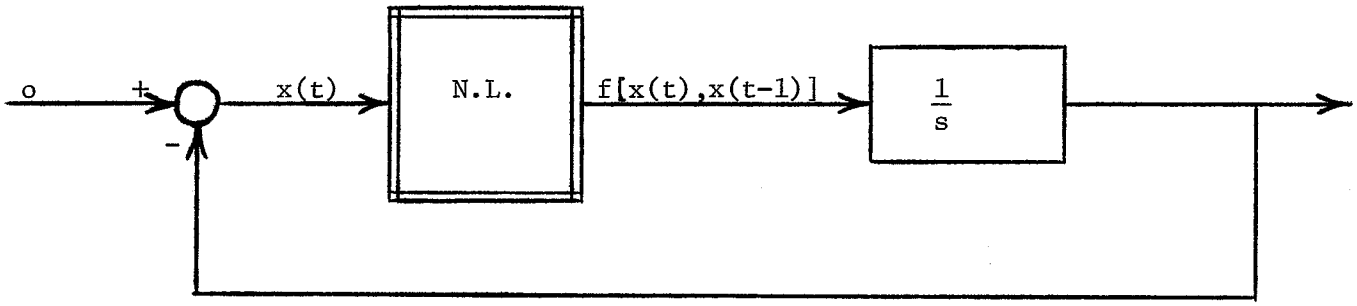

Fig. 7.2 SIMPLIFIED BLOCK DIAGRAM OF JONES SYSTEM

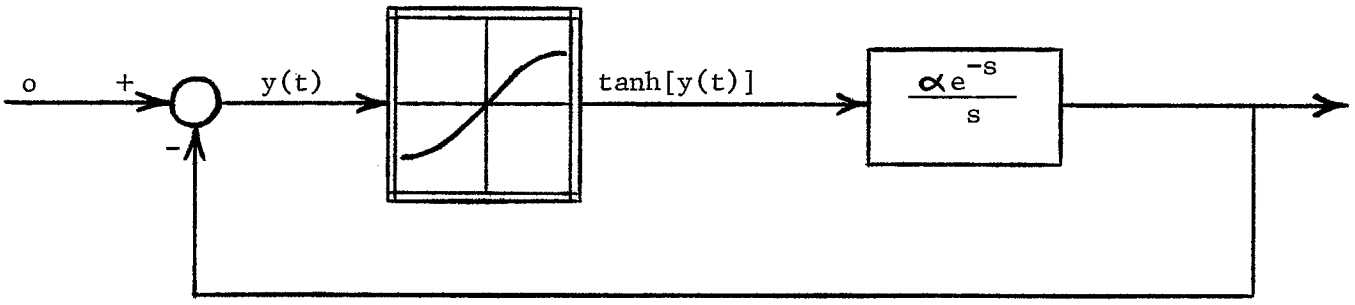

Fig. 7.3 BLOCK DIAGRAM FOR SYSTEM EQUATION 7.8

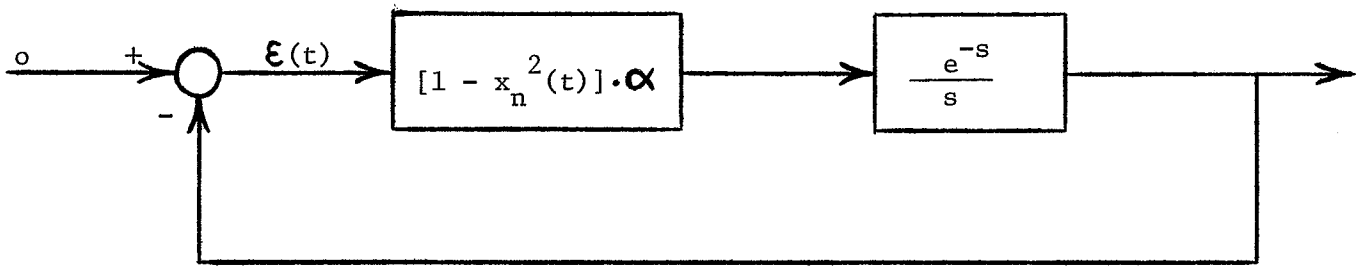

Fig. 7.4 VARIATIONAL SYSTEM FOR PERIODIC SOLUTION $y_n(t)=\tanh^{-1}[x_n(t)]$

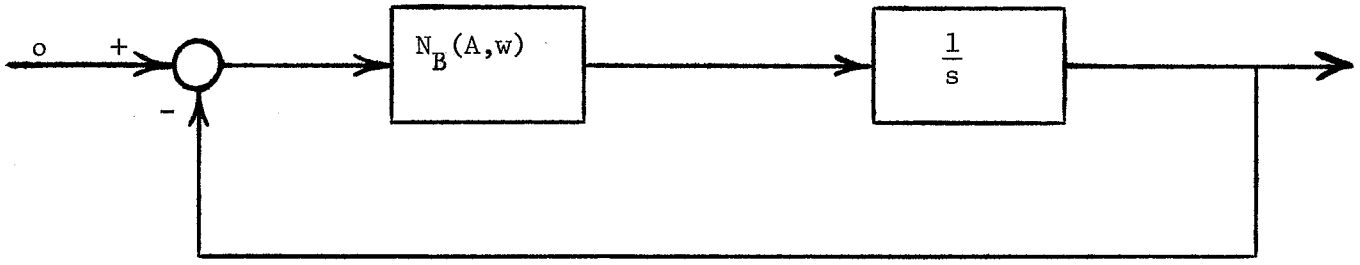

Fig. 7.5 IDF EQUIVALENT LINEAR SYSTEM FOR JONES SYSTEM

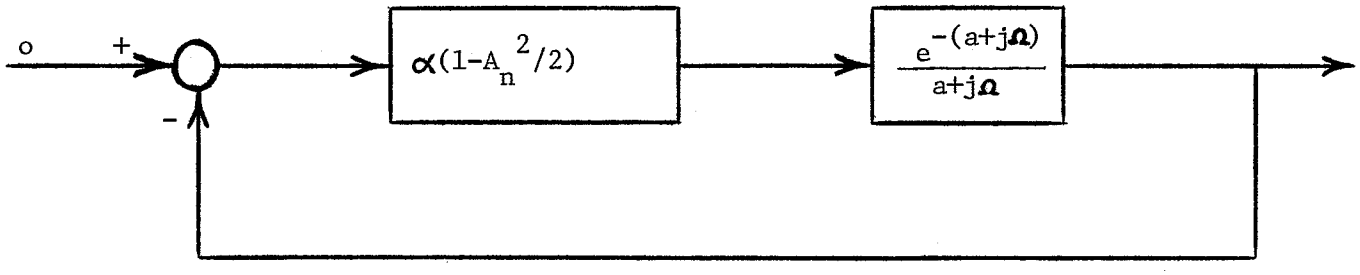

Fig. 7.6 IDF EQUIVALENT LINEAR SYSTEM FOR PERTURBATION $\epsilon e^{at}\sin\Omega t$

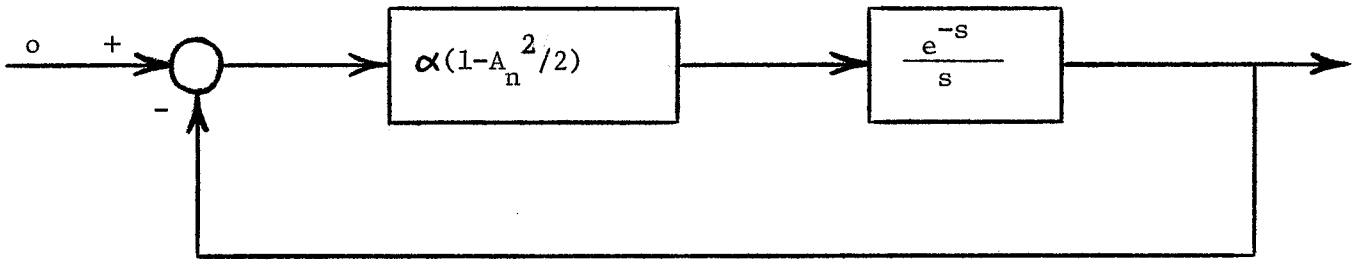

Fig. 7.7 IDF EQUIVALENT LINEAR SYSTEM FOR COMPLEX FREQUENCY s

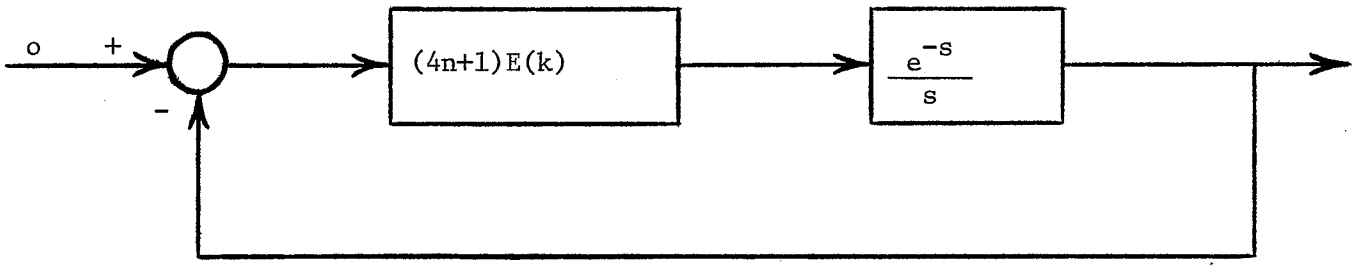

Fig. 7.8 EQUIVALENT LINEAR SYSTEM FOR ACTUAL LIMIT CYCLE.

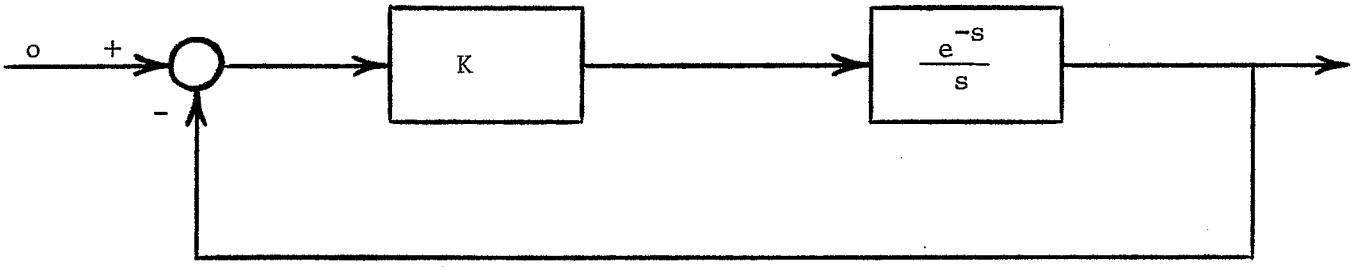

Fig. 7.9 LINEAR TIME DELAY SYSTEM

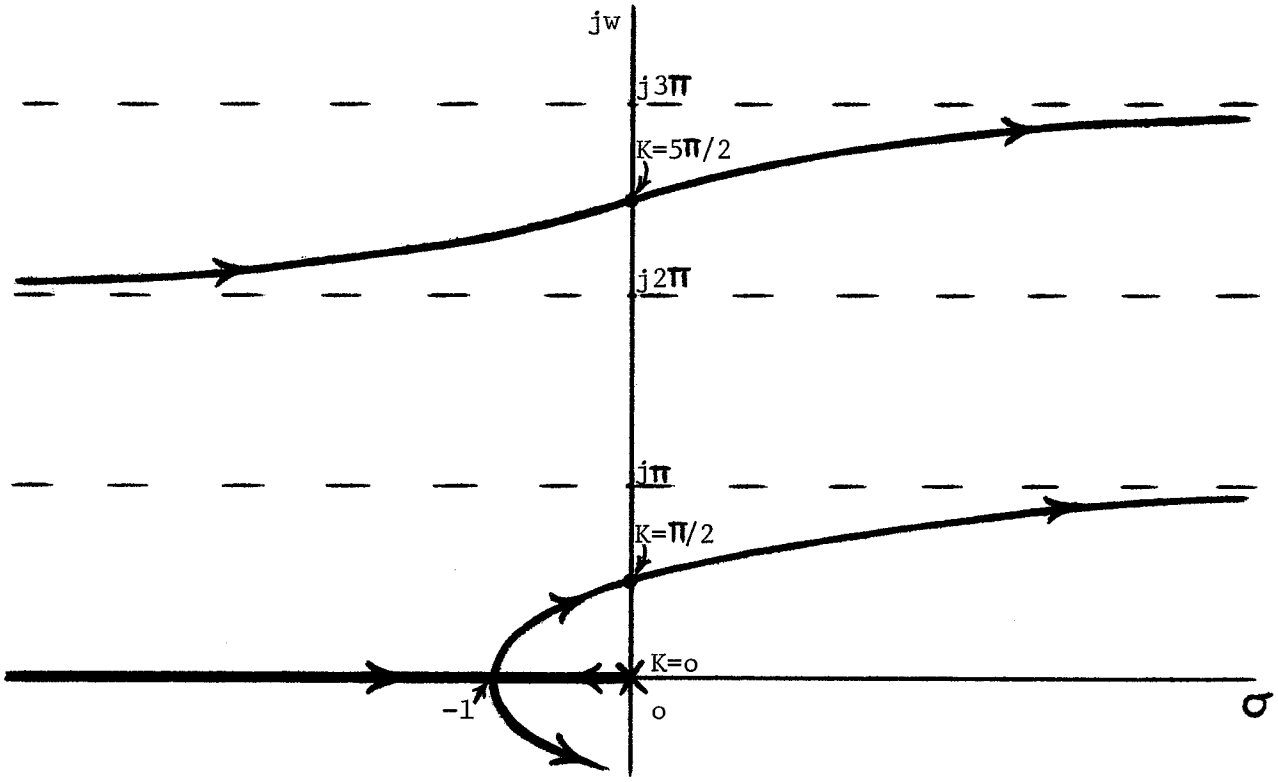

Fig. 7.10 ROOT LOCUS FOR NEGATIVE FEEDBACK

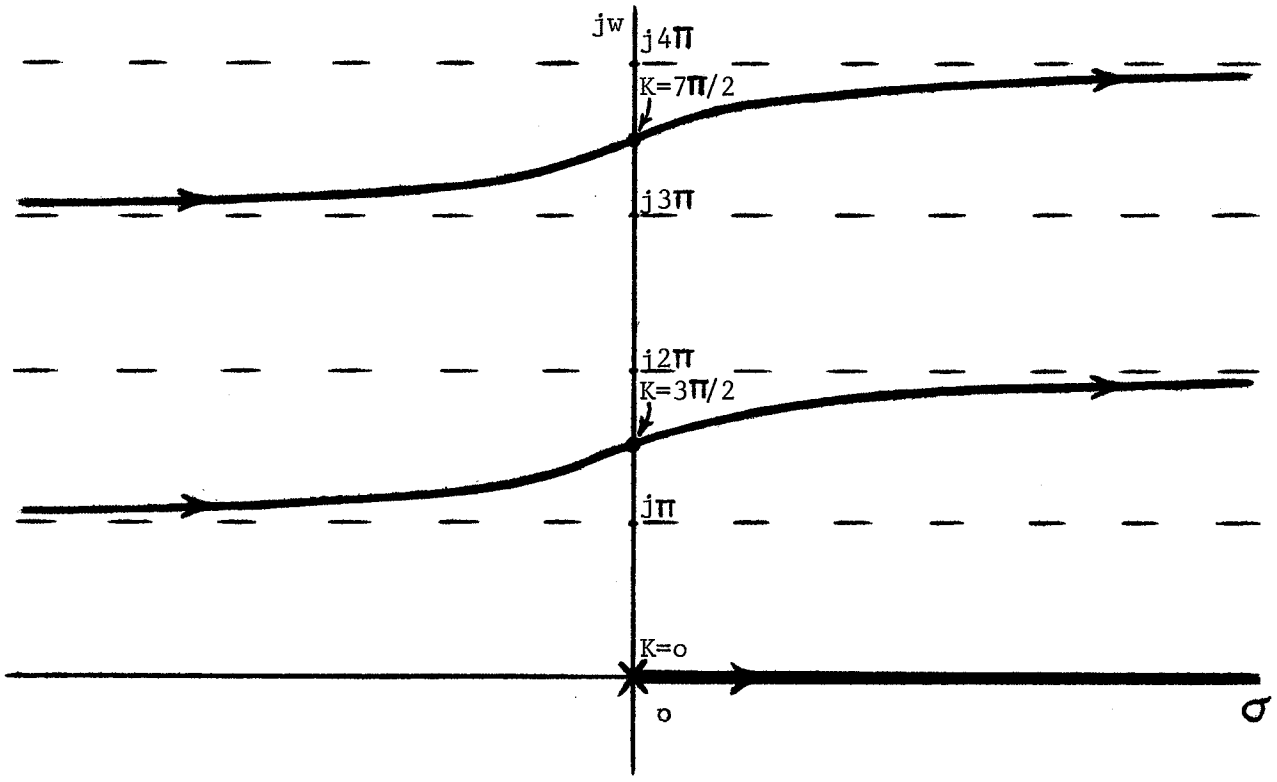

Fig. 7.11 ROOT LOCUS FOR POSITIVE FEEDBACK

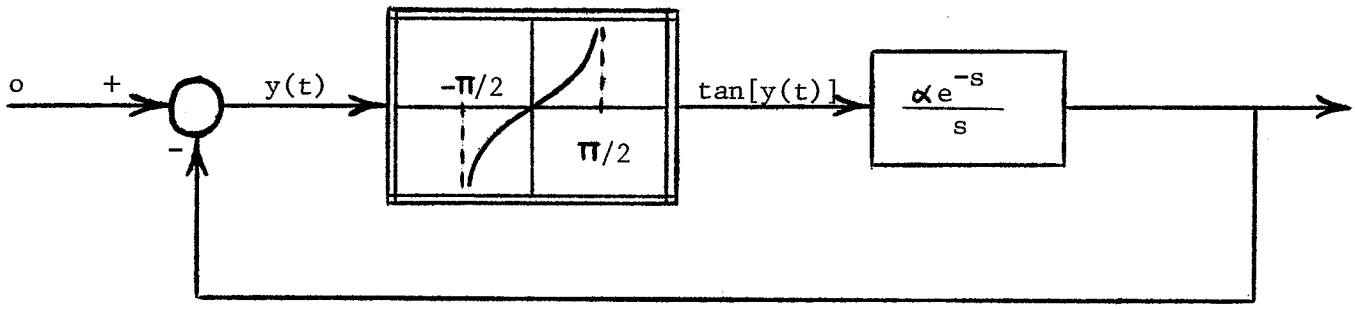

Fig. 7.12 BLOCK DIAGRAM FOR SYSTEM EQUATION 7.60

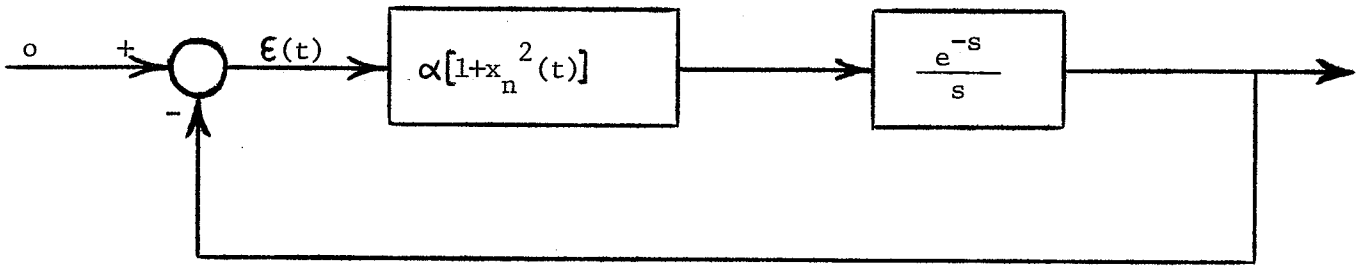

Fig. 7.13 VARIATIONAL SYSTEM FOR PERIODIC SOLUTION $y_n(t)=\tan^{-1}[x_n(t)]$

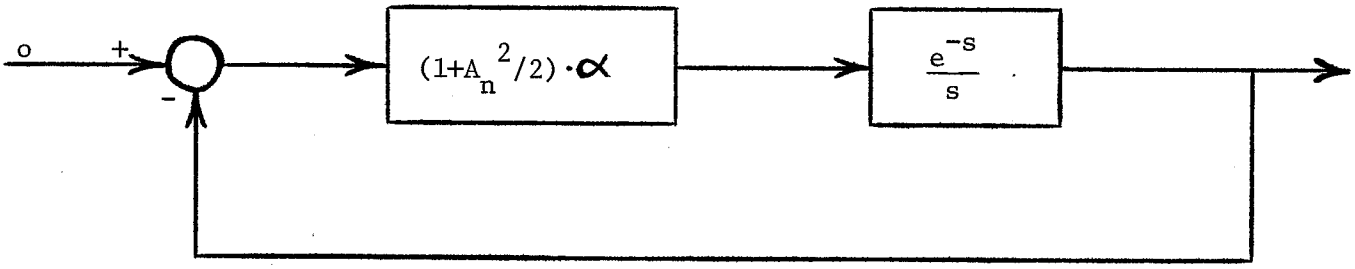

Fig. 7.14 IDF EQUIVALENT LINEAR SYSTEM FOR PERTURBATION $\epsilon e^{at}\sin\Omega t$

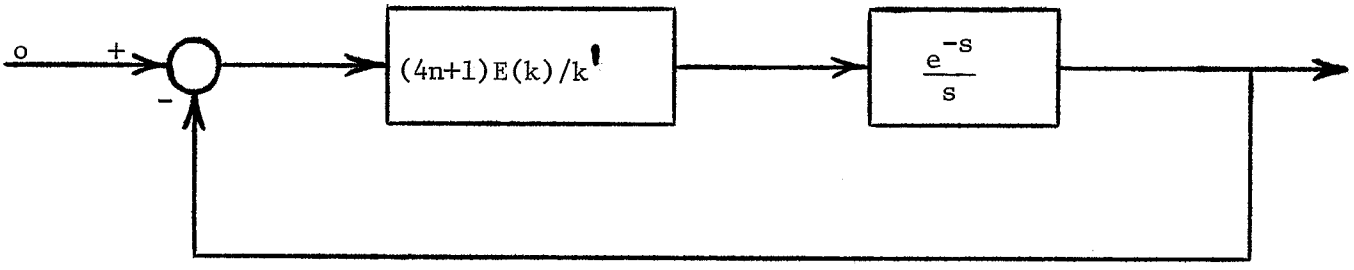

Fig. 7.15 EQUIVALENT LINEAR SYSTEM FOR ACTUAL LIMIT CYCLE

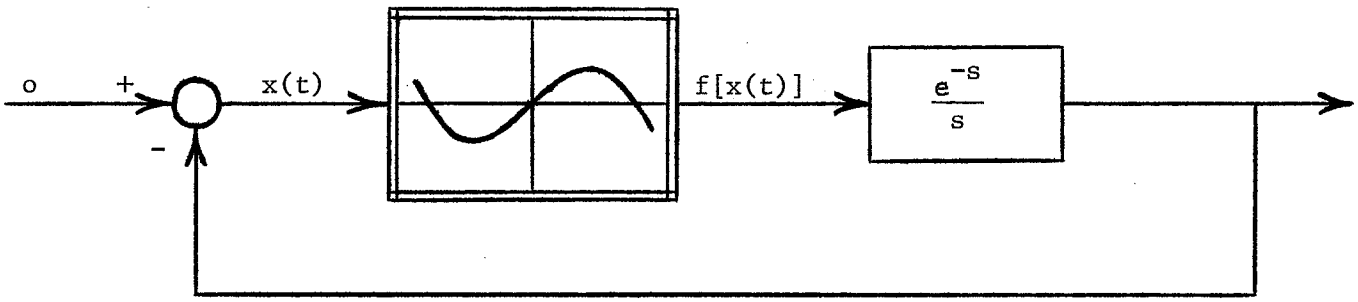

Fig. 7.16 SYSTEM OF GELB AND VANDER VELDE

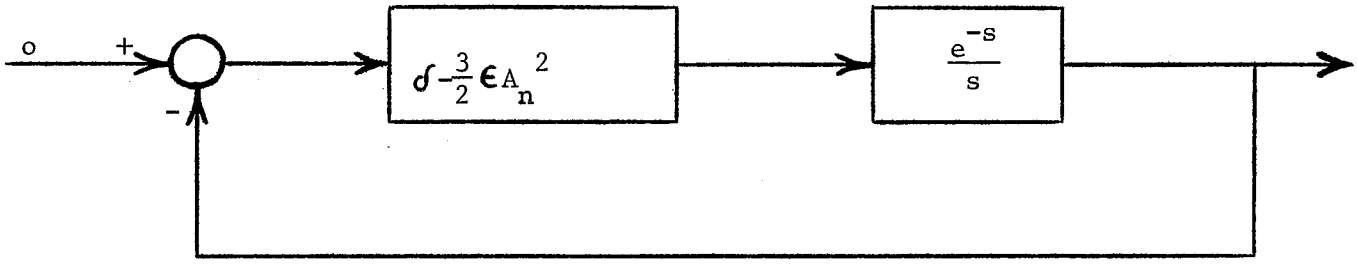

Fig. 7.17 IDF EQUIVALENT LINEAR SYSTEM

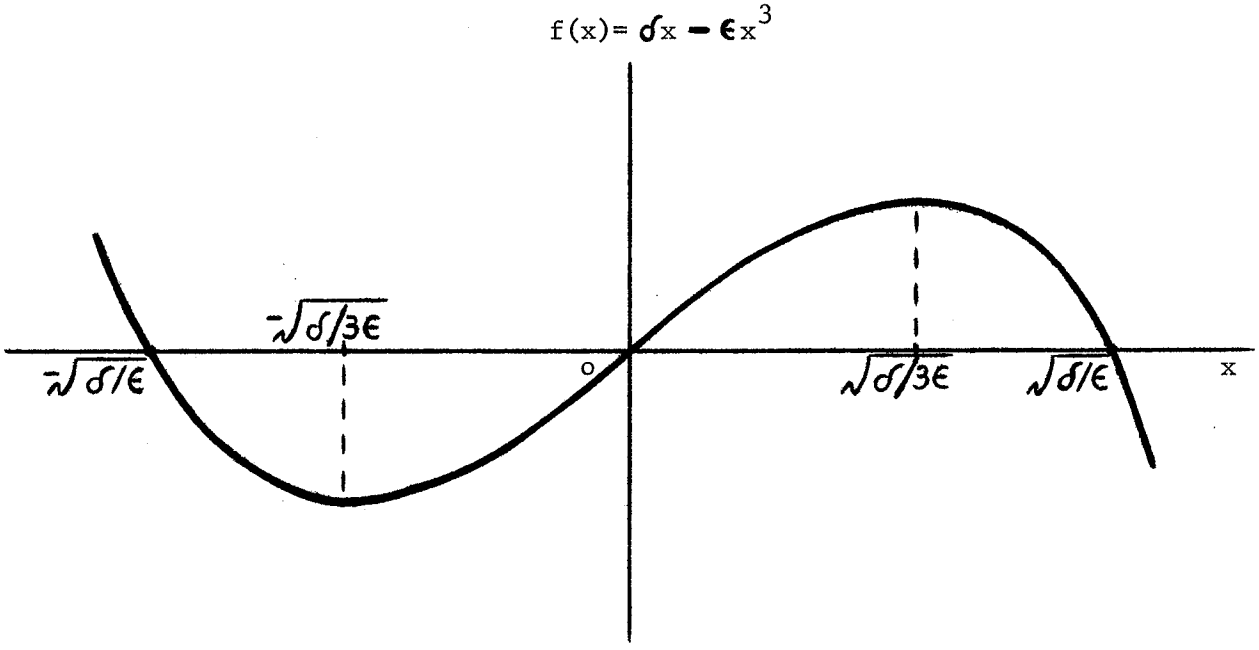

Fig. 7.18 NONLINEARITY OF GELB AND VANDER VELDE SYSTEM

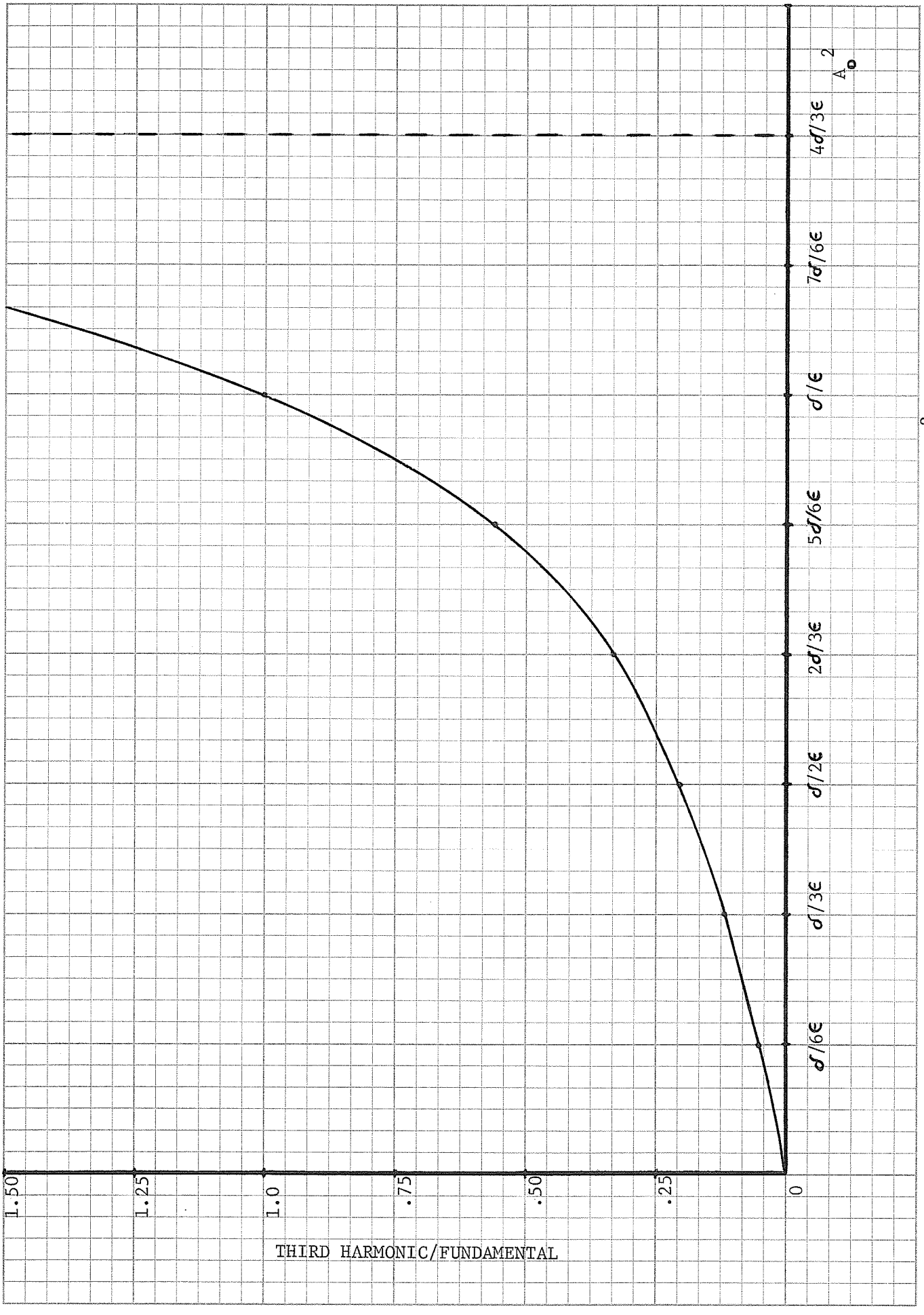

Fig. 7.19 GRAPH OF THIRD HARMONIC/FUNDAMENTAL VERSUS A_o^2

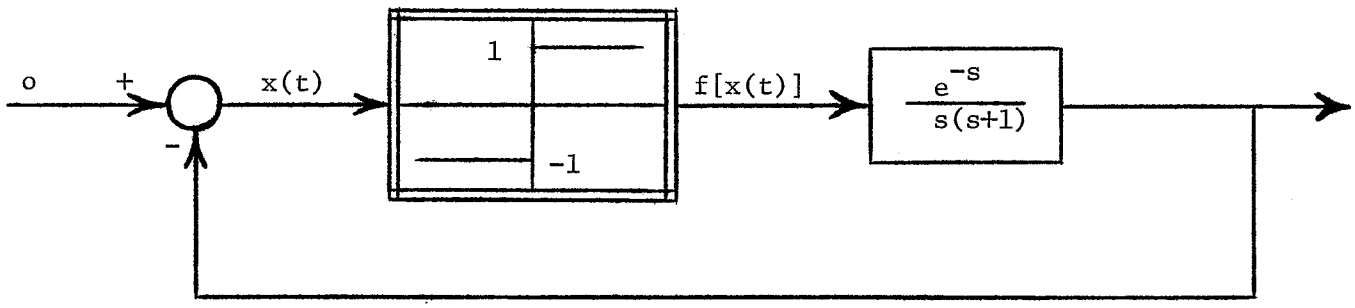

Fig. 7.20 SYSTEM OF BROOKES AND KATZBERG

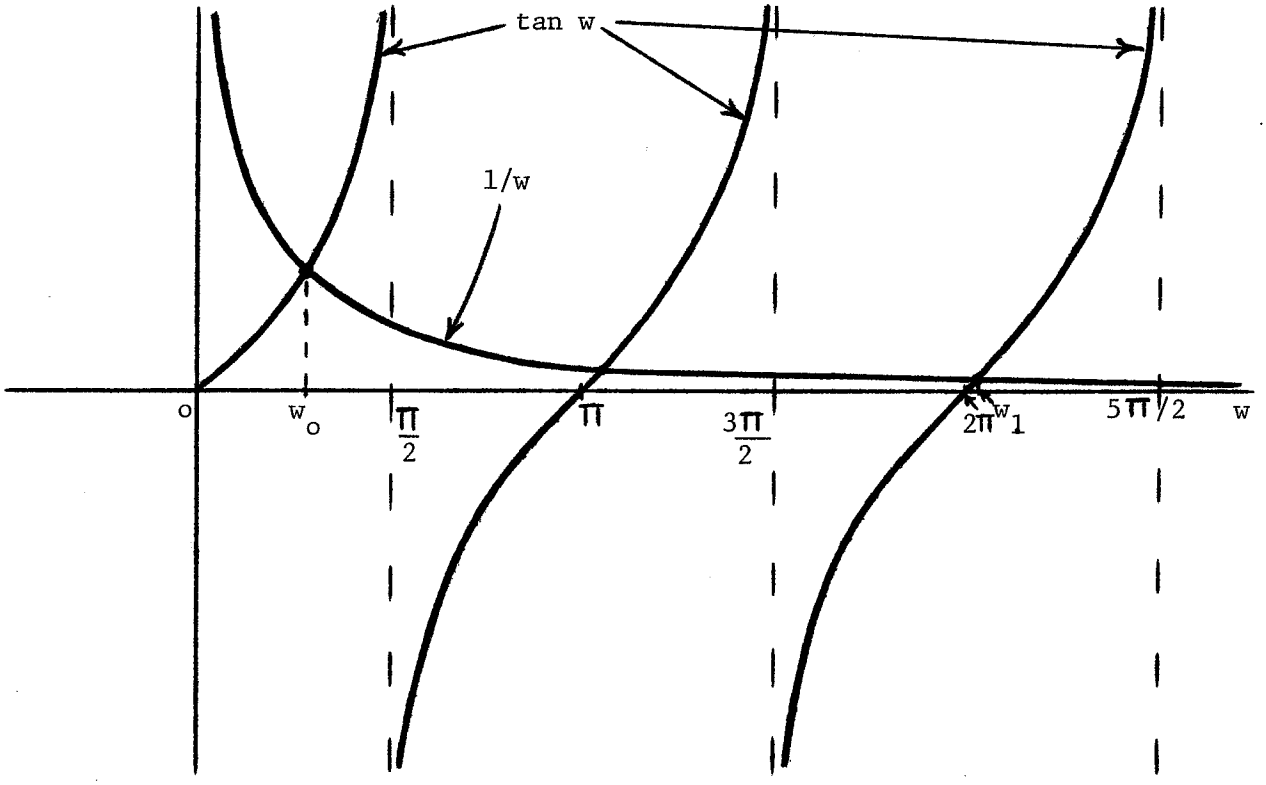

Fig. 7.21 GRAPHICAL SOLUTION OF 7.88

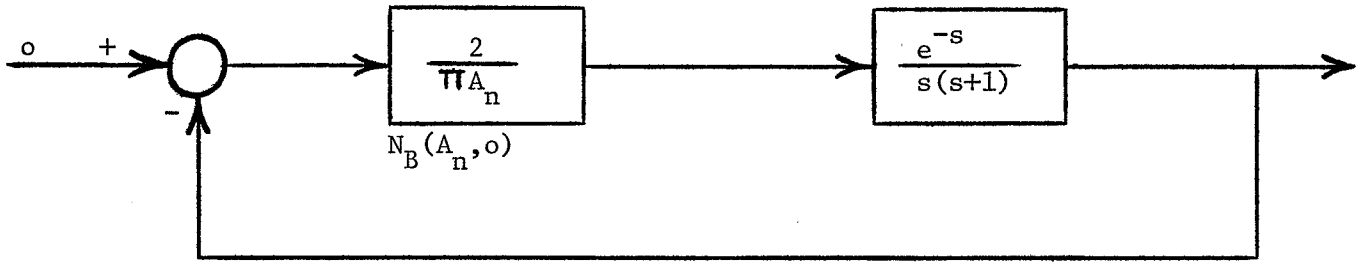

Fig. 7.22 IDF EQUIVALENT LINEAR SYSTEM

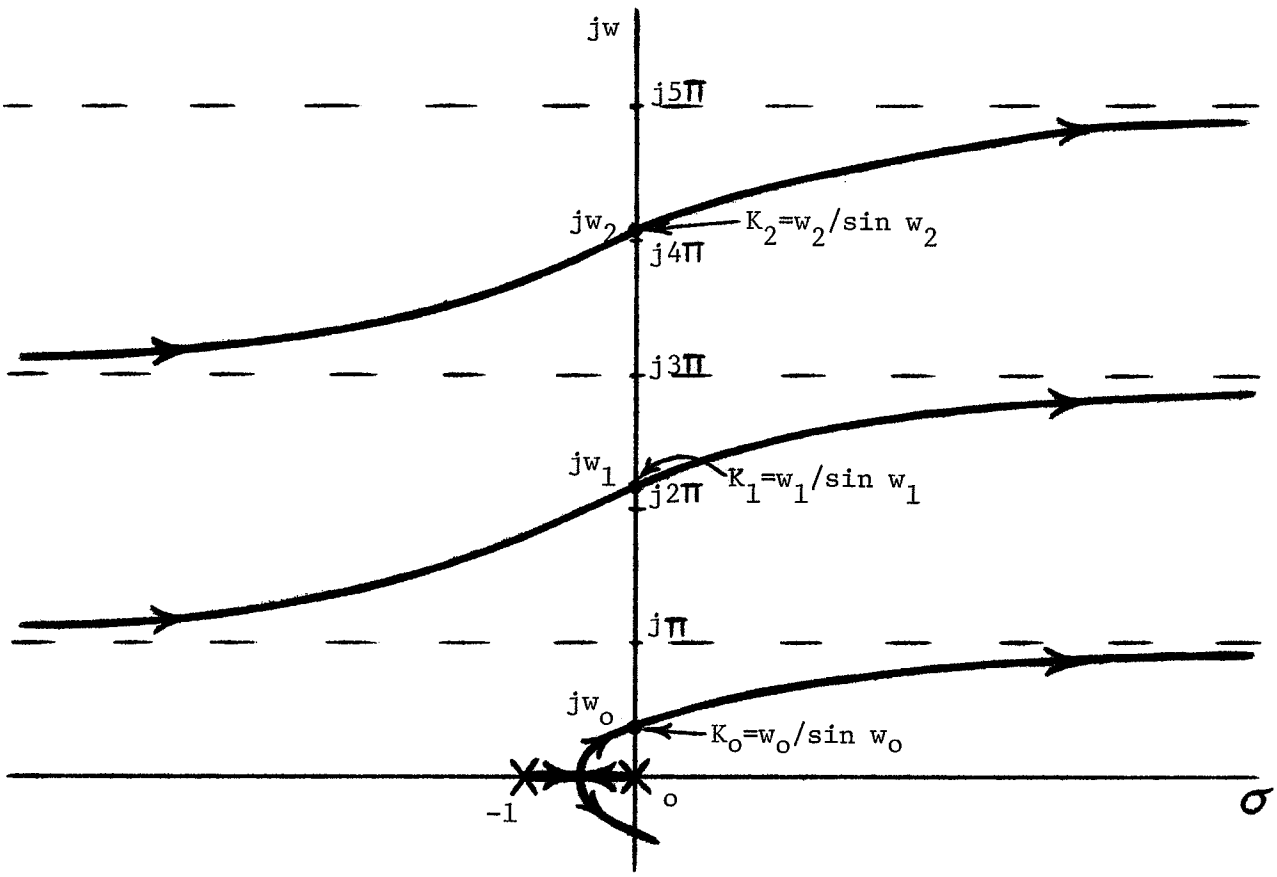

Fig. 7.23 ROOT LOCUS OF EQUIVALENT LINEAR SYSTEM

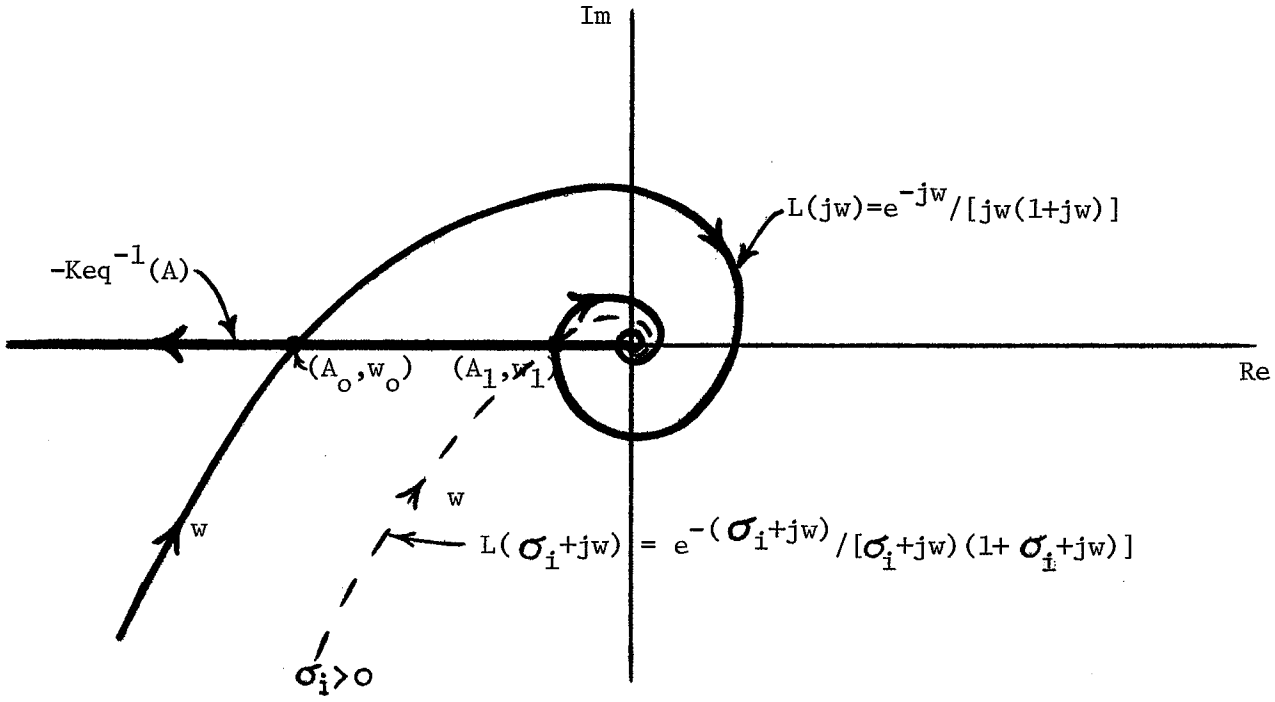

Fig. 7.24 NYQUIST PLOT ANALYSIS OF BROOKES AND KATZBERG SYSTEM

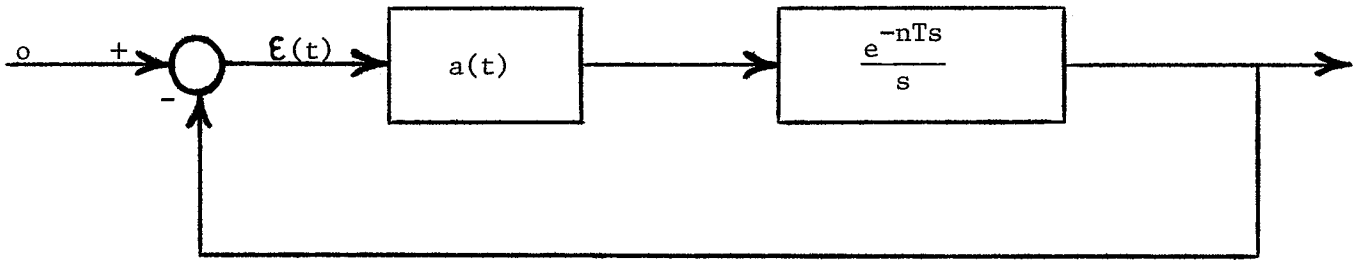

Fig. 7.25 LINEAR SYSTEM OF EL'SGOL'TS

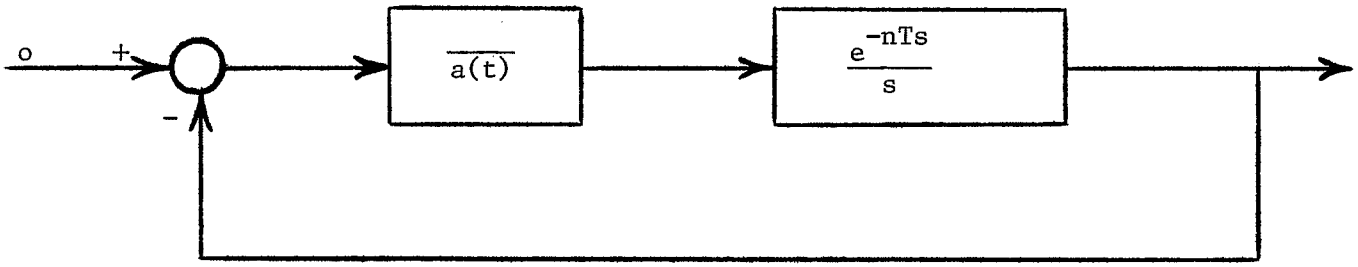

Fig. 7.26 TIME-AVERAGED SYSTEM

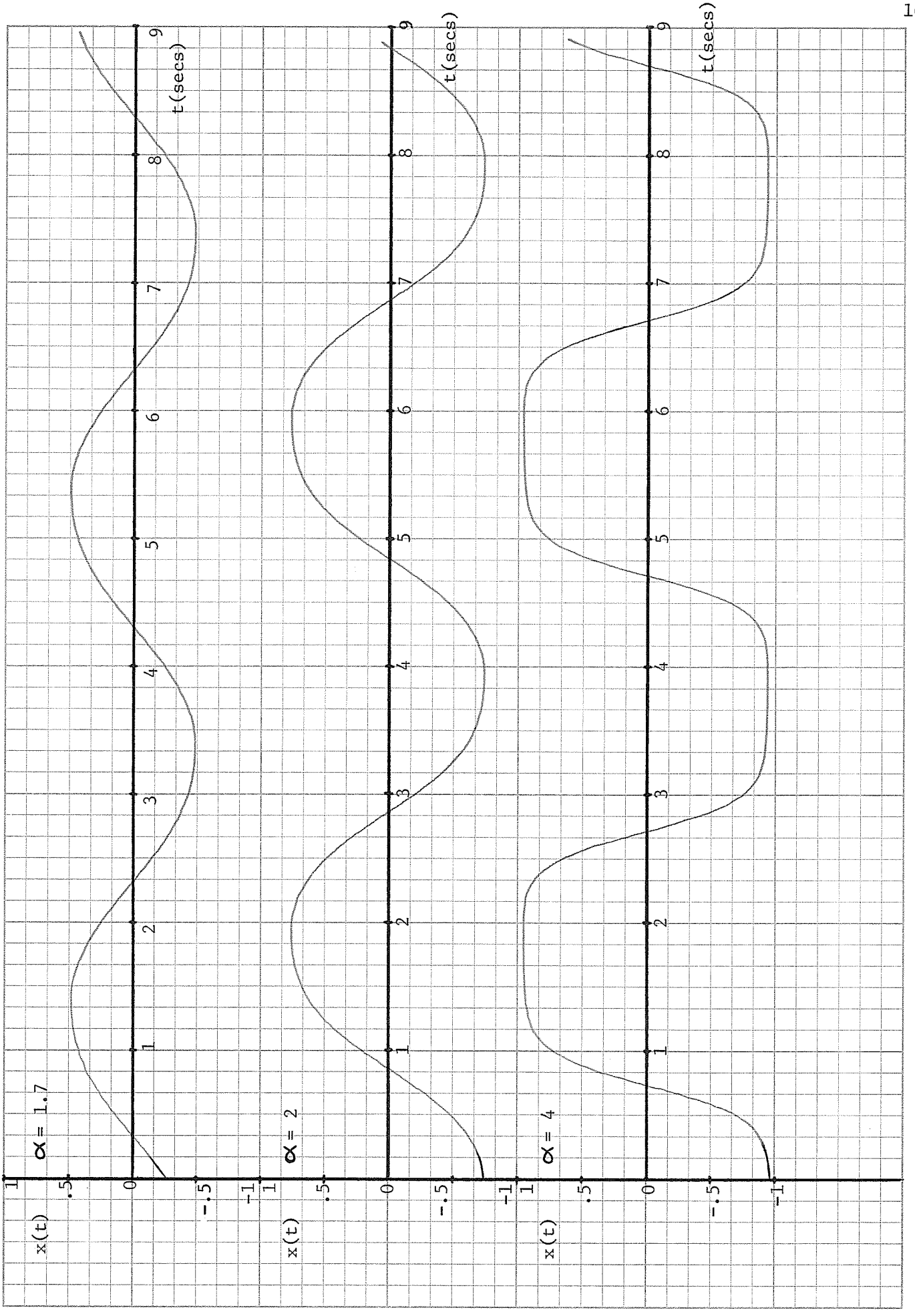

Fig. 7.27 PLOTS OF n = o LIMIT CYCLE OF JONES SYSTEM

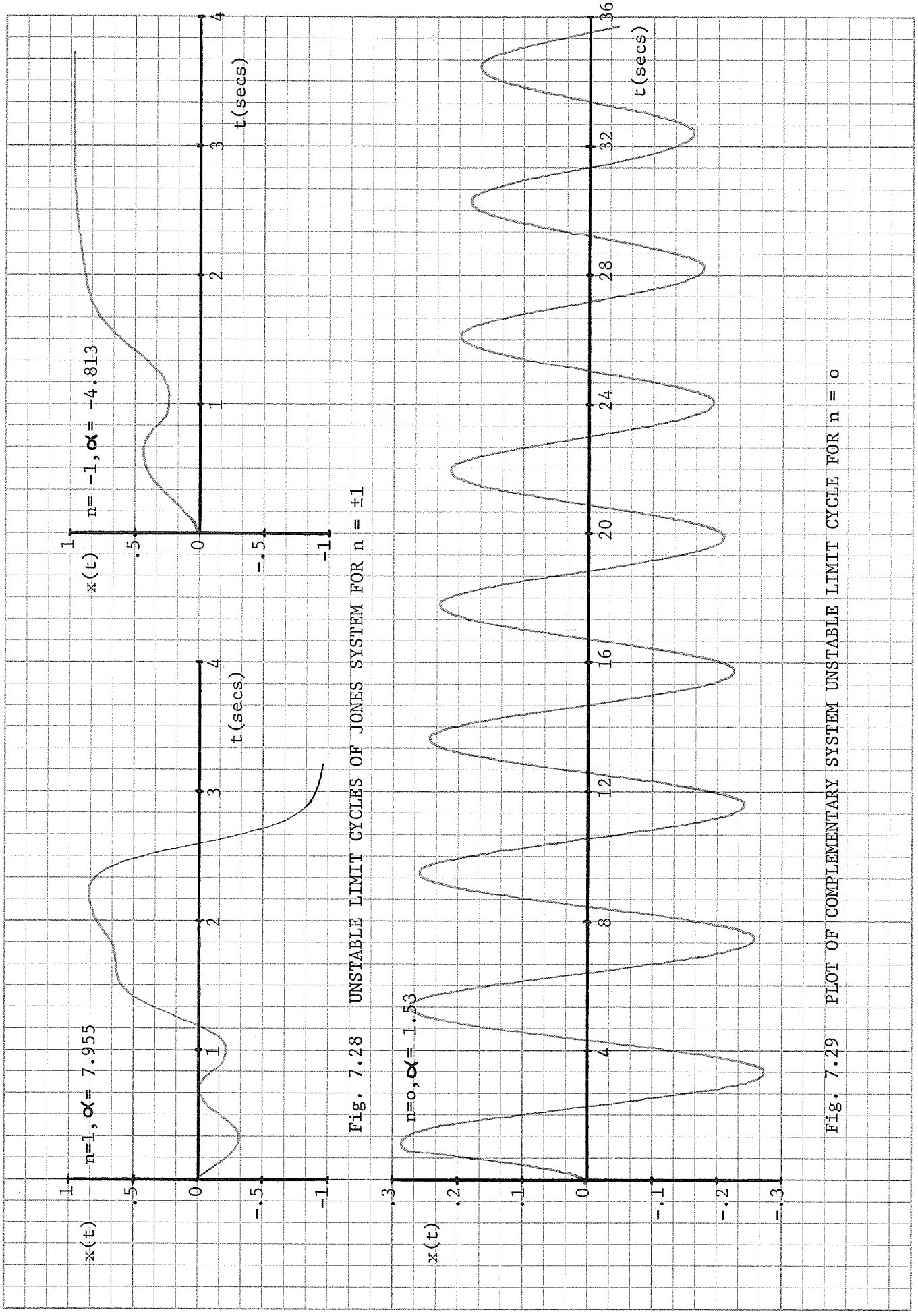

Fig. 7.28 UNSTABLE LIMIT CYCLES OF JONES SYSTEM FOR n = ±1

Fig. 7.29 PLOT OF COMPLEMENTARY SYSTEM UNSTABLE LIMIT CYCLE FOR n = 0

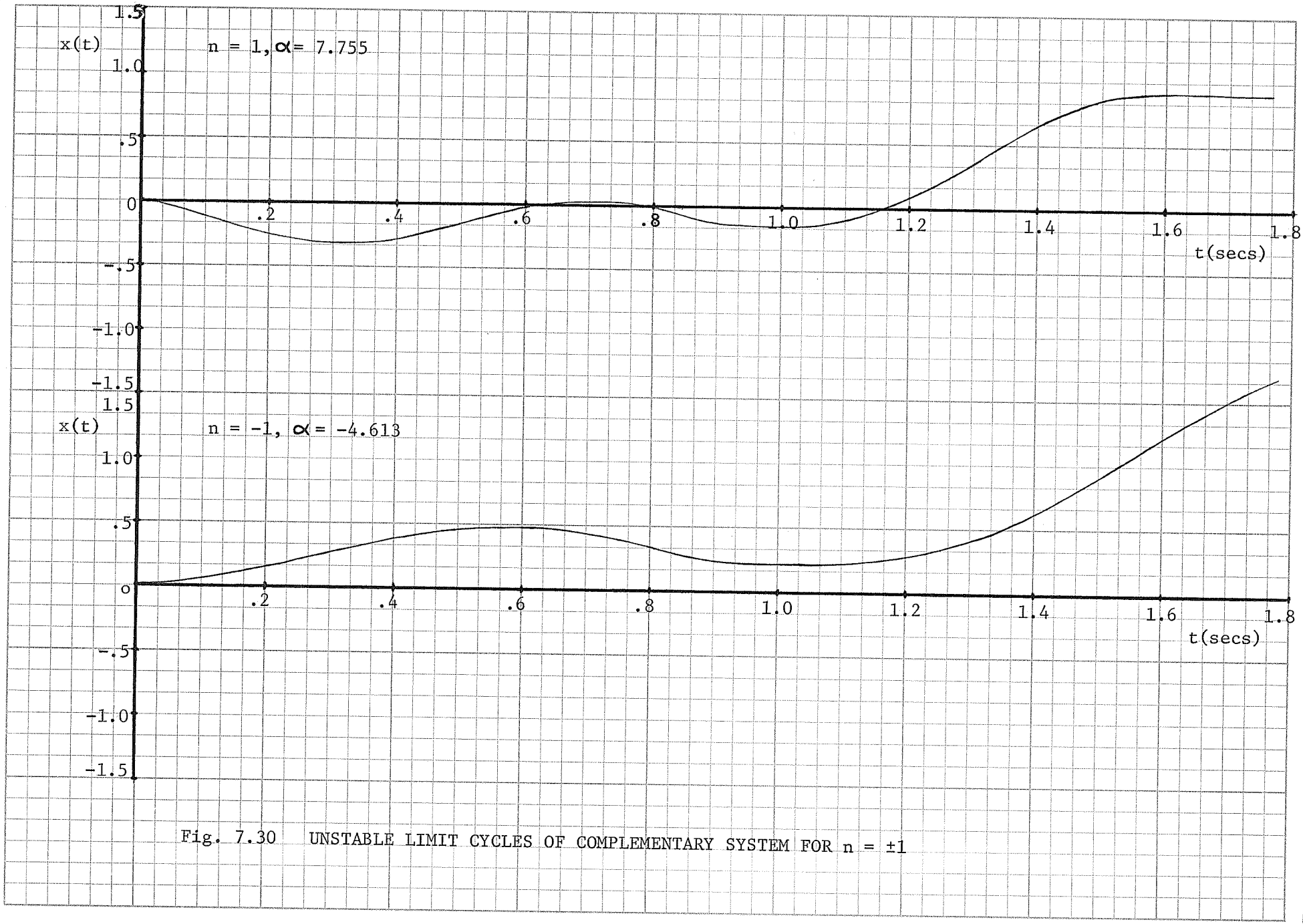

Fig. 7.30 UNSTABLE LIMIT CYCLES OF COMPLEMENTARY SYSTEM FOR n = ±1

CHAPTER 8

SUMMARY AND RECOMMENDATIONS FOR FUTURE WORK

8.1 Summary

It has become obvious from the work in this thesis that a comparison of Loeb's criterion and the IDF stability technique depends a great deal on the form of nonlinear system considered. Certainly it has been demonstrated that one of these techniques is not better than the other in all cases - different types of systems display different results in this respect.

Second order system studies are the most complete, in the theoretical sense, because of the known stability information about second order variational systems. Loeb's criterion is shown to be equivalent to a stability analysis of the DF approximate variational system, while the IDF stability technique involves the additional approximation of time averaging. This establishes Loeb's criterion as the more accurate stability technique for second order systems, assuming a reasonable DF approximation. However, system simulations reveal that discrepancies between Loeb's criterion and the IDF stability technique normally occur in regions of poor DF approximation, especially for frequency, due to the nature of typical nonlinearities and second order systems. The IDF stability technique seems to indicate these situations by predicting instability while Loeb's criterion predicts stability - in this sense the IDF stability technique is not entirely incorrect when these discrepancies occur. The problem of additional unstable modes not considered by Loeb's criterion does not arise for second order systems because only the complex conjugate root pair of the DF and IDF systems determines stability.

Studies of third order systems consist mostly of system simulations since only a few theoretical stability results are available. In general, the results indicate the similar trend of second order systems that discrepancies correspond to situations in which the DF approximation is poor - due to either large frequency error or a bias being present in the actual limit cycle. This frustrates any attempt to evaluate which is the better technique for third order systems. The IDF stability technique again appears to be an indicator of these situations of poor DF approximation when it predicts instability while Loeb's criterion predicts stability. Many instances of nonexistence of a DF predicted limit cycle also occur when the IDF stability technique predicts instability.

It appears that mode theory in terms of the IDF system does not work in general for third order systems - especially for the prediction of unstable limit cycles. The only consistent result from the examples studied is the fact that the pair of roots predicting an oscillation in the DF system must move into the RHP in the IDF system in order to have an unstable DF predicted limit cycle. However, this is shown not to be a sufficient condition for existence of an unstable limit cycle. One encouraging aspect in the use of the IDF stability technique is the demonstrated prediction of a stable limit cycle for certain cases of unstable DF systems - although regions of existence are not predicted very accurately, a lot of this error can be attributed to the poor filtering properties of the systems. It is interesting that an example could not be found illustrating the clear failure of Loeb's criterion when it neglects the third (unstable) mode - all examples of this sort that were tried resulted in nonexistence of a limit cycle rather than existence of an unstable limit cycle. For both second and third order

systems, Loeb's criterion and the IDF stability technique should probably be used together so that discrepancies may be identified and interpreted properly.

The time delay systems studied definitely show the inaccuracy of Loeb's criterion with its assumption of perturbations only about the limit cycle amplitude and frequency. The IDF stability technique is seen to work quite well in predicting stability, and there is evidence that it is fairly accurate in predicting the actual unstable modes of the variational system as well.

8.2 Recommendations for Future Work

The nonlinearities studied in this thesis have been restricted to the hard and soft spring types. However, many of the approximate techniques apply generally to any static, single-valued, odd symmetric nonlinearity. All that is really required is a knowledge of Keq(A), $N_B(A,o)$, and the relationship between these two quantities. Studies of other than hard and soft spring nonlinearities might produce further interesting results.

Nondelay systems of higher than third order should be studied for possible discrepancies between Loeb's criterion and the IDF stability technique. In fact, Gelb and Vander Velde [6, pp. 324-326] cite the hypothetical example of a saturation nonlinear system with conditionally stable equivalent linear system in which they claim Loeb's criterion can fail when compared to the IDF stability technique. Dorf [39,pp. 248-249] gives a realization of the linear portion of the system in terms of a fifth order plant with two zeros (root locus shown in Fig. 3.5). If Loeb's criterion indeed fails here then the nature of the failure is quite different from discrepancies in second and third order systems. In this system, the unstable mode in the IDF system is contributed by

the motion of the root pair generating the oscillation (A_3,w_3) in the DF system. Also, there is the possibility of Loeb's criterion failing in an entirely new way - predicting instability of (A_2,w_2) in Fig. 3.5 when the true situation given by the IDF stability technique is a stable limit cycle. These possibilities of course depend upon proper gain calibration of the root locus and the relationship between Keq and N_B. Clearly, different situations may arise in higher order systems, and these must be recognized and studied.

The prediction of the modes in the variational systems of nonlinear time delay systems, through the use of the IDF system, is particularly interesting in the light of the results of Chapter 7. A thorough study of the accuracy of these approximate modes should be done. Also, more work must be done on evaluating the stability of time varying variational systems with time delay, such as the variational system for periodic solutions of the Jones equation.

More generally, the relationship between stability of variational systems and stability of their time-averaged counterparts - basic to the IDF stability technique - must be determined for the various types of systems. It is apparent that time averaging is not always an approximation with respect to stability prediction, but just when it may be used successfully is not entirely known. Also, use of the IDF system for predicting modes in the variational system for nondelay cases should be studied.

COMMENT ADDED AFTER PRESENTATION: The sentence struck out on p. 27 is incorrect. The procedure outlined in [43] could be used to obtain the IDF stability of the biased sinusoid limit cycles of Examples I and III and should be a topic of future work.

APPENDIX I

THE SECOND CHARACTERISTIC SOLUTION OF 5.2

The first characteristic solution of 5.2 is $e_1(t) = \dot{x}^*(t)$, a periodic solution of period T. The second characteristic solution is assumed in the form $e_2(t) = a(t)\, e_1(t)$. Substitution in 5.2 yields

$$\ddot{a}(t)e_1(t)+2\dot{a}(t)\dot{e}_1(t)+a(t)\ddot{e}_1(t)+\left\{p_1+q_1g[x^*(t)]\right\}\left\{\dot{a}(t)e_1(t)+a(t)\dot{e}_1(t)\right\}$$

$$+\left\{p_o+q_og\,[x^*(t)]+q_1\dot{g}\,[x^*(t)]\right\}a(t)e_1(t) = o \qquad (I.1)$$

which, upon rearrangement, becomes

$$e_1(t)\ddot{a}(t)+\left\{2\dot{e}_1(t)+e_1(t)\,[p_1+q_1g(x^*)]\right\}\dot{a}(t)+\left\{\ddot{e}_1(t)+[p_1+q_1g(x^*)]\dot{e}_1(t)\right.$$

$$\left.+\,[p_o+q_og(x^*)+q_1\dot{g}(x^*)]\,e_1(t)\right\}a(t) = o, \qquad (I.2)$$

and, since $e_1(t)$ is a solution of 5.2, this simplifies to

$$e_1(t)\ddot{a}(t)+\left\{2\dot{e}_1(t)+e_1(t)\,[p_1+q_1g(x^*)]\right\}\dot{a}(t) = o. \qquad (I.3)$$

Equation I.3 may be written in the form

$$\frac{\ddot{a}(t)}{\dot{a}(t)} + \frac{2\dot{e}_1(t)}{e_1(t)} + \left\{p_1+q_1g\,[x^*(t)]\right\} = o, \qquad (I.4)$$

and integrated with respect to time as follows:

$$\int_{t_o}^{t}\frac{d\dot{a}(\tau)}{\dot{a}(\tau)} = -2\int_{t_o}^{t}\frac{de_1(\tau)}{e_1(\tau)} - p_1\int_{t_o}^{t}d\tau - q_1\int_{t_o}^{t}g[x^*(\tau)\,]d\tau,$$

to give

$$\ln\left\{\frac{\dot{a}(t)}{\dot{a}(t_o)}\right\} = -\,2\ln\left\{\frac{e_1(t)}{e_1\,(t_o)}\right\} - \left\{p_1+q_1\overline{g\,[x^*(t)]}\,\right\}(t-t_o)$$

$$-\,q_1\int_{t_o}^{t}\left\{g[x^*(\tau)] - \overline{g\,[x^*(\tau)]}\,\right\}d\tau. \qquad (I.5)$$

Solving for $\dot{a}(t)$ yields $\dot{a}(t) = \phi(t)\, e^{\rho t}$, where

$$\phi(t)=\dot{a}(t_o)\exp\left\{ - 2\ln\left\{\frac{e_1(t)}{e_1(t_o)}\right\} - q_1 \int_{t_o}^{t} \left\{g[x^*(\tau)] - \overline{g(x^*)}\right\} d\tau \right.$$

$$\left. + [p_1+q_1\overline{g(x^*)}]t_o \right\} \qquad (I.6)$$

is periodic of period T, and

$$\rho = -\left\{p_1+q_1\overline{g[x^*(t)]}\right\}. \qquad (I.7)$$

If now $a(t) = \phi_1(t)\, e^{\rho_1 t}$, with $\phi_1(t)$ periodic of period T, then

$$\dot{a}(t) = [\dot{\phi}_1(t) + \rho_1 \phi_1(t)]\, e^{\rho_1 t}. \qquad (I.8)$$

With the identifications $\phi(t) = [\dot{\phi}_1(t) + \rho_1\phi_1(t)]$ and $\rho = \rho_1$ it becomes clear that

$$e_2(t) = e_1(t)a(t) = \dot{x}^*(t)\ \phi_1(t)e^{\rho t} = P_2(t)e^{\lambda_2 t}, \qquad (I.9)$$

where $P_2(t) = \dot{x}^*(t)\ \phi_1(t)$ is periodic of period T and

$$\lambda_2 = \rho = -\left\{p_1+q_1\overline{g[x^*(t)]}\right\}. \qquad (I.10)$$

APPENDIX II

EQUIVALENT LOEB'S CRITERION FOR SECOND ORDER SYSTEMS

Equation 4.5 shows that

$$\frac{d}{dA} Keq(A) = - \frac{2Keq(A)}{A} + \frac{2\ N_B(A,o)}{A} . \qquad (II.1)$$

Now

$$L(jw)=\frac{jwq_1+q_o}{p_o-w^2+jwp_1} = \frac{[q_o(p_o-w^2)+q_1p_1w^2] + j[-q_op_1w+wq_1(p_o-w^2)]}{(p_o-w^2)^2+ w^2p_1^2}, \qquad (II.2)$$

so that

$$Im\ L(jw) = \frac{- q_op_1w+wq_1(p_o-w^2)}{(p_o-w^2)^2+ w^2p_1^2} . \qquad (II.3)$$

Then

$$\frac{d}{dw} Im\ L(jw) = \Big\{[p_1q_ow-q_1w(p_o-w^2)]\ [2wp_1^2-4w(p_o-w^2)]$$

$$+ [(p_o-w^2)^2+p_1^2w^2]\ [-q_op_1+q_1(p_o-w^2)-2w^2q_1]\Big\} / [(p_o-w^2)^2+w^2p_1^2]^2 \qquad (II.4)$$

and, since $w_o^2 = p_o-q_op_1/q_1$ (5.16),

$$\frac{d}{dw} Im\ L(jw)\Big|_{w=w_o} = \frac{[(p_o-w_o^2)^2+p_1^2w_o^2]\ [-2q_1w_o^2]}{[(p_o-w_o^2)^2+p_1^2w_o^2]^2} = \frac{-2q_1w_o^2}{(p_o-w_o^2)^2+p_1^2w_o^2} . \qquad (II.5)$$

Also, from 5.15, $Keq(A_o) = - p_1/q_1$, so that

$$\frac{d}{dw} Im\ L(jw)\ \frac{d}{dA} Keq(A)\Big|_{(A_o,w_o)} = \frac{-4w_o^2[p_1+q_1N_B(A_o,o)]}{[(p_o-w_o^2)^2+p_1^2w_o^2]\ A_o} . \qquad (II.6)$$

The Loeb condition for a stable (unstable) limit cycle, $\frac{d}{dw} Im\ L(jw) \cdot \frac{d}{dA} Keq(A)\Big|_{(A_o,w_o)} < o\ (>o)$, is then equivalent to

$$p_1+q_1N_B(A_o,o) > o \ (< o), \tag{II.7}$$

and the conservative oscillation condition, $\frac{d}{dw}$ Im L(jw) $\frac{d}{dA}$ Keq(A)$\Big|_{(A_o,w_o)}$ = o, is equivalent to

$$p_1+ q_1 N_B(A_o,o) = o. \tag{II.8}$$

APPENDIX III

RELATIONSHIPS BETWEEN $N_B(A,o)$, $\frac{f(A)}{A}$, AND Keq(A)

Express Keq(A), $N_B(A,o)$, and $\frac{f(A)}{A}$ in the forms

$$Keq(A) = \frac{1}{\pi}\int_0^{2\pi} f'(A\sin\theta)\cos^2\theta\, d\theta = \frac{4}{\pi}\int_0^{\pi/2} f'(A\sin\theta)\cos^2\theta\, d\theta, \tag{III.1}$$

$$N_B(A,o) = \frac{1}{2\pi}\int_0^{2\pi} f'(A\sin\theta)\, d\theta = \frac{2}{\pi}\int_0^{\pi/2} f'(A\sin\theta)\, d\theta, \tag{III.2}$$

and

$$\frac{f(A)}{A} = \frac{1}{A}\int_0^{A} f'(x)dx = \frac{1}{A}\int_0^{\pi/2} f'(A\sin\theta)\, A\cos\theta d\theta = \int_0^{\pi/2} f'(A\sin\theta)\cos\theta d\theta. \tag{III.3}$$

Now

$$\frac{f(A)}{A} - Keq(A) = \int_0^{\pi/2} f'(A\sin\theta)\cos\theta\,[1-\frac{4}{\pi}\cos\theta]\, d\theta, \tag{III.4}$$

so that, if θ_1 is defined such that $1 - \frac{4}{\pi}\cos\theta_1 = o$ or $\cos\theta_1 = \frac{\pi}{4}$, then $\theta_1 = 38^o15'$ and

$$\frac{f(A)}{A} - Keq(A) = \int_{0^o}^{38^o15'} f'(A\sin\theta)\cos\theta\,[1-\frac{4}{\pi}\cos\theta]d\theta + \int_{38^o15'}^{90^o}\{f'(A\sin\theta)\cos\theta\,[1-\frac{4}{\pi}\cos\theta]\}d\theta \tag{III.5}$$

$$= I_1 + I_2, \tag{III.6}$$

where $I_1 < o$ and $I_2 > o$. If $f'(x)$ is monotonic decreasing then

$$-I_1 = \int_{0^o}^{38^o15'} f'(A\sin\theta)\cos\theta\,[\frac{4}{\pi}\cos\theta - 1]d\theta \geqslant \int_{0^o}^{38^o15'}\{f'(A\sin 38^o15')\cos\theta[\frac{4}{\pi}\cos\theta - 1]\}d\theta = f'(.619A)\int_{0^o}^{38^o15'}\cos\theta\,[\frac{4}{\pi}\cos\theta - 1]\,d\theta = [.116]f'(.619A), \tag{III.7}$$

and

$$I_2 = \int_{38^o15'}^{90^o} f'(A\sin\theta)\cos\theta\,[1-\frac{4}{\pi}\cos\theta]d\theta \leqslant f'(.619A)\int_{38^o15'}^{90^o}\cos\theta[1-\frac{4}{\pi}\cos\theta]d\theta.$$
$$= [.116]f'(.619A). \tag{III.8}$$

Thus $I_2 \lesseqgtr - I_1$ or $I_1 + I_2 \lesseqgtr o$, and $\frac{f(A)}{A} - Keq(A) = I_1 + I_2 \lesseqgtr o$ or $\frac{f(A)}{A} \lesseqgtr Keq(A)$. Similarly, if $f'(x)$ is monotonic increasing then $I_1 \gtreqless - I_2$ and $\frac{f(A)}{A} - Keq(A)$ $= I_1 + I_2 \gtreqless o$ or $\frac{f(a)}{A} \gtreqless Keq(A)$.

Also,

$$\frac{f(A)}{A} - N_B(A,o) = \int_o^{\pi/2} f'(A \sin\theta) \quad [\cos\theta - \frac{2}{\pi}]d\theta \qquad \text{(III.9)}$$

so that, if θ_1 is defined such that $\cos\theta_1 - \frac{2}{\pi} = o$ or $\cos\theta_1 = \frac{2}{\pi}$, then $\theta_1 = 50^o28'$ and

$$\frac{f(A)}{A} - N_B(A,o) = \int_{0^o}^{50^o28'} f'(A \sin\theta) \quad [\cos\theta - \frac{2}{\pi}]d\theta + \int_{50^o28'}^{90^o} \{f'(A\sin\theta)$$

$$[\cos\theta - \frac{2}{\pi}]\}d\theta \qquad \text{(III.10)}$$

$$= \qquad I_1 \qquad + \qquad I_2 , \qquad \text{(III.11)}$$

where $I_1 > o$ and $I_2 < o$. If $f'(x)$ is monotonic decreasing then

$$I_1 = \int_{0^o}^{50^o28'} f'(A \sin\theta) \; [\cos\theta - \frac{2}{\pi}]d\theta \gtreqless \int_{0^o}^{50^o28'} \{f'(A \sin 50^o28') \; [\cos\theta - \frac{2}{\pi}]\}d\theta = f'(.771A) \int_{0^o}^{50^o28'} [\cos\theta - \frac{2}{\pi}]d\theta = [.211] \; f'(.771A), \qquad \text{(III.12)}$$

and

$$- I_2 = \int_{50^o28'}^{90^o} f'(A \sin\theta) \; [\frac{2}{\pi} - \cos\theta] \; d\theta \lesseqgtr f'(.771A) \int_{50^o28'}^{90^o} [\frac{2}{\pi} - \cos\theta]d\theta$$

$$= [.211] \; f'(.771A). \qquad \text{(III.13)}$$

Then $- I_2 \lesseqgtr I_1$ or $I_1 + I_2 \gtreqless o$, and $\frac{f(A)}{A} - N_B(A,o) = I_1 + I_2 \gtreqless o$ or $\frac{f(A)}{A} \gtreqless N_B(A,o)$. Similarly, if $f'(x)$ is monotonic increasing then $I_1 + I_2 \lesseqgtr o$ and $\frac{f(A)}{A} - N_B(A,o) \lesseqgtr o$ or $\frac{f(A)}{A} \lesseqgtr N_B(A,o)$.

Thus, if $f(x)$ is a soft spring nonlinearity ($f'(x)$ monotonic non increasing) then

$$N_B(A,o) \lesseqgtr \frac{f(A)}{A} \lesseqgtr Keq(A), \qquad \text{(III.14)}$$

and if f(x) is a hard spring nonlinearity ($f'(x)$ monotonic non decreasing) then

$$Keq(A) \leq \frac{f(A)}{A} \leq N_B(A,o). \qquad \text{(III.15)}$$

If $f'(x)$ is monotonic decreasing or increasing then III.14 and III.15 become

$$N_B(A,o) < \frac{f(A)}{A} < Keq(A) \qquad \text{(III.16)}$$

and

$$Keq(A) < \frac{f(A)}{A} < N_B(A,o) \qquad \text{(III.17)}$$

respectively for $A > o$ and finite.

APPENDIX IV

CALCULATION OF $w_{o_{exact}}$ IN 5.43

The system equation for the ideal relay example of case ii) is

$$\ddot{x}(t) + p_o\, x(t) + q_o\, M \operatorname{sgn}[x(t)] = o. \tag{IV.1}$$

For $x(t) > o$ the general solution of IV.1 is

$$x(t) = A^{+} \sinh\left(\sqrt{-p_o}\, t\right) + B^{+} \cosh\left(\sqrt{-p_o}\, t\right) - q_o M/p_o, \tag{IV.2}$$

and for $x(t) < o$ the general solution is

$$x(t) = A^{-} \sinh\left(\sqrt{-p_o}\, t\right) + B^{-} \cosh\left(\sqrt{-p_o}\, t\right) + q_o M/p_o. \tag{IV.3}$$

In the phase plane, $x(t) - \dot{x}(t)$, it is assumed that the periodic motion begins with $x(o) = A_o > 0$, $\dot{x}(o) = o$. Then as long as $x(t) > o$ the solution is

$$x(t) = [A_o + q_o M/p_o] \cosh\left(\sqrt{-p_o}\, t\right) - q_o M/p_o. \tag{IV.4}$$

If t_1 is defined as the minimum $t > o$ such that $x(t_1) = o$, then

$$t_1 = \frac{1}{\sqrt{-p_o}} \operatorname{arc\,cosh}\left\{\frac{q_o M}{p_o A_o + q_o M}\right\} \tag{IV.5}$$

under the constraint, $M/A_o > -p_o/q_o$.

For $t = t_1^{+}$, $x(t)$ goes negative and the solution is IV.3, where

$$A^{-} = \sinh\left(\sqrt{-p_o}\, t_1\right)\left[q_o M/p_o + (A_o + q_o M/p_o) \cosh\left(\sqrt{-p_o}\, t_1\right)\right] < o, \tag{IV.6}$$

and

$$B^{-} = -\frac{q_o M}{p_o} \cosh\left(\sqrt{-p_o}\, t_1\right) - \left[\frac{p_o A_o + q_o M}{p_o}\right] \sinh^2\left(\sqrt{-p_o}\, t_1\right) > o. \tag{IV.7}$$

Let t_2 be the minimum $t > t_1$ such that $\dot{x}(t_2) = o$, then

$$t_2 = \frac{1}{\sqrt{-p_o}} \operatorname{arc\,cosh}\left\{\frac{B^{-}}{\sqrt{B^{-2} - A^{-2}}}\right\}. \tag{IV.8}$$

It can be shown that $x(t_2) = -A_o$, and $t_3 = 2\,t_2$ is such that $x(t_3) = A_o$, $\dot{x}\,(t_3) = o$ from a symmetry argument. Thus the trajectory closes on itself in time t_3 which is then the period of the periodic motion, T_o. Then

$$T_o = 2t_2 = \frac{2}{\sqrt{-p_o}} \text{ arc cosh}\left\{\frac{M^2 - 2MA_o p_o/q_o - A_o{}^2(p_o/q_o)^2}{[M + A_o p_o/q_o]^2}\right\} \qquad \text{(IV.9)}$$

from IV.8, IV.7, IV.6, and IV.5. Also,

$$w_{o_{exact}} = \frac{2\pi}{T_o} = \frac{\pi\sqrt{-p_o}}{\text{arc cosh}\left\{\frac{M^2 - 2MA_o p_o/q_o - A_o{}^2(p_o/q_o)^2}{[M + A_o p_o/q_o]^2}\right\}} \cdot \qquad \text{(IV.10)}$$

APPENDIX V

EVALUATION OF LOEB'S CRITERION FOR GENERAL THIRD ORDER L(s)

The analytical Loeb's criterion conditions, $\frac{d}{dw}\,\mathrm{ImL}(jw_o)\frac{d}{dA}\,\mathrm{Keq}(A_o) < o\ (> o)$ for a stable (unstable) limit cycle are applied to the general third order nonlinear system of Fig. 6.1. Equation 4.5 gives

$$\frac{d}{dA}\,\mathrm{Keq}(A_o) = \frac{2}{A_o}\,[N_B(A_o,o) - \mathrm{Keq}(A_o)]\ . \tag{V.1}$$

Since

$$L(jw) = \frac{q_2(jw)^2 + q_1 jw + q_o}{(jw)^3+p_2(jw)^2+p_1 jw+p_o}\ , \tag{V.2}$$

$$\mathrm{ImL}(jw) = \frac{wq_1(p_o-p_2w^2) - (wp_1-w^3)\ (q_o-w^2q_2)}{(p_o-p_2w^2)^2 + (wp_1-w^3)^2} \tag{V.3}$$

with

$$q_1\ (p_o-p_2w_o^{\,2}) - (p_1-w_o^{\,2})\ (q_o-q_2w_o^{\,2}) = o \tag{V.4}$$

from the DF oscillation requirement that $\mathrm{ImL}(jw_o) = o$. Then

$$\frac{d}{dw}\,\mathrm{ImL}(jw_o) = \frac{2w_o^{\,2}[q_o+q_2p_1-p_2q_1-2q_2w_o^{\,2}]}{(p_o-p_2w_o^{\,2})^2 + (w_op_1-w_o^{\,3})^2}\ . \tag{V.5}$$

The general DF conditions are

$$(p_1+q_1\mathrm{Keq})\ (p_2+q_2\mathrm{Keq}) - (p_o+q_o\mathrm{Keq}) = o \tag{V.6}$$

and

$$w_o^{\,2} = \frac{p_o+q_o\mathrm{Keq}}{p_2+q_2\mathrm{Keq}} = p_1 + q_1\,\mathrm{Keq} > o. \tag{V.7}$$

The solutions of V.6 are

$$\mathrm{Keq}_{1,2} = -\frac{(p_1q_2+q_1p_2-q_o)}{2\,q_1q_2} \pm \sqrt{\frac{(p_1q_2+q_1p_2-q_o)^2}{4q_1^{\,2}\,q_2^{\,2}} - \frac{-(p_1p_2-p_o)}{q_1\,q_2}}\ . \tag{V.8}$$

If

$$\frac{(p_1q_2 + q_1p_2 - q_o)^2}{4q_1^2 q_2^2} - \frac{(p_1p_2 - p_o)}{q_1 q_2} > o \qquad (V.9)$$

and

$$\sqrt{\frac{(p_1q_2+q_1p_2-q_o)^2}{4 q_1^2 q_2^2} - \frac{(p_1p_2-p_o)}{q_1q_2}} > \left| \frac{p_1q_2+q_1p_2-q_o}{2 q_1q_2} \right| \qquad (V.10)$$

then $Keq_1 > o$ and $Keq_2 < o$ with

$$Keq(A_o) = Keq_1 = - \frac{(p_1q_2+q_1p_2-q_o)}{2 q_1q_2} + \sqrt{\frac{(p_1q_2+q_1p_2-q_o)^2}{4q_1^2q_2^2} - \frac{(p_1p_2-p_o)}{q_1q_2}} . \qquad (V.11)$$

Now $w_o^2 = p_1 + q_1 Keq(A_o)$, so that

$$\frac{d}{dw} ImL(jw_o) = - \frac{4w_o^2 q_1q_2 \sqrt{\frac{(p_1q_2+q_1p_2-q_o)^2}{4q_1^2q_2^2} - \frac{(p_1p_2-p_o)}{q_1q_2}}}{(p_o-p_2w_o^2)^2 + (w_op_1-w_o^3)^2} . \qquad (V.12)$$

Then

$$\frac{d}{dw} ImL(jw_o) \frac{d}{dA} Keq(A_o) = \frac{-8w_o^2 \sqrt{\frac{(p_1q_2+q_1p_2-q_o)^2}{4q_1^2q_2^2} - \frac{(p_1p_2-p_o)}{q_1q_2}} \; q_1q_2[N_B(A_o,o)-Keq_1]}{A_o [(p_o-p_2w_o^2)^2 + (w_op_1-w_o^3)^2]} , \qquad (V.13)$$

and Loeb's criterion becomes

$$q_1q_2 [N_B(A_o,o) - Keq_1] > o \; (< o) \qquad (V.14)$$

for a stable (unstable) limit cycle. Also, $Keq_2 < o$ implies $N_B(A_o,o) - Keq_2 > o$, and

$$q_1q_2[N_B(A_o,o) - Keq_1] [N_B(A_o,o)-Keq_2] = q_1q_2N_B^2(A_o,o) + (p_1q_2 + q_1p_2 - q_o) N_B(A_o,o) + p_1p_2 -p_o. \qquad (V.15)$$

Hence Loeb's criterion may also be written as

$$q_1 q_2 N_B^2(A_o,o) + [p_1 q_2 + q_1 p_2 - q_o]\, N_B(A_o,o) + p_1 p_2 - p_o > o \ (< o) \tag{V.16}$$

for a stable (unstable) limit cycle. Condition V.16 is the Loeb's criterion condition for L(s) with two zeros . If L(s) has only one zero then $q_2 = o$ and V.16 becomes

$$(q_o - q_1 p_2)\, N_B(A_o,o) + p_o - p_1 p_2 < o \ (> o) \tag{V.17}$$

for a stable (unstable) limit cycle. Also, if L(s) has no zeros then $q_1 = q_2 = o$ and V.16 becomes

$$q_o\, N_B(A_o,o) + p_o - p_1 p_2 < o \ (> o) \tag{V.18}$$

for a stable (unstable) limit cycle.

APPENDIX VI

CALCULATION OF $N_i(A_n, a, , w_n)$

The input to the nonlinearity is assumed in the form $x(t) = \epsilon e^{at} \sin\Omega t + A \sin wt$. Expansion of the output of the nonlinearity yields

$$f[x(t),x(t-1)] = \alpha x(t-1)\ [1-x^2(t)]$$

$$= \alpha[\epsilon e^{-a} e^{at} \sin(\Omega t-\Omega) + A \sin(wt-w)] \cdot$$

$$[1 - \epsilon^2 e^{2at} \sin^2\Omega t - 2\epsilon A e^{at} \sin\Omega t \sin wt - A^2 \sin^2 wt]. \quad \text{(VI.1)}$$

Linear terms in $\epsilon e^{at} \sin(\Omega t - \Omega)$ are

$$\alpha[\epsilon e^{-a} e^{at} \sin(\Omega t - \Omega) - \epsilon e^{-a} e^{at} \sin(\Omega t - \Omega) \cdot \frac{1}{2\pi} \int_0^{2\pi} A^2 \sin^2\theta\, d\theta$$

$$- 2\epsilon e^{at} \sin\Omega t \frac{1}{2\pi} \int_0^{2\pi} A^2 \cos w \sin^2\theta\, d\theta], \quad \text{(VI.2)}$$

or

$$\alpha[1 - A^2/2 - A^2 \cos w]\ e^{-a} \epsilon e^{at} [\cos\Omega \sin\Omega t - \sin\Omega \cos\Omega t]. \quad \text{(VI.3)}$$

The incremental gain is then identified as

$$N_i(A,a,\Omega,w) = \alpha[1 - A^2/2 - A^2 \cos w]\ e^{-(a+j\Omega)}, \quad \text{(VI.4)}$$

and

$$N_i(A_n,a,\Omega,w_n) = \alpha[1 - A_n^2/2 - A_n^2 \cos w_n]\ e^{-(a+j\Omega)}$$

$$= \alpha[1 - A_n^2/2]\ e^{-(a+j\Omega)}. \quad \text{(VI.5)}$$

CALCULATION OF $N_i(k,a,\Omega,n)$

The input to the nonlinearity is $x(t) = \epsilon e^{at} \sin\Omega t + k\ sn[(4n+1)Kt,k]$. Expansion of the output of the nonlinearity yields

$$f[x(t),x(t-1)] = \alpha[\epsilon e^{at} e^{-a} \sin(\Omega t - \Omega) + k\ sn[(4n+1)K(t-1),k]] \cdot$$

$$[1 - \epsilon^2 e^{2at} \sin^2\Omega t - 2\epsilon e^{at} \sin(\Omega t) k\ sn(\cdot) - k^2 sn^2(\cdot)]. \quad \text{(VI.6)}$$

Linear terms in $\epsilon e^{at} \sin(\Omega t - \Omega)$ are

$$\alpha[\epsilon e^{-a}e^{at}\sin(\Omega t - \Omega) - \epsilon e^{-a}e^{at}\sin(\Omega t - \Omega)\frac{1}{T_n}\int_0^{T_n} k^2 sn^2[(4n+1)Kt,k]dt$$

$$- 2\epsilon e^{at}\sin\Omega t \ \frac{1}{T_n}\int_0^{T_n} k^2 sn[(4n+1)Kt,k]\ sn\ [(4n+1)K(t-1),k]\ dt] \ , \qquad \text{(VI.7)}$$

or

$$\epsilon e^{-a}e^{at}(4n+1)E(k)\ [\cos\Omega \sin\Omega t - \sin\Omega \cos\Omega t] \ . \qquad \text{(VI.8)}$$

The incremental gain is then identified as

$$N_i(k,a,\Omega,n) = (4n+1)E(k)e^{-(a+j\Omega)} \ . \qquad \text{(VI.9)}$$

CALCULATION OF $N_B^*(k,n)$

The input to the nonlinearity of the transformed system of Fig. 7.3 is assumed in the form $y(t) = B + \tanh^{-1}\{k\ sn[(4n+1)Kt,k]\}$. The equivalent gain to the bias B is defined as

$$N_B^*(k,n,B) = \frac{\alpha}{T_n B}\int_0^{T_n} \tanh\left\{B + \tanh^{-1}\{k\ sn[(4n+1)Kt,k]\}\right\} dt$$

$$= \frac{\alpha}{T_n B}\int_0^{T_n} \frac{\{\tanh(B) + k\ sn\ [(4n+1)Kt,k]\}\ dt}{1+\ \tanh(B)\ k\ sn[(4n+1)Kt,k]}$$

$$= \frac{\alpha \tanh(B)}{T_n B}\int_0^{T_n} \frac{dt}{1 + \tanh(B)k\ sn[(4n+1)Kt,k]}$$

$$+ \frac{\alpha}{T_n B}\int_0^{T_n} \frac{k\ sn[(4n+1)Kt,k]\ dt}{1 + \tanh(B)k\ sn[(4n+1)Kt,k]} \ , \qquad \text{(VI.10)}$$

and the incremental gain becomes

$$N_B^*(k,n) = \lim_{B\to o} N_B^*(k,n,B) = \lim_{B\to o}\left\{\frac{\alpha\tanh(B)}{T_n B}\int_0^{T_n} \frac{dt}{1+\tanh(B)k\ sn[(4n+1)Kt,k]}\right\}$$

$$+ \lim_{B\to o}\left\{\frac{\alpha k}{T_n B}\int_0^{T_n} \frac{sn[(4n+1)Kt,k]dt}{1+\tanh(B)k\ sn[(4n+1)Kt,k]}\right\}$$

$$= \alpha + \lim_{B\to o}\left\{\frac{\alpha k}{T_n B}\int_0^{T_n} \frac{sn[(4n+1)Kt,k]dt}{1+\tanh(B)k\ sn[(4n+1)Kt,k]}\right\}. \qquad \text{(VI.11)}$$

Now

$$\frac{\alpha k}{T_n B}\int_0^{T_n}\frac{sn[\cdot]dt}{1+\tanh(B)k\ sn[\cdot]} = \frac{\alpha k}{T_n B}\int_0^{T_n} sn\,[\cdot]\left\{1-\tanh(B)k\ sn[\cdot]+\right.$$

$$\left.\tanh^2(B)k^2sn^2[\cdot]- \cdots\right\} dt$$

$$= \frac{\alpha k}{T_n B}\int_0^{T_n} sn[.]dt - \frac{\alpha k^2\tanh(B)}{T_n B}\int_0^{T_n} sn^2[\cdot]dt + \text{higher order terms}$$

$$= o - \frac{\alpha k^2\tanh(B)}{T_n B}\int_0^{T_n} sn^2[\cdot]dt + \text{higher order terms in } \tanh(B). \qquad \text{(VI.12)}$$

Then

$$\lim_{B\to o}\left\{\frac{\alpha k}{TnB}\int_0^{T_n}\frac{sn[\cdot]dt}{1+\tanh(B)k\ sn[\cdot]}\right\} = \frac{-\alpha k^2}{T_n}\int_0^{T_n} sn^2[(4n+1)Kt,k]\,dt, \qquad \text{(VI.13)}$$

and

$$N_B^*(k,n) = \alpha\left\{1 - \frac{k^2}{T_n}\int_0^{T_n} sn^2[(4n+1)Kt,k]\ dt\right\}$$

$$= \alpha\left\{1 - \frac{k^2\ sgn(4n+1)}{4K}\cdot\int_0^{4Ksgn(4n+1)} sn^2[u,k]du\right\} = \alpha\left\{1 - \frac{1}{K}\int_0^{K} k^2sn^2[u,k]du\right\}$$

$$= \frac{\alpha}{K}\int_0^{K} dn^2[u,k]du = \frac{\alpha}{K}\,E(k) = (4n+1)E(k). \qquad \text{(VI.14)}$$

REFERENCES

1. Gibson, John E., Nonlinear Automatic Control. New York : McGraw-Hill Book Company, Inc., 1963.

2. Gille, J-C., M.J. Pelegrin and P. Decaulne, Feedback Control Systems. New York : McGraw-Hill Book Company, Inc., 1959.

3. Graham, Dunstan, and Duane McRuer, Analysis of Nonlinear Control Systems. New York : John Wiley and Sons, Inc., 1961.

4. Truxal, John G., Automatic Feedback Control System Synthesis. New York : McGraw-Hill Book Company, Inc., 1955.

5. West, J.C., Analytical Techniques for Non-linear Control Systems. Princeton, N.J. : D. Van Nostrand Company, Inc., 1960.

6. Gelb, A., and W.E. Vander Velde, Multiple-input Describing Functions and Nonlinear System Design. New York : McGraw-Hill Book Company, Inc., 1968.

7. Loeb, J., "Phénomènes Héréditaires dans les Servomécanismes; un Critérium Général de Stabilité", Annales des Télécommunications, Vol. 6, No. 12, 1951, pp. 346-356.

8. Loeb, J., "Recent Advances in Nonlinear Servo Theory." (1953) In Frequency Response, ed. R. Oldenburger, New York : The Macmillan Book Company, 1956, pp. 260-268.

9. Brookes, Barry Edward, "The Stability of Limit Cycles in Time-Lag Relay Control Systems", M.Sc. Thesis, Department of Electrical Engineering, University of Manitoba, May, 1967; IJC.

10. Katzberg, Jack David, "Self-Oscillations in Relay Control Systems with Delay", M.Sc. Thesis, Department of Electrical Engineering, University of Manitoba, October, 1968.

11. Menzies, Don F., "On the Differential-Difference Equation $\dot{x}(t) = - \alpha x(t-1) (1-x^2(t))$", Summer Research Project, Department of Electrical Engineering, University of Manitoba, September, 1969.

12. Cosgriff, R.L., "Application of Linear Differential Equations with Periodic Coefficients in the Study of Non-linear Phenomena", Proc. of First International Congress of the I.F.A.C. Vol. 2, 1960,pp. 883-887.

13. Coddington, E.A., and N. Levinson, Theory of Ordinary Differential Equations. New York : McGraw-Hill Book Company, Inc., 1955.

14. Minorsky, N., Nonlinear Oscillations. Princeton, N.J. : D. Van Nostrand Company, Inc., 1962.

15. Mufti, I.H., "The Stability of Systems with Lag", N.R.C. Mechanical Engineering Report MK-16, Ottawa, March, 1965.

16. Bellman, Richard, and Kenneth L. Cooke, Differential-Difference Equations. New York : Academic Press Inc., 1963.

17. Kaplan, W., Operational Methods for Linear Systems. Reading, Massachusetts : Addison-Wesley Publishing Company, Inc., 1962.

18. Stokes, A., "A Floquet Theory for Functional Differential Equations", Proc. Nat. Acad. Sci., Vol. 48, 1962, pp.1330-1334.

19. Stokes, A., "On the Stability of a Limit Cycle of an Autonomous Functional Differential Equation", Contributions to Differential Equations, Vol. 3, 1964, pp. 121-140.

20. Krylov, N., and N. Bogoliubov, Introduction to Nonlinear Mechanics. Princeton, N.J. : Princeton University Press, Annals of Mathematical Studies, Vol. 11, 1947.

21. Kochenburger, J.R., "Analysis and Sythesis of Contactor Servomechanisms", Sc. D. Thesis, Department of Electrical Engineering, Massachusetts Institute of Technology, 1949.

22. Tustin, A., "The Effects of Backlash and of Speed Dependent Friction on the Stability of Closed-cycle Control Systems", J.I.E.E. , Vol. 94, Part II, May, 1947, pp. 143-151.

23. Oppelt, W., "Locus Curve Method for Regulators with Friction", Z. Deut. Ingr., Vol. 90, 1948, pp. 179-183.

24. Goldfarb, L.C. "On Some Nonlinear Phenomena in Regulatory Systems", Avtomatika i Telemekhanika, Vol. 8, No. 5, 1947, pp. 349-383.

25. Dutilh, J., "Théorie des Servoméchanisms à Relais", Onde Élec., Vol. 30, 1950, pp. 438-445.

26. Bower, J.L., and P.M. Schultheiss, Introduction to the Design of Servomechanisms. New York : John Wiley & Sons, Inc., 1958.

27. West, J.C., J.L. Douce, and R.K. Livesley, "The Dual Input Describing Function and Its Use in the Analysis of Non-linear Feedback Systems", J.IEE, Vol. B-103, July, 1956, pp. 463-474.

28. McLachlan, N.W., Theory and Application of Mathieu Functions. London : Oxford University Press, 1951.

29. Willems, J.L., "The Stability of Oscillations in Nonlinear Networks", IEEE Trans. on Circuit Theory, Vol. CT-15, No.3, September, 1968, pp. 284-286.

30. Jones, G.S., "Periodic Functions Generated as Solutions of Nonlinear Differential-Difference Equations", Proceedings of International Symposium on Nonlinear Differential Equations and Nonlinear Mechanics, 1961.

31. Jones, G.S., "Periodic Motions in Banach Space and Applications to Functional-Differential Equations", Tech. Report 63-9, RIAS, Baltimore, Md., 1963; Contribs. Differential Eqs., Vol. III, 1964, pp. 73-106.

32. Jahnke, E., F. Emde, and F. Lösch, Tables of Higher Functions. New York : McGraw-Hill Book Company, Inc., 1960.

33. Birkhoff, G., and L. Kotin, "Asymptotic Behavior of Solutions of First-Order Linear Differential-Delay Equations", Journal of Mathematical Analysis and Applications, Vol. 13, 1966, pp. 8-18.

34. El'sgol'ts, L.E., Introduction to the Theory of Differential Equations With Deviating Arguments. San Francisco : Holden-Day, Inc., 1966.

35. Grensted, P.E.W., "The Frequency Response Analysis of Non-Linear Systems", Proc. I.E.E., Vol. 102, part C, 1955, pp.244-255.

36. Grensted, P.E.W., "Frequency Response Methods Applied to Non-Linear Systems", Progress in Control Engineering, Vol. 1, pp. 105-139.

37. Zverkin, A.M., "On the Completeness of a System of Particular Solutions of a Differential Equation with Retardation and Periodic Coefficients", Proc. Seminar on the Theory of Differential Equations with Deviating Argument, Moscow Friendship Univ., Vol. 2, 1963, pp. 94-112.

38. Zverkin, A.M., "On the Theory of Linear Differential Equations with Retarded Argument and Periodic Coefficients", Dokl. Akad. Nauk SSSR, Vol. 128, 1959, pp. 882-885.

39. Dorf, R.C., Modern Control Systems. Reading, Massachusetts : Addison-Wesley Publishing Company, Inc., 1967.

40. Sommerville, M.J. and D.P. Atherton, "Multi-gain Representation for a Single-valued Non-linearity with Several Inputs, and the Evaluation of Their Equivalent Gains by a Cursor Method", Proc. I.E.E, Vol. 105c, 1958, pp. 537-549.

41. Rajagopalon, P.K., and Y.P. Singh, "Analysis of Harmonic and Almost Periodic Oscillations in Forced Self-oscillating Systems", Paper 41.6, IFAC Congress, Warsaw, June, 1969.

42. Bonenn, Z., "Relative Stability of Oscillations in Non-linear Control Systems", Proc. IFAC, Basel, Switzerland, p. 214/1-4, August, 1963.

43. Balasubramanian, R, and D.P. Atherton, "Response of Multi-dimensional Nonlinearities to Inputs Which are Separable Processes", Proc. I.E.E., Vol. 115, 1968, pp 581-590.